METAL CATALYSED INTUMESCENCE OF POLYHYDROXYL COMPOUNDS

FJWJ Labuschagné

METAL CATALYSED INTUMESCENCE OF POLYHYDROXYL COMPOUNDS

Frederick Johannes Willem Jacobus (Johan) Labuschagné

Submitted in partial fulfilment of the requirements for the degree of *Philosophiae Doctor* (Chemical Engineering) in the Faculty Engineering, Built Environment and Information Technology, University of Pretoria, Pretoria

2003

METAL CATALYSED INTUMESCENCE OF POLYHYDROXYL COMPOUNDS

by: Frederick Johannes Willem Jacobus (Johan) Labuschagné
Supervisor: Prof. Walter W Focke
Department: Chemical Engineering
Degree: PhD (Chemical Engineering)

SYNOPSIS

Fire presents a great risk to humans and their possessions. Polymeric compounds are highly flammable and compounds are added to increase their fire resistance. These additives are referred to as flame retardants. Intumescent flame retardants are systems that form a carbon rich foam on the surface of the polymer during thermal degradation. A new field of metal catalysed intumescence is discussed in this document. The influence of both the metal ion and organic backbone of polyhydroxylcarboxylic acid metal salts was studied. The intumescence and foaming properties of selected salts were studied in more detail.

Gluconic acid proved to be the best intumescent and showed the best combination of carbon char yield, foam structure and volume, stability and open flame characteristics. As a general rule of thumb, the char volume and structure improved with an increased number of hydroxyl groups in the compound. Carbon char yield increased with an increase in the number of hydroxyl groups for a constant number of carbons in the complex. The number of acid groups in the compound played a lesser role in intumescence. Most metal complexes catalyse intumescent decomposition of polyhydric compounds such as polyhydroxylcarboxylic acids and pentaerythritol. The reduction in the volatilisation losses implies that the metal cations catalyse carbonisation reactions in the polyhydroxyl compound. Unfortunately, the resultant carbon-foams are unstable: the metal residues also catalyse the further oxidative degradation of the char. The low thermal stability of the compositions tested, as well as the afterglow effect makes them unsuitable for use as flame retardant additives in plastics. From the studies of the different metal complexes with acetylacetone and gluconic acid, it was concluded that the calcium ion exhibited the most promise.

When pyrolysed in air with an open gas flame or in a furnace, calcium gluconate monohydrate produces voluminous foam. The foam is of a closed cell structure, densely packed and has no mechanical strength. The cell walls are very thin (5 to 50 nm) and the cells are between 50 μm and 200 μm in size. If the sample is compressed before heating, the resultant foam produced during pyrolysis is less voluminous than that of the loose powder. The BET surface area of the calcium gluconate monohydrate foamed at 300°C for 5 min. is 16.0 m^2/g. The foam produced after 5 min heating at 300°C has a thermal conductivity similar to standard polystyrene foam.

Adding leached silica to the calcium gluconate monohydrate increases mechanical strength of the foam, but influences the foam volume negatively. The optimum silica level was calculated to be 1:1 gluconate to silica on a mole ratio (11.8% SiO_2 by mass). The mechanical strength of the foam can also be increased with the addition of expandable graphite. The graphite has a lesser influence on the foam volume than the silica, but also reduces the foam volume. However, the addition of the expandable graphite gives the sample more "opening" force, as the foam volume of a compressed sample pyrolysed, is similar to that of the heated loose powder.

Calcium gluconate monohydrate starts to degrade at 120°C, losing its crystal water and shows a mass loss of 4% at 180°C. The exothermic peak (shown in the DSC/TGA data) associated with the metal catalysed carbon oxidation (afterglow) is observed at 570°C in air. For the calcium gluconate monohydrate the transition from $CaCO_3$ to CaO occurs above 650°C in air.

It has been shown that the foaming of polyhydroxylcarboxylic acids is due to the formation of water vapour during degradation. For calcium gluconate monohydrate, foaming starts due to the loss of crystal water and is continued by the loss of hydroxyl groups as water. The bulk of the foaming is due to the second reaction. It has been shown that compounds with crystal waters produce a more voluminous and lower density foam. The foam is an amorphous carbon rich residue. The molecular mass of the carbon residue increases up to a heating temperature of 300°C. This implies that the carbon residue crosslinks during formation, forming a stretchable cell wall for the foam. Compounds with a "free" hydroxyl group at the end of the carbon chain produce a foam of larger volume and lower density. This supports the crosslinking theory. The foam produced when calcium

gluconate monohydrate is heated for 5 min at 300°C in air is of very low density – 2.5 kg/m^3 based on residual mass.

The density of the calcium gluconate monohydrate pyrolysed at 1000°C for 5 min in air yields a CaO with a density of 20 kg/m^3. This implies that the high temperature pyrolysis of calcium gluconate can produce an inorganic oxide of low bulk density and possible high specific surface area. The BET surface area of $CaCO_3$ from the gluconate pyrolysed at 600°C is ~ 12 m^2/g.

An intumescent coating containing calcium gluconate monohydrate, leached silica and expandable graphite as a system was prepared and compared to commercial formulations. This gluconate based system was at least as efficient as the commercial formulations when painted on balsa wood planks or aluminium plates. On cardboard sheets it did not perform as well as the commercial systems.

More work should be done to overcome the afterglow effect observed with metal-based intumescent systems. The crystal structure of calcium gluconate monohydrate should be determined as to understand the decomposition better. It is unclear whether the decomposition is catalysed inter- or intramolecularly.

KEY WORDS: carbon foam, char, latent base catalysed intumescence, metal catalysed intumescence, carbonisation, intumescent flame retardants

ACKNOWLEDGEMENTS

A PhD dissertation is never complete. There is always something else still to be done, something more to be added, to make it … even more complete.

CONTENT

LIST OF FIGURES

LIST OF TABLES

NOMENCLATURE

Symbol	Property	Unit	
A	cross section area	square meter	$[m^2]$
I	electric current	Ampere	$[A]$
l	electric path length	meter	$[m]$
R	electrical resistance	Ohm	$[\Omega]$
V	electric potential	volt	$[V]$
Σ	electric conductivity	-	$[\Omega^{-1}.m^{-1}]$

ABBREVIATIONS

ABS	acrylonitrile-butadiene-styrene
ASTM	American Society for Testing of Materials
APP	ammonium polyphosphate
ATH	aluminium trihydroxide or alumina trihydrate
BET	Brunauer, Emmett and Teller

ca.	*circa* (approximately)
CaDex	calcium complexes produced from dextrose monohydrate
DMSO	dimethyl sulfoxide
DSC	differential scanning calorimetry
DTA	differential thermal analysis
e.g.	*exempli gratia* (for example)
EDS	energy dispersive spectroscopy
EDX	energy dispersive analysis of X-rays
et al.	*et alibi* (and elsewhere)
etc.	*et cetera* (and so forth)
FeDex	iron complexes produced from dextrose monohydrate
FEP	perfluoro(ethylene/propylene)
IR	infrared
LCP	liquid crystal polymers
LOI	limiting oxidation index
LPG	liquefied petroleum gas
LV	low vacuum
MALDI-TOF-MS	matrix assisted laser desorption ionisation – time of flight – mass spectrometry
MetDex	metal complexes produced from dextrose monohydrate
P	property
PA	polyamide
PAI	poly(amide imide)
PAN	polyacrylonitrile
PBT	poly(butylene terephthalate)
PC	polycarbonate
PE	polyethylene
PEEK	poly(ether ether ketone)
PEI	poly(ester imide)
PEO	poly(ethylene oxide)
PER	pentaerythritol
PES	polyethersulphone
PET	poly(ethylene terephthalate)
PMMA	poly(methyl methacrylate)

POM	polyoxymethylene
PP	polypropylene
PPO	poly(phenylene oxides)
PPS	poly(phenylene sulphide)
PS	polystyrene
PSU	polysulphone
PTFE	poly(tetrafluoroethylene)
PUR	polyurethane
PVA	poly(vinyl alcohol)
PVC	poly(vinyl chloride)
rpm	revolutions per minute
SABS	South African Bureau of Standards
SAN	styrene-acrylonitrile
SDTA	simultaneous differential thermal analysis
SEM	scanning electron microscope
TEM	transmission electron microscope
TGA	thermo gravimetric analysis
vs.	*versus* (against)
XRD	X-ray diffraction

1.   Introduction

Due to the great risk of fires to humans and their possessions, new methods are continuously being investigated and developed to prevent fires and reduce their effects. Some additives to polymers increase the materials resistance to ignition, the amount of fire stress it can withstand, retard the rate of combustion of the materials and prevent sustained burning (Gann, 1993). These additives incorporated in polymeric materials are called flame retardants.

Intumescent flame retardants form a foamed carbon barrier layer on the polymer surface when it is exposed to heat (Vandersall, 1970; Camino, Costa, & Martinasso, 1989). Conventional organic systems are based on the acid catalysed dehydration of carbon rich polyols such as dipentaerythritol. It is known that metal oxides (Cullis & Hirschler, 1984) and other metal compounds (Gann; 1993, Green; 1996) have utility as catalytic char forming flame retardants. Both antimony and tin have been used to improve the flame resistance of cellulosics without the assistance from halogen containing compounds (Ramsbottom; 1947). Apparently they alter the condensed phase thermal degradation pathways in such a manner that more non-volatile char residues and less flammable gases are generated on the thermal decomposition of the polymeric material (Wills; 1952).

Furthermore, it was found that low levels of potassium bicarbonate significantly modified the pyrolysis kinetics of α-cellulose and led to greater char yields (Tang & Neill, 1964). Recently it was also discovered that potassium carbonate enhances the charring of polymers containing pentaerythritol-silica combinations as flame retardants (Gilman *et al.,* 1997). This consequently led to the discovery of the base catalysed intumescence of potassium bitartrate (Focke, Labuschagné & Strydom, 2000).

Combinations of potassium bitartrate and pentaerythritol showed improved intumescence but carbon char oxidation by glowing combustion remained a problem (Focke *et al.,* 2000). Base catalysis is an attractive alternative to conventional acid catalysed intumescent flame retardant systems as it could help to alleviate corrosion problems during polymer processing.

The problem is that strongly basic residues catalyse the oxidative destruction of the char-foam at high temperatures. These observations suggested the need for a more detailed investigation on the effect of the metal cation in such systems. It was decided to do a more comprehensive study on metal base catalysed intumescent systems.

The aim of the study was to investigate a great number of different organometallic complexes. The effect of both the organic part and metal ion was investigated. For the organic backbone, properties such as number of carbons, functionalities, molecular structure and other elements in the organic compound were taken into account. The effects of different metal ions in the organometallic complex on the char foam structure and volume, carbon yield and char oxidation (afterglow effect) were studied. This was done to identify suitable metal ions and organic molecules, which in combination are effective intumescent systems with possible commercial interest.

Because of time constraints and the great number of complexes studied, screening tests were carried out on all the samples as to identify those with greater potential. These tests are very quick and are in some cases unscientific, but are good indications of which compounds will not work as intumescent systems. Further studies that are more comprehensive were carried out on the materials showing potential. Several of the metal complexes were synthesised and may therefore be slightly different to commercial samples.

2.   Background

2.1.   Thermal degradation, flammability and flame retardancy

Organic compounds degrade thermally, as is the case with polymers (plastics). If this thermal degradation of the combustible materials is oxidative and characterised by the generation and emitting of heat and light, the process is called a fire. The light emitted from the fire is the flame, which is a visual sign and is an indication of the heat generated.

In the early 1990's it was estimated that 29 000 injuries and 4 500 deaths are caused by fires each year in the United States alone and that the total global cost is over $100 billion annually (Gann, 1993). Today a fire in a structure occurs every 60 seconds, residential fires every 82 seconds, every 85 seconds in a vehicle and every 34 seconds in an outside property in the United States; 1.8 million fires a year. This resulted in $10 billion in property damage, 3 570 civil deaths and 21 875 injuries in 1999, down from the early 1990's (Nelson & Wilkie, 2001).

Combustion is usually a gas phase phenomenon. Volatile combustible species oxidise exothermically in the gas phase. Afterglow or glowing combustion is a form of non-gas phase combustion. Here the substrate is oxidised in the condensed phase to form both solid and gaseous products. This usually takes place at temperatures well below the ignition temperature of the material. For instance, the carbon residue in a carbon rich material is oxidised in the solid phase.

Emman's fire triangle is generally used to illustrate how combustion works and is shown in Figure 2-1 (Wolf & Lal Kaul, 1992). For a sustained fire, three elements are needed (Sutker, 1988):

- Fuel – Volatile combustibles from carbon rich substance thermally degrading
- Heat – Supplied by the exothermic oxidative destruction of fuel
- Oxidising agent – Oxygen provided by air

In the case of polymers, an external heat source is needed to ignite the substrate. The heat, to which the material is exposed, causes the high molecular weight polymer to thermally decompose (Hirschler, 2000). On thermal decomposition, the polymer releases smaller

volatile compounds that act as fuel to the fire. These combustible species mix with the oxygen in the air to form an ignitable mixture. Exothermic oxidation of the volatiles occurs and the material burns. Light and more heat are generated. The process becomes self-sustaining and functions with a feed back loop as can be seen in the fire triangle (Figure 2-1). The product of the fire differs for each combustible compound. In the case of polymers, the gases produced by combustion tend to be mainly carbon dioxide (CO_2), carbon monoxide (CO) and water vapour (H_2O). The solid residue is mostly carbon (C) and ash (oxidised metals) (Wolf & Lal Kaul, 1992; Sutker, 1988).
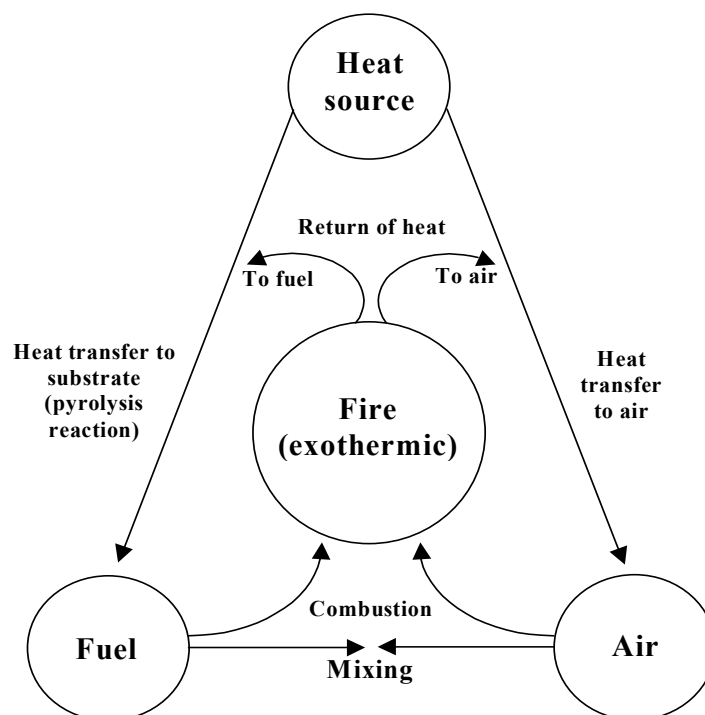
Figure 2-1   Emman's fire triangle

A flame retardant system is a compound or compositions added to materials, which increases a given material's resistance to combustion. The flame retardant system can either be added to the polymer during the polymer's manufacturing step, during master batching of the polymer additives or during the production of the plastic artefacts.

An effective flame retardant needs to hinder the supply of one or more of the elements required for sustained combustion (Sutker, 1988). The objective of flame retardants is to lower a polymers inherent fire risk by lowering the rates of combustion and flame spreading under fire conditions (Benbow, 1987). The use of flame retardants may prevent a small fire from becoming a major catastrophe (Green, 1996). In order for a flame retardant to be

effective, it must interact and interfere with the degradation of the host polymer at the polymer's degradation temperature (Schmidt, 1965). The degradation temperatures for the most widely used polymers are between 200°C and 400°C (Pearce, 1986). Increased fire resistance can be achieved through several mechanisms, as can be seen in Figure 2-2 (Focke, Strydom & Bartie, 1997). The interference with the combustion process may take place in the gas or vapour (flame zone) or condensed or solid phases (polymer melt).

Gas Phase
Oxidation (Flame)
(Inhibition of the oxidation reactions)

Volatile products
(Dilution with inert gas)

Heat
(Endothermic decomposition)

Phase Boundary

(Protective coating or char barrier)

Thermal Degradation
Condensed Phase
(Cooling of substrate, matrix dilution and char formation)

Solid
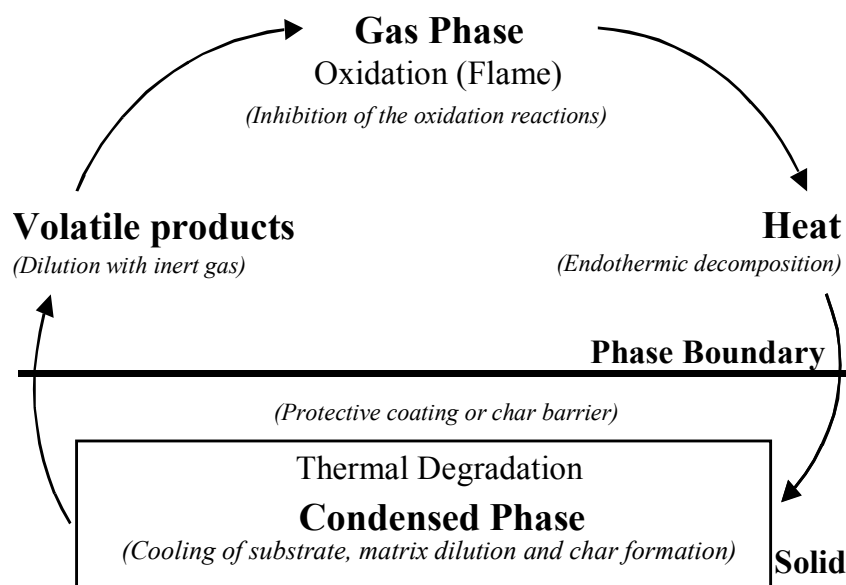
Figure 2-2   A simplified model for combustion and flame retardancy

A flame retardant is not designed to prevent the material from igniting, but to keep the flame spread rate to a minimum and prevent sustained burning. Flame retardants tend to retard the spread of flames by increasing the given polymer's resistance to ignition. Ignition is unavoidable, because most substances will flame up if subjected to high enough levels of fire stress – thermal radiation (Sutker, 1988).

A useful and complete description of the mechanisms of general retardant systems is provided in the review articles of Green (1996; 1997). Different flame retardant systems can be identified, all of which function by different mechanisms. Flame retardants interfere with the thermal decomposition pathway of the polymeric material. Different compositions interact differently with different polymers and a flame retardant's use is thus very specific to the particular substrate for which it was designed.

Some flame retardants which form acids during combustion – like the halogens – operate through gas-phase free-radical inhibition. Other groups of retardants produce many non-combustible gases and dilute the amount of fuel or oxygen supplied to the fire. The formation of solid residues on the surface of the burning material is another way of reducing flame spread. Some reduce the rate of heat release during combustion by affecting the heat transfer pathway to the polymer substrate. Another group of flame retardants form a foaming char on the surface of the combusting material. These additives are called intumescent systems. A system can also operate through combinations of the above-mentioned mechanisms (Green, 1996).

The following terms and definitions are used to describe the different mechanisms by which flame retardants operate (Pettigrew, 1993):

- **Inert gas dilution:** Large quantities of inert and *non-combustible* gasses are produced on thermal decomposition of the additive. The concentration of oxygen and combustible species are reduced and the fire dies.

- **Thermal quenching:** The surface temperature of the polymer is reduced or kept low by the *endothermic degradation* of the additive. Due to the lower substrate temperature, less combustible products are produced and the thermal degradation is retarded.

- **Physical dilution:** Large quantities of inorganic fillers (such as glass fibre) are added to the polymer matrix. The amount of *flammable material (polymer) is thus reduced* and the substrate's fire resistance increased.

- **Chemical interaction:** Some flame retardants thermally dissociates into radical species that then *interferes with the gas phase combustion* of the combustibles.

- **Protective char:** On thermal decomposition, the additive forms an *insulating char barrier* on the surface of the polymer. This char reduces heat transfer for to the polymer, diffusion of oxygen to the area of decomposition and diffusion of combustibles to the flame zone, retarding the combustion.

An ideal flame retardant will have the following properties: (Gann, 1993; Green, 1996; Green, 1997; Sutker, 1988; Wolf & Lal Kaul, 1992; Miller, 1995)

- It reduces flammability to the required standard;
- It is thermally stable at the processing temperatures;
- Have long term compatibility with the polymer matrix (i.e. does not "bloom")

- Maintains or improves the mechanical properties of the polymer;
- Represents no health hazard; and
- Is cost effective

The flame retardant must not decompose at temperatures below the processing temperatures of the polymer. Ideally, the flame retardant's decomposition temperature should be several degrees higher than the polymer processing temperature. A list of typical processing temperatures for the most widely used polymers is given in Appendix A.

Large-molecule flame-retardants in the form of polymeric and oligomeric compounds are gaining ground in the industry because they are more resistant to blooming and leach-out and promise greater compatibility with host plastics than traditional flame-retardant additives (Gilman *et al.,* 1997).

2.2.   The history of flame retardants

The need for fireproofing polymers became important in the nineteenth century due to the commercialisation of cellulose nitrate plastics (Green, 1997). These materials are highly flammable and presented a major fire risk.

The early large-volume polymers, including phenolics, melamine resins and rigid polyvinylchloride (PVC), possessed adequate intrinsic flame resistance. Unfortunately, the more recent volume plastics such as polyolefins (e.g. polyethylene, polypropylene), styrenics (e.g. polystyrene, acrylonitrile-butadiene-styrene copolymer (ABS)) and polyesters, are significantly more flammable than wood. Polyolefins have the same basic structure of fuels such as petrol, handy gas and flammable waxes (Sutker, 1988). Clearly, something needed to be done to reduce the fire risk presented by these polymers. This subsequently led to the development of different formulations that increased the fire resistance of polymers.

By the early 1970's, the flame retardant industry already produced $\pm$ 50 000 metric tons per year (Green, 1997). Unsaturated polyesters, PVC and cellulose photographic films, were the mayor groups of fire resistant polymers in use by 1970. Early flame retardant systems were mainly based on aluminium trihydroxide $(Al(OH)_3)$, also referred to as alumina trihydrate $(Al_2O_3.3H_2O)$ or ATH, halogenated compounds and antimony – if the price allowed it (Green, 1997; Gann, 1993). Some phosphate esters were also used.

Since the early 1980's, mixtures of pentaerythritol and melamine were used as intumescent flame retardant systems, together with additives such as phosphates (Green, 1997). Both ATH and halogenated compounds were still dominant. Antinomy was now widely used as synergist with the halogen compounds.

In the early 1990's trends suggested that the market was beginning to move away from halogenated flame retardants (Green, 1997). These compounds work very well in most cases but release poisonous and corrosive gases when decomposing in a fire and these retardants are not readily disposable after use. In especially Europe, the environmentalists are putting more pressure on companies to produce more environmentally friendly products to protect the environment and humans (Miller, 1996). The flame retardant world market for 1990 was estimated to be approximately 500 000 metric tons (Wolf & Lal Kaul, 1992). A breakdown of the market is given in Table 2-1. The dominant inorganic flame retardant was still ATH as it is also the least expensive flame retardant. Current flame retardants are still based on inorganic compounds (such ATH) and halogen containing compounds; but the use of intumescent systems is increasing (Miller, 1996; Nelson, & Wilkie, 2001).

Table 2-1   Estimated flame retardant consumption for 1990

Flame retardant system	Metric tons
Total inorganic	290 000
Brominated organics	80 000
Chlorinated organics	50 000
Organophosphates	60 000
Other	20 000
Total	**500 000**

A newly issued patent of particular interest is a patent for the production of open-celled porous plastics or natural product flame retardants (Blount, 1998). Different types of flame retardants, including intumescent systems with and without the addition of fillers, were used. All were implemented with great success. Another new field of interest is the use of nano-clay composites as flame retardants (Gilman & Kashiwagi, 1997). In these materials the layered nano-clays are dispersed throughout a polymer as exfoliated sheets each of about one nanometre in thickness. Reasonable flame retardancy can be achieved at very low dosages, in the order of 5%.

2.3.   Flame retardants and synergism

As with many other multi-component products, flame retardant systems are regularly produced by simply mixing two or more ingredients together. The efficiency of flame retardants can be greatly influenced by synergy between the formulation components (Weil, 2000). The properties of the final product or system depend on the proportion of the individual components used. Synergy is the phenomenon when a compound formulation (a combination of two or more components) leads to a desirable property that is better than the property obtained with the ratio of the individual compounds. However, such component combinations can unfortunately also lead to undesirable effects. A reduction in the desirable property due to the combination is called antagonism. Figure 2-3 shows possible responses for a two-component system (Cornell, 1981).

Synergy
$(\beta_{12} > 0)$

No interaction
$(\beta_{12} = 0)$

P_2

Desirable property (P)

Antagonism
$(\beta_{12} < 0)$

P_1

$P = \alpha_1 x_1 + \alpha_2 x_2 + x_1 x_2 \beta_{12}$

$\alpha_1, \alpha_2, \beta_{12}$ - constants

x_i - fraction component i

0   1.0

Fraction component 2 (x_2)
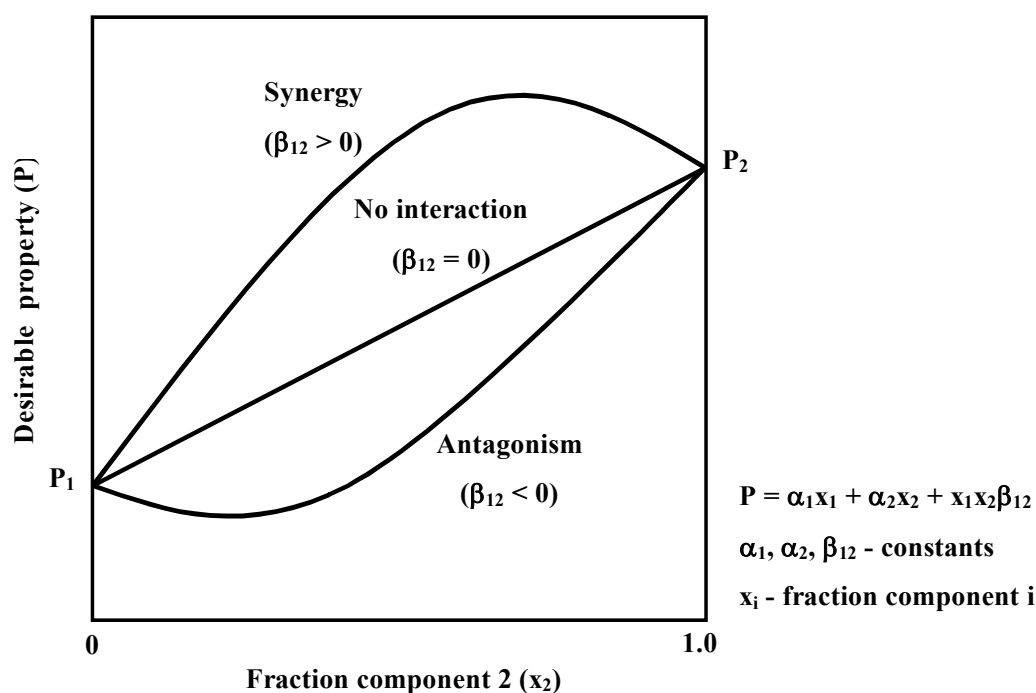
Figure 2-3   The property (P) evaluation of a two component system blend

2.4.   Inorganic flame retardants

Inorganic fillers act as flame retardants due to their endothermic decomposition which withdraws heat from the fire and simultaneously releases inert gasses such as H_2O, CO_2, NH_3, etc. that dilute the oxygen and volatile fuel supplies to the fire (Sobolev & Woycheshin, 1974; Horn, 2000). Furthermore, these inorganic compounds are non-combustible materials and thus physically dilute the amount of combustible polymer in the solid phase. Rothon (1995) discussed several inorganic filler flame retardant systems. Metal oxide residues are

formed during the decomposition of the inorganic systems. These metal oxides may catalyse further oxidation of the condensed phase (afterglow effect).   The latter includes the carbonaceous residues formed during the charring step and the remaining polymer (Delfosse *et al.,* 1989).

In order for inorganic flame retardant fillers to be effective, the following decomposition reactions' characteristics are desirable (Schmidt, 1965; Rhys, 1969; Sobolev & Woycheshin, 1974; Delfosse *et al.,* 1989 and Focke *et al.,* 1997):

- Their degradation onset should be above the polymer's processing temperature.
- Their degradation temperature range should be similar to that of the host polymer.
- Their decomposition rate should be rapid at, or just below, the polymer's decomposition temperature.
- Their reaction enthalpy should be large and positive.
- They should release voluminous quantities of inert gasses.
- They should not promote the formation of smoke.
- Their oxide residues should not promote afterglow.

Unfortunately, in practice very high dosage levels (50% to 60%) of the inorganic fillers are needed in the polymer in order to be effective. This compromises the polymeric material's mechanical properties. For instance, $\pm$ 60% $Mg(OH)_2$ is needed in polyethylene-vinyl-acetate or polyester (PE) for adequate flame retardancy. The flame retarded material should also be processed at temperatures below 220 ºC (Touval, 1993).

In the early 1970's the main inorganic flame retardants used were ATH, zinc borate and antimony compounds (Green, 1997; Gann, 1993). Although antimony was one of the most popular and frequently used compounds in flame retardant systems over the years, it was expensive and thus used sparingly (Gann, 1993).

ATH is the least effective in terms of dosage, but also the least expensive of all flame retardants. It is therefore widely used. Some 66 000 ton of ATH were used during 1990 and 110 000 ton in 1991 (Touval, 1993). ATH provides the best balance of flame retardant properties (endothermic decomposition, volumes inert gas produced, char catalysis and little afterglow) versus cost of the commercially available inorganic filler type flame retardants

(Sobolev & Woycheshin, 1974; Focke *et al.,* 1997). It unfortunately starts to decompose just above 200°C and needs to be used in high dosages. $Mg(OH)_2$ systems are used when higher processing temperatures are needed (Rothon & Hornsby, 1996). Its metal oxide, which is formed on decomposition, is however a stronger char oxidation catalyst than those of ATH and leads to increased afterglow (Delfosse *et al.,* 1989).

For many years now, antimony based inorganic compounds have been used for flame retardants, for example Sb_2O_3, Sb_2O_5 and Na_3SbO_4 (Touval, 1993). In 1990 some 20 000 metric tons of Sb_2O_3 were used in the USA as flame retardants. Unfortunately, antimony based compounds are very expensive. The basic Na_3SbO_4 is ideal for polymers which hydrolyse when processed in the presence of acidic additives. Currently antimony compounds are not used as flame retardant on their own, but are used as synergists with other flame retardants. The addition of antimony compounds to halogen systems can increase their efficiency considerably and thus reduces the total additive loading in the polymer. Antimony trioxide on its own has been reported to be a catalyst for carbon oxidation (Day, 1936). However, more recent studies showed that antimony trioxide has an inhibiting effect on char oxidation (Baillet & Delfosse, 1990) when used with other inorganic fillers. Unfortunately, a chemical explanation for this unexpected effect was not given.

Boron compounds are also widely used as flame retardants (Touval, 1993). Compounds such as borax (sodium borate), zinc borate, barium metaborate ($BaB_2O_4.xH_2O$) and ammonium fluoroborate (NH_4BF) are well known retardant systems. Some 4 500 metric tons of boron flame retardants are used in the USA annually of which zinc borate is used most widely. Boron compounds act in both the condensed and vapour phase as fire suppressants. Most boron complexes are Lewis acids, which promote crosslinking of the polymeric material on thermal degradation and thus minimising decomposition and volatile combustibles. Boron compounds can also react with the hydroxyl group in polymers containing such groups (e.g. cellulose) to form a glassy ester. This ester forms a char coating on the substrate surface and reduces solid-state carbon oxidation by protecting the underlying material. Moreover, it is common knowledge in commercial practice that the addition of zinc borate to metal hydroxide flame retardant systems can help to reduce the afterglow effect.

Molybdenum compounds are also used as flame retardants (Touval, 1993), and it was one of the first elements to be used as flame retardant additives for cellulose (Ramsbottom;

1947). Molybdic oxide, molybdenum trioxide, zinc molybdate and ammonia octamolybdate are used. Molybdenum trioxide acts as a condensed phase retardant by increasing char yields.

Cellulose could be made fire retardant by the addition of tin compounds as well (Ramsbottom; 1947). Since the 1970's tin compounds have been used as synergist with halogen systems (Touval, 1993). Tin is both a vapour and condensed phase flame retardant. Compounds such as zinc hydroxyl stannate ($ZnSn(OH)_6$), zinc stannate ($ZnSnO_3$) and stannic oxide ($SnO_2.xH_2O$) have been used commercially

Clays can be used as flame retardant systems. Experiments showed that the heat release rate – the most important parameter for predicting fire hazard – is reduced by 63% in a nylon-6-clay nanocomposite containing 5% of a modified montmorillonite clay (Gilman & Kashiwagi, 1997). Nanocomposites used are clays. According to Gilman & Kashiwagi, 1997) the clay additive does not degrade the overall material properties and caused no increase in carbon monoxide or soot levels during combustion.

2.5. Halogenated flame retardants

The use of halogen containing flame retardants started to grow in the 1970's. The 1980's saw a large increasing in the use of brominated systems. Currently bromine based flame retardants are the most widely used of the halogen systems. In the early 1990's approximately 150 000 metric tons of halogen based flame retardants were consumed annually world wide, which is more than 25% of the total flame retardant market (Gann 1993, Wolf & Lal Kaul, 1992).

Halogen based flame retardants function in the vapour phase. On heating, they decompose to form halogen radicals. These halogen radicals interfere with the oxidation of the volatile fuels. They react with the oxygen and hydrogen radicals in the gas phase, thereby reducing their concentration and extinguishing the fire (Lyons, 1987; Pettigrew, 1993; Georlette, Simons & Costa, 2000).

Antimony and phosphorous based compounds are very effective synergists with halogen based flame retardants (Touval, 1993; Weil, 1993). These compounds help with the scavenging of free radicals and regeneration of the halogen radicals.

In the 1990's the market started to move away from halogen based flame retardants (Green, 1997). This is because they produce toxic gases (e.g. hydrobromic and hydrochloric acid fumes) and high levels of smoke. These gases are also highly corrosive. The halogen containing retardants are also difficult to dispose of, which implies that they are an environmental risk (Green, 1997; Pettigrew, 1993). The shift to more environmentally friendly flame retardants is of interest world wide but especially in Europe. The majority of current research focuses on non-halogen systems. However, alternative systems are usually less effective and more expensive (Mount, 1992).

2.6.   Phosphorous flame retardants – Non intumescent

Phosphorous containing flame-retardants include phosphate esters and inorganic phosphates (Green, 1996). The mechanism whereby phosphorus flame retardants function varies depending on both the types of phosphorus compound and the specific polymer. Phosphorous-based flame retardants work in both the condensed and vapour phases (with the condensed phase being predominant), and interact according to both physical and chemical mechanisms (Weil, 1993; Weil, 1992a; Green, 2000; Lyons, 1987). Each of these mechanisms will be discussed separately. For example, they appear to function by promoting char formation, dripping of the burning polymer or by gas phase radical scavenging. Studies have however shown that condensed phase mechanisms are significantly more effective than the vapour phase mechanisms (Weil, 1992a).

It is well known that both phosphorous and boron compounds act as inhibitors of carbon oxidation (Rakszawski, 1964; Green, 1997; Weil, 1993). Thus, phosphorous systems prevent this glowing combustion. Although the exact mechanism is unknown, it is believed that it involves the deactivation of the active centres on the carbon (Weil, 1993).

Flame retardants based on phosphorous are widely used as synergists for halogen systems, inorganic compounds and organic systems. Organic flame retardants such as intumescent formulations are dependant on phosphorous compounds (Weil, 1993).

Intumescence will be discussed separately. Unfortunately, phosphorous containing systems are expensive (Green, 1997).

2.6.1.   Condensed phase

Different mechanisms, such as flame inhibition, heat loss due to melt flow and dripping, surface obstructions with char formation, acid-catalysed dehydration and char enhancement, have been identified in polymer systems using phosphorous based flame retardants (Weil, 1992a). It is thus very possible that two or more different mechanisms are involved in a given system.

Phosphates and other phosphoric acid derivatives decompose thermally to form phosphoric acid, which is a good flame retardant due to its own low volatility (Weil, 1993). The phosphoric acid acts as dehydration catalyst in cellulose or in the presence of hydroxyl rich compounds or polymers. Furthermore, it forms polyphosphoric acid when strongly heated. The polyphosphoric acid is an even more effective dehydration catalyst of cellulose than phosphoric acid itself. Char (shielding the material) and water (acting as heat sink and diluting gas) is formed during the dehydration step. The char formed is coated by the phosphoric acid, making it less permeable and protecting the char from solid phase oxidation or afterglow (Weil, 1992a). The addition of nitrogen compounds act as a synergist in retaining phosphorous in the char and thus increasing char yields (Weil, 1993). This is however not a general phenomenon and some nitrogen compounds are antagonistic. The compound used depends on the polymer flame retardant system. Compounds such as melamine, urea and dicyandiamide have been known to work well as synergists.

In some polymers, the phosphorous rich flame retardants cause an initial crosslinking reaction through the polymer (Weil, 1993; Weil, 1992a). This implies that the polymer is prevented from volatilising and thus less combustible species are formed. The phosphorous containing additives can also catalyse the clipping of the polymer chains thereby reducing its molecular weight. This reduces the viscosity of the polymer melt allowing it to drip away from the fire zone. This dripping removes material that can burn from the fire zone.

Red phosphorous is an example of a retardant acting by chemical mechanism (Weil, 1993). The non-oxidative pyrolysis of the polymer (which is a radical scission of the

material) is retarded by the phosphorous. It acts by scavenging the free radicals formed during the thermal degradation of the polymer (similar to halogenated flame retardants but only in the condensed phase) and thus prevents further thermal degradation.

2.6.2.   Vapour phase flame retardants

The branching step, in the flame chemistry of the vapour phase, is rate controlling. In this step the hydrogen radicals react with oxygen to form hydroxyl- and oxygen radicals as indicated below (Weil, 1992a). The hydroxyl- and oxygen radicals react with the fuel and combustion is sustained.

$$H^{\bullet} + O_2 \rightarrow {}^{\bullet}OH + O^{\bullet}$$
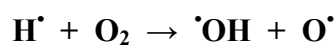
The volatile phosphorous compounds produced during the thermal decomposition of the phosphorous based flame retardants, are effective flame retardants (Weil, 1993). Mass spectroscopy studies have shown that triphenyl phosphate thermally degrades to form small volatile species such as P_2, PO, PO_2 and HPO_2. These volatile phosphorous species interfere and inhibit the branching step in the vapour phase. They extinguish the flame by reducing the hydrogen atom concentration in the vapour phase, (Weil, 1992a). Many phosphorous based flame retardants form water during a fire situation. This water is volatilised forming inert water vapour. The presence of water vapour may help to extinguishing the flame: it dilutes the combustible and starves the fire of O_2 (Weil, 1993; Weil, 1992a).

2.7.   Intumescent flame retardants

In French, the verb *tumere* means *"to swell"*, while *tumescere* in Latin is translated with *"to swell up"* and *tumescent* refers to something *"swollen"*. According to the Webster's dictionary, **intumescence** is *"the process of swelling up"* or *"that which is swollen or bubbled up"* (Taylor, 1966). The process of *"swelling something up"* or *"getting to a swollen state"* or *"that which is swollen up"* is what is referred to with **intumescence** in flame retardant terms. **Intumescent flame retardants** are thus those that reduce flame spread and fire risk through the formation of a swollen, bubbled or foamed up char residue on the material's surface.

Intumescent materials have been in use in coatings, long before their application in plastics (Vandersall, 1970, Bishop, Bottomley and Zobel, 1983). The early formulations were based on ammonium polyphosphate and nitrogen rich compounds. Such intumescent coatings operate by the same mechanism as intumescence in plastics (Brook, 1985; Lyons, 1987). The main function of an intumescent coating is to shield the underlying material from the heat of a fire (O'Rourke, 1974). Several publications on the background, operation, application and new areas of focus in intumescent coatings are available (Bishop *et al.,* 1983; Aslin, 1989; Vandersall, 1970; Brook, 1985; O'Rourke, 1974; Chang, Scriven & Ross, 1975).

For a mixture to be an efficient intumescent system, three elements are needed – see Figure 2-4 (Mount, 1992; Camino *et al.,* 1989):

- An inorganic acid (dehydrating agent)
- A polyhydric material rich in carbon – called a carbonific or char former
- A blowing agent – called a spumific
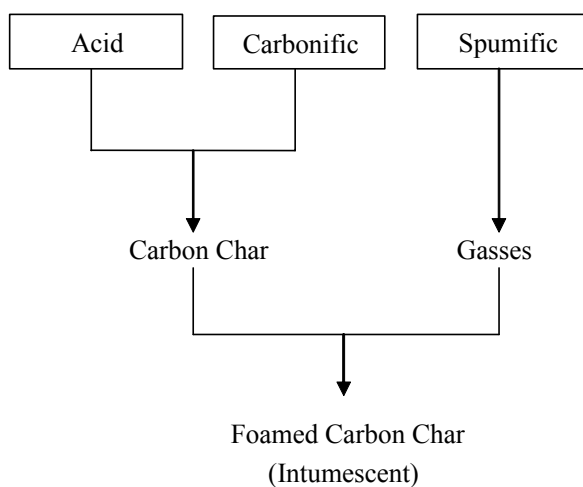
Figure 2-4   Schematic diagram for acid catalysed intumescence

In plastics, intumescent systems are a recent trend. In the early 1980's, mixtures of ammonium polyphosphate, pentaerythritol and melamine were used in some polymers as flame retardants (Green, 1997). These were the first real intumescent systems for polymeric materials. A comprehensive summary of the use of intumescence as flame retardants for polymer are given by Le Bras *et. al.* (1998)

A problem encountered with the early intumescent systems was their water solubility. This leads to the retardant compounds leaching out from the polymer structure during normal use. Other drawbacks of these systems are limitations in their thermal stability, processing difficulties and high cost (Sutker, 1988; Weil, 1993; Gann, 1993).

The fire fighting capabilities of the intumescent flame retardants is due to the swollen or foamed char formed on the surface of the burning material (Camino *et al*., 1989; Camino & Delobel, 2000). The char forms a physical, protective barrier for heat transfer to the surface of the combustible material acting as a "shield" to the polymer from the fire. This lowers the temperature of the surface beneath the char and causes a lag in the surface temperature rise. The char layer furthermore hinders the diffusion of oxygen to the site of combustion (see Figure 2-2). Dripping of the molten plastic is reduced by char formation thereby eliminating a possible source of further propagation. Compounds that promote the formation of char under fire conditions are good flame retardants and can improve current systems (Pearce, 1986). Charring also reduces the amount of the polymer that is converted into volatile fuel. There is a positive correlation between char yield and the flammability of a polymer when the LOI is used as the measure of fire resistance (Van Krevelen, 1975).

The char formation in intumescent systems is often expressed in terms of simple acid catalysed dehydration reaction of hydroxyl compounds as shown in Figure 2-5 (Mount, 1992). The mechanism for carbon-carbon double bond formation is indicated below. The formation of $-CH=CH_2$ fragments leads to carbon rich residues or char. Pentaerythritol and dipentaerythritol are polyalcohols frequently used as carbonifics.

The acid catalyst for the char formation is phosphoric acid derivatives. Phosphoric acid is produced when phosphate containing flame retardants degrade thermally. The phosphoric acid reacts with polyols (polyhydroxyl compounds) to form polyol phosphates. These polyol phosphates can break down to form material rich in carbon-carbon double bonds (char) (Mount, 1992; Weil, 1993). Water is released during the reaction. The mechanism is shown in Figure 2-6.

$$-CH_2-CH_2-OH \ + \ H^+ \ \longrightarrow \ -CH_2-CH_2-OH_2^+ \ \longrightarrow$$

$$-\underset{H}{\overset{H}{C}}H-CH_2^+ \ + \ H_2O \ \longrightarrow \ -CH=CH_2 \ + \ H^+$$
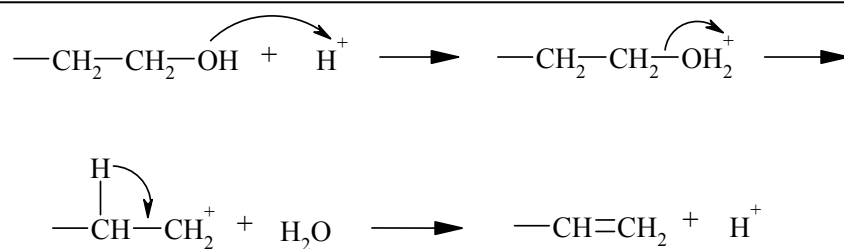
Figure 2-5   Acid catalysed dehydration of a hydroxyl compound
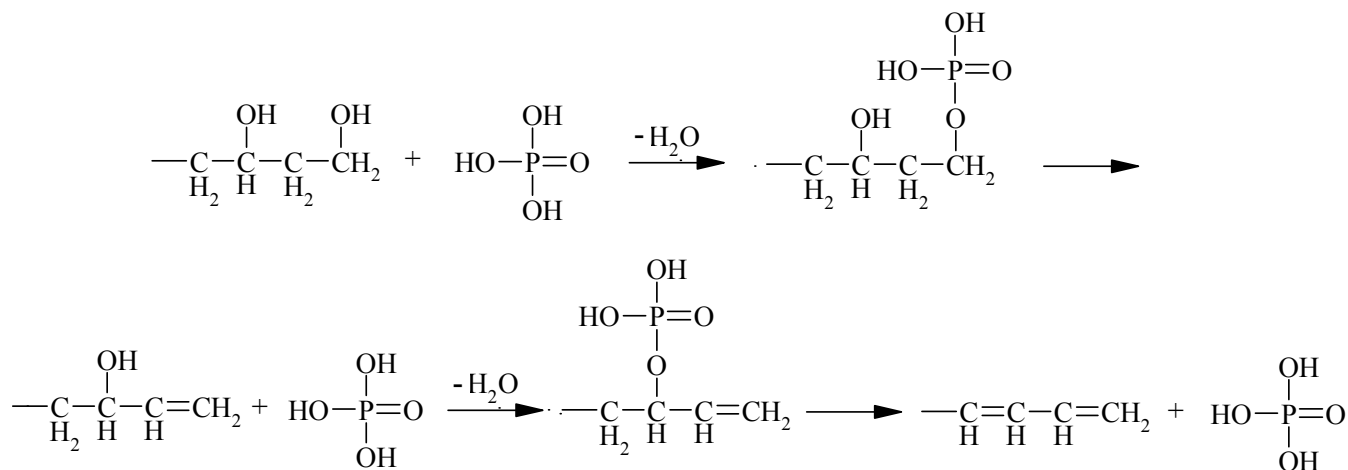
Figure 2-6   The action of the phosphoric acid in char formation mechanism

The water evolved during the reaction also acts as the blowing agent. The blowing agent forms gasses during the degradation reaction that cause the carbon residue to foam, bubble or swell up (intumesce).

Nitrogen rich compounds are nearly always used in intumescent systems. Such compounds improve char yield and intumesces the carbon through the formation of gasses – acting as the spumific. Nitrogen compounds are environmentally friendly; they do not produce corrosive gasses, are easily disposable, produce fewer toxic gasses and less smoke than for example halogen based systems (Zaikov & Lomakin, 1996; Horacek & Grabner, 1996). This holds true for almost all char forming flame retardant systems. Melamine is often used as a compound in an intumescent flame retardant system and melamine-based compounds have shown promise as fire retardants (Horacek & Grabner, 1996; Stern & Horacek, 1994).

Further studies showed that "tailor-made" substances incorporating two or more of the elements needed for an intumescent system are more effective than arbitrary chosen compounds (Camino *et al.*, 1989). Figure 2-7 shows one such a complex; a melamine salt of

a pentaerythritol-phosphoric acid derivative. The ratios in which the different compounds are added to each other are also important.   The optimum ratio should be determined experimentally. One or more of these substances could be replaced with others of the same class or group. These intumescent flame retardants work well in numerous polymers (Weil, 1993; Miller, 1996).
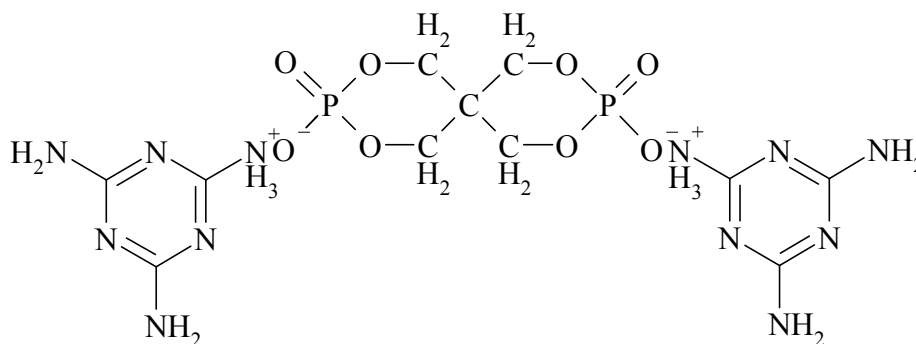
Figure 2-7   **A single intumescent complex containing all three functionalities**

Bertelli *et al.* (1989) studied the effect of adding a range of inorganic fillers to intumescent systems. They found that the fillers did modify the char structure. Chars were harder and less voluminous and less of it formed in the presence of filler. The foamed char volume was reduced and the efficiency of the flame retardant system reduced considerably. Bertelli *et al.* (1989) suggested that reactions between the acid phosphorus moieties and the fillers could explain some of their observations.

The addition of some metal-based fillers may also lead to a catalytic solid state oxidation or afterglow of the formed char (Day, 1936; Baillet & Delfosse, 1990; Delfosse *et al.,* 1989).   However, titanium oxide (TiO_2) can act as synergist with ammonium polyphosphate in polypropylene. Char yield is increased and a stronger more cohesive char is formed (Weil, 1992a).

Potassium bicarbonate in combination with silica and pentaerythritol as intumescent flame retardant composition, showed increased char yield (Gillman *et al.,* 1997; Miller, 1996). Unfortunately, these systems are water-soluble that is unfavourable for outdoor use. It was found that the potassium carbonate could be replaced with potassium bitartrate. It is more effective and less water-soluble. It was also found that the presence of silica gel is not very important (Focke *et al.* 1997, Labuschagné, 1998).

Expandable graphite flakes expand their initial thickness by up to 100 times when exposed to heat (Miller, 1996). This added thickness significantly boosts the fire retardancy of coatings by producing a thicker char layer. Expandable graphite flakes also toughen the char and reduce the formation of cracks that would let the flames penetrate to the substrate.

The addition of zeolite 4A ($Na_{12}((AlO_2)_{12}(SiO_2)_{12}).27H_2O$) to intumescent systems of ammonium polyphosphate (APP) and pentaerythritol (PER) in polypropylene, polyethylene and ethylene copolymers, improved the temperature stability of the char (Bourbigot *et al.,* 1996; Bourbigot *et al.,* 1997). The zeolite helps to form a protective aromatic nitrogen rich top layer. This delays the oxidation of the char and turns the degradation of the material to the formation of a phosphor-carbonaceous structure covered by a "carbonaceous coating".

2.8.   Oxygenated hydrocarbon flame retardants

Recently it was discovered that oxygenated hydrocarbons could be used as flame retardants on their own (Bisschoff, 2000; Bisschoff & Focke, 2001) in polyester fabrics. These compounds are food additives - containing only carbon, hydrogen and oxygen - and are thus environmentally friendly, non-toxic and relatively inexpensive.

Compounds such as pentaerythritol, dipentaerythritol, benzophenone, 2-furoic acid etc. can be used. The main mechanism by which these systems operate is by enhancing the dripping of the polymer melt. Heat is removed from the polymer when molten polymer drips away from the flame zone. The rate of dripping for the treated polyester fabrics were up to 80% faster than the untreated fabrics, resulting in shorter self extinguishing times. These systems showed an optimum dosage level (Bisschoff, 2000; Bisschoff & Focke, 2001).

2.9.   Smoke suppressants

Smoke is a hazard to fire victims. According to statistics, 80% of injuries caused by fires are due to smoke inhalation (Green, 1996). Smoke causes asphyxia or oxygen depravation in victims. It is the mayor cause of death in a fire situation with approximately four out of five of fire deaths attributable to smoke inhalation (Green, 1997).

Commercial smoke suppressants include zinc borate, molybdenum and tin compounds. Molybdenum increases char yield, thus reducing smoke (Touval, 1993). It is known that polymers that unzip to monomers on heating burn cleanly and give very little smoke (Green, 1996; Green 1997). These include polyacrylates, polyformaldehyde and polyacetals. Dense smoke is produced by polymers that decompose and rearrange to form aromatic polymers.

Both $Al(OH)_3$ and $Mg(OH)_2$ act as smoke suppressants in polymeric materials (Cullis & Hirschler, 1981; Green, 1997). The soot precursors formed during a fire by the host polymer is trapped and oxidised by the high surface area oxides generated by the mineral decomposition of the metal hydroxides (Hornsby, 1986). Antimony oxide often is used to impart flame resistance to flexible PVC wire and cable compounds, but usually at the cost of increased smoke. Experiments showed that mixtures of alumina trihydrate used alone or in combination with zinc borate, could replace most of the antimony oxide and reduce smoke.

2.10. Metals in flame retardants

From the previous sections, it is clear that metal compounds play an important role in flame retardant systems. In most formulations they are however not the functional compound but only part thereof (e.g. ATH). Of importance to this study are those metals that influence the char yield, char properties and smoke generation in intumescent systems.

It is a well known fact that some metals increase the char yield in specific polymers on their own and/or when used as synergists in other systems (Tang & Neill, 1964; Ramsbottom, 1947; Touval, 1993; Sutker, 1988; Wolf & Lal Kaul, 1992; Gilman *et al.*, 1997; Zaikov & Lomakin, 1996; Levchik *et al.,* 1996; Wilkie, 1999; Bourbigot *et al.,* 1996; Bourbigot *et al.,* 1997; Ebdon *et al.,* 1998). Unfortunately, most metals and their oxides catalyse the solid-state carbon oxidation, increasing afterglow (Oshima & Fukuda, 1935; Day, 1936; Weil, 1993; Rakstaski, 1964; Delfosse *et al.,* 1989). The carbon oxidation catalyst efficiency decreases in the order (Rakstaski, 1964):

alkali metals > alkali earth metals > group IIIA - IVA elements

2.11. Fire testing

Over the years, hundreds of different tests to evaluate the reaction of plastics to fire and test flame retarded plastic materials have been developed in various countries. Almost all literature dealing with flame retardancy for plastics, also elaborates on fire testing methods (Babrauskas, 2000; Furches, 1993; Gann, 1993; Innes & Cox, 1997; Paul, 1999; Shields & Silcock, 1987; Sutker, 1988; Troitzsch, 1990; Van Krevelen, 1990). Most of these tests consider plastic fire behaviour in terms of the following factors:

- Ease of degradation or decomposition
- Ease of ignition
- Rate of combustion
- Heat of combustion and the rate of heat release
- Ease of extinction
- Smoke evolution
- Toxic gas generation
- Corrosivity of generated fumes

The three most widely used fire tests to characterise the flame retardancy of a material is the Cone Calorimeter test, UL94 Small Flame Standard test and the Limiting Oxidation Index (LOI) test.

A material's resistance to ignition can be quantified by measuring the LOI (also referred to as the oxygen index) of the material. The LOI is the lowest oxygen gas concentration that still sustains combustion of the sample. It is an indication of the ease with which a material will burn. The lower the LOI value, the easier the polymer burns. The effectiveness of a flame retardant could thus also be determined with the LOI. By measuring the LOI of a flame retarded polymer and comparing it with that of the host polymer only, the efficiency of the flame retardant can be evaluated. A higher LOI value for the treated material indicates that the sample burns less easily and that the retardant increased the polymer's resistance to ignition (Van Krevelen, 1990; Weil, 1992b; Lyons, 1987). A list of LOI's for the most widely used commercial polymers is given in Appendix B.

Underwriters Laboratory Inc. developed a small flame test for the fire testing of polymeric materials in 1970. The UL 94 test is divided into four test configurations, namely:

- UL 94HB – Horizontal Burning test
- UL 94V – Vertical Burning test (50 W)
- UL 94-5V – Vertical Burning test (500 W)
- UL 94VTM – Vertical Burning test for thin materials

The UL 94V test is currently the most common procedure specified and used commercially. In this test, the same specimen is exposed to two successive 50 W methane gas flame applications. The material is classified into three categories depending on the performance with respect to the individual duration of burning for each specimen, the total duration of burning for all specimens and the presence or absence of burning drips. Generally, burning and dripping can remove both the flame and the heat from a sample but are likely to ignite the cotton. The specimen (127 mm by 127 mm with a thickness of 1.6 mm or 3.2 mm) is mounted vertically so that the lower end is located 305 mm above a 6 mm thick surgical cotton layer. The specimens are ignited from below for 10 s with a defined gas flame. If the specimen extinguishes after removing the ignition source, it is ignited once more for 10 seconds. Based on these test results, materials are classified as follows:

- *Class 94 V-0:* In a series of 5 specimens with 10 ignitions, the sum of the afterflame times should not exceed 50 s and no specimen should burn for longer than 10 s. During ignition and combustion the cotton layer should not be set on fire by dripping material.
- *Class 94 V-1:* In a series of 5 specimens, which are ignited twice, the sum of afterflame times should not exceed 250 s, no specimen should burn longer than 30 s and the dripping material should not ignite the cotton layer.
- *Class 94 V-2:* Similar to V-1 except that the cotton layer is ignited by burning drops.

The Cone Calorimeter test is probably the most widely used test method in use today to calculate the rate of heat released by a burning material. Ignitability polymer formulations can also be tested in the calorimeter. It is the bench-scale test method used most commonly for the majority of polymer fire testing and was developed in 1982 by Babraukas at the National Institute of Standards and Technology (NIST). A 100 mm by 100 mm sample (up to 50 mm thick) is placed horizontally in the apparatus and exposed to a radiant heat flux of

10 kW/m^2 to 100 kW/m^2 with a spark ignition system. The effluent is monitored and temperature, gas flow rate and oxygen concentration measured. The amount of smoke produced along with carbon dioxide and carbon monoxide concentrations can be determined with some instruments. Flame retarded coatings can also be evaluated with the cone calorimeter.

Flame retarded coatings are commonly tested under fire tests developed for materials used in the construction of buildings. Examples of such tests are the American Society for Testing and Materials (ASTM) E 84 and E 119 tests. The Steiner Tunnel is the basis for the ASTM E 84 test. It is possibly the oldest fire test for flame retarded materials in use in North America and is used to test the surface burning characteristics of building materials. The test was developed by Albert J. Steiner of Underwriters Laboratory Inc. and Simon Ingberg and was first described in 1943. A 0.514 m wide and 7.32 m long sample is placed in the ceiling of a 7.62 m (25 ft) long tunnel with a 88 kW burner at the one side of the tunnel and an air draft forced through the tunnel at a velocity of 1.22 m/s. The flame spread is recorded as a function of time. The tunnel is also fitted with a photometer to determine smoke. The test results for some plastics are however questionable. Due to its size, large samples were needed for testing. From the 25 ft Steiner tunnel test several smaller tunnel tests were developed e.g. the 18 ft, 8 ft and 2 ft tunnel tests (Bishop *et al*, 1983).

3.   Experimental

3.1.   Planning

Studies showed that tailor-made substances incorporating two or more of the elements needed for intumescence in a single compound are more effective than mixtures of individual compounds (Camino *et al.,* 1989). This is attributed to diffusion effects. In a single complex, the diffusion pathway of the carbonific and spumific to and from the intumescent catalyst (phosphate derivative) is shorter than in a mixture of compounds. Recent studies showed that organometallic compounds could be intumescent, char forming substrates (Labuschagné, 1998). Potassium bitartrate and mixtures thereof with pentaerythritol showed considerable intumescence (Focke *et al.,* 2000). The metal is believed to be the catalyst for the dehydration of a polyol to form an intumescent char.

In this study, a number of organometallic complexes were prepared and investigated for their intumescent action. The char yield calculated for all the samples during the tests only refers to carbon char and excludes the ash. The amount of ash in the char was calculated as the stable metal compound (e.g. metal oxide or carbonate) at the selected pyrolysis temperature for all the samples tested. The effects of both the metal cation and the organic portion of the molecular complex on performance were studied. The best performing intumescent complex was selected. Its thermal decomposition and foaming properties were characterised. Attempts were made at elucidating the mechanism of intumescence. The residues formed at high temperatures were found to be fine metal oxide and carbonate powders. Thus the thermal decomposition of these metal complexes also provides a potential preparation method for nano-sized oxide and carbonate particles. This was also investigated.

3.1.1.   The effect of the organic part of the organometallic complex

Different organic acids were used to study the effect of the organic part of the organometallic complex on char formation and intumescence. Sodium was chosen as the metal cation. It was selected because of the availability of commercial sodium salts and the ease with which its organometallic compounds could be prepared by simple neutralisation of an organic acid with sodium carbonate in aqueous solution.

Important factors that were expected to affect intumescence and pyrolysis of the organic part include:

- Number of carbon atoms in the back bone
- Number of carboxylic acid groups
- Number of hydroxyl groups
- The presence of aromatic groups
- Other elements in the acid molecule (e.g. phosphorous, nitrogen and boron)

Carboxylic acids of different chain lengths were chosen to determine the effect of the number of carbons on intumescence. Other effects considered were aromaticity, the presence of other atoms such as nitrogen in the complex and the number of carboxylic acid and hydroxyl groups. The addition of aromatic material in intumescent systems is known to increase the char yield (Lyons, 1987). The addition of nitrogen rich compounds also tends to increase char yield and intumescence (Horacek & Grabner, 1996). The hydroxyl groups act as spumifics due to the formation of water vapour (Weil, 1993). Both phosphorous and boron are known to reduce solid-state carbon oxidation and afterglow (Rakszawski, 1964; Touval, 1993; Weil, 1993; Gann, 1993; Green, 1996; Green, 1997; Focke *et al.,* 1997). The structures of the sodium compounds and the acids used are listed in Appendix C.

Intumescence of the compounds was evaluated using open flame tests and also by pyrolysing samples, placed in a glass tube, in a furnace.

3.1.2.   The effect of the metal cation of the organometallic complex

The effect of the metal cation on the intumescent behaviour and char formation was studied. Metals, representative of the main groups in the periodic table, were chosen:

- Alkali metals – sodium [Na]
- Alkali earth metals – magnesium [Mg] and calcium [Ca]
- Main group metals – aluminium [Al] and antimony [Sb]
- Transition metals – titanium [Ti], vanadium [V], zirconium [Zr], zinc [Zn], iron [Fe] and copper [Cu]

Potassium is known to improve char formation in cellulose (Tang & Neill, 1964) and in polyamide 6 (nylon 6) when used as synergist with silica compounds (Gilman *et al.*, 1997).

Potassium bitartrate also showed intumescence and char formation on its own (Focke *et al.,* 1997; Labuschagné, 1998). Potassium nitrate can also be used as a flame retardant in nylon 6 as it improves charring of the polyamide (Levchik *et al.,* 1996). Char yield and flame retardancy can be improved in poly(vinyl alcohol) (PVA) by the addition of potassium permanganate ($KMnO_4$) (Zaikov & Lomakin, 1996). It has also been found poly(sodium styrene sulphonate) is a flame retardant providing intumescent char formation (Wilkie, 1999).

Like $KMnO_4$, Cu^{2+} copper complexes can act in the same way in improving char performance (Zaikov & Lomakin, 1996). Copper is also added to current halogen flame retardants as a smoke suppressant (Green, 1996). This is most likely due to the condensed phase reactions such as charring caused by the copper.

Ebdon *et al.* (1998) found that vanadyl acetylacetonate ($VO(CH_3COCHOCH_3)_2$) and $VOCl_2$ increased the LOI of styrene/4-vinyl pyridine- and methylmethacrylate/4-vinyl pyridine copolymers by forming an intumescent char on the surface. The addition of Zn and Ni had little or no effect on char formation.

Antimony trioxide is one of the most widely used flame retardants (Ramsbottom; 1947; Green, 1997; Gann, 1993; Touval, 1993; Weil, 1993; Miller, 1996). It is not known for intumescence, or used as synergist in intumescent formulations, but was chosen to see if it would have any effect on foaming and afterglow.

Other very popular flame retardants are metal hydroxides such as aluminium trihydrate (ATH) and magnesium hydroxide (Rothon & Hornsby, 1996; Green, 1996; Green, 1997; Miller, 1996; Focke *et al.,* 1997; Brown, 1999). Magnesium oxide and magnesium carbonate ($Mg_2(CO_3)_3(OH_2)$) are also used (Sutker, 1988; Wolf & Lal Kaul, 1992; Gann, 1993; Touval, 1993; Green, 1996; Focke *et al.,* 1997; Reyes *et al.,* 1999). In some instances, calcium compounds such as calcium carbonate and calcium hydroxide, calcium sulphate and calcium oxide are also used (Sutker, 1988; Wolf & Lal Kaul, 1992; Gann, 1993; Touval, 1993; Focke *et al.,* 1997). None of these are used in intumescent systems but were included in the study as to identify their influence on charring and carbon oxidation.

Zinc compounds were also used. They mainly act as a source of boron (zinc borate), which helps with smoke suppression and to stabilise carbon chars (Sutker, 1988; Wolf & Lal

Kaul, 1992; Gann, 1993; Touval, 1993; Green, 1996; Green, 1997; Focke *et al.,* 1997; Shen & Ferm, 1999) or as a source of phosphate (ZnPO$_4$) - the catalyst for intumescence (Kuma *et al.,* 1999). In both cases, the effect of the zinc on carbon formation is not investigated or mentioned. The metal may play a part in carbon yield and this was investigated.

Zirconium, titanium and iron were included, because they are used in pigments and because, along with copper, they were expected to represent a "worse case scenario". Because they have more than one oxidation state, it was expected that they would have high catalytic activity with respect to char oxidation. It was expected that they would be unlikely to form stable intumescent chars.

To isolate the specific effects of the metals on intumescence, carbon char yield and thermal degradation, a common organic compound (back bone) had to be used. Acetylacetone, i.e. 2,4-pentanedione was selected for this purpose. It forms very stable complexes with most of the metals listed.

The chemical properties of acetylactone are determined by the keto-enol tautomerism shown in Figure 3-1. It exists in all states of aggregation (Siegel & Eggersdorfer, 1988). The more stable resonance structures a compound have, the higher its stability. At moderate temperatures, it is generally accepted that the enol form predominates in the gas and liquid phases (Lowrey *et al.,* 1971). A description of the structure of 2,4-pentadione in the enol form is given by Gordon & Koob (1973).
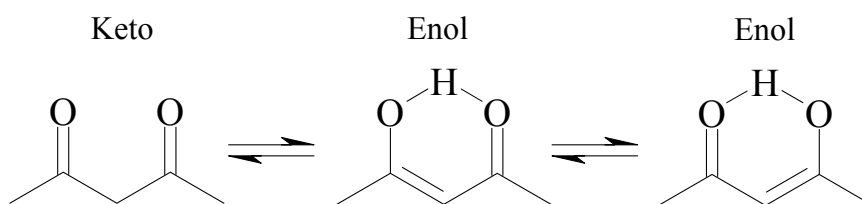
Figure 3-1   2,4-Pentanedione (acetylacetone) and its stable isomers

Acetylacetone is renowned for forming stable metal acetylacetonate complexes (Houben-Weyl, 1988). The metal reacts with the acetylacetonate in the enol form to form bonds between the two oxygen atoms and the metal ion. The inner complexes formed between the metal ions and the β-diketones are unusual since they possess properties usually associated with pure compounds, and not organometallic complexes (Berg & Truemper,

　
1960). A number of metal acetylacetonates were purchased from the chemical suppliers, Sigma-Aldrich and Merck. The following are schematically listed in Appendix D:

- Aluminium acetylacetonate $[Al(C_5H_7O_2)_3]$
- Calcium acetylacetonate hydrate $[Ca(C_5H_7O_2)_2.xH_2O]$
- Copper (II) acetylacetonate $[Cu(C_5H_7O_2)_2]$
- Iron (III) acetylacetonate $[Fe(C_5H_7O_2)_3]$
- Magnesium acetylacetonate dihydrate $[Mg(C_5H_7O_2).2H_2O]$
- Sodium acetylacetonate monohydrate $[Na(C_5H_7O_2).H_2O]$
- Titanium oxide acetylacetonate $[TiO(C_5H_7O_2)_2]$
- Vanadium oxide acetylacetonate $[VO(C_5H_7O_2)]$
- Zirconium (IV) acetylacetonate $[Zr(C_5H_7O_2)_4]$

The volatile character of acetylacetonates is well known in the literature (Berg & Truemper, 1960). Reactions such as oxidation, isomerisation, hydrogenation, dehydrogenation, esterification and transesterification can be catalysed by metal acetylacetonates (Merkblatt Wacker-Chemie, 1988).

It was also decided to consider some metal complexes of gluconic acid. This was done because, in the first set of experiments with the different sodium salts of the organic acids, sodium gluconate showed appreciable intumescence, high carbon char yield and good char properties. Ammonium was also used as a cation with this acid in order to be clear on the influence of the metals on intumescence and char properties. Gluconic acid is a good chelating agent for most metals (Sawyer, 1964). The following gluconic acid metal salts were studied:

- Aluminium [Al]
- Antimony [Sb]
- Calcium [Ca]
- Copper [Cu]
- Iron [Fe]
- Magnesium [Mg]
- Sodium [Na]
- Zinc [Zn]
- Zirconium [Zr]

The calcium gluconate monohydrate, magnesium gluconate hydrate, iron (II) gluconate hydrate and copper (II) gluconate were commercial products from Merck and used as is. The other salts were synthesised in the laboratory and used for further work. The pyrolysis properties of the other ammonium and metal gluconates were then compared with that of the sodium gluconate.

D-Gluconic acid is a sugar derivative. It is produced by the oxidation of D-glucose. A summary of the commercial preparation of gluconic acid and calcium gluconate (Green, 1980; Theander, 1980; Hustede, Haberstroh, & Schinzig, 1988) is given in Appendix E. The structures of D-glucose and D-gluconic acid are shown in Figure 3-2. Glucose is also referred to as dextrose.

Metal salts of gluconic acid are environmentally friendly. Gluconic acid and its derivatives are commonly used in the food and beverage industries (as additives and synergists to other additives) and the pharmaceutical industries (Hustede *et al.,* 1988; Lück & Von Rymon Lipinski, 1988). A number of the salts of gluconic acid are important pharmaceutical chemicals (Theander, 1980). Appendix F contains a picture of the label of a multivitamin supplement. The metals complexes (several gluconates) included in the tables are shown.
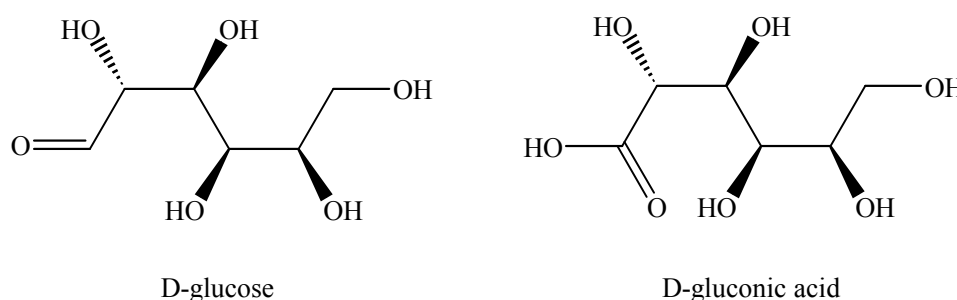
Figure 3-2   **The structures of D-glucose and D-gluconic acid**

The efficiency of each of the metals in the organometallic complexes (both acetylacetonates and gluconates) was quantified through thermal analysis, open flame tests and furnace pyrolysis in glass tubes. The metal acetylacetonates were also mixed with pentaerythritol. In current intumescent compositions, pentaerythritol acts as carbonific (Weil, 1993; Green, 1997; Bourbigot *et al.,* 1996; Bourbigot *et al.,* 1997; Gillman *et al.,* 1997; Miller, 1996). It was expected to act similarly and char in the presence of the

acetylacetonates. Aluminium acetylacetonate was mixed with tartaric acid and fumaric acid as these compounds are also expected to promote intumescence. Studies showed that mixtures containing potassium bitartrate and fumaric acid showed improved intumescence (Focke *et al.,* 1997; Labuschagné, 1998). From the experimental data, the influence of all the metals on carbon char yield and properties, intumescence and char oxidation (afterglow) were evaluated.

3.1.3. The intumescence of calcium gluconate monohydrate and ammonium gluconate hydrate

From all the experiments carried out on the above-mentioned complexes, calcium gluconate monohydrate proved to be the best. It showed excellent intumescence, very good carbon char yield and good char stability. Ammonium gluconate showed adequate foaming but no afterglow and a strong, hard, glassy char. All further studies focused on these compounds. The structures of the calcium and ammonium gluconate salts are shown in Figure 3-3 and Figure 3-4 respectively.
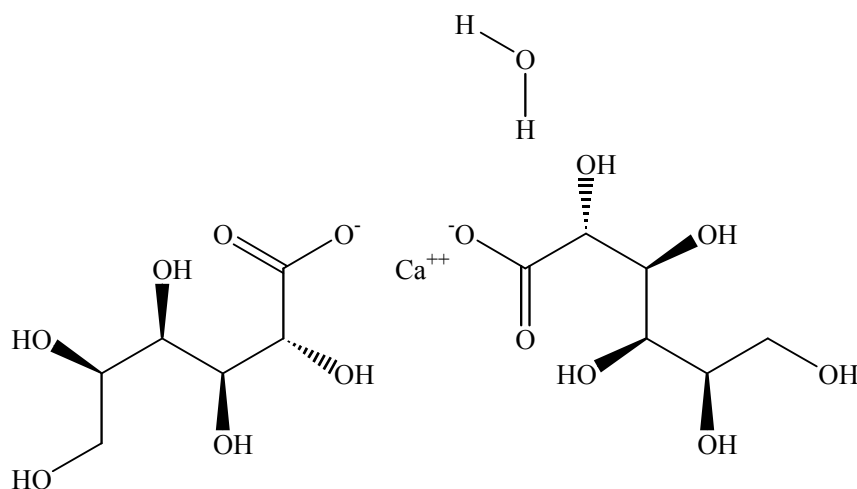
Figure 3-3   The structure of calcium D-gluconate monohydrate
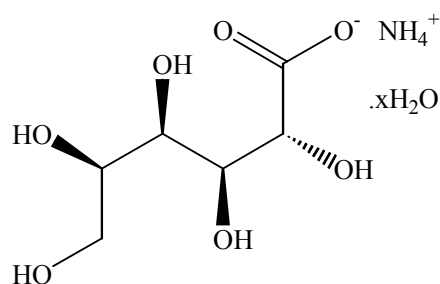
Figure 3-4   The structure of ammonium D-gluconate hydrate

Calcium gluconate has several other commercial and pharmaceutical uses. For instance, it is used as a corrosion inhibitor for mild steel in low concentration chloride solutions (Rajendran, Apparao & Palaniswamy, 1998). Hydrofluoric acid burns are treated with a water based gel containing 2.5% to 5% calcium gluconate (Smith; 1994; Sheridan *et al.,* 1995; Kono *et al.,* 2000). In the field of medicine, regular mention is made to calcium gluconate and its uses (Theander, 1980; Weinstein, 1996; Kaneko *et al.,* 1998; Moser, Smythe & Tisdale, 2000). Calcium gluconate monohydrate has a low water solubility. Only 3.0 g gluconate dissolves in 100 mℓ water at 20°C.

Several inorganic fillers were added to the calcium gluconate monohydrate to study the influence these compounds may have on the intumescence and char yield of the gluconate and the thermal stability of the chars. Expandable graphite flakes were also added to the calcium gluconate to determine its influence on intumescence and char properties. The fillers used with the gluconate were:

- Amorphous silica flakes obtained from acid leached mica
- Attapulgite
- Bentonite
- Fillersite
- Filter dried silica
- Flogopite
- Mica, 325 mesh
- Mica, 60 mesh
- Talc

In order to understand and describe the thermal degradation of the complexes, further thermal studies were carried out. Thermal analysis was done on both the gluconates. Temperature scans up to 1000°C in both air and inert (nitrogen or argon) atmospheres were done. The composition of the solid pyrolysis products as a function of temperature was determined using X-ray diffraction, infra-red and Raman spectroscopy. The foam structure and other intumescent properties of the compounds as a function of pyrolysis temperature were studied and characterised using electron microscopy. The electric conductivity of the foams produced by both the ammonium and calcium gluconates in an inert atmosphere was measured. Pyrolysis gas chromatography – mass spectrometry analysis of the calcium

gluconate monohydrate and similar calcium compounds were done to identify the gaseous pyrolysis products. The density of the intumescent foam from the heated calcium gluconate monohydrate as a function of pyrolysis temperature and time was measured. The thermal conductivity of the foam produced at the optimum foaming temperature was determined. Mass spectrometry studies were done on the foams produced at different temperatures in both air and inert atmospheres to try to determine the molecular mass of the carbon residues.

Two commercial intumescent formulations were used for comparison with the foaming and char character of the calcium gluconate monohydrate. These were, Hostaflam AP750 from Clariant GmbH (referred to as AP750), and Xyro-flam PEN (referred to as PEN) from Xyris Technology.

Water-based polyvinyl acetate emulsions (paint resins) were used with the calcium gluconate monohydrate and mixtures thereof with fillers and/or expandable graphite for an intumescent coating formulation. The resins used were, MC 56 resin from Makeen Polymers and ATEBIN ES/BA resin from Boehme Africa. Similar coatings were also prepared from the commercial intumescent systems and the resins. The flame retardant and thermal insulation properties of the paint were studied and compared to the commercial compositions on wood and aluminium. The corrugations of double-layered cardboard were filled with calcium gluconate monohydrate and mixtures thereof with fillers and/or expandable graphite and the commercial products and tested.

In order to determine the mechanism of intumescence for the calcium gluconate monohydrate, a comprehensive understanding of the compound's crystal orientation and structure is needed. Attempts were made to grow single crystals of the calcium gluconate monohydrate in order to obtain full crystallographic data for the compound.

3.1.4.   The foaming properties of metal glucose (dextrose) derivatives

As mentioned before, gluconic acid is prepared from glucose by the oxidation of the sugar. Since the late 1830's it has been known that acidic sugar derivatives are formed by the treatment of sugars with alkali solutions (Sowden, 1957; Pigman & Anet, 1972). Glucose degrades in the presence of limewater at ambient temperatures to form a number of acidic

compounds (Sowden, 1957; Pigman, 1957; Pigman & Anet, 1972). These compounds are commonly referred to as saccharinic acids.

Extensive research has been done to identify the acids formed during the alkali degradation of sugars (Kenner & Richards, 1954; Sowden, 1957; Pigman, 1957; Marchell & Richards, 1960; O'Meara & Richards, 1960; Isbell & Pigman, 1969; Pigman & Anet, 1972). The reaction mechanism is not yet fully understood. Several three, four, five and six carbon saccharinic acids have been identified in the product spectrum, including a large number of isomers. The structures of a number of common six carbon saccharinic acid isomers are schematically shown in Figure 3-5 (Sowden, 1957; Pigman & Anet, 1972). These acids are similar in structure to gluconic acid with one less hydroxyl group and one additional carboxylic acid group.
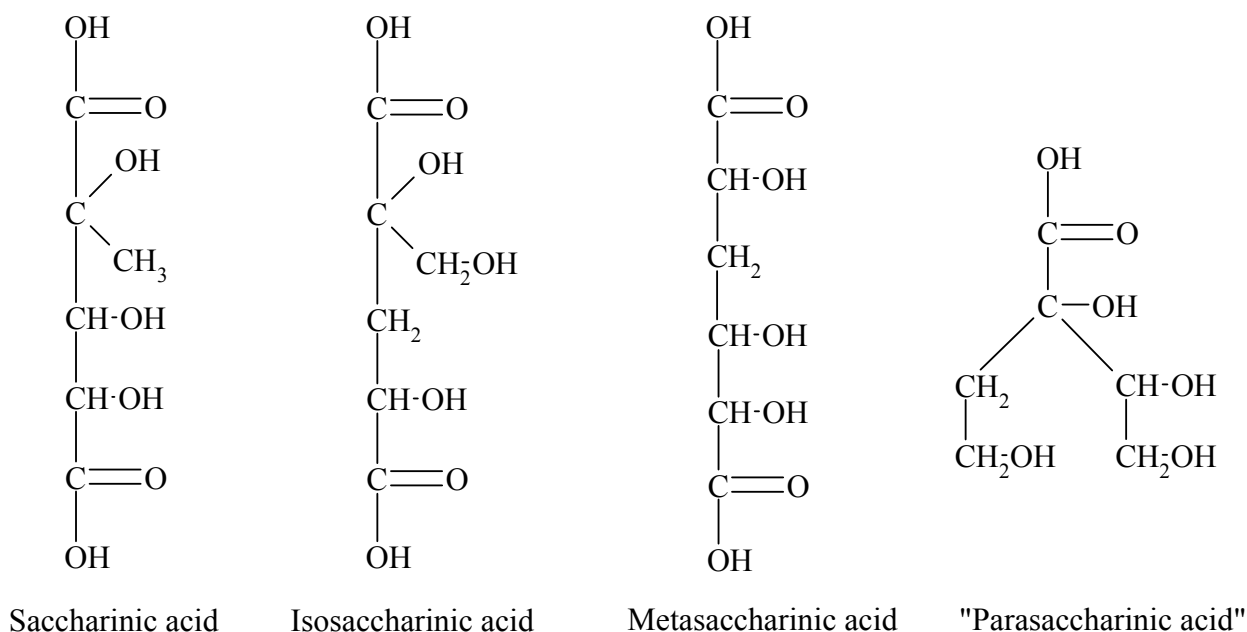
Figure 3-5   Schematic representation of saccharinic acids

A solution of dextrose monohydrate was reacted with $Ca(OH)_2$ to form calcium salts of the saccharic acids. The acids act as chelating agent for the calcium. These calcium complexes are highly soluble in water. It is believed that the high water solubility is due to the variety of compounds in the solution, hindering the crystallisation or precipitation of the different salts. For convenience, the resultant solution is referred to as CaDex.

Other metal complexes were prepared by the addition of a metal sulphate solution to the CaDex solution. The resultant calcium sulphate precipitate was removed by filtration leaving a MetDex solution. The sulphates used were:

- Copper sulphate [$Cu(SO_4).5H_2O$]
- Iron sulphate [$Fe_2(SO_4)_3.7H_2O$]
- Iron ammonium sulphate [$Fe(SO_4)_2.(NH_4)_2.6H_2O$]
- Aluminium ammonium sulphate [$(NH_4) Al(SO_4)_2.12H_2O$]
- Zinc sulphate [$Zn(SO_4).7H_2O$]
- Zirconium sulphate [$Zr(SO_4)_2.4H_2O$]

The solids in the MetDex solutions are similar in structure to the gluconates and may operate similarly. The major differences are their high water solubility, ease of preparation and relative low cost. It was evident from the thermal decomposition of most of the gluconates that a high percentage of carbon is retained during pyrolysis in the form of voluminous foam. The pyrolysis properties of these MetDex solutions were investigated.

3.1.5.   The formation of fine metal carbonates and oxides

In industry, burnt lime (CaO) is often used as a desulphurisation sorbent (Sasaoka, Sada, & Uddin, 1998; Nimmo *et al.,* 1999). The CaO scrubs H_2S and SO_2 from air. Recently the preparation of a macroporous CaO from lime was investigated (Sasaoka, Sada, & Uddin, 1998). The CaO is prepared by first swelling lime with acetic acid vapours followed by calcination of the swelled material. The reactivity of the resultant macro porous CaO is higher than the calcinated raw lime and SO_2 removal is greatly improved. Spray calcinated calcium acetate has also proven effective in the desulphurisation of flue gasses (Nimmo *et al.,* 1999).

Several metal oxides and carbonates are frequently used in the paints and coatings industry as extenders (Roelle, 1991). These include $CaCO_3$, $MgCO_3$, MgO and Al_2O_3. For an extender to be effective, several properties are of importance. Two of the most important are particle size distribution and specific surface area. For a $CaCO_3$ extender typical values are listed in Table 3-1. The typical particle size distribution of a commercial fine $CaCO_3$ powder is 2 μm to 5 μm.

Table 3-1   Typical properties for CaCO₃ paint extenders

Material	Natural	Synthetic
Particle size distribution	0.5-100 μm	0.2-0.8 μm
Specific surface area	0.5-3 m²/g	7-10 m²/g

It is believed that microporous or fine powder carbonates and oxides can be prepared from the pyrolysis of both the MetDex and gluconates. The intumescence of these compounds leads to the formation of small particles and/or very porous high temperature decomposition products. The powders produced from the high temperature decomposition of the gluconates and MetDex solutions were characterised. Particle size and porosity are of great importance. The surface areas of these powders were determined and SEM analysis done on the samples.

3.2.   Apparatus

3.2.1.   Laboratory furnace

All pyrolysis experiments were carried out in a Nabertherm L9 laboratory furnace with a Logotherm S17 programmable controller. The controller is programmable in 1°C increments. Maximum operation temperature if the furnace is 1100°C. The furnaces' chamber dimensions were:

- height – 175 mm
- width – 255 mm
- depth – 285 mm

3.2.2.   Pyrolysis glass tubes

Glass tubes 100 mm long with an inner diameter of 7 mm and wall thickness of 1 mm were used to evaluate sample foaming (intumescence) in air. Figure 3-6 shows a glass tube next to a R1 coin. An aluminium block with several holes of 10 mm diameter and 25 mm deep was used to hold the glass tubes in the furnace.

A glass tube in the aluminium block is also shown in Figure 3-6 placed on the door of the laboratory furnace. The block was placed in the furnace and preheated to the desired temperature.
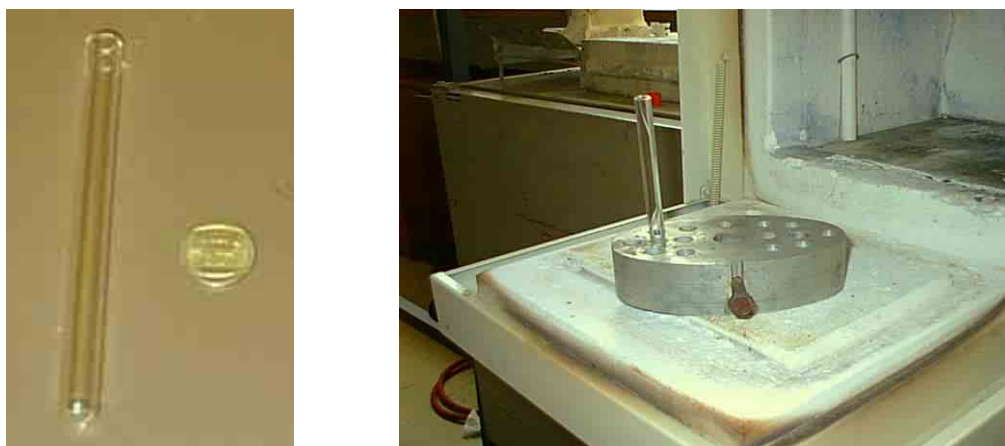
Figure 3-6   Glass tube for the pyrolysis of the samples and a tube in the aluminium block on the furnace door

3.2.3.   Open flame tests

For the open flame tests, a handy gas or liquefied petroleum gas (LPG) cylinder with a standard round nozzle was used. LPG is predominantly a mixture of liquefied propane and butane gasses. The samples were placed on an asbestos plate and exposed to the open flame.

3.2.4.   Inert atmosphere pyrolysis chamber and silica tube

A special glass chamber to be used with the laboratory furnace was custom made for the pyrolysis of the samples in the inert atmosphere. The inert gas pyrolysis of the samples at temperatures of up to 600°C was done in this chamber in the laboratory furnace. A nitrogen gas cylinder was linked to the chamber. The pyrolysis chamber could be placed in the furnace, preheated and the samples then inserted into the chamber at the desired temperature. Pictures of the chamber and accessories are shown in Figure 3-7.

Figure 3-7   Glass chamber used for the pyrolysis in an inert atmosphere

For the inert atmosphere pyrolysis above 600°C, a silica tube with 20 mm inside diameter and 2 mm wall thickness was used (seeing that most glasses melt at approximately 650°C). The one end of the tube was reduced to a 5 mm hole. A nitrogen cylinder was linked to the other end of the tube. The tube was preheated in the furnace. Samples were placed into the preheated tube on silica stubs.

3.2.5.   Thermal analysis

A Netsch STA 409 simultaneous TGA/DSC instrument and a Mettler Toledo TGA/SDTA 851^e high temperature, large-furnace instrument were used for the thermal analysis of the samples. Between 5 and 25 mg of each of the samples were placed in the crucibles. For all scans of up to 650°C, aluminium crucibles were used. The scans of above 650°C were done with platinum crucibles. All the runs were done in either air or inert (nitrogen or argon) and at a scan rate of 10°C/min unless stated otherwise.

3.2.6.   X-ray diffraction analysis

X-ray diffraction (XRD) was used to identify the decomposition products formed during pyrolysis and other materials used. The sample was ground with an agate mortar and pestle and the loose powder was pressed into a diffractometer sample holder. The XRD analysis was performed on a Siemens D-501 automated diffractometer. Instrumental conditions are summarised in Table 3-2.

Table 3-2   XRD instrument and data collection parameters

Instrument	Siemens D-501
Radiation	Cu $K\alpha$ (1.5418 A)
Temperature	25 °X
Specimen	flat-plate, rotating (30 RPM)
Power Setting	40 kV, 40 mA
Soller slits	2 ° (diffracted beam side)
Divergence slits	1 °
Receiving slits	0.05 °
Monochromator	Secondary, graphite
Detector	Scintillation counter
Range of 2θ	3-75 ° 2θ
Step width	0.05 ° 2θ
Time per step	1 second

3.2.7.   Infrared and Raman spectroscopy

Infrared spectroscopy (IR) spectra were obtained using a Brooker IFS 113 spectrometer at low pressures and operated at 32 scans, 2 cm^{-1} resolution. These were also used to study the thermal decomposition of the samples. Approximately 0.05 g of each of the samples were ground with equal amounts of KBr and pressed into pellets with a hydraulic press.

Raman spectra were recorded with a XY Raman spectrometer from Dilor®, using the λ=514.5 nm laser line of a Coherent Innova® 90 Ar^+-laser, with a resolution of at least 2 cm^{-1}. The samples were recorded in a backscattering configuration under the microscope attached to the instrument, using a 50 times objective. A liquid nitrogen cooled CCD detector was used with the laser power 200 mW at the laser exit, resulting in a laser power < 20 mW at the sample. The spectra were baseline corrected, using the Labspec software program supplied by Dilor®.

3.2.8.   Matrix assisted laser desorption ionisation – time of flight – mass spectrometry

MALDI-TOF-MS (Matrix Assisted Laser Desorption Ionisation – Time of Flight – Mass Spectrometry) was preformed on the pyrolysed calcium gluconate samples using a PerSeptive Biosystems Voyager-DE STR time of flight mass spectrometer. This instrument is equipped with a nitrogen laser (337 nm), a delayed extractor and a reflector. The accelerating potential was set to 25 kV in the reflection mode. Laser shot frequency was set at 20 Hz. A spectrum represents the accumulated spectra of 100 shots. The instrument was calibrated with polystyrene standards of known molecular mass.

3.2.9.   Pyrolysis gas chromatography – mass spectrometry

The gaseous decomposition products from the pyrolysed samples were identified with Gas Chromatograph – Mass Spectroscopy (GC-MS). For the work, a Thermal Desorber, Gas Chromatograph and Mass Spectrograph combined setup was used. A Gerstel TDSA thermal desorber was used to heat the samples to the desired temperature. The Gas Chromatograph was an Agilent 6890 with a PTV inlet (CIS4) and the Mass Spectrograph a GCT – Micromass time-of-flight (TOF) high-resolution accurate mass spectrometer run in full scan mode.

3.2.10. Thermal conductivity measurements

Thermal conductivity tests of the foamed calcium gluconate were conducted on a Lasercomp Fox 314 heat flow meter that conforms to ISO 8301 or ISO 8302. The tests were conducted according to ASTM C518 test method, titled "Standard test method for steady-state thermal transmission properties by means of the heat flow meter apparatus". The South African Bureau of Standards (SABS) did the measurements.

3.2.11. Electric conductivity measurements

A HP 4140B pA/DC voltage source was used for electric conductivity measurements of the ammonium and calcium gluconates pyrolysed in nitrogen. The samples were measured on a probe station and tungsten tusters (probes) were used.

3.2.12. Electron microscopy

Samples of the materials used, their pyrolysis products and the prepared crystals were studied with electron and light microscopes.

The crystals prepared of the calcium gluconate monohydrate along with the gluconate powder itself, were viewed with a Nikon Optiphot light microscope. A Nikon DXM 1200 digital camera is attached to the microscope for digital imaging. A top and/or bottom light source was used.

A JEOL JSM 840 SEM (Scanning Electron Microscope) operated at 5 kV was used for the characterisation of the carbon chars produced as well as for general sample viewing. The microscope's optimum usable magnification is between 20 and 30 000 times, but it can produce acceptable images up to 50 000 times. Samples were coated with gold (99.9995% purity) using a Polaron E5200 sputter coater. The samples were coated for a total of 90 seconds; three times for 30 seconds at 60 second intervals.

For wall thickness calculations of these foams and the viewing of very small metal oxide particles, a JEOL JSM 6000F cold field emission gun SEM operated at between 3 kV to 10 kV was used. The optimum field of operation is between 20 000 and 300 000 times magnification, although magnifications of up to 900 000 can be used. The intumesced samples were viewed uncoated since the material contained mostly carbon and was thus

sufficiently conductive. The non-conductive metal oxides were coated with ca. 5 nm high-purity chromium with a Gatan Model 681 high-resolution ion beam coater.

Elemental analysis of the metal oxide particles were carried out using Energy Dispersive Spectroscopy (EDS) of the oxides on a JEOL 5800 LV (Low Vacuum) SEM linked to a Noran Voyager 4 EDS. EDS is also referred to as EDX (energy dispersive analysis of X-rays). The samples were viewed at 10 kV and the analysis time was 100 seconds. Carbon tape was used to stick the samples to aluminium stubs.

The carbon chars produced from both the ammonium and calcium gluconates were viewed for crystallinaty with a Philips EM 301 Transmission Electron Microscope (TEM) using electron diffraction techniques. The TEM was operated at 100 kV. Copper G100/200 mesh folding grids were used to clamp the carbon samples for viewing.

3.2.13. Surface area measurements

BET analysis is a widely used technique for surface area measurements developed by Brunauer, Emmett and Teller; hence the name. Single point BET surface area analyses were carried out on a Micromeritics Flowsorb II 2300 instrument. Between 5 mg and 200 mg of each sample was used for the analysis.

3.2.14. Burn tests

All the tests used to evaluate flame retardant coatings are large scale, destructive and expensive (See Section 2.11) and not really suitable for screening of potential systems. A test, loosely based on work done by Bishop *et al* (1983) and on the ASTM E119 and E84 test methods, was developed to test small samples of possible metal catalysed intumescent flame retardant coatings.

The same LPG cylinder as used for the open flame tests was used for the burn tests. A Brooks Instruments B.V. model 1357 rotameter with a maximum flow rate (calibrated for air) of 255 normal ℓ/h was linked to the gas bottle. The flow rate of the gas could be set and measured with the rotameter and was set at 30% (76.5 normal ℓ/h). The nozzle was held in position with a retort stand and clamp. The samples were placed 50 mm from the nozzle.

Two 300 mm square steel plates were used to clamp the samples. A 60 mm diameter hole was cut in the middle of the front plate, while a cross-shaped cut was made in the middle of the back plate. The aluminium and wood assembly housing the thermocouples was placed in the cut made in the back plate (see Figure 3-8). Five thermocouples were used in the assembly and a sixth as reference. The thermocouples were placed in the assembly at the back of the sample in such a way that they made good contact with the samples. The setup was held in position with a set of retort stands and clamps and placed in a steel tray. Pictures of the experimental setup are shown in Figure 3-9 and Figure 3-10. More pictures of the setup for the burn tests are shown in Appendix G.
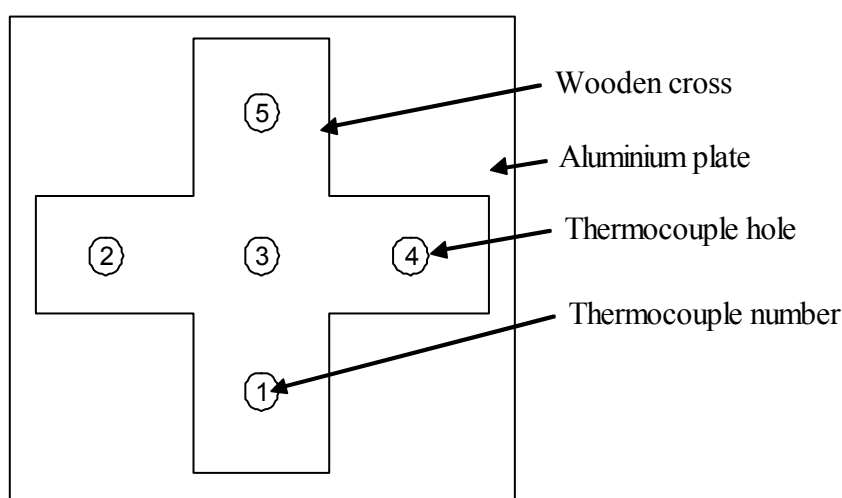
Figure 3-8   Assembly housing the five thermocouples
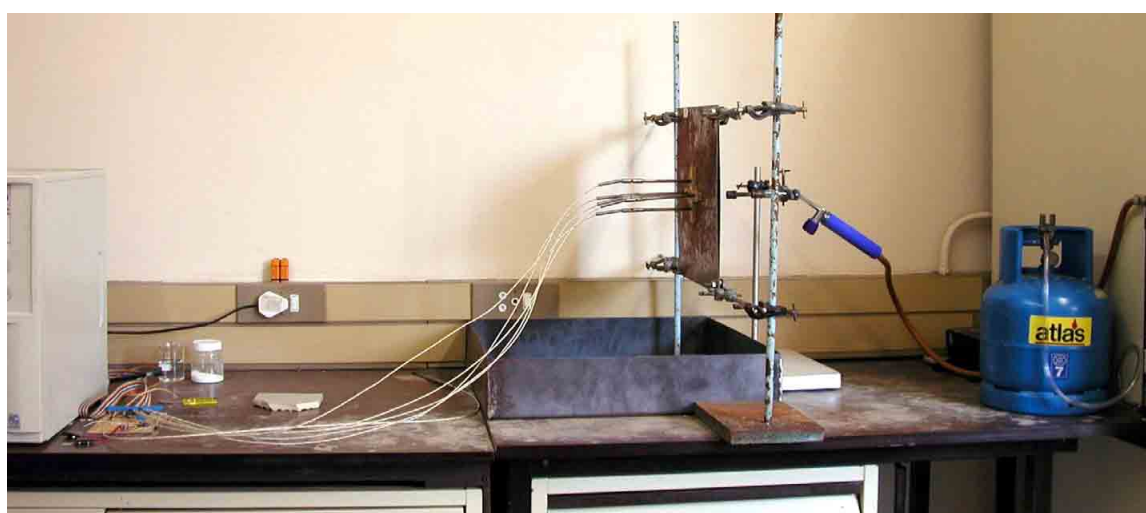
Figure 3-9   Side view of the burn test setup

Figure 3-10   Back view of the burn test setup showing the thermocouples

Chromel-Alumel type K ceramic-coated 6 mm thermocouples with a one meter lead wire were used. The temperature at the back of the samples was measured as a function of time. An Eagle Technology PC30F data logging card was used to record the thermocouple temperature profiles on a personal computer with Windows95™ as operating system and software specially written for the data logging by Dr. S. van der Walt (2000). The software supported the use of 8 thermocouples. Thermocouple 1 (see Figure 3-8) was attached to channel 2 of the software, thermocouple 2 to channel 3, etc. A "screen grab" of the program can be seen in Appendix H showing six thermocouples heated to 90°C and left to cool slowly.

In the preparation of the paints a Hamilton Beach Commercial model 936-220 high speed mixer (milkshake make) operated at 21 000 rpm was used to mix the intumescent formulation, water and resin. The mixing was done in plastic containers. The intumescent coatings were painted onto the samples with a 25 mm paintbrush.

3.2.15. Growing single crystals of calcium gluconate monohydrate

Solutions of calcium gluconate monohydrate in water and other solvents were used to grow single crystals of the gluconate. A water bath with a Grant type VFP submersion heater/circulator was used to heat certain solutions or maintain a chosen solution temperature to induce crystallisation. The submersion heater/circulator can be set in increments of 0.1°C

to a maximum of 200°C. A standard thermo flask was used for the slow cooling of a saturated solution of the calcium gluconate monohydrate in water.

Sublimation crystallisation techniques were used to grow crystals of the calcium gluconate. A cold finger was used to crystallise the sublimated material. Sublimation of the material was done under vacuum at 80°C. A Welch Gem 1.0 vacuum pump was used for the vacuum and the water bath with the submersion heater/circulator to heat the material to the desired temperature. A schematic of the cold finger used for sublimation crystallisation is shown in Figure 3-11 and pictures in Appendix I.
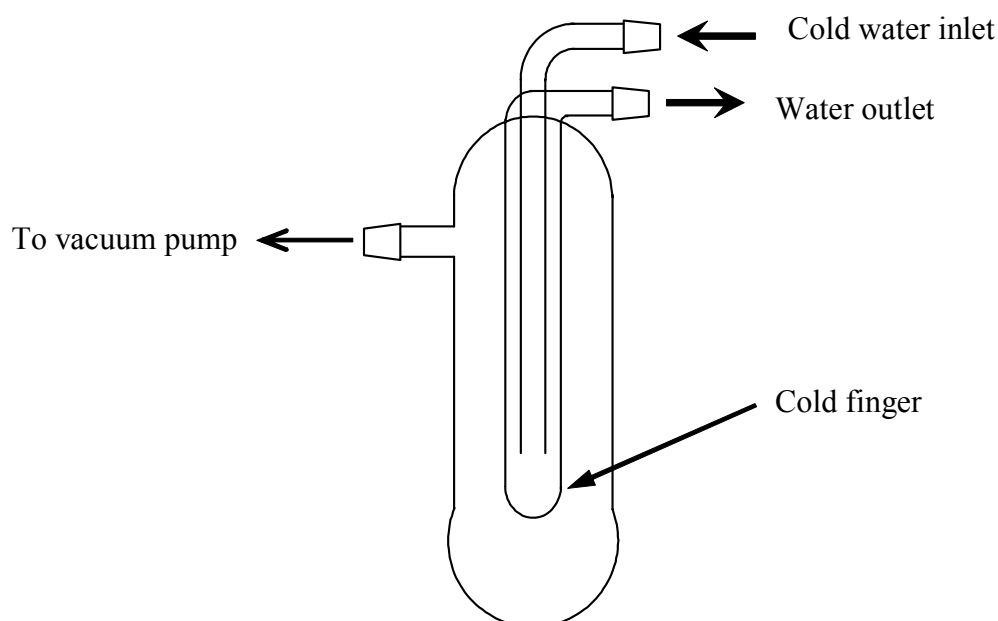
Figure 3-11   Setup for the sublimation crystallisation of calcium gluconate

3.3.   Method

3.3.1.   Preparation and study of the organic acids' sodium salts

For the preparation of the organic acid sodium salts, an aqueous solution of known concentration of sodium carbonate was prepared. This was reacted with the organic acids in a chosen mole ratio of 1:1 by the addition of the stoichiometric amount of acid to the sodium carbonate solution. The solutions immediately began bubbling. After the bubbling stopped, the reacted solutions were poured into Petri dishes and left for up to 14 days for the water to evaporate and the salts to crystallise.

It is important to note that some of the acids used in the synthesis were monocarboxylic acids and that one mole sodium carbonate was added per mole of acid. This implies that some of the sodium carbonate would still be left and would re-crystallise with the organic acid sodium salts. For the acids with two or more carboxylic acids, this would not be true. By reacting the acids and sodium carbonate in a 1:1 mole ratio an easy standard was selected for the amount of sodium metal in the complex and would be equal for all the samples. The carbonate left could help with intumescence as it would form carbon dioxide on thermal decomposition.

After the sodium salts crystallised and all the free water evaporated at ambient conditions, the solid residues were ground in a mortar and pestle. Grinding ensures that the products were homogeneous for further experiments. Both the theoretical yield and percentage yield obtained was calculated. From these values, an approximation was made for crystal water in each of the sodium salts.

A small amount of each of the sodium salts (ca. 0.1 g to 0.3 g) was placed in the glass tubes. The sample mass and the height of the powder in the tube were noted. The laboratory furnace was preheated to a temperature of 500°C. The samples were placed in the aluminium block in the furnace and left for 5 minutes to thermally decompose. After cooling, the mass loss was determined and the height of the char (only the "solid" foam) measured. Of great importance was the type of foam produced. Figure 3-12 shows the glass tubes used and a tube containing a pyrolysed sample.

Figure 3-12   An empty glass tube (left) and tubes with pyrolysed samples (right) of the sodium salts

Open LPG flame tests were carried out on all the organic acid sodium salts. A small sample of the salts were placed on an asbestos plate and exposed to the flame. In this way, the behaviour of the salts in a flame could be studied. Attention was given to intumescence, foam characteristics, afterglow, char formation and stability.

3.3.2. Preparation and studies of the metal complexes of acetylacetone and gluconic acid

The following metal acetylacetonates were used:

Al	Ca	Cu
Fe	Mg	Na
Ti	V	Zr

Gluconic acid salts of the following metals were obtained or prepared and used

Al	Ca	Cu
Fe	Mg	Na
Sb	Zn	Zr

3.3.2.1.   Acetylacetone metal complexes

Pentaerythritol was added to each of the acetylacetonates in a 1:1 mass ratio. The mixtures were ground together in a mortar and pestle until the samples appeared homogeneous. The aluminium acetylacetonate was also ground together with fumaric acid and tartaric acid in a 1:1 mass ratio in order to be compared with the pentaerythritol mixture.

The pure acetylacetonate along with all the mixtures with the pentaerythritol, fumaric acid and tartaric acid were exposed to an open LPG flame. The gas flame was intermittently applied to a small amount (ca. 3 g) of the powder samples for short time intervals (varying from 3 seconds up to about two minutes). The behaviour of the samples in the flame was observed and noted. Attention was given to solid-state carbon oxidation, ignition, melting and the extent of foaming. The volume of the carbonaceous foam-char formed was taken as a measure of the tendency of the compound to intumesce. A scale ranging from 1 to 5 was used with higher numbers indicating more vigorous generation of voluminous foam-char.

Thermal analysis up to approximately 650 ºC was carried out on all the pure acetylacetonate complexes and on the acetylacetonates/pentaerythritol mixtures. The results were compared and analysed.

3.3.2.2.   Gluconic acid metal salts

For the laboratory reactions, a 50% solution of gluconic acid in water (aqueous solution) was obtained from Merck and used as is. Pure calcium gluconate monohydrate and magnesium gluconate hydrate were obtained and used in the research.

For the preparation of the ammonium gluconate, 100% excess of the stoichiometric amount of a 35% ammonia solution was added to the gluconic acid solution. The reaction was left stirring for a day on a magnetic heater/stirrer. The ammonium gluconate was left to crystallise from the solution and dried over phosphor pentoxide (P_2O_5).

The sodium gluconate was prepared by adding the stoichiometric amount of sodium carbonate to the gluconic acid solution. More gluconic acid was used to acidify (acidulate) the solution to a pH of ca. 4. After the bubbling stopped, ethanol was added to the solution and a cream to brownish precipitate formed. The solubility of gluconic acid in ethanol was confirmed beforehand. The precipitate was washed with excess ethanol after filtration of the solution.

Aluminium hydroxide ($Al(OH)_3$) was added to gluconic acid. A 20% excess gluconic acid was used. A new container of $Al(OH)_3$ was used. The suspension of $Al(OH)_3$ in the acid was placed on a magnetic heater/stirrer. The reaction mixture was stirred continuously while it was slightly heated (approximately 50°C) for seven days. The unreacted $Al(OH)_3$ was filtrated and discarded. Ethanol was added to the clear filtrate solution and the aluminium gluconate immediately precipitated. It was again filtrated and the precipitate was washed with ethanol and air dried for a week.

The gluconic acid antimony salt was prepared from the 50% gluconic acid solution (20% excess) and antimony trioxide (Sb_2O_3). The raw materials were added to a glass beaker, slightly heated and stirred for seven days. As with the aluminium hydroxide, the unreacted Sb_2O_3 was removed through filtration. A precipitate of antimony gluconate formed

with the addition of ethanol and was collected through filtration. The precipitate was washed and air dried similarly to the other gluconates.

A basic zinc carbonate ($ZnCO_3.12H_2O$) was used for the synthesis and reacted with the stoichiometric amount of gluconic acid. The bubbling solution was acidulated (acidified) to a pH of ca. 3. A precipitate formed with the addition of ethanol. The solution was then filtrated and the precipitate washed with excess ethanol.

For the synthesis of the gluconic acid zirconium salt, the stoichiometric amount of zirconium basic carbonate (approximated as $Zr_2(OH)_2O_2CO_3.14H_2O$) was added to the gluconic acid. The solution started to bubble immediately and was acidified to a pH of 2 with an excess gluconic acid. When the solution stopped bubbling, the zirconium salt was precipitated out by the addition of ethanol. The precipitate was filtrated and washed with ethanol and left to air dry.

After air-drying the gluconic acid salts for a week, they were placed in a desiccator filled with P_2O_5. This was done in order to remove as much water as possible and to further keep the samples dry.

All the salts were standardised in order to determine the ratio of metal to organics and thus gluconic acid. The standardisation was done by placing each of the gluconates in a preheated furnace at 1000°C for approximately 20 minutes. The residual mass as metal oxides and carbonate in the case of sodium was calculated.

Thermal analysis was also done on the gluconates as well as the tube pyrolysis and open flame tests. These experiments were done as described for the acetylacetonates.

3.3.3. Characterisation and evaluation of the intumescence calcium gluconate monohydrate and ammonium gluconate hydrate

The intumescent properties of calcium gluconate monohydrate were studied more comprehensively. Several of the foam properties of ammonium gluconate hydrate were also investigated more comprehensively. A range of analyses was carried out on the intumesced

gluconates. The analysis done and foaming temperatures and atmospheres are listed in Table 3-3 for the calcium gluconate and Table 3-4 for the ammonium gluconate.

Table 3-3   Temperatures selected pyrolysis for the calcium gluconate monohydrate

Atmosphere	Temp. (°C)	IR	XRD	SEM	MALDI	BET	Thermal conduc.	Electric conduc.	Density
Air	100	✓	✓		✓				
	150	✓	✓		✓				✓
	200	✓	✓	✓	✓				✓
	250	✓	✓		✓				
	300	✓	✓	✓	✓	✓	✓		✓
	400	✓	✓	✓	✓	✓			✓
	500	✓	✓	✓		✓			✓
	600	✓	✓	✓		✓			✓
	700	✓	✓	✓					✓
	750	✓	✓						
	800	✓	✓	✓					✓
	1000	✓	✓	✓					✓
Inert	200	✓	✓	✓	✓				
	300	✓	✓	✓	✓				
	400	✓	✓	✓	✓				
	500	✓	✓						
	600	✓	✓						
	700	✓	✓						
	850	✓	✓					✓	
	1000	✓	✓						
Pure powder		✓	✓	✓	✓				✓

Table 3-4   Temperatures selected pyrolysis for the ammonium gluconate hydrate

Atmosphere	Temperature (°C)	IR	XRD	SEM	Electric conductivity
Air	300	✓	✓	✓	
	400	✓	✓	✓	
	500	✓	✓		
	600	✓	✓		
	700	✓	✓		
	800	✓	✓		
	1000	✓	✓		
Inert	300	✓	✓	✓	
	400	✓	✓	✓	
	500	✓	✓		
	600	✓	✓		
	850	✓	✓		✓
	1000	✓	✓		
Pure powder		✓	✓	✓	

The gluconates were pyrolysed at several selected temperatures ranging from 100°C to 1000°C in both air and inert (nitrogen) atmospheres. All the samples were placed into a

preheated furnace at the selected temperature for 5 minutes unless mentioned otherwise. For the pyrolysis in nitrogen, the special glass chamber or the silica tube was used (depending on the temperature). Sufficient material was pyrolysed to be used for all the analyses.

3.3.3.1.   The characterisation of the intumescent foams

Several samples of the calcium and ammonium gluconates were placed in polytops™ and pyrolysed at selected temperatures.

Furthermore, mixtures of calcium gluconate monohydrate and several fillers on a 1:1 mass ratio, were made. A mortar and pestle was used to homogenise the mixtures. Each of these samples was exposed to the open LPG flame and visually compared with one another. Of importance were afterglow, intumescence and char structure. The best filler was identified as amorphous leached silica from Foskor.

The silica was send to an external laboratory for elemental analysis in order to determine its composition. It was analysed for major metals, silica and other majors. A scanned image of the results can be found in Appendix J.

Mixtures of the calcium gluconate and the leached silica were made on a mole ratio (assuming the silica to be pure SiO_2) and homogenised with a mortar and pestle. Mole ratios were used as it was believed that the calcium and silica could react to form various calcium silicates. The amounts of silica used are listed in Table 3-5. The mixtures were exposed to the open flame and pyrolysed in the glass tubes. Samples of the mixtures were prepared for further analysis and pyrolysed at 400°C, 600°C and 1000°C in air.

Table 3-5   Amounts of leached silica used

Mole ratio Ca gluconate : SiO_2	% SiO_2 (by mass)
0.5:1	21.14%
1:1	11.82%
2:1	6.28%
4:1	3.24%

In a similar manner as with the silica, mixtures of the calcium gluconate with expandable graphite mined in Zimbabwe and distributed by Ferro, were prepared. The mixtures contained between 10% and 50% graphite by mass. The samples were exposed to the open gas flame and the most favourable formulation identified.

BET surface area analysis was done on the calcium gluconate foam prepared at 300°C for 5 minutes. Small amounts of the samples (c.a. 20 mg) were placed in the sample holders and analysed.

SEM was done on the foams of the foamed ammonium and calcium gluconates and the pyrolysed calcium gluconate/silica mixtures. The cell sizes of the foams, cell packing density and the cell wall thickness were of importance. The effects of heating temperature, pyrolysis atmosphere and filler content on the foamed gluconate were investigated. The intumesced chars of some commercial intumescent flame retardants (pyrolysed at 400°C for 5 minutes in air) were also analysed. These chars were compared to the calcium gluconate pyrolysed under similar conditions. Each of the foams was frozen with liquid nitrogen and "broken open" with a razor blade. This was done in order not to damage the cells and best show the foam structure. The samples were mounted on the aluminium stubs with double-sided carbon tape. For the wall thickness calculations, it was important to mount the material with the cell walls perpendicular to the microscope.

3.3.3.2.   Thermal analysis of the gluconates

Thermal analysis of the calcium gluconate monohydrate and ammonium gluconate hydrate was done in both air and inert atmospheres up to 1000°C. The leached silica and expandable graphite were also analysed in air up to 1000°C. Small amounts (less than 20 mg) of the gluconates were placed in platinum crucibles and analysed.

3.3.3.3.   Identification of the gaseous decomposition products

The desorber was set to a temperature of 100°C for 10 minutes and then ramp up at 30°C per minute to 300°C. The samples were then kept at 300°C for 5 minutes. The CIS4 inlet was kept at -40°C for the duration of the desorption. At the completion of the desorption cycle, it was heated to 300°C at 10°C per second and maintained at the temperature for 2 minutes. The samples were placed in the desorber auto sampler and analysed.

The data was interpreted with the instruments' own software. In this way, the same decomposition species were identified and the mass of all volatile decomposition products obtained.

The samples selected were calcium salts of:

- acetic acid (acetate)
- lactic acid (lactate)
- glyceric acid
- threonic acid
- citric acid (citrate)
- propionic acid (propionate)
- saccharic acid (saccharate)
- gluconic acid (gluconate)

3.3.3.4.   Identification of the solid decomposition products

The composition of the char residues of all the pyrolysed materials were analysed with XRD and IR, along with the gluconates themselves and the leached silica. The chars of the calcium gluconate/silica mixtures were also analysed. The TEM was used to identify the crystallinaty of the carbon produced from the pyrolysis of the gluconates in nitrogen at 1000°C.

3.3.3.5.   Molecular mass determination of the carbon foam from the calcium gluconate

Some of the foamed gluconates were analysed with MALDI-TOF-MS to determine the molecular mass of the carbon in the solid phase. A matrix and salt, each dissolved in tetrahydrofurane (THF), should usually be added to the materials to be analysed with this technique. The efficiency of several matrixes and salts were tested each, dissolved in THF. The matrixes used were:

- 1,8,9-Trihydroxyanthracene (Dithranol)
- 2,5-Dihydroxybenzoic acid (DHB)
- trans-Cinnamic acid (CA)
- trans-4-Hydroxy-3-methoxycinnamic acid (FA)
- 2-(4-Hydroxyphenylazo)-benzoic acid (HABA)

- trans-3-(3-Indolyl)-acrylic acid (IAA)
- Thiourea (TU)
- None

The salts used were:

- Sodium trifluoroacetate [$C_2F_3O_2Na$]
- Silver trifluoroacetate [$C_2F_3O_2Ag$]
- None

The material tested is normally dissolved in THF, but water and sulphuric acid were also used, as the carbon foams do not readily dissolve in the THF. The sample was pre-mixed with the matrixes and salts, and deposited on the target (100 well plate) and dried in air (dry-droplet method). In addition, samples where the matrix and salt were first deposited on the target and dried with the materials deposited on top of the dried matrix/salt were also used.

Each sample was exposed to 100 laser shots. The resultant spectra were evaluated with the Voyager software and the best technique chosen. Using this method, the foams were analysed and an average molecular mass calculated. The effect of pyrolysis temperature and atmosphere on the molecular mass of the carbon was determined.

3.3.3.6.   Density calculations of the calcium gluconate monohydrate foam

Small amounts of the calcium gluconate monohydrate were placed into polytops™ with an inner diameter of 23.5 mm. The gluconate samples were placed in the preheated laboratory furnace at selected temperatures for 5 minutes. After the samples were removed from the furnace and left to cool, each sample's mass loss was calculated. The volume occupied by each of the foamed samples in the polytops™ was determined. The foam volume and both original and retained mass was used to calculate the foam density for each of the samples as a function of the foaming temperature.

The foam density of the calcium gluconate as a function of heating time at a selected temperature was determined in a similar fashion. Samples were placed in the preheated furnace at 300°C for selected times from 2 min to 30 hours (1800 min). Mass loss and foam volume were measured and density calculated as a function of temperature.

3.3.3.7.   Thermal conductivity of the intumesced calcium gluconate

For the thermal conductivity measurements of the foamed calcium gluconate, two foamed polystyrene blocks of 300 mm square and 50 mm thick were used. A 200 mm square hole was cut in one of the blocks, to leave a border of 50 mm. Enough of the calcium gluconate was foamed in air at 300°C to fill the hole completely. The foamed gluconate was kept in place by closing the hole with a sheet of brown paper on either side and keeping it in place with brown sticky tape. The solid, uncut polystyrene block was used as reference and compared with the block filled with the gluconate foam.

3.3.3.8.   Electric conductivity measurements

Small amounts of calcium gluconate monohydrate and ammonium gluconate were each pyrolysed at 850°C for 60 minutes in a silica tube in nitrogen. Each of the carbon samples was ground into a fine powder with a mortar and pestle. A piece of commercial graphite was ground in a similar fashion as the other carbon samples.

Each of the carbon powders was imbedded in an epoxy resin. The plastic sample holders containing the carbon and epoxy were centrifuged for 10 minutes at 2 500 rpm. This forced the air from the resin and helped to tightly pack the carbons at the bottom of the sample holders. The epoxy resin was left to set at 60°C in a drying oven. From each of the samples a 1 mm disk – containing the carbon imbedded in the epoxy – was cut with a diamond saw. These disks were used for the electric conductivity tests along with a blank epoxy disk.

The electric conductivity of each of the samples was measured. The samples were placed on a probe station. Two tungsten tusters were placed 5 mm apart on the samples and contact with the samples ensured. The distance between the tusters was kept constant for all the samples and measurements. A selected potential was applied between the two tusters and the current flowing through the samples measured. All the samples were tested at 1 V, 2 V and 5 V. The carbon from the ammonium gluconate was tested more thoroughly. A rang of potentials from 0.1 V in 0.1 V increments up to 1 V and in 1 V increments up to 5 V were used for the measurements.

3.3.3.9.   Paint preparation and burn tests

Intumescent coatings were prepared from the calcium gluconate monohydrate, mixtures of the gluconate with the leached silica and/or the expandable graphite and the commercial intumescent compositions. These were applied to balsa wood, cardboard and aluminium plates.

Balsa wood planks, 100 mm square and 5 mm thick, were painted with intumescent coatings prepared form the MC 56 resin and the different intumescent formulations. The intumescent content of the paint was 70% of the total solids and the ratio intumescent to water was 1:2. For all the mixtures, the ratio silica used were 1:1 moles to the gluconate (11.8% by mass silica to gluconate) and 10% by mass expandable graphite to gluconate. Intumescent systems used for the paints were:

- AP 750
- PEN
- Calcium gluconate monohydrate
- Calcium gluconate monohydrate with amorphous leached silica
- Calcium gluconate monohydrate with expandable graphite
- Calcium gluconate monohydrate with leached silica and expandable graphite

Aluminium plates (2.5 mm thick and 100 mm square) and cardboards (3 mm thick and 100 mm square) were painted with similar intumescent coating prepared form the ATEBIN ES/BA resin and the intumescent formulations. The intumescent to resin ratio was 25:1 and 1:2 to water. For all the mixtures, the ratio silica used were 1:1 moles to the gluconate (11.8% by mass silica to gluconate) and 10% by mass expandable graphite to gluconate. Intumescent systems used for the paints were:

- AP 750
- PEN
- Calcium gluconate monohydrate with leached silica and expandable graphite

The samples were left to dry for a day or two and the mass loading determined. The painted samples were clamped in the sample and thermocouple holder assembly. The rest of the setup was placed in position and the temperature measurement started as soon as the sample was exposed to the flame. The flame was removed when it burned through the sample (in the case of the wood and cardboard) or the paint was completely burned off (for

the aluminium). The data was logged, exported as an ASCII file and imported into Microsoft Excel. The temperature vs. time profiles for each of the samples were compared with those of the untreated samples and used to determine the effectiveness of each of the compositions as a function of loading mass. Each experiment was repeated three times and an average taken.

3.3.3.10.   Growing single crystals of calcium gluconate monohydrate

Attempts were made to grow sizable single crystals of the calcium gluconate monohydrate. The solubility of the calcium gluconate monohydrate at 20°C is only 3.0 g gluconate per 100 mℓ water. At 25°C, the solubility rises to 3.5 g per 100 mℓ and 20.0 g per 100 mℓ at 100°C.

Solutions of the calcium gluconate monohydrate varying in concentration from 0.5 g per 100 mℓ water to 3.0 g per 100 mℓ water were prepared at room temperature. These solutions were left to crystallise at ambient conditions. Seed crystals were grown in a similar fashion from a 0.5 g per 100 mℓ solution. The seed crystals were added to a saturated solution at room temperature and the solution with seed crystals left to crystallise at ambient conditions. A small rough surfaced stone was added to a 3.0 g per 100 mℓ solution of the gluconate in water and left to crystallise at ambient conditions.
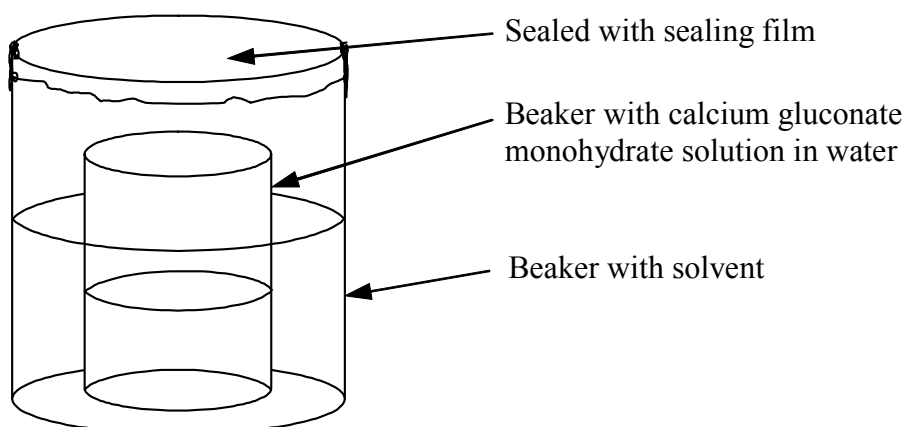
Solutions of concentrations between 0.5 g and 3.0 g per 100 mℓ water were prepared and placed in a fridge and left to cool and crystallise. A saturated solution of the calcium gluconate was prepared in boiling water (ca. 95°C). The solution was sealed, placed in a thermo flask filled with boiling water, closed and left for two weeks to crystallise.

Super saturated solutions of the gluconate in water, acetone, ethanol and methanol were prepared at room temperature. Calcium gluconate monohydrate is only very slightly soluble in acetone, methanol and ethanol. The solutions were strained through cotton wool to remove the undissolved material and left to crystallise at ambient conditions.

Solutions of 3% calcium gluconate in both DMSO and acetonitrile were made. These were left in the open for a few days to crystallise. A solution of 2 g gluconate per 100 mℓ water was prepared. A few drops (± 10 drops) DMSO were added to the solution and left to crystallise at ambient conditions. The crystals were retained and used as seed crystals in a similar solution.

Attempts were made to grow crystals by solvent diffusion. Solutions of the calcium gluconate in water varying in concentration form 0.5 g per 100 mℓ to 3.0 g per 100 mℓ were placed in small beakers. The beakers were placed in larger beakers containing a second, volatile solvent in which the gluconate is less soluble than in water. The large beakers were sealed with sealing film. The volatile solvent should diffuse into the water and "force" the crystals out of solution. A schematic of the experimental setup is shown in Figure 3-13. The experiment was repeated with seed crystals being added to the solutions of the gluconate in the water. The volatile solvents used were:

- Dimethyl sulfoxide (DMSO) [$(CH_3)_2SO$]
- 1,4-Dioxan [$C_4H_8O_2$]
- Acetonitrile [CH_3CN]
- Acetone [$(CH_3)_2CO$]
- Methanol [CH_3OH]
- Ethanol [C_2H_5OH]
- 2-Propanol (iso-propanol) [C_3H_7OH]
- Buthanol [C_4H_9OH]
- Octanol [$C_8H_{17}OH$]

Sealed with sealing film

Beaker with calcium gluconate monohydrate solution in water

Beaker with solvent

Figure 3-13   Diffusion crystallisation of calcium gluconate monohydrate

A "U"-tube with agar in the bottom, a saturated solution of calcium gluconate monohydrate in water in the one tube leg and ethanol in the other, was also used. The solvents should diffuse through the agar and the calcium gluconate crystallise from the solution.

Some of the calcium gluconate monohydrate powder was placed in the sample holder of the cold finger. The cold finger was placed in the water bath set to 80°C. Cold water was used as cooling medium for the cold finger. The vacuum pump operating at 87% to 90% vacuum was used for the sublimation of the gluconate at 80°C. The setup was left for 10 days for the sublimation/crystallisation to take place. Prior to the crystallisation, it was confirmed with XRD that the calcium gluconate monohydrate would not dehydrate and change crystal structure if left at 80°C for 10 days.

3.3.4.   Preparation of the calcium and other metal dextrose derivatives and study of their intumescence

A solution of dextrose monohydrate (glucose) was heated with calcium hydroxide [$Ca(OH)_2$] to prepare the CaDex solution. The preparation procedure was obtained from Venter (2000) and the full method is given in Appendix K. The method was optimised for yield and calcium hydroxide consumption, but only small quantities (ca. 200 mℓ) could be prepared and the reaction medium was only stirred occasionally.

For the preparation of the CaDex the reagents were increased ten fold from the above-mentioned method and the medium continuously stirred. The $Ca(OH)_2$ was added slowly to the heated dextrose solution, as the reaction is exothermic at these conditions. After all the $Ca(OH)_2$ was added, the reaction was kept at 60°C for 20 minutes. The unreacted $Ca(OH)_2$ was removed by filtration. The CaDex solution was standardised for calcium in the solution by heating the solution to 1000°C and maintaining the temperature for 20 hours. The mass CaO left was calculated and from that the percentage calcium in the solution.

The metal sulphates used for the preparation of the MetDex solutions were dissolved in distilled water and the concentrations noted. The stoichiometric correct amounts of the sulphates needed to react with all the calcium in the CaDex solution was calculated and 5% excess (on mass) added. After the solutions were stirred for four hours, the precipitated calcium sulphate ($CaSO_4$) was removed by filtration and weighed.

The MetDex solutions were poured into 400 mℓ beakers and pyrolysed in the preheated furnace at 500°C for 30 minutes. The foaming and after glow effect for each of the samples was observed. CaDex samples containing 1%, 5%, 10%, 20%, 50% and 100% boric

acid by mass, based on the mass calcium in the solution, were prepared. Pure CaDex and the CaDex samples containing boric acid were used to treat several pieces of newspaper, filter paper and polyester fabric. The treated materials were dried and the mass loading determined. The samples were exposed to the open gas flame to evaluate the intumescent flame retarding properties of the CaDex and boric acid solutions. Attention was given to foaming and ignition resistance.

3.3.5. Characterisation of the metal carbonates and oxides

All the MetDex solutions, along with the CaDex and the calcium gluconate monohydrate were pyrolysed for 24 hours at 1000°C using alumina (Al_2O_3) crucibles and for 60 hours at 600°C using glass crucibles in the preheated furnace. The surface area of the resultant metal oxides and carbonates were determined. SEM analysis of the metal oxides and carbonates was done to identify particle sizes and characterise them. EDS analysis was used to determine the elemental composition of the samples.

3.3.6. Understanding metal catalysed intumescence of polyols

Only some organometallic complexes containing hydroxyl groups show appreciable intumescence when heated. Although most of these complexes contain calcium as the metal ion, this is not always the case. Furthermore, all hydroxyl rich calcium containing organometallic compounds do not intumesce as appreciable as calcium gluconate monohydrate does. The reason and mechanism for this was further investigated. Relevant results from the previous sections were compared and studied. Furthermore, thermal analysis was done on the compounds studied in the pyrolysis GC-MS. Open gas flame tests were also carried out on these samples. The structures of these compounds are shown in Figure 3-14. The samples were calcium salts of:

- acetic acid [calcium acetate hydrate]
- propionic acid [calcium propionate]
- lactic acid [calcium lactate tetrahydrate]
- glyceric acid [glyceric acid hemicalcium salt monohydrate]
- threonic acid [threonic acid hemicalcium salt]
- citric acid [tricalcium dicitrate tetrahydrate]
- saccharic acid [calcium saccharate tetrahydrate]
- gluconic acid [calcium gluconate monohydrate]

The effect of a compound's crystal waters on its intumescence was investigated. In an attempt to remove the bound crystal water of the calcium gluconate monohydrate and the glyceric acid hemicalcium salt monohydrate (calcium glycerate dihydrate) the samples were placed in a drying oven at respectively 120°C and 140°C for 24 hours. Small amounts (ca. 1 g) of the gluconate and glycerate were placed in polytops® and 10 ml ethanol added to each. The calcium salts did not dissolve (or dissolved very slightly) in the alcohol. The samples in the ethanol were stirred for a week, filtered, dried and immediately pyrolysed at 300°C. The foam densities were calculated. Density measurements were done on the glyceric acid hemicalcium salt monohydrate and the threonic acid hemicalcium salt when heated for 5 minutes in the laboratory furnace at 200°C, 300°C and 400°C. All the dehydrated samples of the calcium gluconate and glycerate were heated for 5 minutes at 300°C in the furnace and their foam densities calculated. These were compared with the density of calcium gluconate when heated under similar conditions. SEM images of the heated glyceric acid calcium salt at 200°C, 300°C and 400°C were compared with calcium gluconate pyrolysed at the same temperatures.

Calcium acetate hydrate

Propionic acid calcium salt

Calcium lactate pentahydrate

Glyceric acid hemicalcium salt monohydrate

Threonic acid hemicalcium salt

Tricalcium dicitrate tetrahydrate

Calcium saccharate tetrahydrate

Calcium gluconate monohydrate
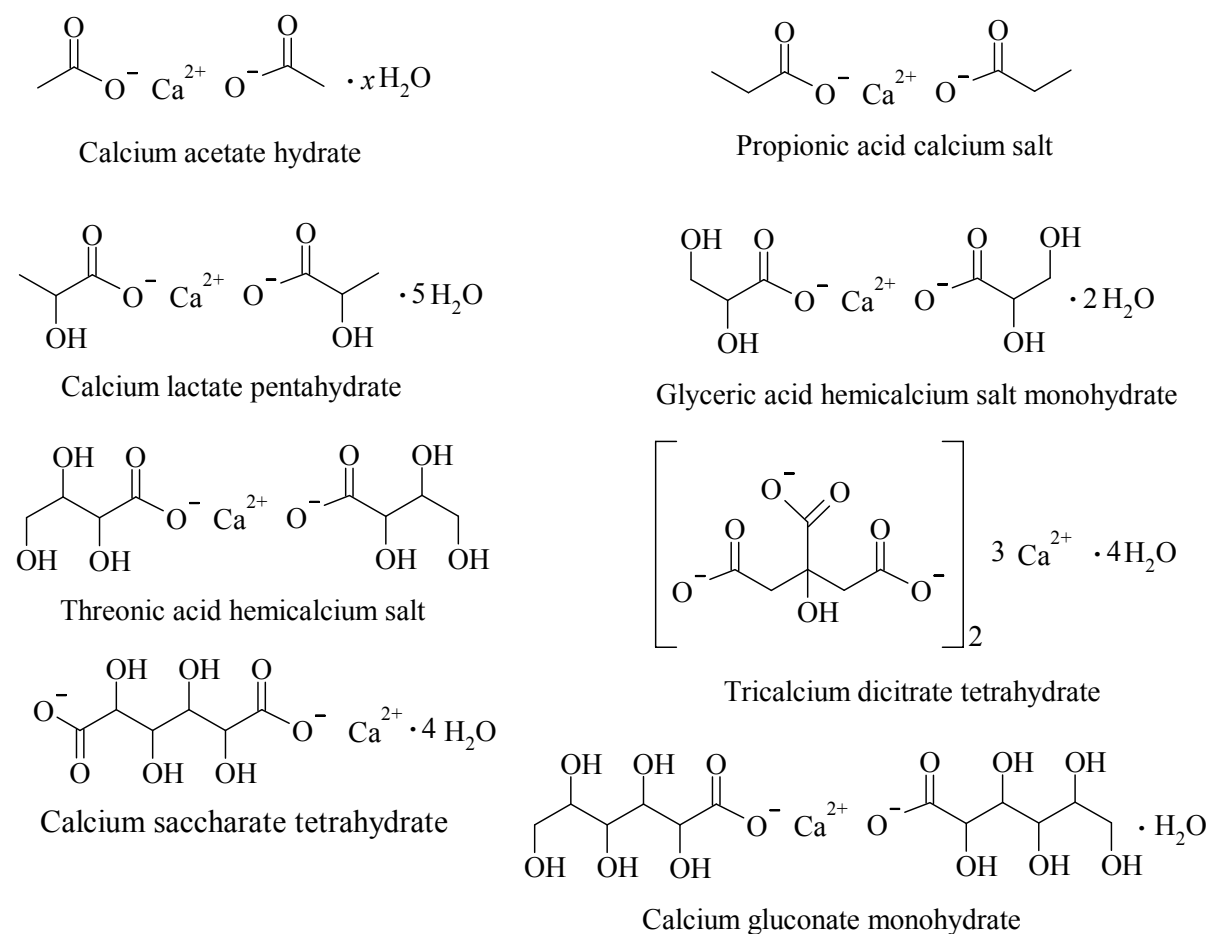
Figure 3-14   Structures of the compounds studied in this section

4.   Results and Discussion

4.1.   The organic acid sodium salts

All the results of the synthesis of the sodium salts and their pyrolysis are tabulated in Appendix L. With the addition of the sodium carbonate solution to the acids, most of the solutions started to bubble. The rate and degree of bubbling varied for each of the solutions. Several of the acids are insoluble or only partially soluble in water. Reactions with these acids produced little or no bubbling, while others bubbled slowly but steadily. Bubbling was steady and some times vigorous for the soluble acids. The bubbling is an indication of the reaction as the carbonate in the sodium carbonate is replaced with the carboxylic acid and CO_2 is released. The reaction was complete when the bubbling stopped.

Two of the reactions of the sodium carbonate with the carboxylic acids failed to produce solid products (carboxylic acid sodium salts). These were the phytic acid and aspartic acid solutions. Phytic acid is a liquid at room temperature and contains 12 acidic protons per mole. The addition of two moles of sodium per mole acid is thus insufficient for the formation of the sodium salt, as it is possible that some of the phytic acid will stay in the free form (liquid) while others contain two, three and maybe more sodium ions per acid molecule. These may be bound to the remaining liquid free acid. This will explain the difficulty in the formation of crystalline material with this synthesis method. In the case of the aspartic acid, the reason for it not crystallising is not obvious. In fact, it cannot be explained at all.

With the addition of one mole of Na_2CO_3 per mole of organic acid (irrespective of the number of acid hydrogens per mole acid), the ratio of sodium to organic acid was constant for all. In the case of the unreactive organic compounds, there would still be two moles of sodium per mole acid after crystallisation, although the sodium will be as carbonate (Na_2CO_3). The insoluble acids might only have reacted partially. Still there will be two moles of sodium per mole of acid because the unreacted sodium will be present as Na_2CO_3.

The most important results for the pyrolysis tests on the sodium salts can be seen in Table 4-1, with all the results listed in Appendix L. The compounds listed in Table 4-1 represent some of the best intumescent compounds, but were mainly chosen to indicate trends

and for comparative reasons. Some of the samples showed little or no intumescence, with others showing very low carbon char yields. The char yield only refers to carbon char and excludes the ash. The compounds are grouped according to their chemical structure. The aromatic and aliphatic compounds are listed separately. Those with alcohol functionalities (hydroxyl groups) are grouped together. Compounds with other functionalities made up a separate group.

Table 4-1   The effect of organic structures on carbon formation

Acid compound	Aromatic	No. of carbon atoms	No. of acid groups	No. of hydroxyl groups	Other groups in complex	% Carbon char yield (excluding ash)	Relative char rating (in group)	Relative char rating (overall)
Oxalic		2	2	-	-	15	1	
Malonic		3	2	-	-	5	2	
Succinic		4	2	-	-	40	2	
Maleic		4	2	-	-	25	**5**	1
Levulinic		5	1	-	-	20	2	
Glutaric		5	2	-	-	5	3	
2-Ketoglutaric		5	2	-	-	30	3	
Adipic		6	2	-	-	50	4	
Phenyl acetic	✓	8	1	-	-	10	1	
Anisic	✓	8	1	-	-	20	2	
4-*t*-Butyl benzoic	✓	11	1	-	-	55	2	
Benzoic	✓	7	1	-	-	35	2	
Homophthalic	✓	9	2	-	-	40	3	
Phthalic	✓	8	2	-	-	60	4	2
i-**Phthalic**	✓	8	2	-	-	55	**5**	
Phthalic anhydride	✓	8	2	-	-	60	4	
Trimesic	✓	9	3	-	-	50	4	
Pyromellitic	✓	10	4	-	-	50	4	
Phenylpyruvic	✓	9	1	-	-	55	1	
Coumaric	✓	9	1	1	-	25	3	
Pyrogallic	✓	6	-	3	-	60	1	3
Gallic	✓	7	1	3	-	30	**5**	
Cyanuric	✓	3	-	3	3 x N in ring	50	2	
Diaminobenzoic	✓	7	1	-	2 x NH$_2$	45	**5**	
Tetraphenyl borate	✓	24	1	-	Borate	75	1	
Uric		5	-	-	4 x NH	40	3	4
3-Picolinic		6	1	-	Pyridine	30	2	
Glycine		2	1	-	NH$_2$	15	3	
Pyrazinecarboxylic		5	1	-	Pyrazine	25	4	
Nitrilo triacetic		6	3	-	Nitrile	70	3	
Glycolic		2	1	1	-	10	2	
Tartaric		4	2	2	-	10	2	
Malic		4	2	1	-	10	3	
Citric		6	3	1	-	10	1	5
Mucic		6	2	4	-	20	3	
Galacturonic		6	1	4	-	20	4	
Gluconic		6	1	5	-	35	**5**	

1 – worst; 3 – medium; 5 – best.

The materials were visually evaluated during open flame pyrolysis. The tests give a better indication of the intumescent ability of the compounds in terms of char volume (height) than the tube tests. All the sodium salts were heated and their foams compared relative to each other for char volume. In this way compounds with good, little and no intumescence were identified. Attention was also given to the structure of the foamed chars during this visual evaluation. This visual evaluation along with the measured char heights was used to form a relative char rating.

The scale used for the relative ratings are: 1 – worst; 3 – medium; 5 – best.

The sodium salt of pyruvic acid performed best in the char height (furnace tube) tests and recorded the highest char height. Unfortunately this test was not as good an indication for intumescence as was hoped for. Some of the samples left very little or no foam in the tubes, but instead foamed out of the tube and left a small ball of foam on top of the tube opening or foamed char down the side of the tube. Yet, the same compounds show some to extensive intumescence in the open flame tests. Char heights for these samples were approximated.

The highest overall char yield was calculated for sodium tetraphenyl borate at just over 75%. The other aromatic compounds showed substantial char yields, but were lower than that of the sodium tetraphenyl borate. The nitrogen containing complexes also showed high char yields and were on a par with the aromatic compounds. The sodium salt of nitrillo triacetic acid showed the highest char yield of the nitrogen rich compounds at ~ 70%. All the sodium salts showed considerable solid-state oxidation during the open flame tests. This is due to the high catalytic oxidative activity of the alkali metal on the carbon char (Rakstaski, 1964). The only exception was the sodium tetraphenyl borate, which showed considerably less afterglow (but was still noticeable). Boron rich compounds are known to reduce afterglow (Rakszawski, 1964; Touval, 1993; Weil, 1993; Gann, 1993; Green, 1996; Green, 1997; Focke *et al.,* 1997). The afterglow effect would be similar for all the complexes seeing that the ratio of sodium to organic acid was constant (at 2:1 mole ratio). Therefore, the char yield would also be an indication of the material's resistance to after glow. Higher char yields will be associated with lower levels of solid-state carbon oxidation.

The ten compounds showing the best results in terms of all the parameters (char yield, foamed char structure and overall intumescence) are printed in bold in Table 4-1. Phthalic

acid and phthalic anhydride are not marked because *i*-phthalic acid is a similar acid and has been highlighted. The sodium salts of gluconic acid and of 3,5-diaminobenzoic acid were the overall best performers. They showed the best balance between char yield, char structure and char foam volume, although afterglow was a problem.

Several trends can be identified from the results in Table 4-1. A number of factors influence the char yield of the tested compounds. Aromatic compounds showed higher char yields than the aliphatic compounds. If the number of carbons in the complex of a specific group is compared with its char yield after pyrolysis, a general trend becomes apparent. As the number of carbons in the compound increases, so does the char yield. This generally held true for all the groups. The number of carboxylic acid groups in the complex had a lesser influence on the carbon yield. Generally, the more acid groups a compound had, the lower the char yield. This is to be expected as the carboxylic acid will be lost first in the formation of $CaCO_3$ and as CO_2. The presence of other elements (such as boron and nitrogen) had a positive effect on char yield. As mentioned before, boron reduces carbon oxidation and thus led to very high char yields. Compounds with nitrogen give higher char yields than similar aliphatic compounds, but were on a par with the aromatic materials.

Intumescence can only be achieved when a gas is formed during pyrolysis, causing the char to foam up – as discussed earlier. In the cases for the prepared sodium salts, the gases can be steam (from the crystal water and complex's hydroxyl groups), CO and CO_2 (from the carboxylic acid) and ammonia (from the nitrogen in the nitrogen rich compounds). Compounds with more carboxylic acid groups tend to show better foaming, but too many acid groups can be detrimental. This may be because too much carbon is lost as CO and CO_2 for these complexes leaving insufficient material to intumesce. Aromatic compounds show less intumescence than most aliphatic compounds. The carbon char produced by the aromatic complexes may be "harder" and "stiffer" than the aliphatic chars; making them more difficult to foam up.

From the data it was clear why nitrogen rich compounds are frequently used in intumescent compositions. The ammonia formed during pyrolysis is an efficient spumific. Compounds with separate amino groups were more effective than those with nitrogen in the carbon back bone. An example is the sodium salt of 3,5-diaminobenzoic acid, which showed the second best foaming. The compounds with nitrogen in the carbon back may form more

fragmented carbon char bits, causing them to oxidise more readily and thus forming less material to intumesce.

The amount and quality of intumescence is influenced most by the number of hydroxyl groups in the compound. Compounds with more hydroxyl groups tend to show better and more intumescence. This is proven by the fact that the sodium salt of gluconic acid showed the best intumescence.

4.2.   The metal complexes of acetylacetone and gluconic acid

Each of the reactions of the metals with gluconic acid yielded a solid metal gluconate product. The metal gluconates were all standardised to determine the exact metal content of the gluconate along with the ratio of metal to organics in the complex. The results are summarised in Appendix M. The water content (crystal waters) was not calculated separately, but taken as part of the organic part of the gluconates. These synthesised gluconates were satisfactory for the comparative use they were intended.

Table 4-2 gives a qualitative assessment of the behaviour of the compounds when exposed to a small gas flame. The copper acetylacetonate/pentaerythritol mixture ignited easily and continued to burn even after the flame was removed. The other acetylacetonate samples were more difficult to ignite and self-extinguished on removal of the flame, while the aluminium, calcium and titanium acetylacetonates did not ignite. Only the copper gluconate ignited, but was self-extinguishing. None of the other gluconates ignited. All the mixtures charred and foamed when subjected to the gas flame, except for the copper gluconate. It melted, bubbled and started to burn when exposed to the gas flame. Only after considerable exposure to heat did it start to foam. The sodium and calcium salts showed the strongest and the copper and zirconium salts the weakest intumescence. In the case of the metal 2,4-pentanedione complexes, vanadium and magnesium performed well, but were not as good as most of the gluconates.

Continued exposure to the gas flame invariably resulted in a "glowing" combustion mode. In some cases, this glowing combustion occurred virtually simultaneously with the intumescence. This combustion led to complete consumption of the char and the formation of a powdery residue in some of the samples. In some instances, notably in the case of

calcium gluconate, the residual ash retained the expanded or foamed character of the original char. Other samples did not even leave ash behind, as was the case for the sodium complexes, the copper acetylacetonate and the antinomy gluconate. For the antimony gluconate sample, this can be attributed to the known volatility of antimony oxides. The copper gluconate left no char, but a few round copper particles (as metal) were left.

Table 4-2   Response of powder samples to the application of an open LPG flame

Pentaerythritol and Acetylacetonate/ Pentaerythritol mixtures										
Metal	Al	Ca	Cu	Fe^{3+}	Mg	Na	Ti	V	Zr	Penta.
Ignites	No	No	Yes	Yes Slight	Yes Slight	Yes Slight	No	Yes	Yes Slight	No
Foam rating	1	3	1	2	3	2	2	3	2	1
Char foam	Black	Black	Black	Black	Black	Black	Black	Black	Black	Black
Afterglow	Yes Slight	Yes Slight	Not seen Simultaneous	Not seen Simultaneous	Yes Slight	Yes	Yes	Yes	Yes	No
Ash foam	Yes White	Yes White	No residue	No Red-brown	Yes White	No residue	No White	Yes Grey	No White	No residue
Gluconate salts										
Metal	Al	Ca	Cu	Fe^{2+}	Mg	Na	Sb	Zn	Zr	
Ignites	No	No	Yes	No	No	No	No	No	No	
Foam rating	2	5	2	3	4	4	4	3	2	
Char foam	Black	Black	Black - Melts	Black	Black	Black	Black	Black	Black	
Afterglow	Yes Slight	Yes Slight	Yes, Self supported	Yes, Self supported	Yes Slight	Yes	Yes Slow	Yes Slight	Yes	
Ash foam	Yes White	Yes White	No Copper spheres	Yes Red-brown	Yes White	No residue	No residue	Yes Grey	White powder	

Char foam rating: 1 = poor; 3 = medium; 5 = very good (i.e. voluminous)

All the DSC/TGA scans for the gluconates, acetylacetonates and its mixtures with pentaerythritol are given in Appendix M. Only the most relevant scans are repeated in the main text. In these scans, an endothermic peak corresponds to melting, evaporation and/or sublimation of the sample or a part thereof and is indicated as a negative DSC response (W/g or mW/mg). A positive DSC response indicates an exothermic reaction. The two exothermic reactions most important to this study are the intumescent (foaming) and the catalytic carbon oxidation reactions. These can be clearly seen from the DSC/TGA data. Figure 4-1 and Figure 4-2 show the DSC/TGA scans for the copper and calcium acetylacetonate mixtures with pentaerythritol. For the copper acetylacetonate mixture, mass loss commences above 165ºC. Rapid oxidation of the resultant char-foam is indicated by the sharp exothermic peak and rapid mass loss around 265ºC. The endothermic peak identified around 190°C, is the pentaerythritol melting. Little mass loss accompanies this endotherm.
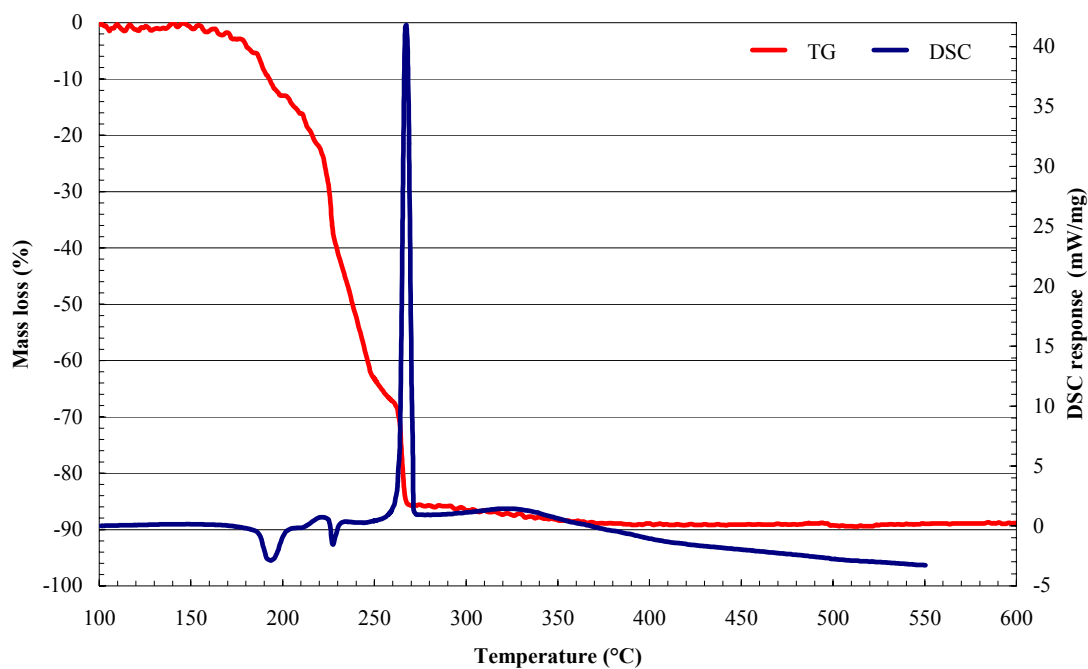
Figure 4-1   **TGA/DSC curves of a 1:1 mass ratio copper (II) acetylacetonate and pentaerythritol mixture obtained at a scan rate of 10ºC per minute in air**
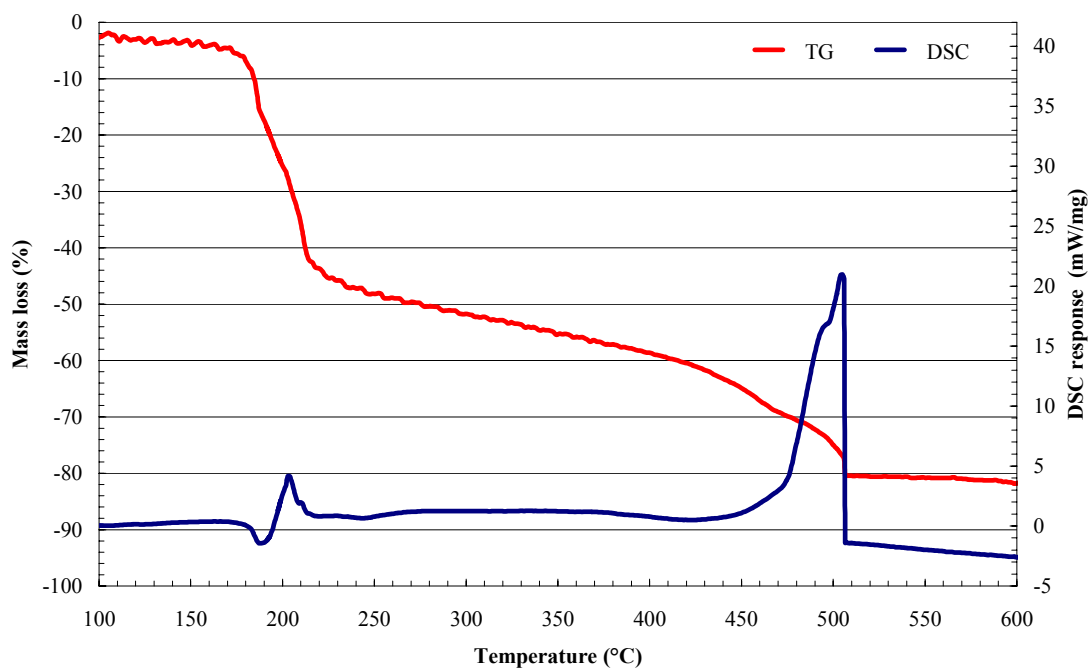
Figure 4-2   **TGA/DSC curves of a 1:1 mass ratio calcium acetylacetonate and pentaerythritol mixture obtained at a scan rate of 10ºC per minute in air**

In contrast, the calcium mixture loses mass from room temperature, with a loss of around 6% at 180°C. The endothermic peak indicating the melting of the pentaerythritol is still visible at 190°C. A small exothermic peak can be identified at 205°C. This is the intumescent (foaming) reaction of the compound. At this temperature, the mass loss curve drastically changes slope and mass loss is much slower. From 420°C onwards, the mass loss curve changes slope again, indicating a more rapid mass loss. The metal catalysed oxidation of the carbon char starts at approximately 420°C as indicated by the strong exothermic peak at 500°C. The peak is only half as high as that of the copper complex and much broader, indicating much slower and thus less catalytic carbon oxidation. This is confirmed by the more gradual mass loss as indicated by the TGA curve.
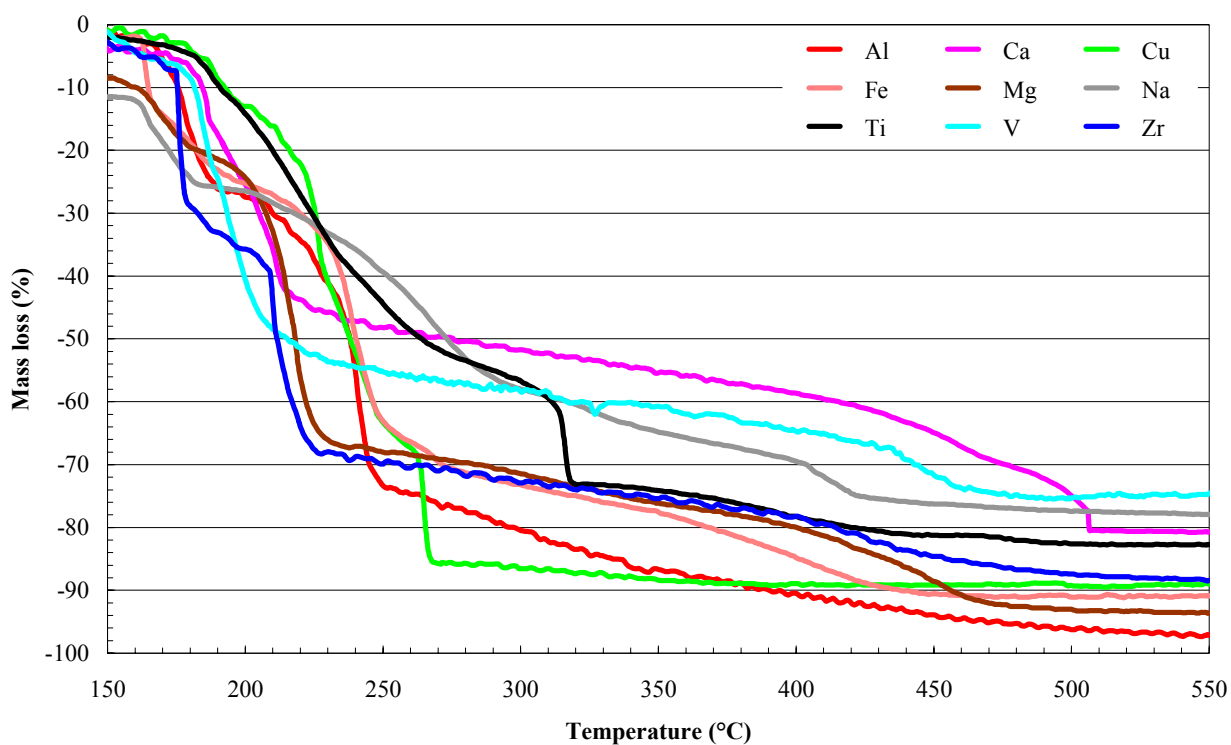
Figure 4-3   Comparison of the acetylacetonate/pentaerythritol mixtures' TGA curves

The TGA data for all the acetylacetonate/pentaerythritol mixtures are shown and compared in Figure 4-3. Except for the sodium acetylacetonate, all the other acetylacetonate compounds mixed with the pentaerythritol showed high temperature stability. This was for both the acetylacetonate compounds on their own and the mixtures with pentaerythritol. The acetylacetonates were stable between 180°C and 250°C (as for magnesium acetylacetonate). With the blending of the compounds with pentaerythritol, the stabilities dropped to between 150°C and 180°C. Copper, titanium and vanadium were the most stable at 180°C. The slow

mass loss of the calcium containing mixture is very clear from the figure. This mass loss also occurs at the highest temperature of all the acetylacetonates tested. DSC data for all the acetylacetonate/pentaerythritol mixtures can be seen in Figure 4-4. The extremely high catalytic activity of the copper can clearly be seen. The high temperature, at which the catalytic carbon oxidation of the calcium containing acetylacetone/pentaerythritol mixture occurs, is evident from the figure. This is the highest of all the acetylacetonate samples tested.
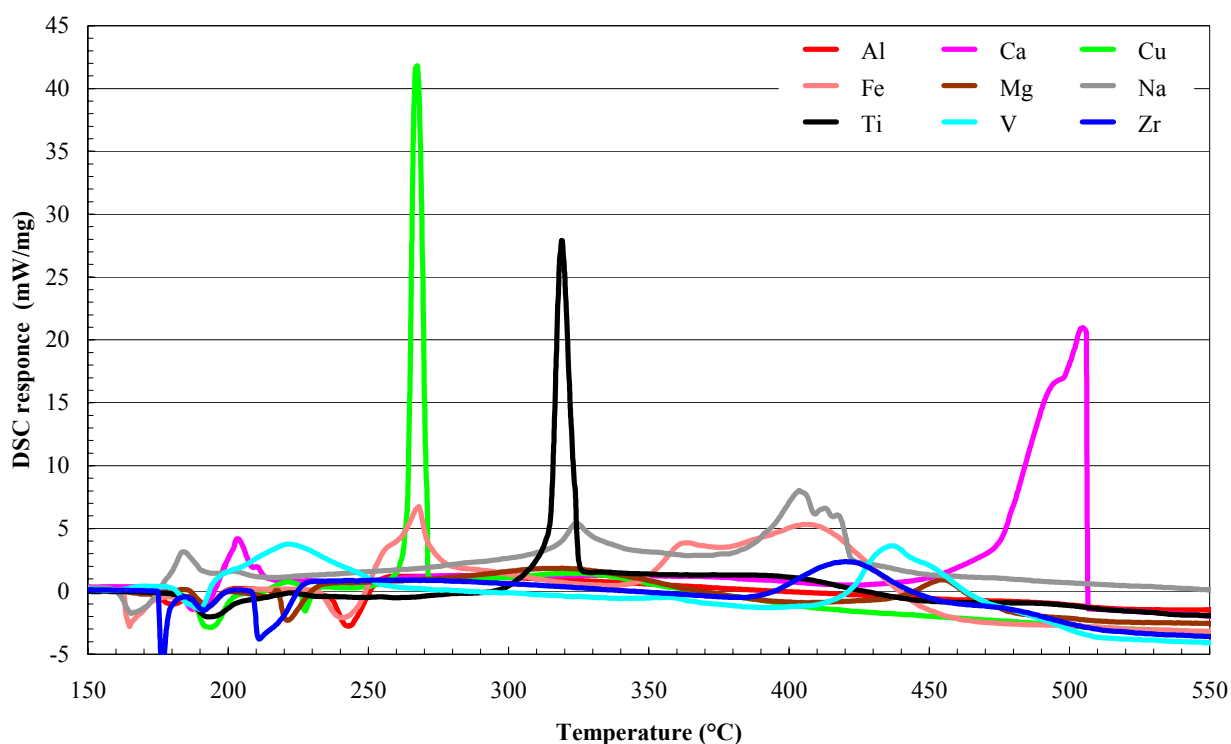
Figure 4-4   Comparison of the acetylacetonate/pentaerythritol mixtures' DSC curves

Figure 4-5, Figure 4-6 and Figure 4-7 show the DSC/TGA scans obtained for the copper, sodium and magnesium gluconates. The decomposition of both the copper and sodium compounds commences at a temperature below 200 ºC. For the copper gluconate, the catalytic char oxidation takes place as low as 350°C with the mass loss curve flattening out at around 400°C. A very sharp exothermic peak and an abrupt mass loss at about 590 ºC characterize the final char oxidation reaction for the sodium salt. The onset of the char oxidation reaction for magnesium gluconate occurs at a lower temperature than the sodium salt, but still higher than copper gluconate. However, the much broader peak suggests that the oxidation reaction is more sluggish than any of the other two compounds.
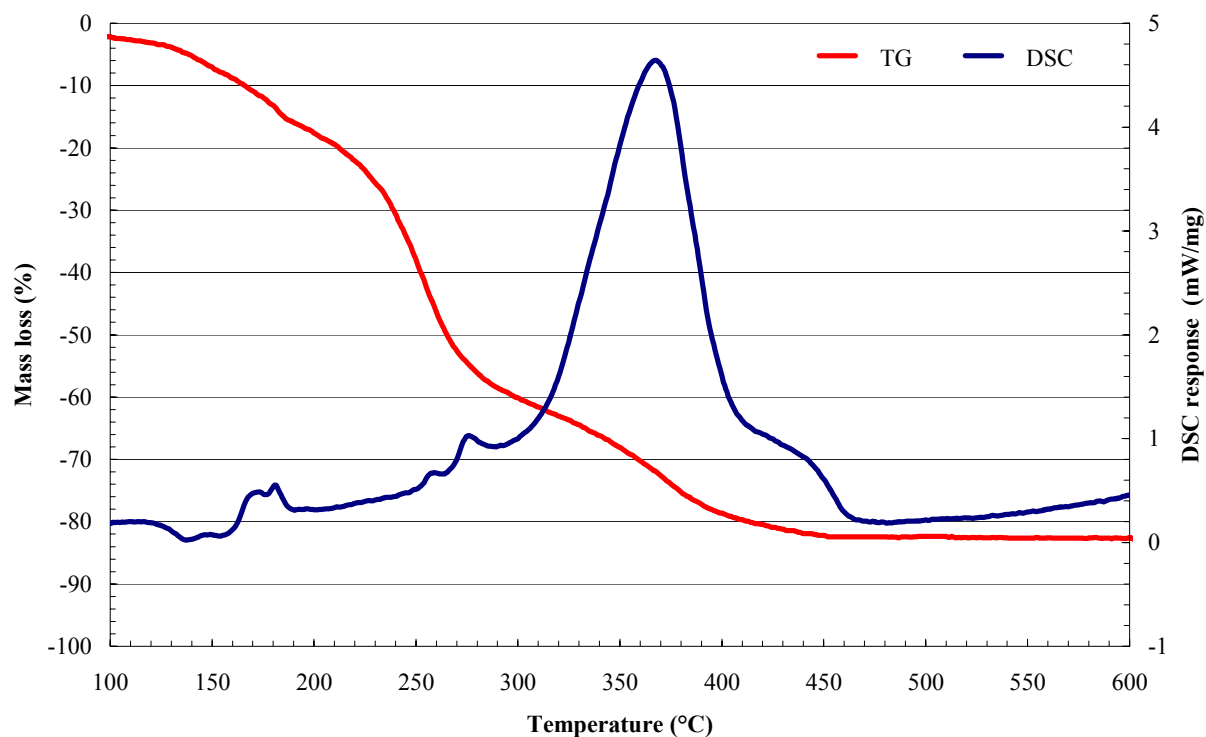
Figure 4-5   **TGA/DSC curves of copper gluconate obtained at a scan rate of 10ºC per minute in air**
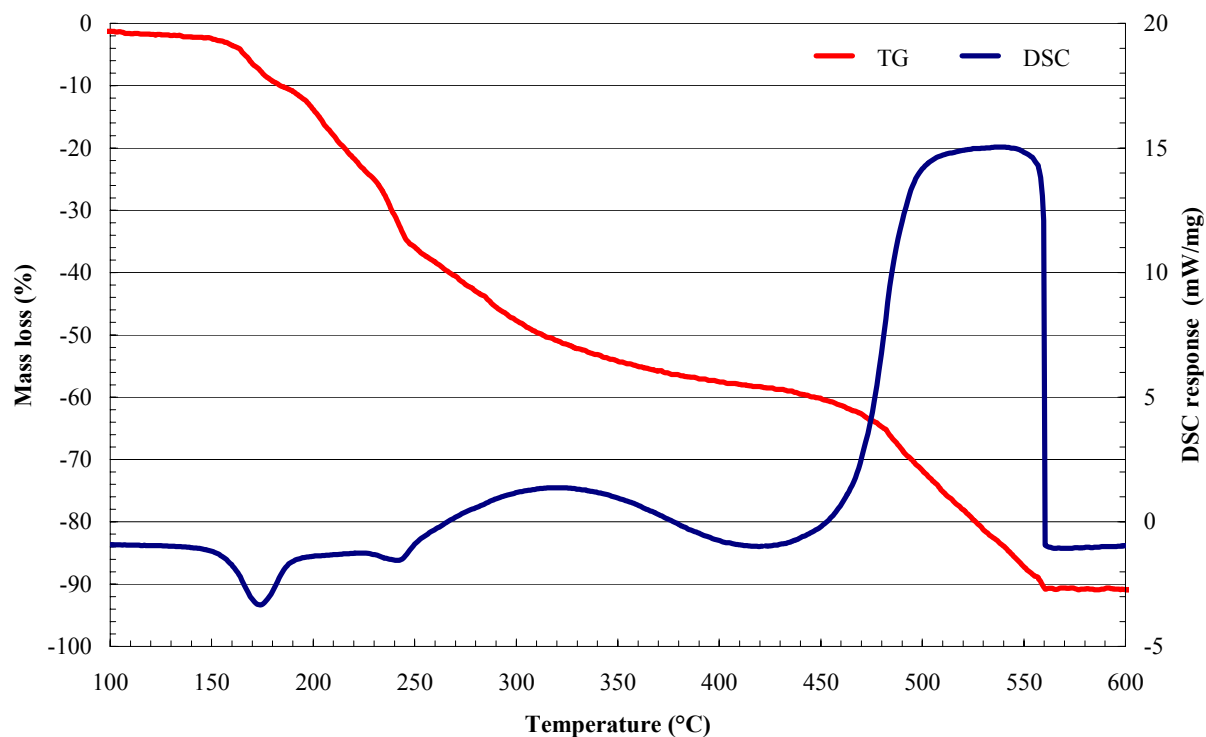
Figure 4-6   **TGA/DSC curves of magnesium gluconate obtained at a scan rate of 10ºC per minute in air**
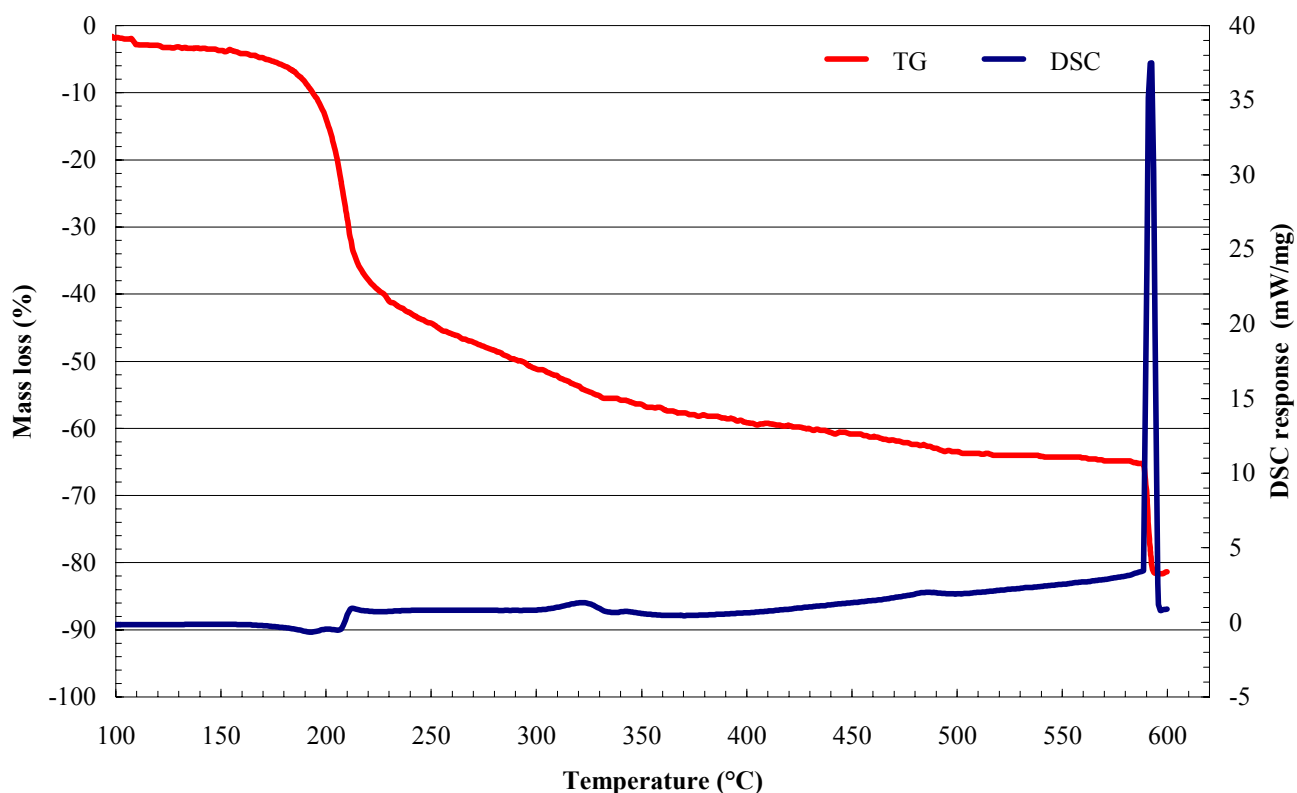
Figure 4-7   TGA/DSC curves of sodium gluconate obtained at a scan rate of 10ºC per minute in air

In order to evaluate the effect of metal complexation, we also obtained a DSC/TGA scan for gluconic acid (as a solution of ca. 50% in water) and they are shown in Figure 4-8. The indicated mass loss of 40% below 200°C by the TGA curve is due to the loss of water in the solution. Some water could have evaporated from the sample holder before the analysis commenced; explaining the reason why the loss is lower than the expected amount of 50%. The endothermic peak at 130°C confirms evaporation of a liquid. The free acid decomposes above 210ºC and the rate of mass loss high above this temperature, but reduces at around 270°C. Char yield is ca. 30% at 280ºC and ca. 10% at 480ºC. More rapid carbon oxidation occurs from 480°C and is completed by 520ºC; accompanied by an exothermic peak at around 510°C. No carbon char is left above this temperature.

The TGA and DSC curves for all the gluconates are separately shown in Figure 4-9 and Figure 4-10. From these figures of the gluconates, it can be seen that none of the compounds are stable at temperatures below 200°C and were less stable than the acetylacetonate compounds. Aluminium, antimony, zinc and zirconium all indicated

considerable mass loss from about 100°C. This is unacceptable for use as a flame retardant in polymers. Calcium, magnesium and sodium gluconates were more stable with magnesium being the most stable of all the gluconate salts. At 177°C, magnesium gluconate showed a mass loss of only 5.8%, while calcium gluconate showed a mass loss of 3.5% at 160°C and sodium gluconate lost 4.85% mass at 170°C. Above these temperatures, the mentioned gluconates degraded quite quickly.
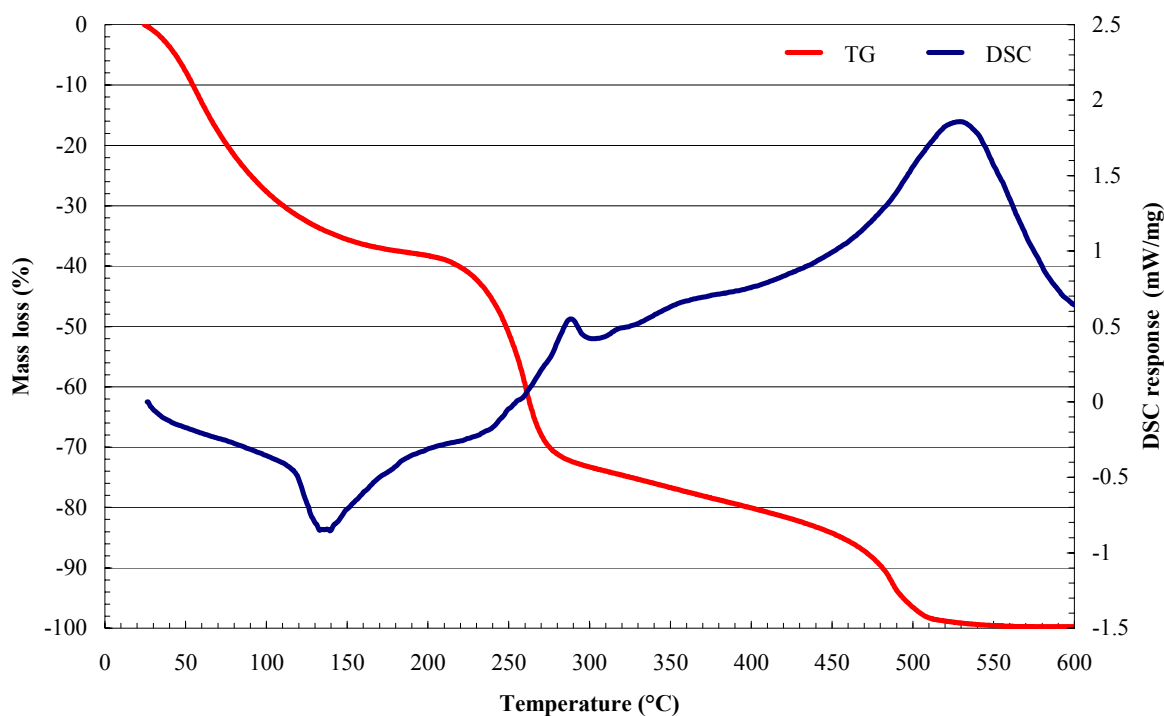
Figure 4-8   TGA/DSC curves of gluconic acid obtained at a scan rate of 10°C per minute in air

The most important information from the DSC/TGA analyses of all the tested samples are summarised in Table 4-3; indicating the onset temperature for the degradation reaction, the peak temperature of the catalysed char oxidation, the peak height of the char oxidation and the half peak width of the char oxidation. The temperatures are listed to the nearest 5°C, while the peak widths are given to the nearest 1°C and the peak height reported to an accuracy of 0.1 W/g.
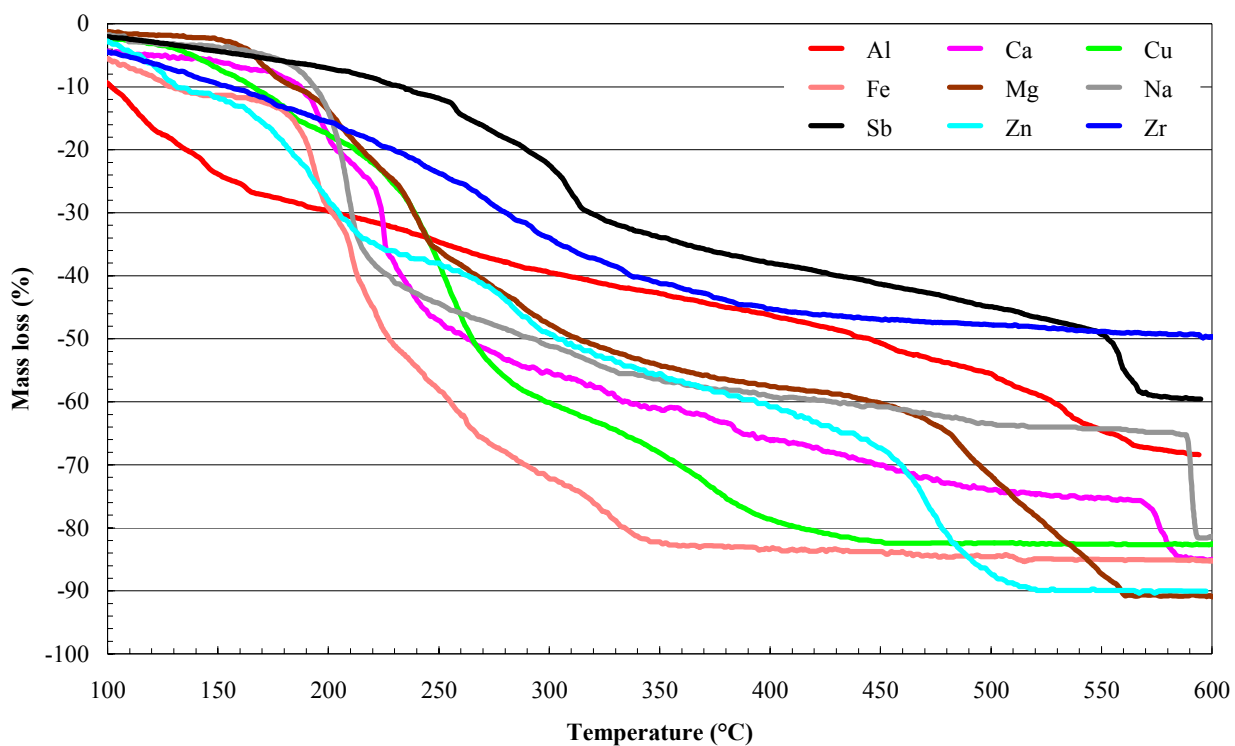
Figure 4-9   Comparison of the gluconic acid salts' TGA curves
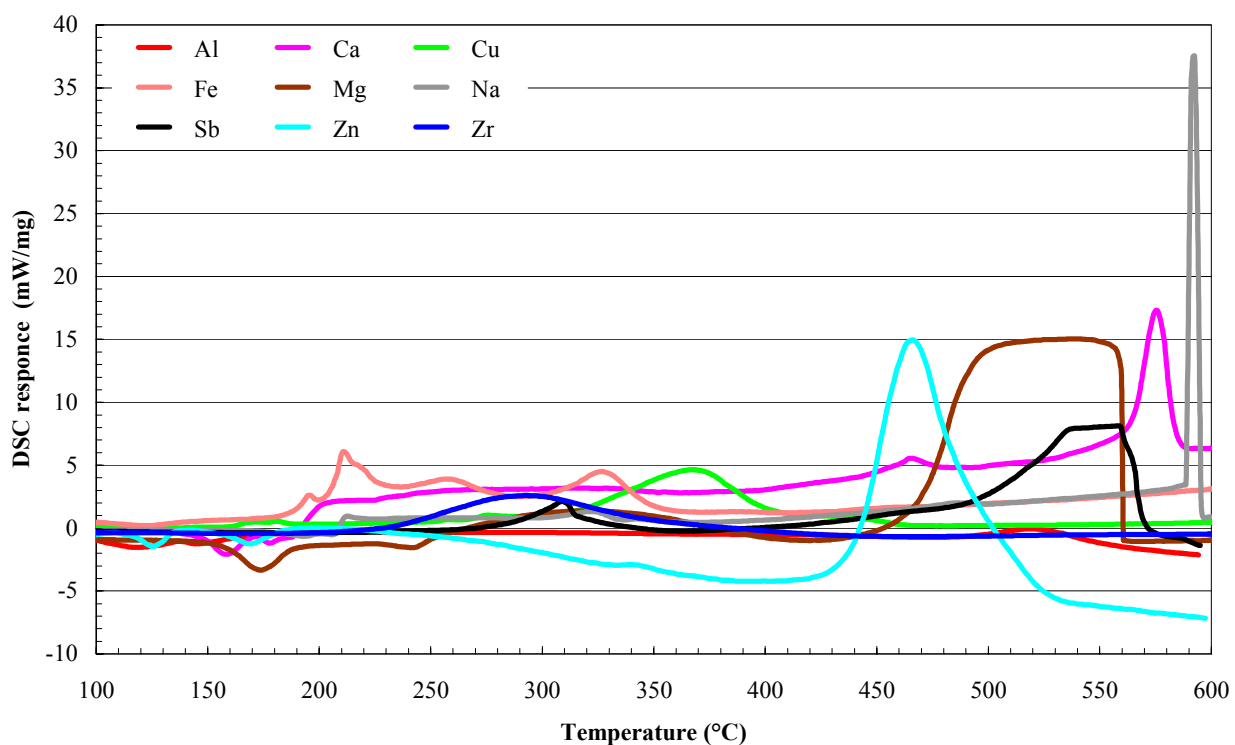
Figure 4-10   Comparison of the gluconic acid salts' DSC curves

Table 4-3   Comparison of the onset and char oxidation temperatures and oxidation exotherm peak width for the metal complexes from the thermal analysis

Complex	T_{onset} degradation	T_{peak} char oxidation	Peak height char oxidation	½ peak width of char oxidation
Gluconates:				
Al	180°C	530°C	1.3 W/g	52°C
Ca	180°C	580°C	11.1 W/g	13°C
Cu	140°C	365°C	3.5 W/g	49°C
Fe	180°C	325°C	2.6 W/g	28°C
Mg	160°C	540°C	16.1 W/g	79°C
Na	200°C	590°C	32.4 W/g	5°C
Sb	220°C	555°C	8.5 W/g	55°C
Zn	160°C	465°C	20.0 W/g	37°C
Zr	120°C	710°C	0.6 W/g	51°C
Acetylacetonate + Pentaerythritol:				
Al	170°C	280°C	3.9 W/g	209°C
Ca	185°C	500°C	22.6 W/g	22°C
Cu	180°C	275°C	41.0 W/g	4°C
Fe	160°C	405°C	6.5 W/g	74°C
Mg	160°C	455°C	2.5 W/g	24°C
Na	160°C	400°C	5.5 W/g	25°C
Ti	185°C	320°C	26.7 W/g	5°C
V	180°C	435°C	6.0 W/g	34°C
Zr	170°C	420°C	3.2 W/g	35°C

The char residue left by each of the gluconates were standardised to obtain the amount of carbon left in the char. The metal residue (as metal oxides or carbonated, depending on the metal) in the char was thus subtracted from the char formed to calculate its carbon content. It was found that antimony gluconate formed 22.6% carbon char at 600°C. This was the highest of all the gluconates. The antinomy was assumed to be in the Sb_2O_3 form. However, Sb_2O_3 is believed to react with O_2 in an oxygen rich environment at low temperatures to form Sb_2O_4 (Li, Archer & Carapella, 1992; Freedman, Dock & Lang, 1992). This explains the apparent high carbon char yield. The second highest char yield was 7.2% at 600°C, formed by zirconium gluconate and worst was zinc gluconate with no carbon char.

When the char formed by the acetylacetonates was standardised to obtain the amount of carbon in the residue, it quickly became apparent that samples left no carbon char when pyrolysed on their own. With the addition of pentaerythritol, titanium oxide acetylacetonate formed 2.1% carbon char at 630 ° C. Both magnesium and copper acetylacetonates left some small amount of carbon residue. None of the other components left any carbon char. This was for a 1:1 mass ratio of the acetylacetonate with pentaerythritol. It is expected that by increasing the percentage of pentaerythritol in the mixture, one would reach an optimum

when the percentage carbon char would be a maximum. This was beyond the scope of the study. The char yields for all the gluconates and the acetylacetonate/pentaerythritol mixtures are summarised in Table 4-4. Since the gluconic acid left only 20% carbon residue at 400°C and none at 600°C, the data in Table 4-4 therefore indicates that complexation of the polyhydroxyl carboxylic acid leads to higher char yields. The reduction in the volatilisation losses implies that the metal cations catalyse carbonisation reactions in the polyhydroxyl compound.

Table 4-4   **Comparison of the carbon char yield at selected temperatures for all the gluconates and acetylacetonate/pentaerythritol mixtures**

Gluconate Complex:	% char @ 400°C	% char @ 600°C	Acetylacetonate/Pentaerythritol complex:	% char @ 400°C	% char @ 630°C
Al	27.8	5.6	Al	0.0	0.0
Ca	19.0	3.4	Ca	53.5	1.0
Cu	5.5	0.8	Cu	0.0	0.0
Fe	3.5	1.4	Fe	0.0	0.0
Mg	35.0	2.1	Mg	15.4	1.4
Na	28.8	6.7	Na	0.0	0.0
Sb	44.1	22.6	TiO	6.6	2.1
Zn	22.9	0.0	VO	0.0	0.0
Zr	10.8	7.2	Zr	9.2	0.0

The observed glowing combustion of the residual char at higher temperatures indicates that the metal residues also catalyze the air oxidation reaction. This was confirmed by the DSC/TGA data and suggests the following approximate order of cation activity:

$$Cu > Fe \approx Zn > Ti > Al \approx V > Na > Ca \approx Mg \approx Sb > Zr$$

Unfortunately, the thermal stability of the compositions tested, as well as the afterglow effect makes them unsuitable for use as flame retardant additives in plastics.

4.3.   The intumescence of the calcium and ammonium gluconates

4.3.1.   The intumescent foam

The theoretical maximum flame temperature of an LP-gas flame in air is 1925°C (Sievert, *s.a.*).When exposed to the high heat of such an open gas flame, calcium gluconate

monohydrate shows profuse foam generation.   Initially the foam is dark brown but on continued exposure to heat, it turns a lighter brown and shrinking slightly, eventually turns white. The white foam is very stable to high heat. It glows with an orange luminosity when held in the gas flame.

Foaming is even more pronounced at certain temperatures when the material is heated in a furnace. Figure 4-11 to Figure 4-13 shows a small sample of the material placed in a polytop™ and subsequently foamed at 300°C in a laboratory furnace. From this series of figures, the enormous change in density at 300°C is evident. A distinctive "caramel" smell is noticeable during the pyrolysis.

Figure 4-11   A small sample (~1 g) of calcium gluconate monohydrate in a polytop®
before pyrolysis in a laboratory furnace at 300°C for 5 minutes

Figure 4-12   The calcium gluconate sample being foamed in the furnace at 300ºC

Figure 4-13   The same calcium gluconate sample after being heated at 300ºC for 5 minutes

When pyrolysed in air, little or no foaming takes place if the calcium gluconate is heated at 100°C, but discolouration is observed. The sample turns a light brown or dark cream colour. Foaming commences at 150°C and is most profuse around 300°C. From 100°C to 300°C, the foam darkens and becomes a dark brown colour at 400°C. Further heating causes the foam to become black and it stays black up to a pyrolysis temperature of 600°C. Between 600°C and 850°C grey (becoming lighter at higher temperatures) and less voluminous foam are formed. A pure white, porous residue is formed when pyrolysed at 1000°C in air.

A hard brittle residue is produced when heated below 200°C. The foamed residue produced between 200°C and 800°C is very soft and shows little mechanical strength. Yet it is pliable and can be pressed into a thin layer or sheet without breaking. The foam is slightly sticky in nature. The white porous foam formed when pyrolysed at 1000°C is soft, but brittle, and forms a powder when broken down.

The foam produced from calcium gluconate monohydrate powder pressed into a lump or pellet is less voluminous than the foam produced from the loose powder. This holds true for both open flame pyrolysis and heating in the furnace. It appears as if the material

decomposition does not generate enough pressure to force open the lump to produce voluminous foam.

Foaming is less pronounced and slower if the calcium gluconate is pyrolysed in the absence of oxygen. As with samples heated in air at 100°C slight burning occurs. However, above 100°C the foam changes to a darker brown more quickly than the samples foamed in air. At a temperature of 400°C the material pyrolysed in nitrogen is completely black. The foams produced at higher temperatures are also black and only at 1000°C is dark grey foam produced. Although the foam produced in nitrogen below 600°C is less voluminous than those formed in air, foam with larger volume is produced in nitrogen at 1000°C compared to air. This foam is also less porous and of a more closed structure than the comparative foam formed when pyrolysed in air.

The ammonium gluconate behaves slightly differently from the calcium gluconate monohydrate. In both air and nitrogen, a dark brown, sticky, caramel like residue is formed when heated below 300°C. This liquid residue hardens on cooling to form something similar to burned sugar in smell, colour, appearance and texture. A black foam char is produced when the calcium gluconate monohydrate is pyrolysed in air at temperatures between 300°C and 1000°C. The foam is most voluminous when pyrolysed at 400°C and is black in colour. At 300°C, the residue is dark brown in colour. Less foam residue is formed when the ammonium gluconate is pyrolysed in air than in nitrogen, due to the oxidation of the carbon-based residue in the air atmosphere.

From the visual comparison of the open gas flame pyrolysis of the filler and calcium gluconate mixtures, it was concluded that the leached silica from Foskor (Pty) Ltd was the best. It produced the highest volume foam and had the least impact on the foam structure while no real increase in afterglow was noticed in comparison to the pure calcium gluconate.

The pyrolysis of the different mole ratio mixtures of the leached silica and calcium gluconate in the glass tubes did not reveal anything. All the samples still foamed too profusely and little of the foam stayed in the tubes. From the visual comparison of the mixtures pyrolysed in the open gas flame, the 1:1 mole ratio of the leached silica to calcium gluconate (11.8% SiO_2 by mass) was identified as the optimum. The leached silica addition at this level had a small effect on foam volume and structure, yet increased the mechanical

strength of the foam and yielded a more voluminous and stronger residue after long exposures to the open gas flame. The foam volume of the mixtures decrease dramatically with an increase in the amount of leached silica. Foams produced at a low leached silica addition showed the best foam structure. The higher the leached silica level, the stronger the resulting foam and the harder the residue after prolonged flame exposure. This was however marginal. The decreasing foam volume was more pronounced and played the biggest role in the identification of the optimum addition level.

A 10% addition of expandable graphite to calcium gluconate was identified as the optimum addition in a similar fashion as with the leached silica. Higher additions of the graphite also caused the foam volume to decrease slightly. The strength of the foam increased with an increase in graphite level. Shrinkage of the produced foam, when exposed to the gas flame for prolonged periods, decreased with an increase of expandable graphite in the mixtures, as did the volume of the resultant residue. However, heating a compressed sample produced a similar volume than a loose powder sample.

It was difficult to do BET analysis on the foam. The sample took approximately 8 hours to analyse and return a surface area value. Some of the foams (e.g. the foam produced at 400ºC) did not return a stable value at all. The reason for this is unknown. The BET analysis returned a surface area of 16.0 m^2/g for the foam produced by heating the calcium gluconate for 5 minutes at 300ºC. This is lower than anticipated. A possible reason for this is the closed cell structure of the foam that will be discussed in detail with the results from the SEM work. The sample that was pyrolysed at 300ºC for 24 hours showed a BET surface area of 12.7 m^2/g.

Several SEM images of the pure compounds and pyrolysed samples are shown in Appendix N. Under SEM, the foam structure for inert and air pyrolysed calcium gluconate samples were similar. The only difference was that the samples pyrolysed in air decomposed quicker than the sample pyrolysed in the inert atmosphere. This implies that the calcium gluconate sample pyrolysed in nitrogen at higher temperatures looked similar under SEM than a sample heated at lower temperatures in air. This is because of the increased carbon oxidation in the air atmosphere causing the degradation not seen in the inert atmosphere.

It was evident from the SEM images that the foams produced at low pyrolysis temperatures are closed cell carbon foams. The wall thickness of the foam cells varied from 15 nm to 50 nm, while the cells (bubbles) varied in size from 10 µm to 100 µm. The SEM pictures (Figure 4-14) show that the carbonaceous foam generated at intermediate temperatures has a closed-cell structure with very thin cell walls. At 400°C in air, the cells were between 50 µm and 200 µm in size. The cell wall thickness was estimated from other SEM photographs and varied from 5 nm to 50 nm. The cell structure started to become open-structured when pyrolysed in air at temperatures above 500°C. The cell wall thickness starts to increase when heated at 500°C and above in air. The cell walls were not as "smooth" and even as the samples pyrolysed at lower temperatures. SEM also revealed that the white residue obtained at 800°C and 1000°C in air has an open-cell structure. The cell walls are grainy and very rough.
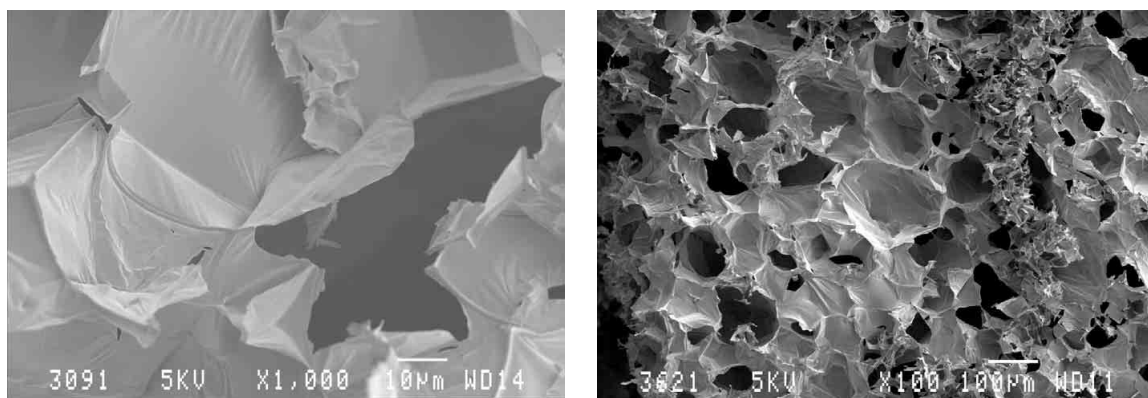
Figure 4-14   SEM images of the foam structure of the oven-pyrolysed sample obtained at 400ºC in air

The 4:1 mass ratio calcium gluconate and leached silica mixtures showed no real differences to the pure calcium gluconate samples pyrolysed at similar temperatures. Even the 2:1 mass ratio mixtures appeared similar under SEM. At a mass ratio of 1:1 gluconate to silica, the material appeared different from the pure gluconate. The foam was also open celled, but the cell walls were less grainy, more dense and "smoother", as if the silica forms "bridges".

The ammonium gluconate foam showed stronger and thicker cell walls than the calcium gluconate. Wall thickness varied from 20 nm to 750 nm when pyrolysed at 300ºC in air. One sample showed a wall thickness of 10.5 µm. The cell sizes are also typically less

homogenous in size. Cells varied from 20 μm to 300 μm in size when foamed at 300ºC in air. The foam produced when ammonium gluconate was foamed at 400ºC in air appeared similar than the foam at 300ºC. There was no apparent difference between the samples pyrolysed in air and nitrogen.
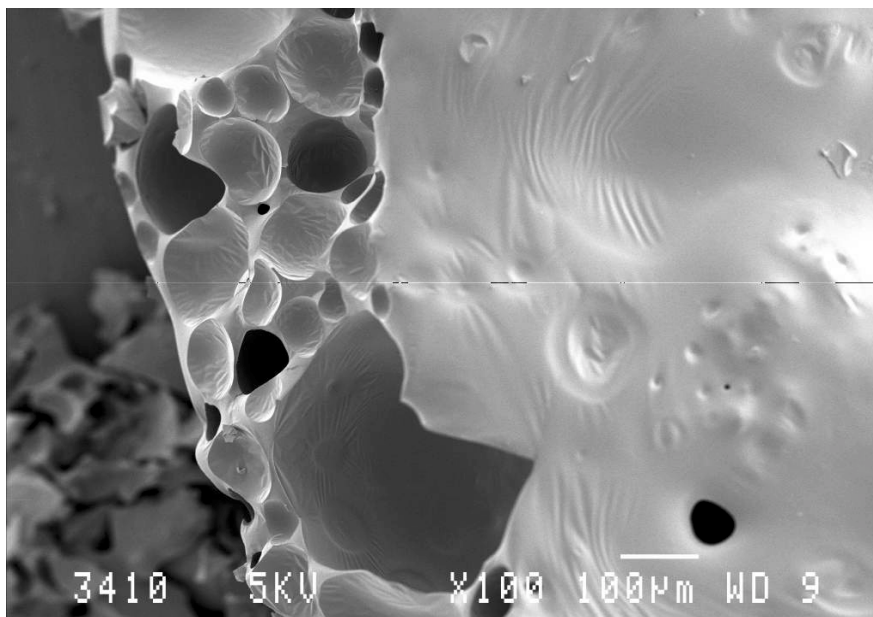
Figure 4-15   AP750 pyrolysed at 400°C in air for 5 minutes

Figure 4-15 shows a sample of AP750 heated at 400ºC in air and Figure 4-16 shows PEN foamed at the same conditions. When comparing the foam structure of AP750 and PEN (commercial samples) to calcium gluconate, all pyrolysed at 400ºC in air, it became apparent that the calcium gluconate foam was more closed celled, thinner walled and the cells packed more densely. The AP750 has a wall thickness up to 10 μm thick and the cells varied from 50 μm to 350 μm in size. The bubbles were scattered through out the material and not "packed" like the calcium gluconate. The cell sizes and wall thickness of the PEN samples were more similar to the calcium gluconate foam than the AP750 foam. Cell sizes were between 50 μm and 200 μm with wall thicknesses below 1 μm. However, the foam was the least dense of all the samples. Both the AP750 and PEN foams were more brittle than the calcium gluconate foam.
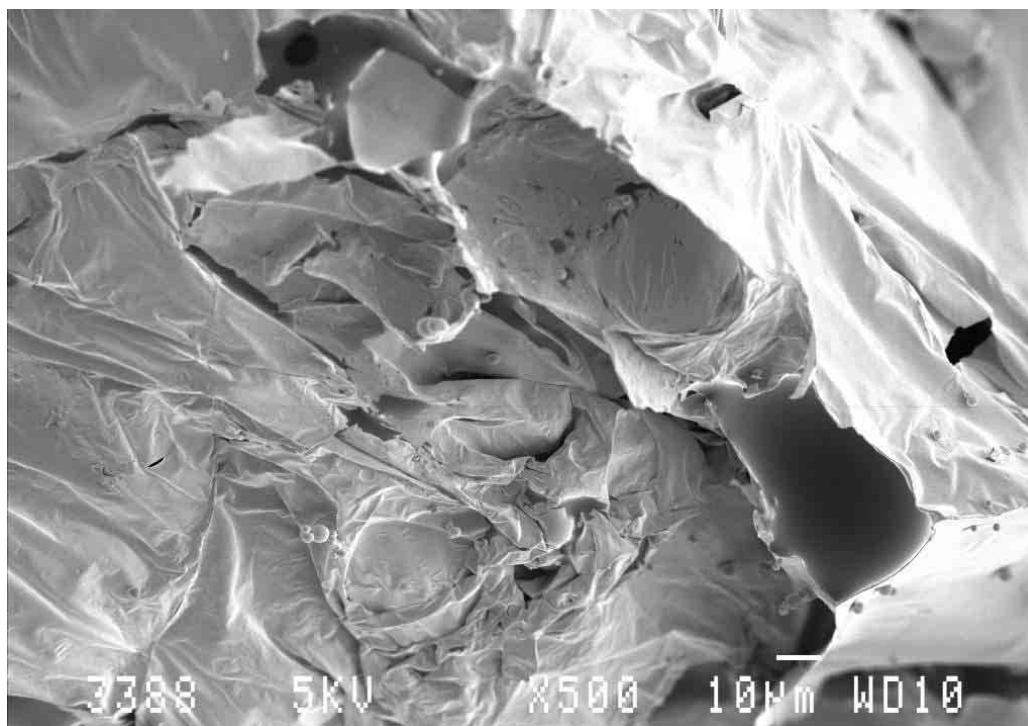
Figure 4-16   PEN pyrolysed at 400°C in air for 5 minutes

4.3.2.   Thermal analysis

Appendix O holds the TGA/SDTA analysis of all the compounds discussed in this section. The thermal analysis of 50% gluconic acid in water is shown in Figure 4-17. The endothermic peak at 70ºC is due to the evaporation of the water. This corresponds to the mass loss of 45% below 220ºC. The loss is lower than the theoretical 50% due to water evaporation at ambient conditions linked to the age of the sample. At 270ºC, a small exothermic peak is evident and corresponds to the 30% mass loss (75% total loss) at 280ºC. This value corresponds exactly with the calculated theoretical loss of all the hydroxyl groups of the gluconic acid as water (which is 45% of gluconic acid or 30% of the total gluconic acid solution). Typically, dehydroxylation is indicated by an endothermic peak. However, this peak may become exothermic due to the cross-linking or double bond formation that may take place in conjunction with the dehydroxylation. The remaining 25% (up to 100% total loss) is due to the carbon in the gluconic acid oxidising (55% of the gluconic acid and 25% of the total gluconic acid solution). The sharp exothermic peak at 530ºC corresponds to the carbon oxidation.
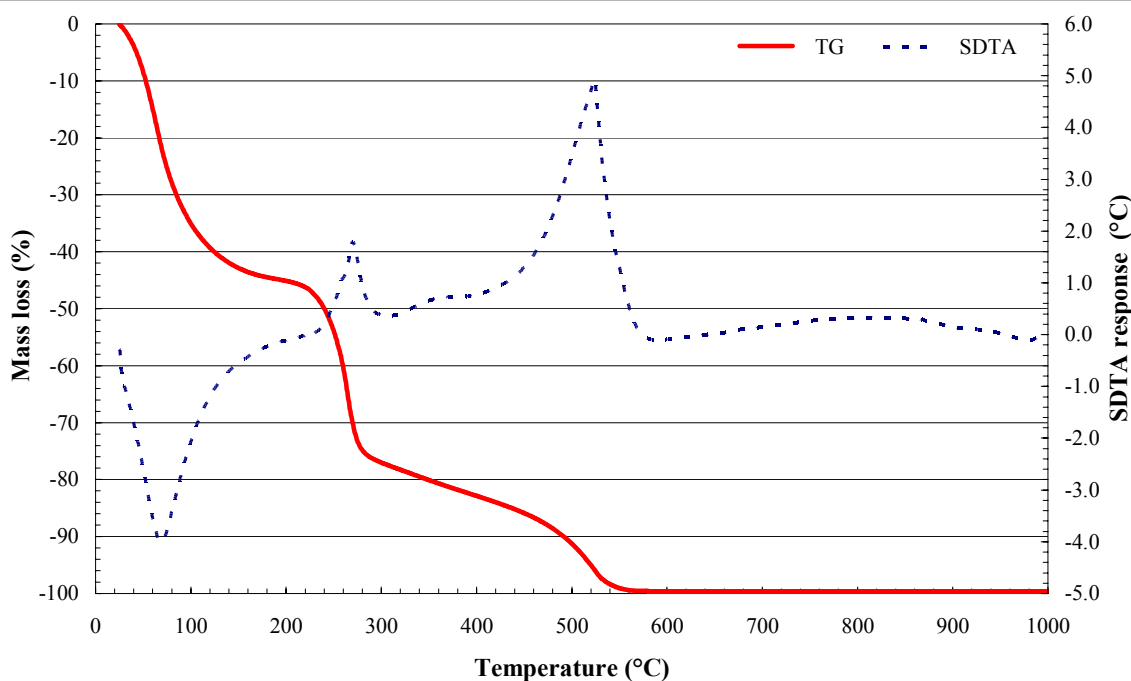
Figure 4-17   SDTA/TGA curves of 50% gluconic acid solution in water obtained at a scan rate of 10°C per minute in air

The thermal analyses for calcium gluconate monohydrate are reported in Figure 4-18 (air atmosphere) and Figure 4-19 (argon atmosphere). The loss of crystal water above 120°C is indicated by the initial mass loss of 4%. This mass loss is associated with an endothermic peak at 150-160°C. The second endothermic peak at 180-210°C probably corresponds with the release of water through dehydration reactions. The overall mass loss in argon of about 42% is only slightly below the expected 44% for removing all the hydroxyl groups as water and the 54% if in addition, one CO_2 is released as well. In the inert atmosphere there is another broad endothermic peak centred at ca 550°C. However, in the air atmosphere there is a sharp exotherm in the DSC signal and a corresponding sudden mass loss in the TGA at approximately 570°C. This corresponds to the catalytic oxidation of the residual carbon by the calcium oxide as observed previously for other base catalysed systems (Focke *et al.,* 2000). This phenomenon is responsible for the afterglow effect in polymers flame retarded with inorganic compounds (Focke *et al.,* 1997). This air-oxidation provides the explanation for the comparatively higher residual mass obtained in an inert atmosphere: more carbon is retained, as it is not oxidised. The mass loss above ca. 650°C for both samples is attributed to the conversion of $CaCO_3$ into CaO.
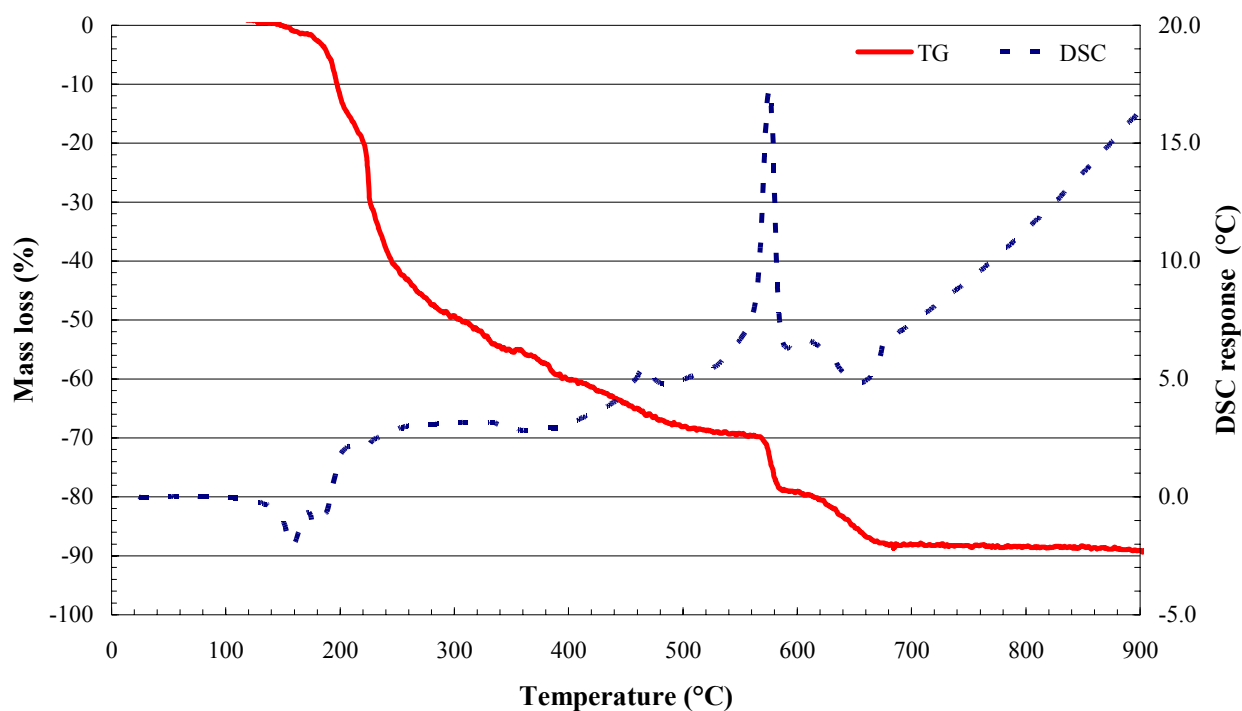
Figure 4-18   TGA/DSC curves of calcium gluconate obtained at a scan rate of 10ºC per minute in air
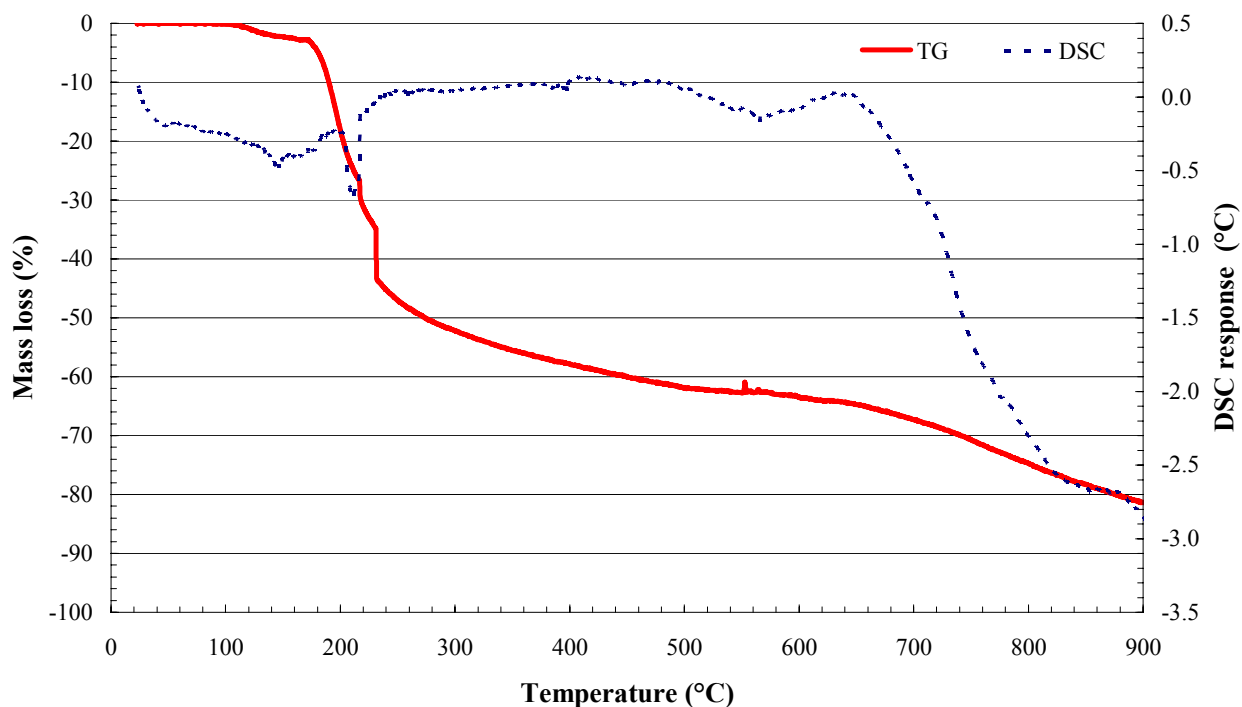
Figure 4-19   TGA/DSC curves of calcium gluconate monohydrate obtained at a scan rate of 10ºC per minute in an inert (argon) atmosphere

The thermal analysis of ammonium gluconate in both air and inert atmosphere are similar. The only difference is the absence of the carbon oxidation peak in the inert sample observed at 510ºC in air. The total mass loss in air is 100% and 83% in nitrogen. At 140ºC, an endothermic peak is evident and should be due to the loss of crystal water. As with the pure gluconic acid (at 270ºC), a small exothermic peak is observed at 240ºC, corresponding to the mass loss of 55% at 280ºC due to the dehydroxylation (loss of hydroxyl groups as water).

The leached silica showed a mass loss of 14% at 1000ºC. An endotherm at 60ºC and mass loss of 6% at 150ºC is due to surface water.

At 260ºC, an endotherm is observed for the expandable graphite, which corresponds to a mass loss of 9% at 280ºC. This is due to the water trapped between the graphite plates. The loss of this water causes the plates to expand, from this the name. A total loss of 91% at 1000°C is observed. Inert materials (e.g. metal traces) may result in the 9% residue at 1000°C. The strong exothermic peak at 880°C indicates the oxidation of the carbon in the graphite.

4.3.3.   The gaseous decomposition products

The idea behind this work is to identify the volatile thermal decomposition products formed when calcium gluconate monohydrate and similar compounds are pyrolysed. This should help us understand the decomposition mechanism of the gluconate.

Acetone was commercially prepared by the dry distillation of calcium acetate until World War I (Everitt, 1911; Howard, 1991; Sifniades, 1985; Case, 1999). The calcium acetate decomposes to form acetone vapour and calcium carbonate as shown in Figure 4-20. The circled section becomes the solid phase, calcium carbonate. Similarly, benzene can be prepared from the dry distillation of benzoates (Everitt, 1911).

Several problems were experienced with the experiments. Firstly, the instrument and instrumental setup was unable to cope with the large volume of water evolved upon the heating of the samples (especially those containing alcohol groups) to 300°C. This masked most of the volatile species. The instrument was also set up in such a way that only species

with relative low molecular weights (Mw < ~200) could be identified. This was not ideal as most of the volatiles expected from the large molecular mass samples, had molecular weights larger than 200. Another problem was the foaming of the samples upon heating. These foams caused the gas tubes to block, resulting in inaccurate readings. Further more, each of the samples produced a large number of decomposition species upon heating, making it difficult for the operator to distinguish between them and identify them. There was an unwillingness to optimise the instrumental setup and experimental conditions to alleviate the problems. However, some useful results were achieved.
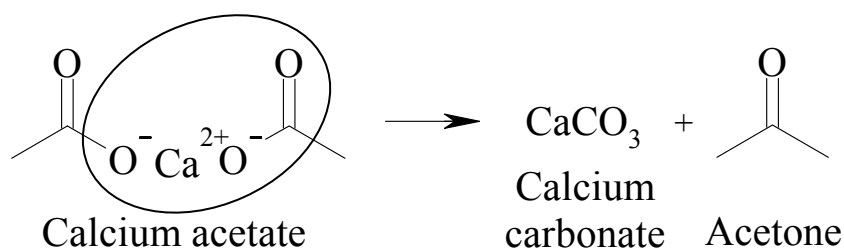
Figure 4-20   Thermal decomposition of calcium acetate

From the mass spectroscopy work, it was identified that the primary gaseous species evolved was water. The amount of water was higher from the samples containing alcohol (-OH) groups as part of the backbone. Only in the case of calcium lactate heated to 300°C was carbon dioxide identified as a decomposition species. None of the other samples showed carbon dioxide evolution. This implies that for the samples where foaming was observed, the foaming was due to the evolution of water, i.e. steam and not carbon dioxide, that was trapped and produced a foamy residue.

In the case of the calcium acetate heated to 300°C, acetone was identified as one of the decomposition products. This proves that calcium acetate decomposes to calcium carbonate and acetone when heated to moderate temperatures. Proving that something similar happens for the other samples was not possible, due to the problems experienced as mentioned above.

For the calcium gluconate monohydrate, small amounts of propanol, tetra hydro furan and other furan like compounds were identified, but were overwhelmed and masked by the water released during pyrolysis.

4.3.4.   The solid decomposition products

From the TEM, no crystalline diffraction patterns for the carbon samples produced from the pyrolysed of the gluconates in nitrogen at 1000°C were identified. Only ring diffraction patterns could be seen, indicating a polycrystalline or amorphous carbon.

Because of the low level of silica addition, it had no real influence on the decomposition species identified in the XRD and IR work. All the XRD and IR spectra of the samples are shown in Appendix P. A graphical summery of the results obtained from the IR spectra are given in Appendix P

4.3.4.1.   XRD analysis

*XRD was used as a **qualitative** tool* and was not employed to quantify how much of the individual compounds were in a sample. The following phases were identified in the powder diffraction patterns of the pyrolysis residues: the precursor compound in its hydrated and anhydrous forms, calcium carbonate, calcium oxide and calcium hydroxide. The presence of calcium hydroxide is attributed to the reaction of the high-surface area oxide with atmospheric moisture during handling and sample preparation subsequent to pyrolysis.

From the XRD analysis it became apparent that all the samples contained large amounts of amorphous material, as indicated by the amorphous halo. This could only be amorphous carbon, as the other decomposition products expected all had clear powder diffraction patterns. This was confirmed by the TEM work, where the carbon was shown not to be crystalline but polycrystalline or amorphous. Samples heated in the inert atmosphere were slower to decompose and contained relatively larger amorphous halo at all temperatures. This was to be expected. Due to the absence of oxygen, the metal catalysed oxidation of carbon to CO and/or CO_2 does not occur. This conclusion is supported by the fact that pyrolysis in air resulted in a higher mass loss than pyrolysis in the inert atmosphere. As mentioned earlier, more carbon is left when oxygen is absent during pyrolysis. It is believed that this abundance of carbon "shields off" the calcium complexes, slowing their decomposition to $CaCO_3$ and CaO. However, oxygen may also play a role in the formation of $CaCO_3$ and CaO.

For the samples pyrolysed in air the results of the XRD spectra indicate the following sequence of events: The dehydration of the mono-hydrate commences at ca. 150°C and is essentially complete at 200°C. Calcium carbonate formation starts at 300°C and is converted to the oxide above 750°C. Essentially the same sequence of events is observed for the samples pyrolysed in a nitrogen atmosphere except that the onset of $CaCO_3$ formation is delayed until about 700°C.

Air atmosphere

The species identified in each of the air pyrolysed samples are listed in Table 4-5. It is concluded that the loss of crystal water (at around 150°C) starts the intumescence of the gluconate. Further foaming is due to the loss of the compound's hydroxyl groups as water, producing the low-density foam. At temperatures of 300°C and above, $CaCO_3$ is formed along with the amorphous carbon. The onset of decomposition of $CaCO_3$ to CaO lies between 700°C and 750°C. The $Ca(OH)_2$ identified in all the samples above 750°C is due to the absorbance of water by CaO to form $Ca(OH)_2$. This water was absorbed during preparation of samples for XRD analysis. Some of the XRD analysis of a number of samples heated in air is presented in Figure 4-21 to Figure 4-24.

Table 4-5   Decomposition products of calcium gluconate monohydrate (air)

Temperature	Products in residue					
	Amorphous carbon	Calcium gluconate monohydrate	Calcium gluconate	$CaCO_3$	CaO	$Ca(OH)_2$
100°C	✓	✓				
150°C	✓	✓	✓			
200°C	✓		✓			
250°C	✓					
300°C	✓			✓		
400°C	✓			✓		
500°C	✓			✓		
600°C	✓			✓		
700°C	✓			✓		
750°C	✓			✓	✓	✓
800°C	✓				✓	✓
1000°C	✓				✓	✓

✓   Species Identified
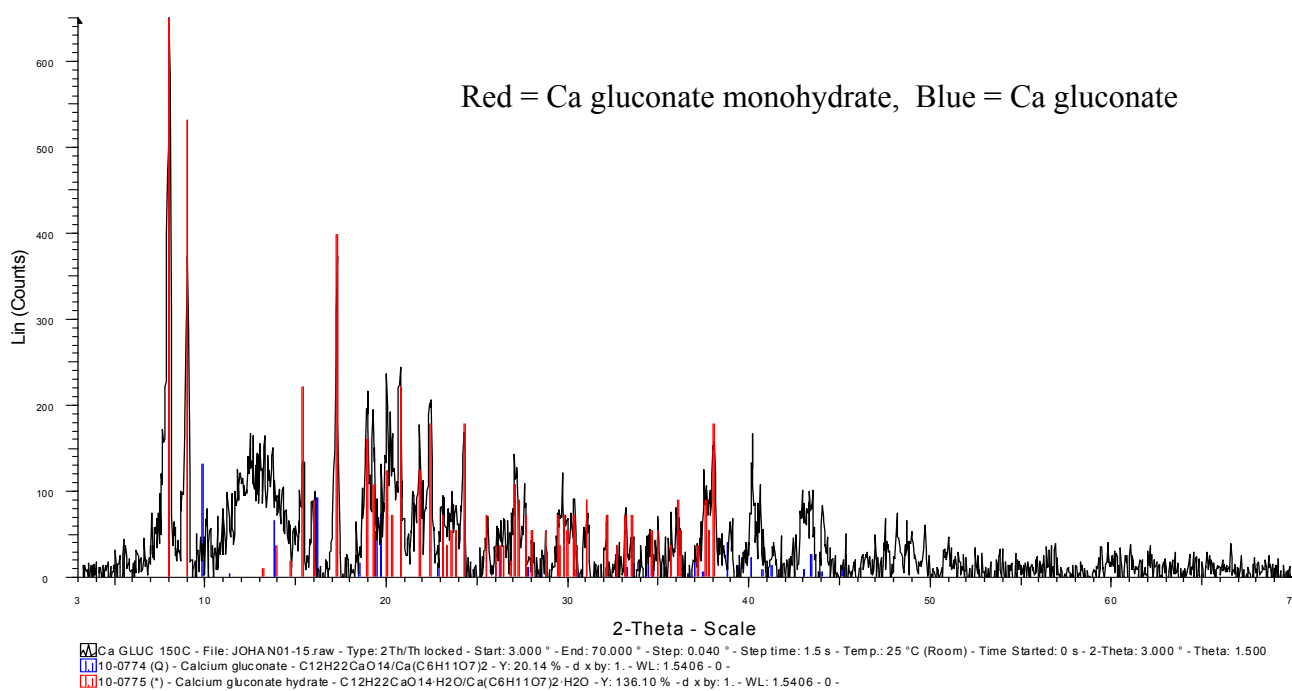
Figure 4-21   Calcium gluconate monohydrate heated at 150°C for 5 minutes (air)
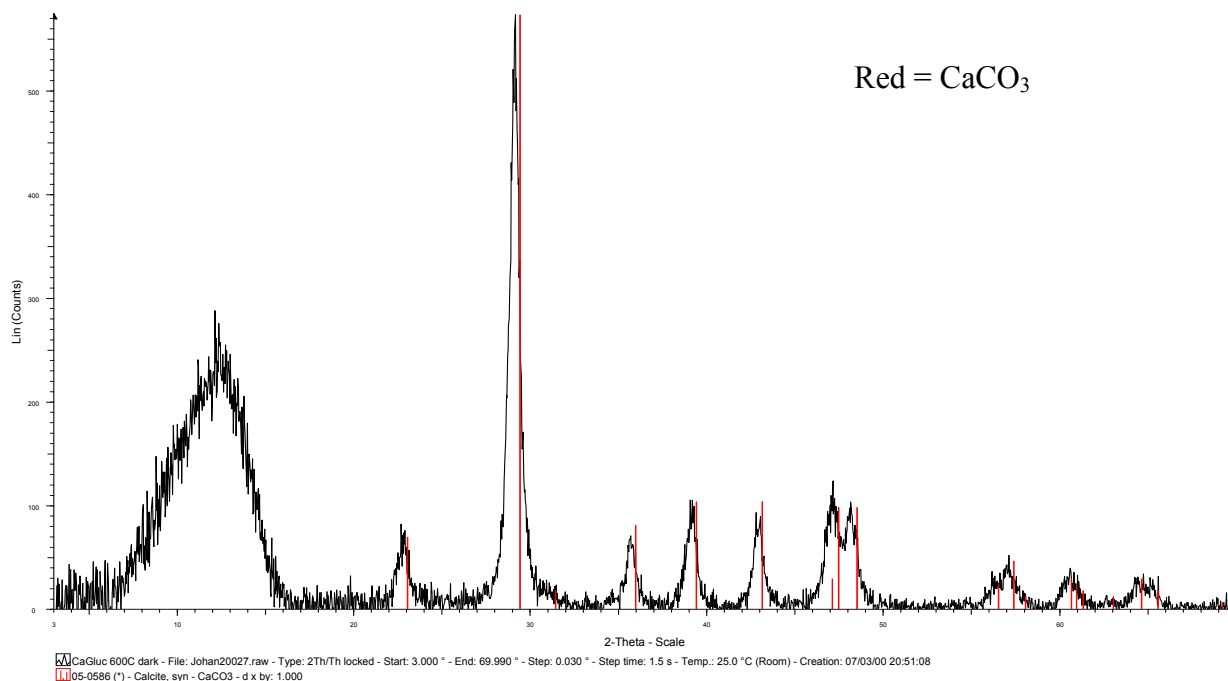
Figure 4-22   Calcium gluconate monohydrate heated at 600°C for 5 minutes (air)
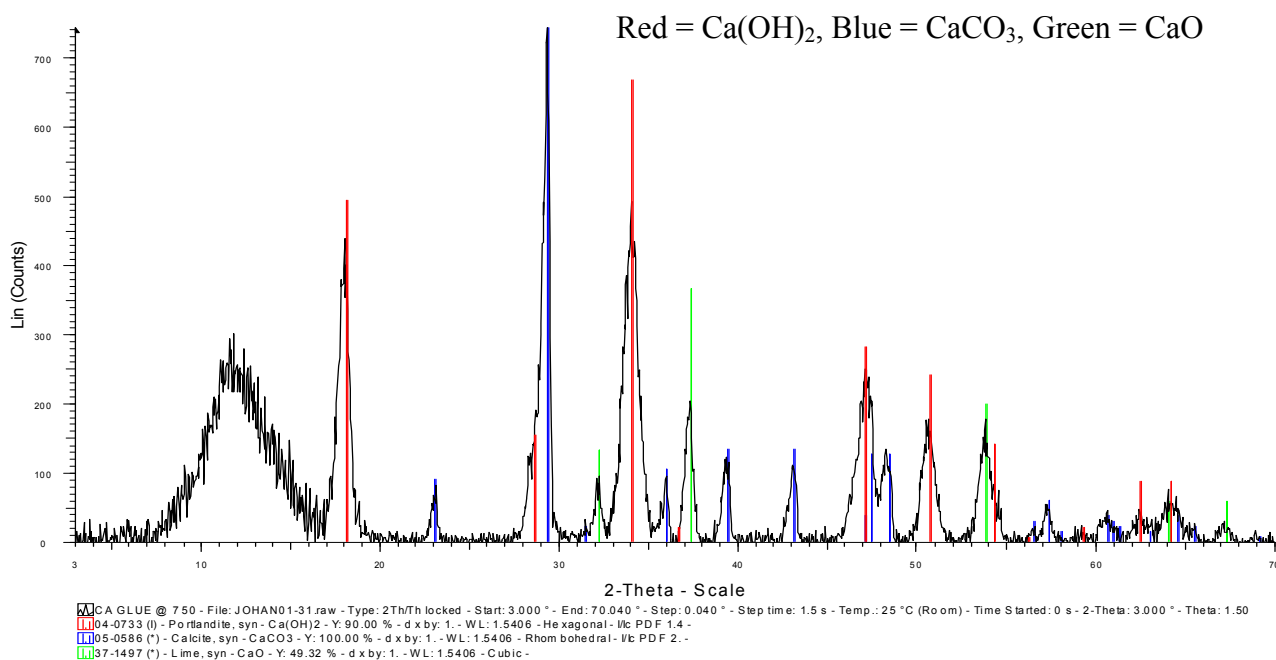
Figure 4-23   Calcium gluconate monohydrate heated at 750°C for 5 minutes (air)
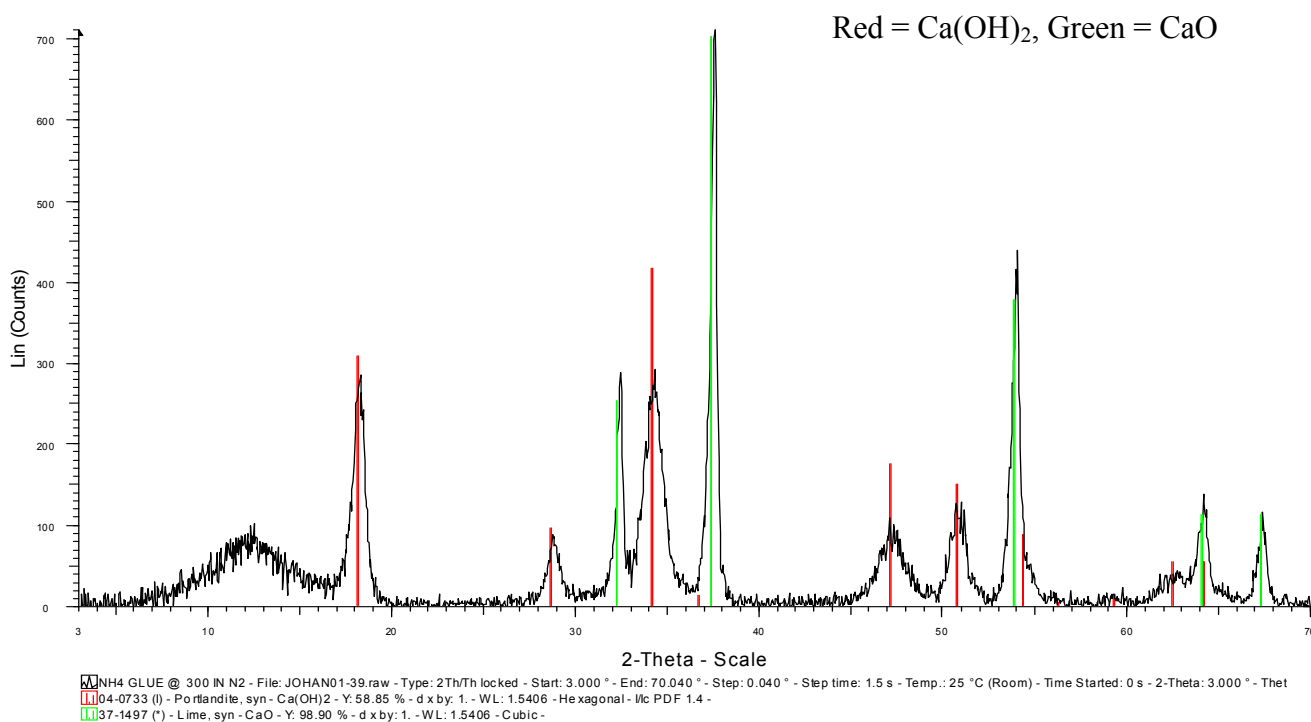
Figure 4-24   Calcium gluconate monohydrate heated at 1000°C for 5 minutes (air)

Inert atmosphere

The intumescence of the gluconate is similar in the inert atmosphere to that in air. As mentioned before: the samples show relatively more amorphous carbon and slower decomposition. The decomposition products confirm this, as listed in Table 4-6. Figure 4-25 shows some of the XRD data of the samples heated in the inert atmosphere.

Table 4-6   Decomposition products of calcium gluconate monohydrate (inert)

Temperature	Decomposition products					
	Amorphous carbon	Calcium gluconate monohydrate	Calcium gluconate	$CaCO_3$	CaO	$Ca(OH)_2$
200°C	✓		✓			
300°C	✓					
400°C	✓					
500°C	✓					
600°C	✓					
700°C	✓			✓		
850°C	✓			✓	✓	✓
1000°C	✓				✓	✓

✓   Species Identified

Red = $CaCO_3$
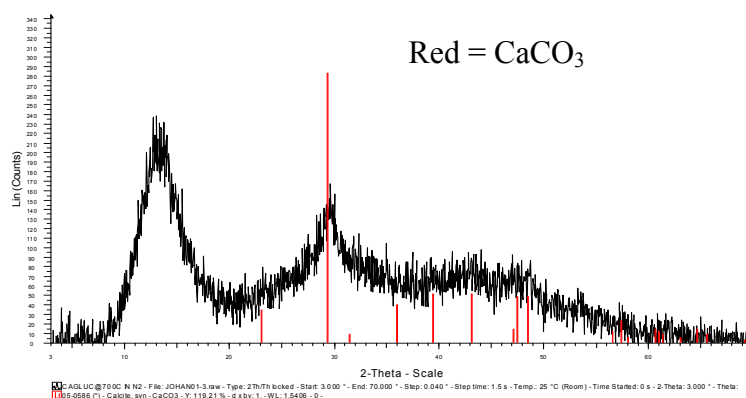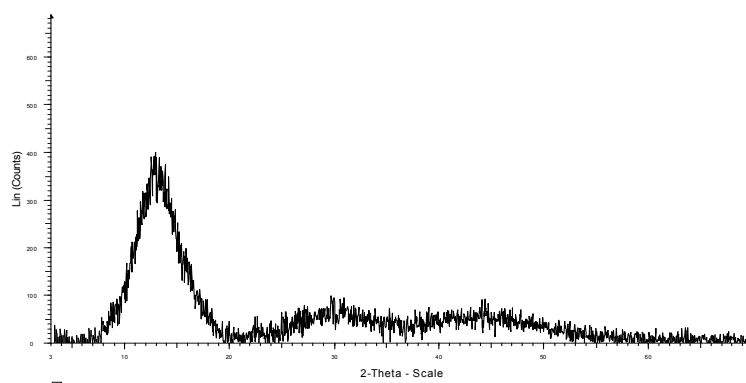
Figure 4-25   Calcium gluconate monohydrate heated at 600°C (top) and 700°C (bottom) for 5 minutes (inert)

From the XRD analysis of the thermal decomposition of calcium gluconate monohydrate in both air and inert atmospheres, the following was established:

- Foaming below 200°C is due to the loss of crystal water

- Foaming above 200°C is continued due to the loss of hydroxyl groups as water

- The primary product of decomposition is amorphous carbon

- More amorphous carbon is retained in the absence of oxygen

- Decomposition is slower in the absence of oxygen

- At temperatures of 300°C and above $CaCO_3$ is formed in air

- At temperatures of 700°C and above $CaCO_3$ is formed in inert atmosphere

- The conversion of $CaCO_3$ to CaO lies between 700°C and 750°C

A graphical summary of the solid decomposition products identified from the XRD data is given in Appendix P

4.3.4.2.   IR spectroscopy

On comparison of the samples pyrolysed in the different atmospheres at the same temperatures, it became apparent that the decomposition is slower in the inert atmosphere than in air. Alcohol groups and hydrogen-carbon bonds were identified at higher heating temperatures in the absence of oxygen. In air, $CaCO_3$, $Ca(OH)_2$ and CaO all formed at lower temperatures than in nitrogen. From the spectrum in Figure 4-26 it can be seen that in the inert atmosphere, more alcohol groups are retained at higher temperatures than in air. Carbonate groups are shown in only the 400°C air spectrum.

At temperatures below 150°C, no significant deviation from the spectrum of the pure calcium gluconate monohydrate can be seen, although the spectra showed a more amorphous material. From temperatures above 200°C, the material began losing alcohol groups and hydrogens. Double bonds between carbon atoms can be identified from relatively low temperatures (200°C in nitrogen and 250°C in air).

Figure 4-27 shows that the concentration of hydroxyl and $-CH_2$ / -CH groups decreases as the pyrolysis temperature in air increases. This is especially clear for the $-CH_2$ / -CH rocking peaks.
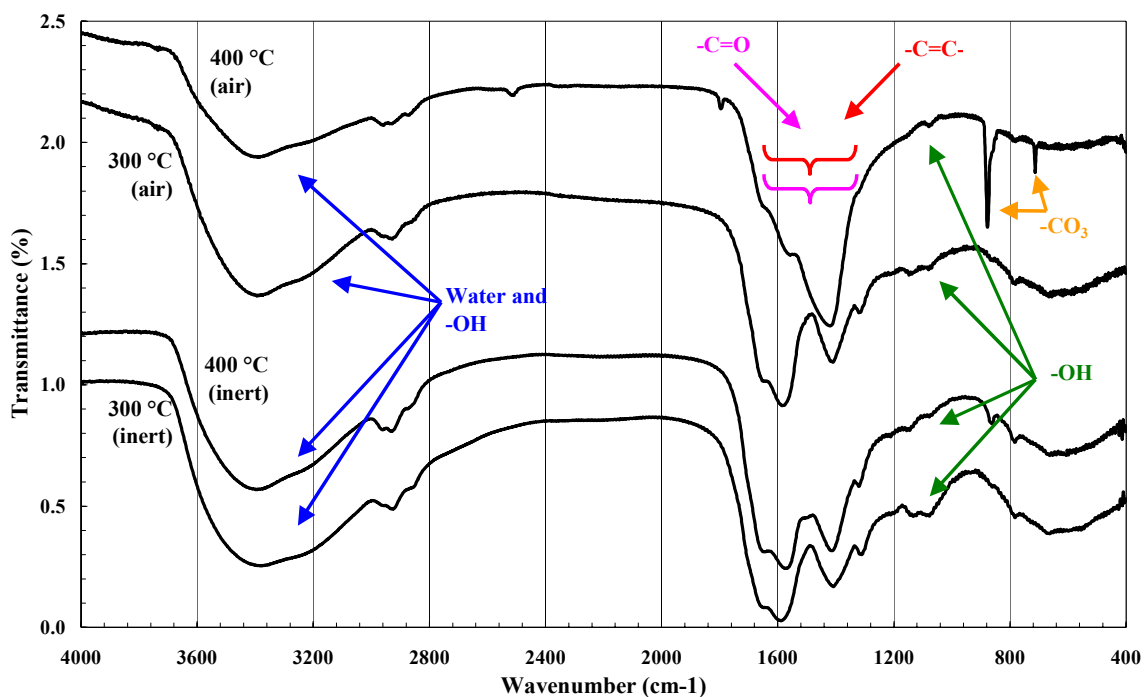
Figure 4-26   Comparison of pyrolysis in air and inert atmospheres
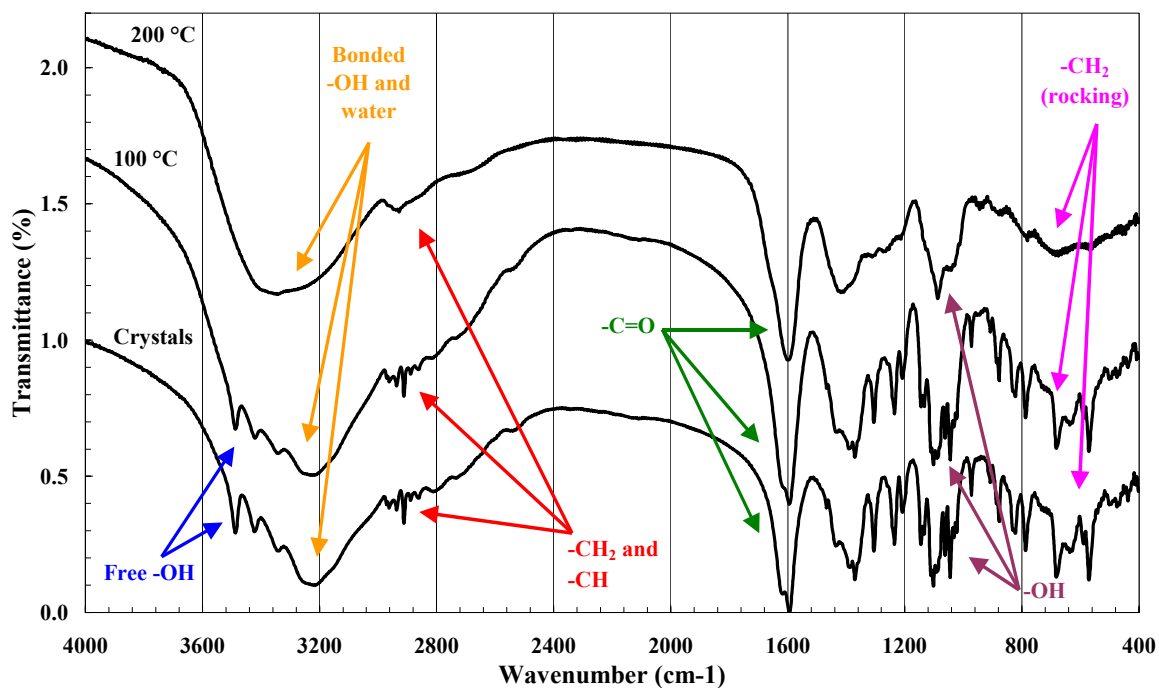
Figure 4-27   Comparison of calcium gluconate monohydrate and samples pyrolysed at low temperatures in air

Above 700°C double bonds could not be observed. The onset for the decomposition to calcium carbonate ($CaCO_3$) lies between 250°C and 300°C in air. For the decomposition to CaO, the onset lies between 700°C and 750°C. The $Ca(OH)_2$ identified in the samples was

due to the absorbance of atmospheric water during the preparation of the samples for IR analysis.

The conversion of calcium carbonate to calcium oxide when pyrolysed in air, is shown in Figure 4-28. The hydroxide identified in the spectra is because calcium oxide strongly absorbs atmospheric water to form the hydroxide.
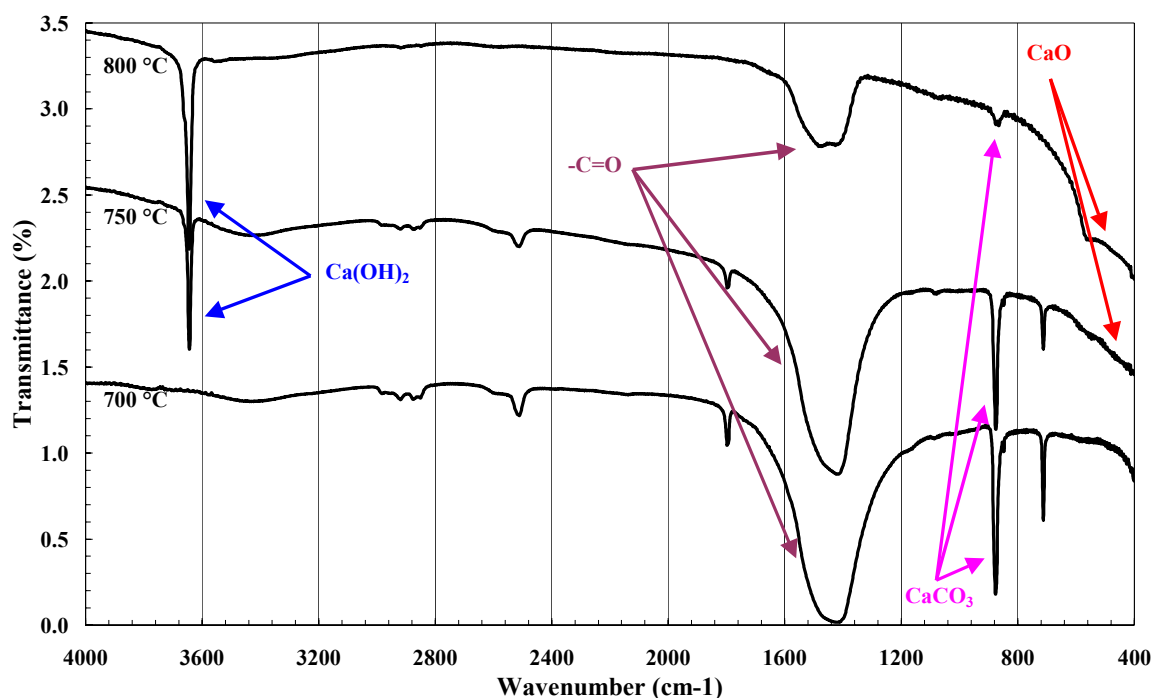
Figure 4-28   Comparison of samples heated at temperatures of 700°C and above in air

At temperatures below 150°C, the spectrum is similar to that of the pure material. Above 200°C, the peaks associated with free (3500 cm^{-1}) and bound (3200 cm^{-1}) –OH groups decrease in intensity indicating a progressive loss in alcohol groups. The absorption peak at ca. 1450 cm^{-1} indicates the formation of carbon-carbon double bonds. This peak can be identified at temperatures as low as 200°C in nitrogen and at 250°C in air. It grows stronger with increasing temperature and then wanes again above 700°C. The onset for the decomposition to calcium carbonate ($CaCO_3$) occurs at about 300°C in air. A sharp peak at 800cm^{-1} is well established at 700°C and is characteristic for calcium carbonate. By 800°C it has virtually disappeared. Simultaneously a sharp peak at 3650 appears that is indicative of the presence of $Ca(OH)_2$. The latter formed when the CaO pyrolysis residue reacted with atmospheric moisture.

From the IR spectroscopy analysis of the thermal decomposition of calcium gluconate monohydrate in both air and inert atmospheres, the following was established:

- Decomposition is slower in the absence of oxygen

- -CH / -CH$_2$ are identified below 400°C in air and below 500°C in inert atmosphere

- -OH are identified below 300°C in air and below 500°C in inert atmosphere

- Carbon-carbon double bonds appear between 250°C and 700°C in air and appear between 200°C and 700°C in inert atmosphere

- From 300°C and upwards, CO_3^{2-} ($CaCO_3$) is formed in air and above 700°C in inert atmosphere

- The conversion of $CaCO_3$ to CaO lies between 700°C and 750°C in air and above 850°C in inert atmosphere

4.3.5.   The molecular mass of the carbon residue

Although the results obtained for the given samples analysed with this technique was not as accurate as expected, some usable information was obtained. In most cases the molecular mass reported was lower than the true molecular weight of the solid phase carbon residues of the samples. The reasons for this are easy to explain and understand. The residues formed by the pyrolysis of the calcium gluconate monohydrate are not readily soluble in THF and water. Only the lower molecular weight species are dissolved and carried to the sample spots. Secondly, the residues showed a high affinity for the stainless steel sample spot holder. They stuck to the sample holder. It was very difficult to volatilise the material with low intensity laser shots. Upon increasing the laser intensity, some of the sample material was volatilised. The bumpiness and high noise level of the background in Figure 4-29, indicates a level of fragmentation of the carbon sample. However, the results showed that the carbon residue is of high molecular weight relative to the molecular mass of the starting material. This implies that some sort of cross-linking was taking place during the pyrolysis of the calcium gluconate. The mechanism for crosslinking could not be explained, but its occurrence could be seen.

The best results were achieved with the following procedure: DHB was used as matrix and dissolved in THF. The pyrolysed calcium gluconate samples were shaken up in water. No salt was used with the matrix. The matrix solution was placed on the spot and left to dry. The samples in water were placed on top of the dried matrix and left to dry. The ratio

of matrix to sample was 20:5. A medium to high laser intensity was used and 1000 shots were taken on each sample to report one set of molecules mass data. The results are reported in Table 4-7. All results for a given sample (pyrolysis condition) were used to calculate an average molecular weight for the sample and the molecular weight of the specie in the sample with the highest intensity are reported. The molecular weight of calcium gluconate monohydrate is 448.39 g/mol. A spectrum obtained under these conditions is shown in Figure 4-29.

Table 4-7   Summary of the molecular masses obtained from the MALDI-TOF-MS

Temperature (°C)	Air Atmosphere		Inert Atmosphere	
	Sample Average Mw	Mw specie with Highest Intensity	Sample Average Mw	Mw specie with Highest Intensity
100	478.2	288		
150	479.6	316		
200	535.8	288	457.5	288
300	643.9	760	705.6	550
400	342.2	316	400.1	522
Pure powder	479.4	288		
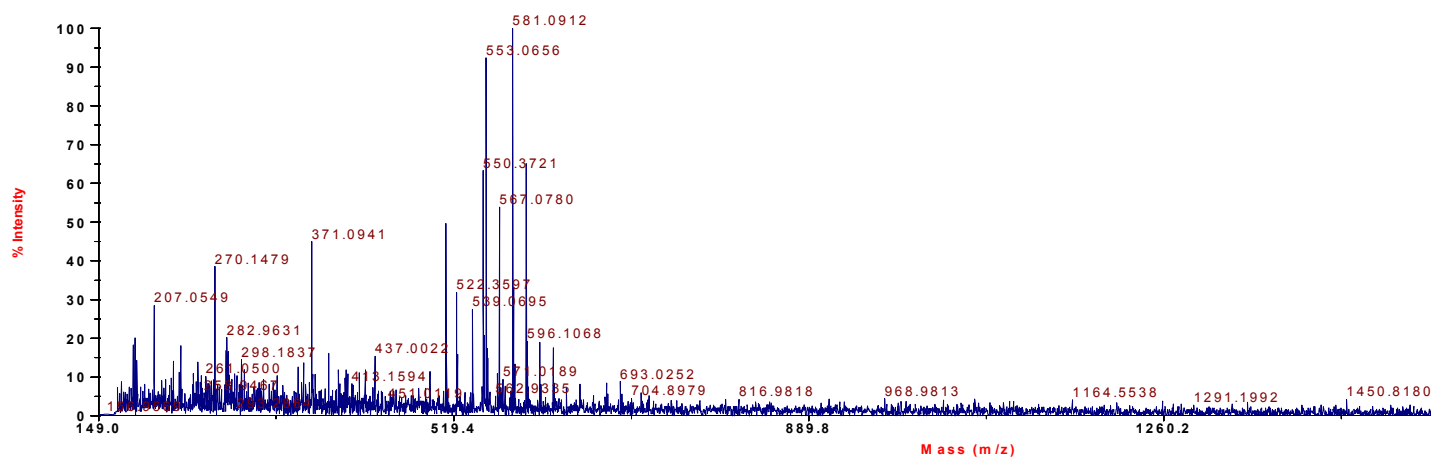
Figure 4-29   MALDI-TOF-MS spectrum of calcium gluconate monohydrate pyrolysed at 300°C for 5 min in air

4.3.6.   Foam density as a function of pyrolysis temperature and time

Figure 4-30 shows the temperature dependant mass loss and apparent density of the foams obtained by the oven-pyrolysis of calcium gluconate monohydrate in an air atmosphere. Mass loss commences above 100°C and the residual sample mass reaches a plateau value of 12.5% at 1000°C consistent with the complete conversion of the calcium

gluconate monohydrate to calcium oxide. The mass loss calculation indicates that complete decomposition to calcium oxide occurs above 800°C. Density decreases from the initial bulk density of 560 kg/m^3 for calcium gluconate monohydrate to a minimum of ca. 2.5 kg/m^3 based on the residual mass and 4.3 kg/m^3 based in the initial mass for the sample pyrolysed at 300°C for 5 minutes. Beyond this temperature, gradual densification of the foam occurs reaching a value of ca. 20 kg/m^3 based on the residual mass and 200 kg/m^3 on the initial sample mass when heated at 1000°C.
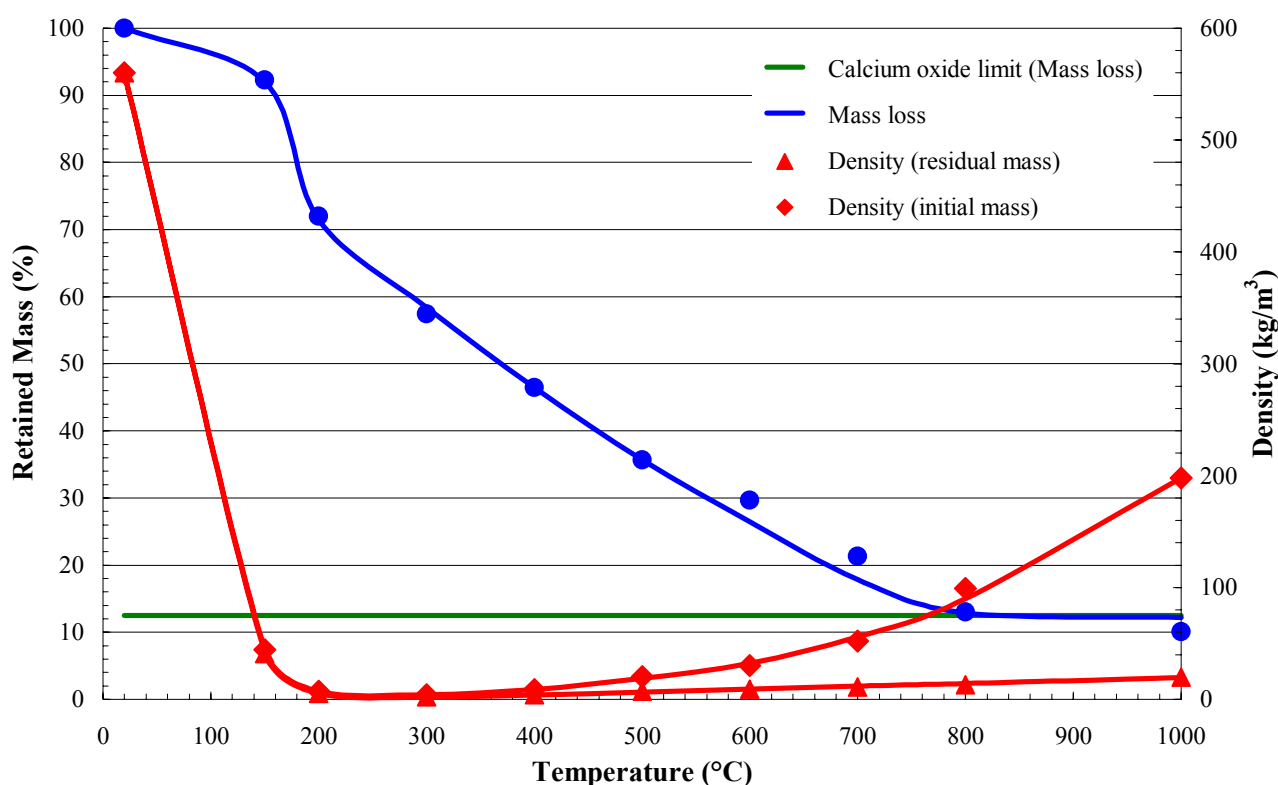
Figure 4-30   Mass loss and density of calcium gluconate foam as a function of temperature, pyrolysed for 5 minutes in air

The time dependent mass loss and density data for calcium gluconate at 300ºC are shown in Figure 4-31. The foam density decreases rapidly from the calcium gluconate monohydrate's bulk density to 4.3 kg/m^3 based on the residual mass and 5.7 kg/m^3 based on the initial mass after 2 minutes. A minimum density of 3.0 kg/m^3 (residual mass) and 5.7 kg/m^3 (initial mass) was observed after 5 minutes pyrolysis time. With increasing heating times, the foam started to densify. After 900 minutes the foam density was 7.1 kg/m^3 (residual mass) and 17.7 kg/m^3 (final mass) and after 1800 minutes, 6.9 kg/m^3 (residual mass) and 20.6 kg/m^3 (final mass). Similarly, the mass loss occurred rapidly up to 30 minutes.

After 2 minutes of heating, the sample retained 75% mass and 53.3% mass after 5 minutes. Mass loss slowed down after 300 minutes of heating. After 1800 minutes of heating the mass loss was 33.3%, short of the theoretical 22.3% mass retained as $CaCO_3$.
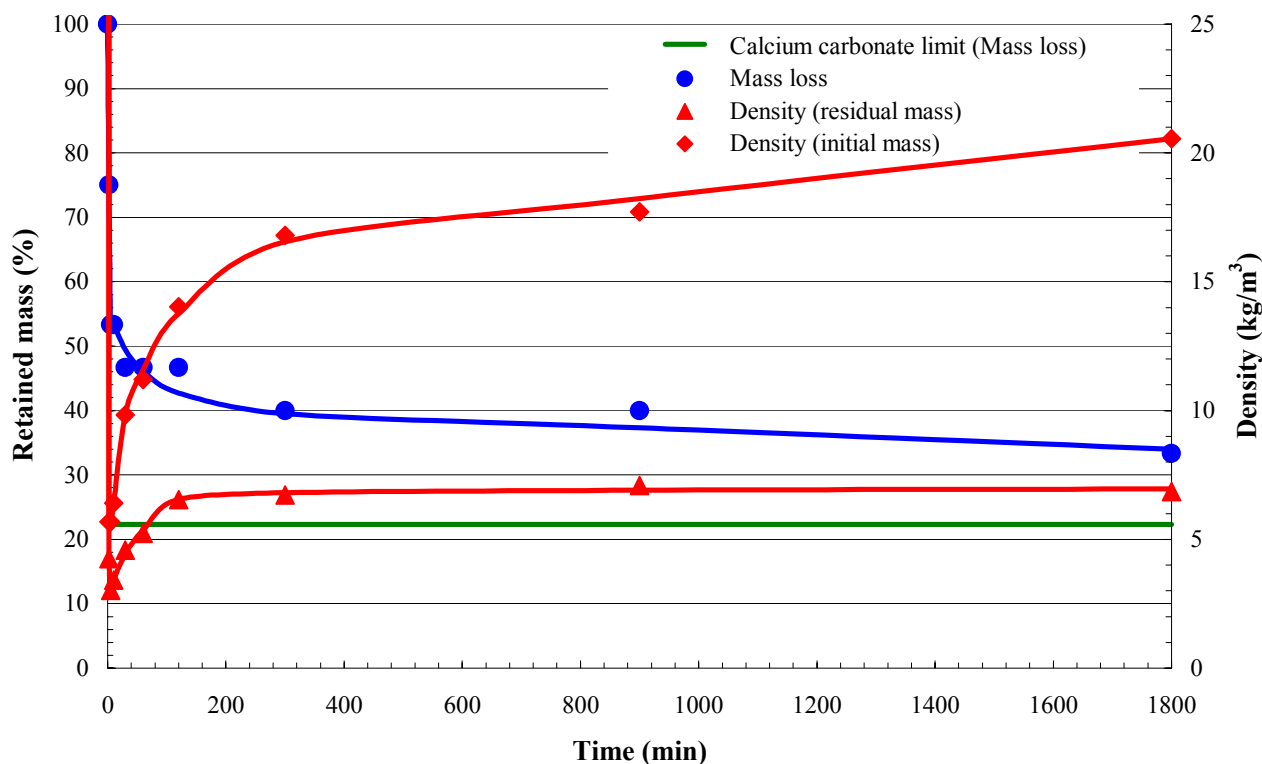
Figure 4-31   Mass loss and density of calcium gluconate foam as a function of pyrolysis time at 300°C in air

4.3.7.   The thermal conductivity of the foam

The thermal conductivity at 300 K (27°C) of three commonly used commercial insulating materials are listed in Table 4-8 (Incropera & DeWitt, 1996). From the results of the analysis, it was found that the thermal conductivity of the foamed calcium gluconate was comparable to foamed polystyrene. It is similar to the materials in Table 4-8. The full results of the tests are listed in Appendix Q.

The heat transfer coefficient for the moulded bead polystyrene block was calculated as 0.04003 W/mK at a mean temperature of 22.52°C and 0.04253 at a mean temperature of 40.02°C. For the block filled with the foamed calcium gluconate, the heat transfer coefficient was 0.04022 W/mK at a mean temperature of 22.52°C and 0.04231 at a mean temperature of 40.02°C. There is only approximately 0.5% difference between the values at the different

temperatures. This small deviation in the thermal conductivity of the polystyrene block and the block filled with the foamed gluconate indicates that the materials are of very similar thermal conductivity.

Table 4-8   Thermal conductivity (at 300 K) and density of insulating materials

Material	Thermal conductivity [W/mK]	Density [kg/m^3]
Polystyrene board (expanded, moulded beads)	0.040	16
Glass fibre (blanket, paper faced)	0.035 – 0.046	16 – 40
Cork (natural material)	0.039	120

The results indicate that the material can be used as a material for insulation from a pure heat transfer point of view. However, the low material strength and integrity of the foam is a great drawback and will adversely affect its applications. Means to improve the foam's material strength without rendering it much less insulative will be advantageous.

4.3.8.   The electric conductivity of the foam

The carbon foam produced by heating the calcium gluconate in nitrogen at temperatures above 850°C was dull black, "soft" and ductile (could be compressed without crumbling) and was of a fine cell structure. The carbon produced from the ammonium gluconate was shinier, of an open cell structure and more brittle than that produced from the calcium gluconate. A possible explanation for the differences is the presence of calcium (in whatever form) in the char produced from the calcium gluconate. In a previous section, it was indicated that the calcium is predominately present as the carbonate when pyrolysed in an inert atmosphere at all temperatures above 300°C, while oxide can be present if heated at 1000°C.

The embedded samples appeared to be tightly packed and homogeneous throughout the resin. If the packing of the sample particles were sufficiently tight (each particle touching the next), a continuous path for the electricity to flow through would be established. This was confirmed when the potential was applied over the tusters (probes) positioned on the

samples. Results for the electric conductivity measurements on all the embedded samples are presented in Figure 4-32.

y = 247416x
R^2 = 0.9973

y = 60406x
R^2 = 0.9886

y = 18746x
R^2 = 0.9795

▲ Graphite   ● Ca Gluconate   ■ NH4 Gluconate

— Linear (Graphite)   — Linear (Ca Gluconate)   — Linear (NH4 Gluconate)

Ampere
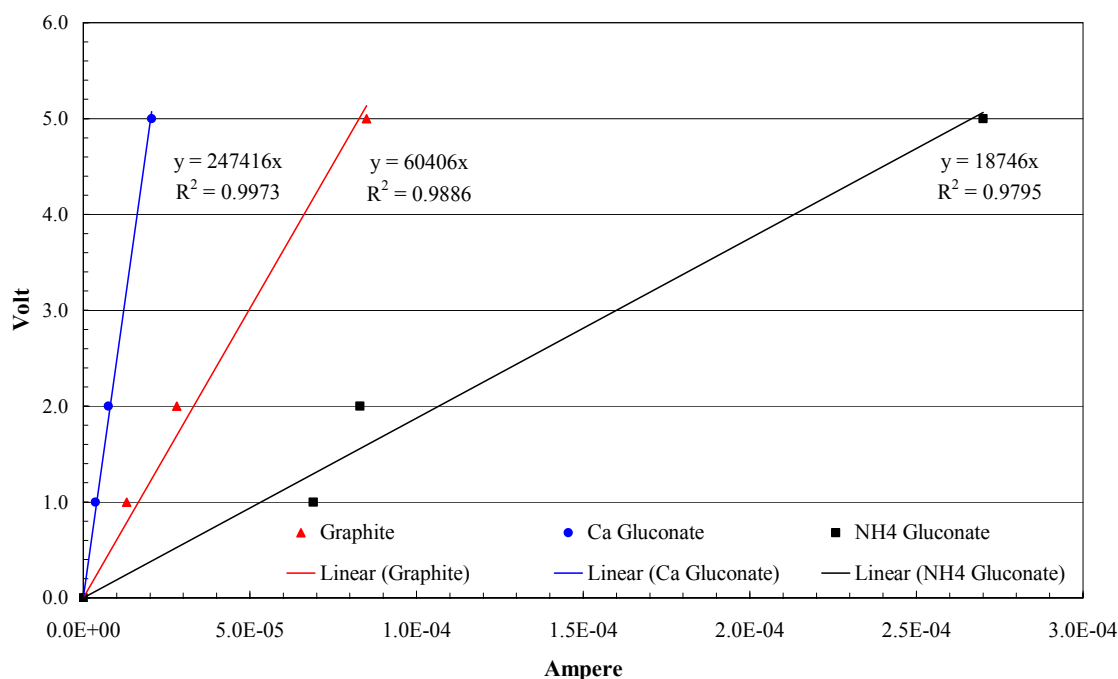
Figure 4-32   Electric conductivity measurements for embedded graphite, coked calcium and ammonium gluconate at 1, 2 and 5 volt

From the data it is concluded that the samples obeys Ohm's Law; which states that the current flowing through an element is directly proportional to the potential applied across it or $V = R \cdot I$ where R is the materials resistance (Rizzoni, 1996). The resistance of the sample depends on the electric path length (*l*), cross sectional area (A) and the materials electric conductivity (σ) according to: $R = \dfrac{l}{\sigma \cdot A}$ However, the electric path length for each of the samples would most certainly not be equal. The particle size and shape of the embedded sample particles for each of the samples were not the same. This implies different packing and thus unequal path lengths. The resistance of the material will be influenced by its path length. A longer path length will lead to a higher resistance. The results were thus only used for comparison. The resistance of the samples were calculated:

Pyrolysed calcium gluconate	247 000 Ω
Pyrolysed ammonium gluconate	19 000 Ω
Graphite	60 000 Ω

Figure 4-33 shows the electric conductivity measurements for the carbon produced from the pyrolysed ammonium gluconate, below 1 volt. The graph for the full potential range (1 V to 5 V) is given in Appendix R.
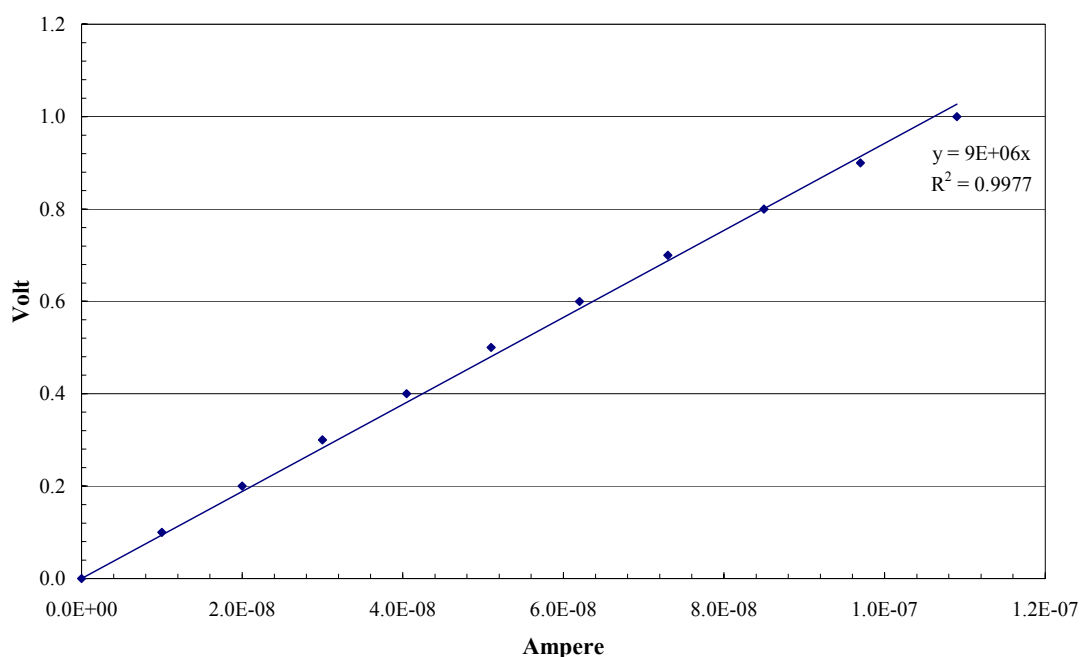
Figure 4-33   Conductivity measurements for embedded coked ammonium gluconate

During the first set of experiments (the 1 V, 2 V and 5 V measurements on all the samples) it was observed that after applying a potential of 5 V to the carbon from the ammonium gluconate for long periods, the current passing through the sample changed. The current slowly started to drop from its initial level after approximately 20 to 30 seconds and then levelled off later. During this reduction in the current, small sparks were observed in the sample. It is believed that the contact points between the different particles in the embedded sample are "burned off" due to the high energy conducted through them. This then leads to an increasing path length – the shortest path now being broken. Accordingly, an increase in the resistance is observed. The data represented in Figure 4-33 is after exposing the material to a 5 V potential for several minutes. Ohm's law is still strongly obeyed by the ammonium gluconate sample, but its resistance has increased to 9 000 000 Ω.

It appears as if the carbon from the pyrolysed ammonium gluconate has a much higher electric conductivity than the others and the carbon from the calcium gluconate much lower than graphite. From the results, it can be concluded that the carbon produced by the pyrolysis of the ammonium gluconate is a good electrically conductive material.

4.3.9.   The fire retardancy of calcium gluconate monohydrate coatings

All the results of the burn-through tests for the painted balsa wood samples, aluminium plates and cardboard sheets are presented in Appendix S. A summary of the results is given in Table 4-9.

Table 4-9   Results form the burn-through tests of the coated balsa wood planks, aluminium plates and cardboard sheets

Coating	Time	Load	Unit load	Resistance	Unit resistance	
Units	sec	g	g/m^2	sec	(sec.m^2)/g	sec/g
Balsa wood planks						
AP750	680	7.34	734	588.6	0.83	83.8
PEN	517	6.64	664	426.1	0.64	64.3
Calcium gluconate	296	7.91	791	205.0	0.26	26.0
Ca Gluconate + Silica	345	8.43	843	254.3	0.30	30.1
Ca Gluconate + Graphite	782	6.47	647	690.8	1.07	107.1
Ca Gluconate + Silica + Graphite	747	7.44	744	656.1	0.88	88.2
Control (untreated)	91	0.00	0	0.0	0.00	0.0
Aluminium plates						
AP750	649	5.51	551	2.3	0.01	0.8
PEN	813	6.04	604	166.0	0.29	29.3
Ca Gluconate + Silica + Graphite	1223	6.39	639	576.3	0.86	86.0
Control (untreated)	647	0.00	0	0.0	0.00	0.0
Cardboard sheets						
AP750	317	15.79	1579	281.5	0.18	17.8
PEN	350	13.21	1321	315.0	0.24	23.8
Ca Gluconate + Silica + Graphite	185	13.61	1361	149.5	0.11	11.0
Control (untreated)	35	0.00	0	0.0	0.00	0.0

Form the untreated balsa wood planks the burn-through temperature was taken as 60°C and the burn-through time average 91 seconds. The burn-through temperature of 60°C was reached after 35 seconds (average) for the unpainted cardboard sheets. For the uncoated aluminium plates a reference burn-through temperature of 80°C was chosen and this was reached after 647 seconds on average. These values were used as reference for the treated samples.

The unit loading for each of the intumescent coatings on the painted samples was determined. This was done by determining the mass coating painted on the plank per unit area (g/m^2). For each coated sample the resistance was calculated as the time needed to reach

the burn-through temperature (60°C for the balsa wood planks and cardboard sheets and 80°C for the aluminium plates), less the average burn-through of the untreated materials. A unit resistance – protection time per unit mass – for each of the samples could now be calculated (sec/g or (sec.m^2)/g). These values are directly comparable for the different coated materials.

From the tests it was established that the calcium gluconate, leached silica and expandable graphite composition were as effective as the AP750 (commercial product) and 25% more effective than the PEN (commercial product) as coating on the balsa wood (see Table 4-9). The gluconate based coating returned a value of 88 sec/g. The gluconate monohydrate and expandable graphite composition returned the highest unit resistance of all the compositions. The calcium gluconate, leached silica and expandable graphite composition performed considerably better than the two commercial products as coating on the aluminium plates. A unit resistance of 86 sec/g were calculated for the gluconate-based composition. On the cardboard sheets, the AP750 performed best. It returned a value of 24 sec/g, more than double the coating prepared from the calcium gluconate composition.

4.3.10. The crystal data of calcium gluconate monohydrate

Calcium gluconate monohydrate is needle like crystals with a very high length to width ratio. These crystals are usually very small and the material is perceived as a course powder. One such a calcium gluconate monohydrate crystal obtained from commercial material is shown in the light microscope image shown in Figure 4-34 and several crystals can be identified in the SEM image (Figure 4-35). More images can be found in Appendix T.

Figure 4-34   Light microscope images of commercial calcium gluconate monohydrate crystals (powder)
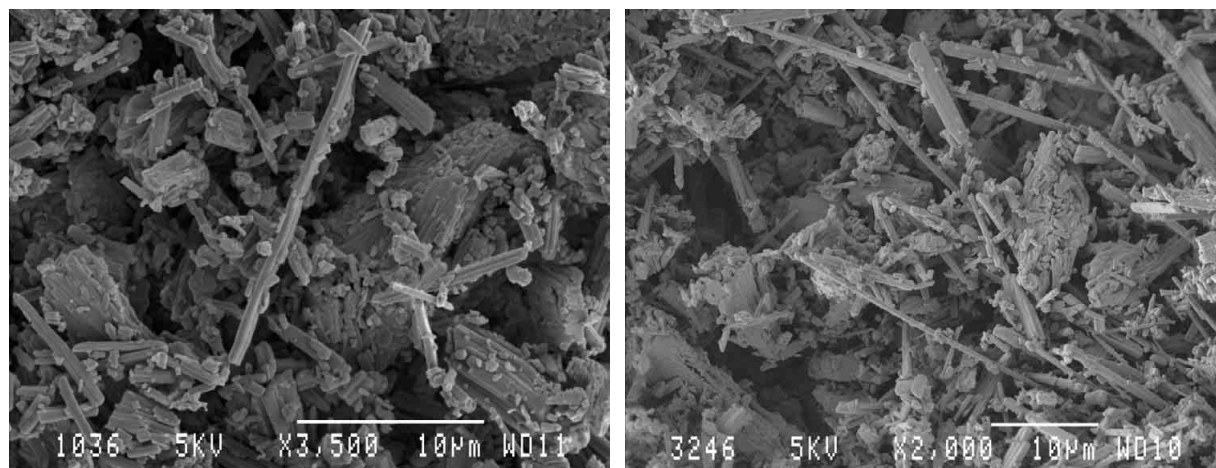
Figure 4-35   SEM images of calcium gluconate monohydrate crystals (powder)

Calcium gluconate monohydrate is one of the most well known gluconates. Yet, it is one of the few for which no crystal data has been published. After all the attempts made, none of the techniques used returned crystals of usable size to obtain the crystallographic data for the gluconate.

The calcium gluconate did recrystallise from the ethanol, methanol and acetone solutions. However, all the crystals were very small. Many small crystals were formed from the solutions with DMSO and acetonitrile and from the water solution where DMSO drops were added. No crystals were formed in the "U"-tube.

All the solutions of the calcium gluconate in water did form crystals when left to crystallise. In fact, many crystals were formed. Unfortunately, the crystals were very small needles. The crystals were in most cases clustered together, with thousands of separate needle like crystals projecting from a single nucleus to form a spiked ball of crystals. Such a sea urchin like ball of crystals was typically 3 mm to 10 mm in diameter.

With the exception of octanol, all the solvent diffusion crystallisation techniques formed crystals. The addition of seed crystals had no influence on the size of the recrystallised crystals. The crystals formed through the diffusion crystallisation of the gluconate from water with ethanol and acetone formed the large crystal aggregates; similar to the balls of crystals formed from the other water solutions. A light microscope image of a piece of such a ball of crystals from the ethanol system is shown in Figure 4-36 and SEM

images in Figure 4-37. From the images, many crystals are visible. Several of the crystals are longer than 1 mm. Some were more than 3 mm in length. However, all the crystals were thinner than 1 µm! None of the crystals could be used for crystallographic analysis.
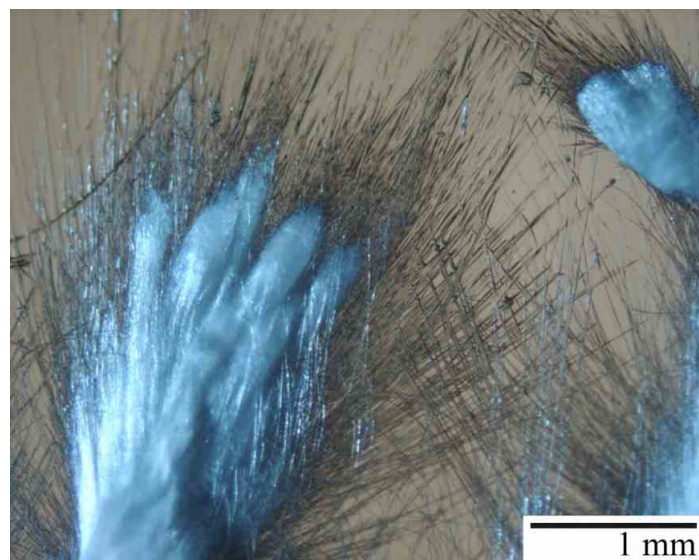
Figure 4-36   Light microscope images of calcium gluconate monohydrate recrystallised from water through diffusion with ethanol
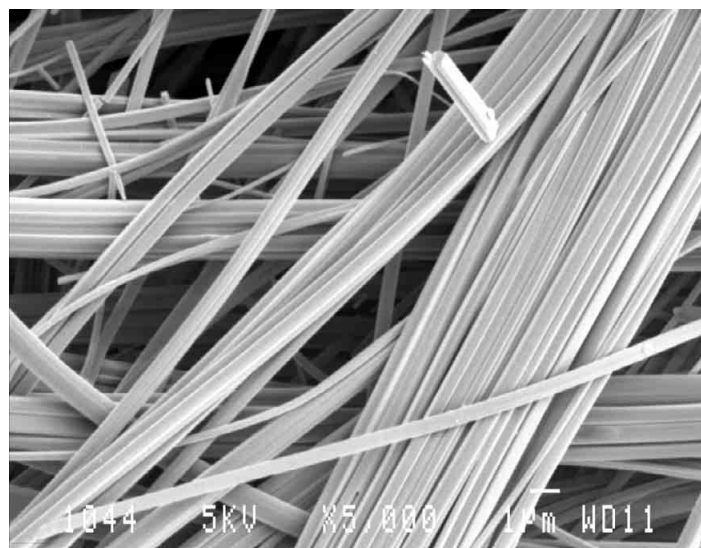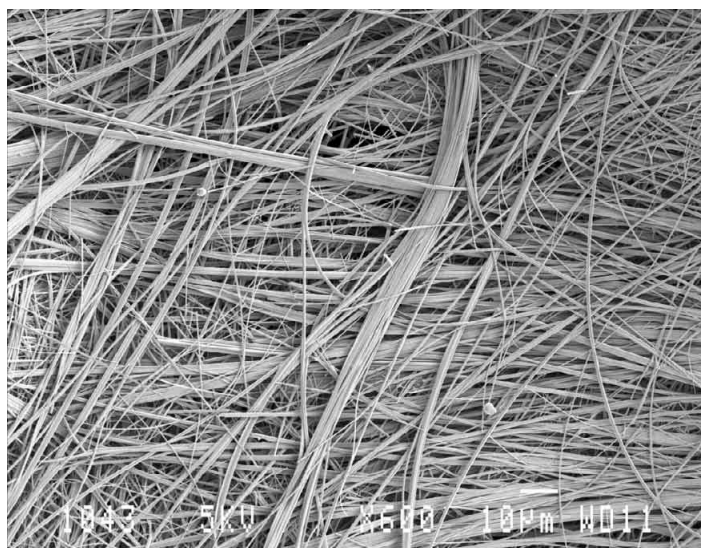
Figure 4-37   SEM images of calcium gluconate monohydrate recrystallised from water through diffusion with ethanol

4.4.   The intumescence of the metal glucose (dextrose) derivatives

Large volumes of the calcium dextrose solution were prepared without problems. Up to 2 litres of the solution could be prepared at a time. The synthesis of all of the metal dextrose solutions were carried out without problems and showed yields above 90%.

None of the metal dextrose solutions poured into the 400 mℓ yielded usable results. All of the samples "foamed" over the sides of the beakers. Due to the high water content of the samples, the amount and rate of foaming was very high. Foaming slowly at first (forming a solid foamed crust on the surface), the foaming increased rapidly as the crust became denser. Even if the amount of water in the samples was reduced through evaporation, the problem persisted. Enough water could not be removed to prevent the boiling over.

As with the acetylacetonates and gluconates, the calcium containing dextrose solution showed the least and slowest afterglow. The aluminium dextrose solution was only slightly worse than the calcium dextrose solution. The copper dextrose solution showed the most pronounced afterglow and very little carbon residue was left.

All the newspaper and filter paper samples treated with calcium dextrose and mixtures of boric acid and calcium dextrose burned when exposed to a gas flame. It is believed that the amount of treatment on the samples was not enough to prevent burning. None of the samples showed any intumescence. All the treated samples of polyester fabric showed intumescence. The pure calcium dextrose treated sample showed the most foaming – but it was much less than the calcium gluconate monohydrate. The sample was difficult to ignite, but did burn when exposed to the gas flame for a few seconds and did not self extinguish. The samples became more and more difficult to ignite as the amount of boric acid added increased up to 50% (mass ratio based on the calcium in the solution) and were self-extinguishing. Above 50% boric acid addition, ignition resistance decreased again and the sample with 1:1 mass ratio boric acid to calcium in the dextrose solution was the easiest to ignite and burned the most profusely. The samples with high levels of boric acid addition "shot" when exposed to the gas flame, increasing with increased addition levels. The optimum boric acid addition level to increase ignition resistance is between 20% and 50% by mass. Further optimisation of the boric acid addition levels was not done.

4.5.   Properties of the fine powder carbonates and oxides

The BET surface area results for the metal oxides and carbonates prepared from the metal dextrose solutions are reported in Table 4-10. The highest surface area was measured for the iron oxide prepared from the iron ammonium dextrose solution, with a surface area of 13.4 m^2/g. The surface areas of the calcium carbonates prepared from both the calcium gluconate and dextrose were very similar.   The calcium carbonate prepared from the gluconate had a surface area of 11.4 m^2/g and the calcium carbonate prepared from the dextrose solution a surface area of 12.0 m^2/g. For most of the samples, the oxides prepared in the glass crucibles at 600°C returned a higher surface area than the samples heated to 1000°C in the alumina crucibles.

Table 4-10   BET surface area results from the metal oxides and carbonates prepared from the metal dextrose solutions

Dextrose sample	Alumina Crucible	Glass crucible	Silica crucible
Units	m^2/g	m^2/g	m^2/g
Al NH$_4$	3.40	0.36	-
Cu	0.35	2.58	-
Fe	0.73	11.20	9.25
Fe NH$_4$	0.26	13.35	-
Zn	0.55	7.36	-
Zr	2.21	1.26	-
Ca	-	11.96*	-
Ca gluconate	-	11.43*	-

* carbonate

No significant differences in the structure of the oxides prepared at 1000°C in the alumina crucibles and the oxides prepared at 600°C in the glass crucibles were evident. Only the SEM images of the oxides obtained at 600°C in the glass crucibles are presented. The SEM images showed that all of the oxide and carbonates produced from the metal dextrose solutions are made up of agglomerates of fine primary particles. Figure 4-38 shows the oxide prepared from the aluminium ammonium dextrose solution. The carbonate prepared from the calcium dextrose solution is shown in Figure 4-39 and in Figure 4-40 the carbonate prepared from calcium gluconate. The differently prepared carbonates appeared very similar under SEM.   Primary particle size, agglomerate size and the structure of the carbonate were virtually identical.
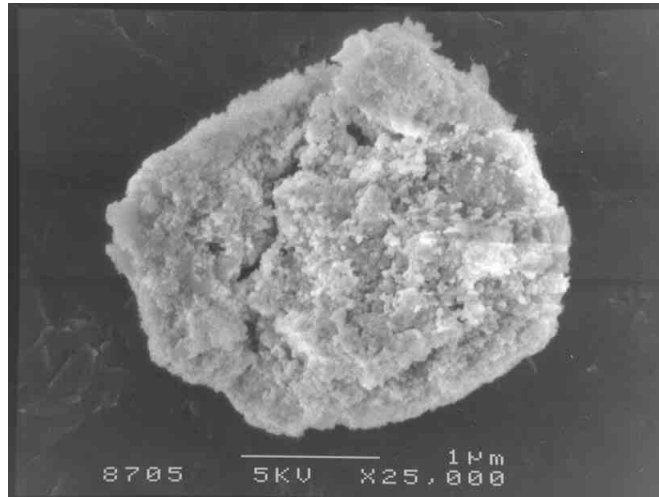
Figure 4-38   Aluminium oxide prepared from aluminium ammonium dextrose solution
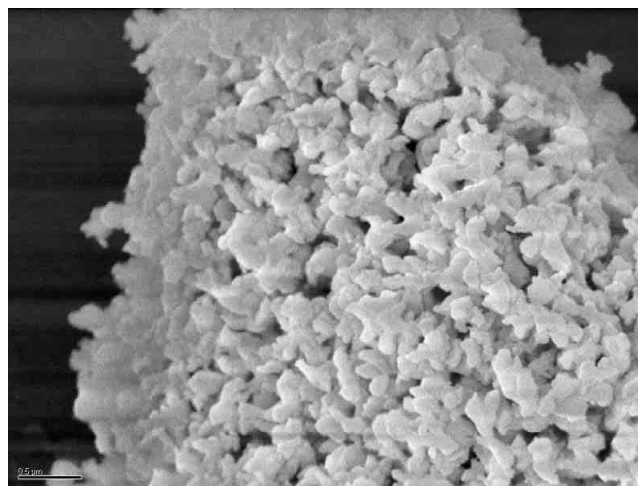
Figure 4-39   Calcium carbonate prepared from calcium dextrose solution
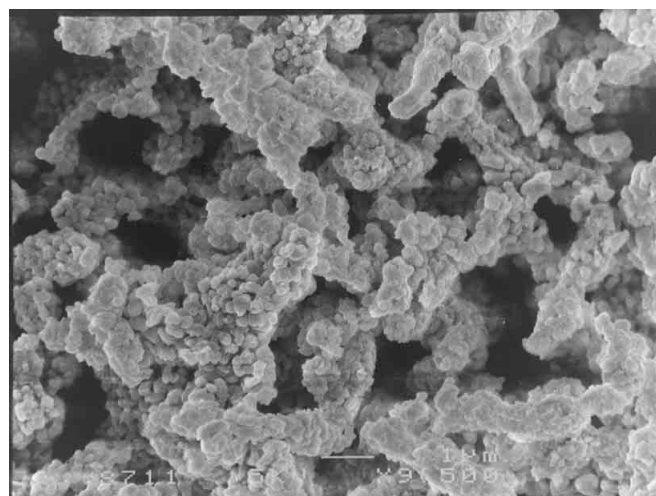
Figure 4-40   Calcium carbonate prepared from calcium gluconate monohydrate

In Figure 4-41 the iron oxide prepared from the iron dextrose solution is shown. The spherical nature of the small primary particles is clear from the image. It appears as if the primary particles are fused to form larger aggregates as seen in the image. More SEM images of the oxides and carbonates prepared from the dextrose solutions are presented in Appendix U.
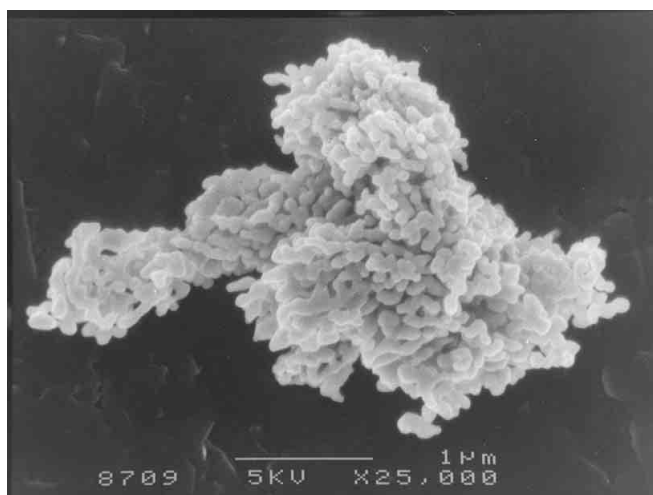
Figure 4-41   Iron oxide prepared form iron dextrose solution

Table 4-11 summarises the results of the oxides analysed with EDS SEM. The EDS SEM analysis showed that most of the oxides prepared from the metal dextrose solutions were impure. Only the aluminium ammonium dextrose solution returned an oxide of less than 80% purity at 48%. All the samples prepared through the precipitation of calcium sulphate showed residual calcium. This implies that some of the calcium sulphate was left in dextrose solutions.

Table 4-11   Elemental analysis of the metal dextrose solutions as obtained from the EDS SEM analysis

Dextrose sample	% metal oxide	% calcium oxide
Al NH$_4$	48%	35%
Cu	83%	11%
Fe	87%	7%
Fe NH$_4$	79%	14%
Zn	91%	6%
Zr	90%	9%
Ca	-	99.9%
Ca gluconate	-	99.5%

4.6.   Understanding metal catalysed intumescence of polyols

The calcium acetate hydrate showed no foaming under the open gas flame. The sample turned grey and lightened, becoming white after long exposure to the flame. At no stage did the acetate form any real carbon residue. When exposed to the open gas flame, the calcium lactate pentahydrate showed very little foaming. The lactate formed no noticeable carbon residue and turned white after continued exposure to the flame. Under the gas flame, the calcium citrate tetrahydrate sample behaved similarly to the lactate sample. Very little foaming and carbon residue were observed. After prolonged exposure, the sample turned lighter grey until finally it turned white. As with the acetate, the propionic acid calcium salt showed no foaming. No carbon residue was noticeable and the residue left after continued exposure to the flame was white. The calcium saccharate tetrahydrate showed foaming more than any of the other samples mentioned previously. A black carbon residue was formed, showing some afterglow, turning grey and becoming white after continued exposure to the flame. The threonic acid hemicalcium salt showed more foaming than the saccharate. At first, the sample turned brown under the flame. The brown residue turned black, then grey and turned white under prolonged exposure to the gas flame. Under the gas flame, the glyceric acid hemicalcium salt monohydrate behaved similarly to the threonic acid salt. However, the sample foamed considerably more. Continued exposure causes the foam to shrink. The foaming of the glyceric acid salt was far less than the calcium gluconate monohydrate sample (refer to section 4.3.1). All the samples forming black carbon showed similar afterglow.

Only the calcium gluconate monohydrate, glyceric acid hemicalcium salt monohydrate and the threonic acid calcium salt showed mentionable foaming. The gluconate foamed the most and the threonic acid salt the least of the three. These three compounds all had one thing in common. They all had a "free" hydroxyl group at the end of the carbon chain, opposing the calcium ion (see Figure 3-14). It appears as if this "free" hydroxyl group can interact with hydroxyl groups on nearby molecules, causing crosslinking of the material. This forms high molecular mass species that can stretch and end up as the flexible cell walls of the foam.

The work done on the sodium salts showed that – as a general rule – samples with longer carbon back bones foamed more and produced more carbon residue, as did materials

with more hydroxyl groups. This however did not hold true for the threonic and glyceric acid salts. Under this theory, the threonic acid hemicalcium salt should have foamed more than the glyceric acid hemicalcium salt monohydrate. The reason for this became apparent when the XRD data of calcium gluconate monohydrate was studied with the density and other pyrolysis data of the gluconate. At approximately 150ºC, the gluconate starts to foam and has formed good foam at 200ºC. The XRD analysis of the gluconate heated at 150ºC shows both calcium gluconate monohydrate and calcium gluconate (with no crystal water). Little amorphous material is detected. At 200ºC the XRD shows more amorphous material, no calcium gluconate monohydrate, but a lot of dehydrate calcium gluconate. This implies that primary foaming is due to the crystal water in the material. It helps to "push" the material open and promotes further foaming. The threonic acid hemicalcium salt is the only one of the three samples without water of crystallisation and it foamed the least.

The densities for the foams produced by the pyrolysis of the calcium gluconate monohydrate, glyceric acid hemicalcium salt monohydrate and threonic acid hemicalcium salt at selected temperatures are presented in Table 4-12 and Figure 4-42. Densities for the dehydrated gluconate and glyceric acid salt are also given.

Table 4-12   Density data of several hydroxyl rich and dehydrated compounds pyrolysed at selected temperatures in air

Sample	Density	Pyrolysis temperature			Dehydration method			Units
					Heated @ 125°C	Heated @ 140°C	Soaked in ethanol	
		200	300	400	300	300	300	°C
Calcium gluconate monohydrate	Based on residual mass	28.1	3.2	5.6	3.2	99.6	9.1	kg/m^3
	Based on initial mass	33.5	5.8	11.8	6.8	158.8	14.7	kg/m^3
Glyceric acid hemicalcium salt monohydrate	Based on residual mass	104.3	4.6	21.3	12.9	33.4	35.2	kg/m^3
	Based on initial mass	123.7	9.2	49.5	23.8	53.9	61.9	kg/m^3
Threonic acid hemicalcium salt	Based on residual mass	237.7	65.5	60.6	-			kg/m^3
	Based on initial mass	247.4	121.3	123.7	-			kg/m^3

The lowest foam densities were achieved at 300ºC heating temperature. The foam of the pyrolysed calcium gluconate monohydrate was the lowest at 3.2 kg/m^3 based on the residual mass and 5.8 kg/m^3 based on the initial sample mass. For the glyceric acid

hemicalcium salt monohydrate, a density of 4.6 kg/m^3 on residual mass and 9.2 kg/m^3 based on initial mass. At both 200ºC and 400ºC, the gluconate produced foam of lower density than the other two samples. All the dehydrated samples pyrolysed at 300ºC produced foams of higher density than the original samples. None of the samples heated at 125ºC for 24 hours fully dehydrated, while the dehydration at 140ºC for 24 hours showed more than 100% dehydration for both samples. This implies that the samples (especially the calcium gluconate monohydrate) lost some of their hydroxyl groups and dehydroxylation; which explains the very high density obtained. The samples dehydrated with the ethanol should be best dehydrated and produced the most reliable results. Densities of 9.1 kg/m^3 (residual mass) and 14.7 kg/m^3 (initial mass) were measured for the dehydrated calcium gluconate and 35.2 kg/m^3 (residual mass) and 61.9 kg/m^3 (initial mass) for the dehydrated glyceric acid hemicalcium salt.
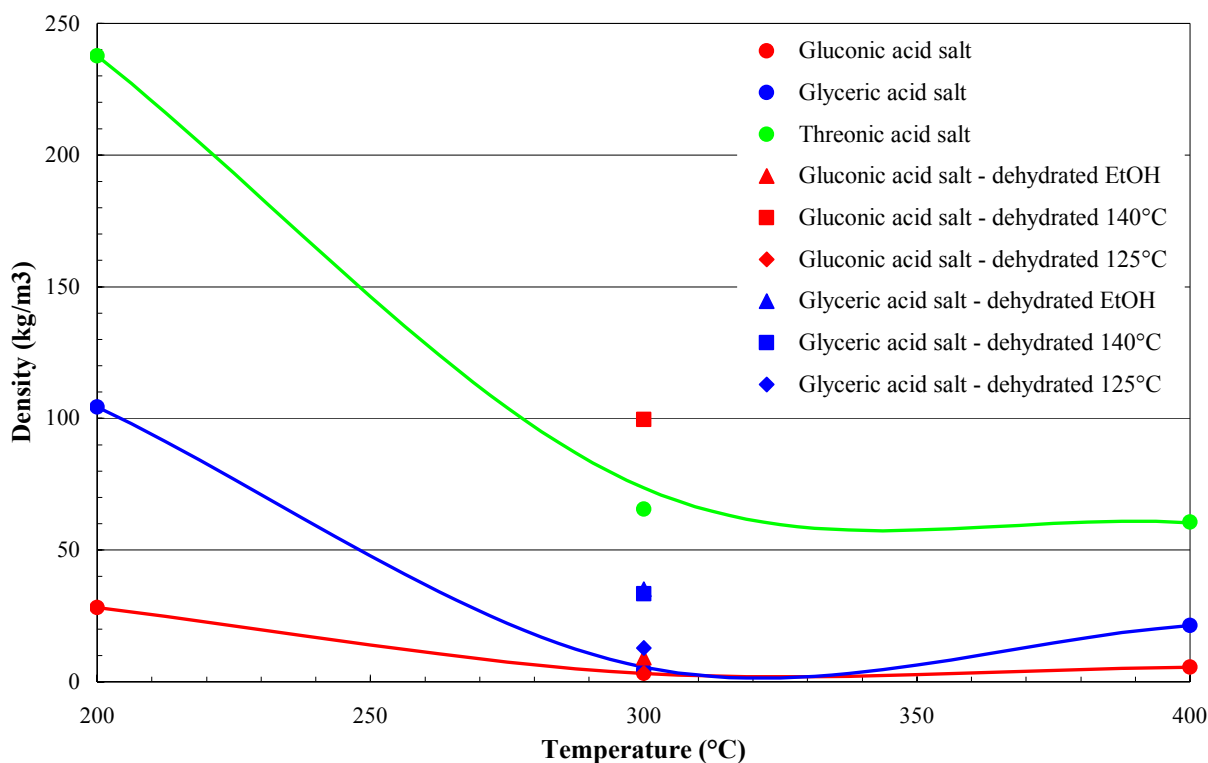
Figure 4-42   Densities of several hydroxyl rich and dehydrated compounds pyrolysed at selected temperatures in air

The TGA/SDTA data for all the above-mentioned compounds can be found in Appendix V. The most important results from the thermal analysis data are summarised in

Table 4-13 and the theoretical contribution of selected species (groups) in the compounds and accumulative percentage loss in Table 4-14.

Table 4-13   Summary of the thermal analysis data for the selected compounds

Acid calcium salts	Dehydration			Dehydroxylation		Carbon oxidation*	CaCO$_3$		CaO	
	Onset	Loss	Endothermic peak	Peak	Endo-/ Exotherm	Exothermic peak	Plateau	Loss	Plateau	Loss
Units	°C	%	°C	°C		°C	°C	%	°C	%
Acetic	60	7	160, 200	-	-	440	460	43	720	68
Propionic	60	3	90	-	-	460, 480	490	48	720	72
Lactic	60	24	90	280	Endotherm	400, 420, 440	460	66	705	81
Citric	60	13	80, 130	420	Exotherm	480	490	47	730	70
Saccharinic	60	22	110, 170	260	Endotherm	460, 550	600	64	820	83
Glyceric	140	12	150	230	Endotherm	430	440	64	660	80
Threonic	220	-	-	260	Exotherm	430, 450	520	67	720	82
Gluconic	130	3	160	220	Exotherm	460, 570	580	76	690	87

* includes losses of all bonded hydrogens and carbons

Table 4-14   Theoretical percentage accumulative loss and percentage contribution of selected species

Acid calcium salts	Crystal waters	Group contribution				Accumulative loss			
		Crystal waters	OH groups	CaCO$_3$	CaO	Crystal waters	OH (as water)	CaCO$_3$ (left)	CaO (left)
Units		%	%	%	%	%	%	%	%
Acetic	0.7	7.4	0	58.6	32.8	7.4	7.4	41.4	67.2
Propionic	0	0	0	53.7	30.1	0	0	46.3	69.9
Lactic	5	29.2	11.7	32.5	18.2	29.2	40.9	67.5	81.8
Lactic	4	24.8	12.4	34.5	19.3	24.8	37.2	65.5	80.7
Citric	4	12.6	6.3	52.6	29.5	12.6	18.9	47.4	70.5
Saccharinic	4	22.5	22.5	31.3	17.5	22.5	45.0	68.7	82.5
Glyceric	2	12.6	25.2	35.0	19.6	12.6	37.8	65.0	80.4
Threonic	0	0	34.8	32.3	18.1	0	34.8	67.7	81.9
Gluconic	1	4.0	40.2	22.3	12.5	4.0	44.2	77.7	87.5

Most of the TGA/SDTA scans correspond well with the theoretical values for mass loss as crystal water and retained calcium carbonate and calcium oxide (see Table 4-13 and Table 4-14). The only exceptions are calcium propionate and calcium lactate. Calcium propionate shows a 3% loss at 105ºC that can be contributed to surface water, seeing that it does not have crystal water. Although the lactic acid calcium salt should be a pentahydrate, the mass loss data from the TGA corresponds much better with a tetrahydrate. In most cases the samples start to degrade at low temperatures (approximately 60ºC) due to the loss of

crystal and surface water. Calcium gluconate monohydrate starts to lose its crystal water at 130ºC with the endothermic peak at 160ºC (3% loss at 180°C). Dehydration starts at 140ºC for the glyceric acid hemicalcium salt monohydrate, with an endothermic peak at 150ºC (12% loss at 190°C). The compound with the highest temperature stability is the threonic acid calcium salt. It only starts to decompose at 220ºC with only 4% mass loss at 260ºC.

The strong exothermic peak associated with the oxidation of the carbon produced during pyrolysis, is clear for all the compounds. This carbon oxidation peak is very similar in size and position for all the compounds. It varies in position from 400ºC for calcium lactate pentahydrate to 570ºC for glyceric acid hemicalcium salt monohydrate; with most of the exothermic peaks being in the mid 400ºC range.

With the exception of calcium citrate tetrahydrate, all the compounds with hydroxyl groups show a weak endothermic or exothermic peak between 220ºC and 280ºC. For the citric acid salt, this energy peak is observed at 420ºC. This peak is due to dehydroxylation – the loss of alcohol groups as water. Typically, the loss of hydroxyl groups as water coincides with an endotherm, but it is believed that the reaction may become exothermic due to crosslinking in the molecule during dehydroxylation.

The SEM images of the glyceric acid hemicalcium salt monohydrate pyrolysed at selected temperatures in air are presented in Appendix V. When heated at 300ºC, the glyceric acid hemicalcium salt monohydrate produces foam similar to the foam produced when calcium gluconate monohydrate is heated at the same temperature. The foam is a closed cell, densely packed foam with thin cell walls. The foam cells vary in size between 100 μm and 300 μm. When heated at 200ºC, the foam produced from the calcium salt of glyceric acid differs from calcium gluconate monohydrate foam produced under similar conditions. The cells are typically smaller (between 20 μm and 150 μm) with much thicker cell walls. The foam is also more brittle. The glyceric acid hemicalcium salt monohydrate foam produced at 400ºC is much different to the foam produced from calcium gluconate monohydrate pyrolysed under the same conditions. The glyceric acid salt is more "decomposed", more open celled with thick cell walls and typically large cells (>>200 μm). The foam compares better with the calcium gluconate monohydrate foamed at 500ºC or even 600ºC. Yet small bubbles (1 μm to 20 μm) are evident in the cell walls. It is as if the cell walls could not stretch enough when heated at 400ºC to form larger cells.

5.   Conclusion and recommendations

In terms of all the organic acid sodium salts tested, gluconic acid proved to be the best intumescent of all. It showed the best combination of char yield, foam structure and volume, stability and open flame characteristics. As a general rule of thumb, the char volume and structure improved with an increased number of hydroxyl groups in the compound. Char yield increased with an increase in the number of hydroxyl groups for a constant number of carbons in the complex. The number of acid groups in the compound played a lesser role in intumescence. Aromaticity led to a reduction in foaming but a higher char yield. The char was stronger and more brittle than the char formed by the aliphatic compounds.

Most metal complexes catalyse intumescent decomposition of polyhydric compounds such as polyhydroxylcarboxylic acids and pentaerythritol. Unfortunately, the resultant carbon-foams are unstable: the metal residues also catalyze the further oxidative degradation of the char. The transition metal based complexes shows the most and strongest afterglow, while the alkali metal based complexes showed less. Foaming is reduced with more pronounced afterglow. From the studies of the different metal complexes with acetylacetone and gluconic acid, it was concluded that the calcium ion exhibited the most promise. It showed the best intumescence, high char yields and the least afterglow; best balance of all the metal ions. Further work is required to overcome this "glowing combustion" effect and to improve the char-foam cell structure before such systems can be considered as flame retardant additives for polymers.

When pyrolysed in air with an open gas flame or in a furnace, calcium gluconate monohydrate produces voluminous foam. Calcium gluconate monohydrate starts to thermally degrade at 120°C, losing its crystal water and shows a mass loss of 4% at 180°C. Compounds that decompose below 200°C (processing temperature of most commonly used polymer) can only be used in unsaturated polyesters and thermoset resins. A possible application is in paints and coatings.

If the sample is compressed, the resultant foam produced during pyrolysis is less voluminous than that of the loose powder. This implies that the foam produced from the gluconate may not be usable in coating applications. Adding leached silica to the calcium gluconate monohydrate increases mechanical strength of the foam, but influences the foam

volume negatively. The mechanical strength of the foam can also be increased with the addition of expandable graphite. The graphite has a lesser influence on the foam volume than the silica, but also reduces the foam volume. However, the addition of the expandable graphite gives the sample more "opening force", as the foam volume of a compressed sample pyrolysed, is similar to that of the heated loose powder. Such a combination could make an efficient intumescent coating.

An intumescent coating containing calcium gluconate monohydrate, leached silica and expandable graphite as a system was prepared and compared with two commercial formulations. This gluconate based system proved to be at least as efficient as or more efficient than the commercial formulations (AP750 and PEN) when painted on balsa wood planks or aluminium plates. On cardboard sheets it did not perform as well as the commercial systems. It appears as if intumescent coatings based on calcium gluconate monohydrate may be of interest. Further work on the performance of such coatings must be done to exploit the potential of calcium gluconate monohydrate based intumescent coating systems.

For the calcium gluconate monohydrate the transition from $CaCO_3$ to CaO occurs at ca. 650°C in air. This is much lower than the expected ca. 800°C. The reason for this can be the "foamed" nature of the produced carbonate having a high surface area and thus reactivity. The BET surface area of $CaCO_3$ from the gluconate pyrolysed at 600°C is ca. $12m^2/g$. Similar results were obtained with the other metal gluconates and metal dextrose solutions. It may thus be possible to produce reactive metal oxides and carbonates with low densities and high specific surface areas. More work should be done on the synthesis of such metal oxides and carbonates.

The amorphous carbon produced by heating ammonium gluconate hydrate at 1000°C in nitrogen for several hours proved to have a higher electric conductivity than graphite. The carbon produced from calcium gluconate monohydrate under similar conditions was also conductive, but was less conductive than graphite. The properties of these carbon residues must be further exploited.

Threonic acid hemicalcium salt also intumesces when exposed to heat. The resultant foam is much less voluminous than that of calcium gluconate monohydrate. However, the threonic acid salt is stable up to 220°C, showing 4% mass loss at 260°C. Due to its high temperature stability, it may be used in applications where calcium gluconate monohydrate could not be used.

From the work it became apparent that several factors influence the intumescence of polyhydroxylcarboxylic acid metal salts. Foaming is due to the formation of amorphous carbon trapping water vapour. Compounds with crystal water tend to foam more than compounds without water of crystallisation. The foam density of calcium gluconate is three times higher than that of calcium gluconate monohydrate. For a given carbon chain length, intumescence increases as the number of hydroxyl groups on the backbone increases.

Another important factor is a "free" hydroxyl group on the end of the carbon chain (opposite the metal ion). Glyceric acid hemicalcium salt monohydrate foams much more than calcium lactate pentahydrate. The only difference in the compounds is the hydroxyl group on the carbons furthest from the carboxylic acid. It is believed that this hydroxyl group crosslinks with other nearby molecules to form high molecular mass carbon species. The high molecular mass species identified in the MALDI-TOF-MS of calcium gluconate monohydrate pyrolysed at 300°C in air supports this theory.

It is unclear whether the decomposition of calcium gluconate monohydrate is catalysed inter- or intramolecularly. It is believed to include both. The colour change that the material undergoes during pyrolysis indicates double bond formation. This would probably be intramolecular. However, the crosslinking mentioned above would be intermolecular. Only if the crystal structure of calcium gluconate monohydrate is known, can this be clarified. All attempts to grow a single calcium gluconate monohydrate crystal of usable size failed. Further studies should include attempts to grow single crystals and determine the crystal structure of calcium gluconate monohydrate.

From the results obtained it appears that is may be possible to develop metal catalysed intumescent flame retardants for bulk polymers. Although threonic acid hemicalcium salt does not form as profoundly as other similar organometallic complexes containing crystal water, it is stable to above 200ºC and the foam produced may be sufficient to act as a flame

retardant. However, the threonic acid salt also foams less if the powder is compressed. This implies that the water vapour produced during pyrolysis is not sufficient to "force open" the foam if compressed. Water has a low vapour pressure at fire temperatures compared to gasses such as carbon dioxide and ammonia. The addition of carbon dioxide or ammonium rich compounds to a metal catalysed intumescent system or such groups to the organometallic complex may improve performance in bulk polymers. Furthermore, the addition of boron rich compounds or groups to such a system, may overcome the afterglow effect (as it inhibits carbon oxidation). Such a system might only be developed through trial and error.

6.   References

Aslin, D.C. (1989) "The design and development of intumescent coatings for structural fire protection", *Journal of the Oil and Colour Chemists' Association, 72,* p. 185-189, 176.

Babraukas, V. (2000) "Fire test methods for evaluation of fire retardant efficiency", in Fire Retardancy of Polymeric Materials, Chapter 3, p. 81-113, Wilkie, C.A. and Grand, A.F. (Editors), Marcel Dekker Inc., New York.

Baillet, C. and Delfosse, L. (1990) "The combustion of polyolefins filled with metallic hydroxides and antinomy trioxide", *Polymer Degradation and Stability, 30,* p. 89-99.

Benbow, J. (1987) "Minerals in fire protection", *Industrial Minerals, 240,* p. 61-73.

Berg, E.W. and Truemper, J.T. (1960) "A study of the volatile characteristics of various metal β-diketone chelates", *Journal of Physical Chemistry, 64,* p. 487-491.

Bertelli, G., Marchetti, E., Camino, G., Costa, L. and Locatelli, R. (1989) "Intumescent fire retardant systems: Effect of fillers on char structure", *Die Andewandte Makromolekulare Chemie, 172,* p. 153-163.

Bishop, D.M., Bottomley, D. and Zobel, F.G.R. (1983) "Fire retardant paints", *Journal of the Oil and Colour Chemists' Association, 66,* p. 373-396.

Bisschoff, J. (2000) *Oxygenated Hydrocarbon Compounds as Flame Retardants for Polyester Fabric,* Masters Thesis, Department of Chemical Engineering, University of Pretoria, South Africa.

Bisschoff, Kobie and Focke, W.W. (2001) "Oxygenated hydrocarbon compounds as flame retardants for polyester fabric", in Fire and Polymers, Materials and Solutions for Hazard Prevention*,* Chapter 19, p. 240-250, Nelson, G.L. and Wilkie, C.A. (Editors), American Chemical Society, Washington DC.

Blount, D.H. (1998) "Flame retardant porous plastics", *US Patent 5,721,281,* assigned to Blount, San Diego, US.

Brook, M. (1985) "How intumescent coatings work", *Fire Prevention,* November 1985, p. 36-37.

Brown, N. (1999) "New aluminium hydroxides for printed circuit boards and public transport applications", paper presented at *The Tenth Annual BCC Conference on Recent Advances in Flame Retardancy of Polymeric Materials*, 24-26 May, 1999, Stamford, Connecticut, USA.

Bourbigot, S., Le Bras, M., Delobel, R., Bréant, P. and Tremillon, J. (1996) "4A zeolite synergistic agent in new flame retardant intumescent formulations of polyethylenic polymers – study of the effect of the constituent monomers", *Polymer Degradation and Stability, 54,* p. 275-287.

Bourbigot, S., Le Bras, M., Delobel, R. and Gengembre, L. (1997) "XPS study of an intumescent coating II. Application to the ammonium polyphosphate-pentaerythritol-ethylenic terpolymer fire retardant system with and without synergistic agent", *Applied Surface Science, 120,* p. 15-29.

Camino, G., Costa, L. and Martinasso, G. (1989) "Intumescent fire retardant systems", *Polymer Degradation and Stability, 23,* p. 359-376.

Camino, G. and Delobel, R. (2000) "Intumescence", in Fire Retardancy of Polymeric Materials, Chapter 7, p. 217-243, Wilkie, C.A. and Grand, A.F. (Editors), Marcel Dekker Inc., New York.

Case, C. (1999) Microbal fermentation: Changed the course of human history, http://www.accessexcellence.org/LC/SS/ferm_background.html, Access Excellence, [2002, August 26].

Chang, W., Scriven, R.L. and Ross, R.B. (1975) "Flame retardant organic coatings", in Flame-Retardancy of Polymeric Materials, p. 399-454, Elsevier, New York.

Cornell, J.A. (1981) *Experiments with Mixtures,* John Wiley & Sons, New York.

Cullis, C.F. and Hirschler, M.M. (1981) *The Combustion of Organic Polymers,* Clarendon Press, Oxford.

Cullis, C.F. and Hirschler, M.M. (1984) "Char formation form polyolefins", *European Polymer Journal, 20* (1), p. 53-60.

Day, J.E. (1936) "Preparation and catalytic oxidation of pure amorphous carbon", *Industrial and Engineering Chemistry,* February 1936, p. 234-238.

Delfosse, L., Baillet, C., Brault, A. and Brault, D. (1989) "Combustion of ethylene-vinyl acetate copolymer filled with aluminium and magnesium hydroxides", *Polymer Degradation and Stability, 23,* p. 337-347.

Ebdon, R.E., Guisti, L., Hunt B.J. and Jones, M.S. (1998) "The effects of some transition-metal compounds on the flame retardancy of poly(styrene-*co*-4-vinyl pyridine) and poly(methyl methacrylate-*co*-4-vinyl pyridine)", *Polymer Degradation and Stability, 60,* p. 401-407.

Everitt, C. (1911) "Distillation" in "The 1911 Edition Encyclopedia", based on "Encyclopaedia Brittanica", http://80.1911encyclopedia.org/D/DI/DISTILLATION.htm, [2002 August 26].

Focke, W.W., Labuschagné, F.J.W. and Strydom, C.A. (2000) "Strong based catalysed intumescent flame retardants", *Journal of Material Science Letters, 19,* p. 617-618.

Focke, W.W., Strydom, C.A. and Bartie, N. (1997) "Thermal analysis of commercial inorganic flame retardants", *South African Journal of Chemical Engineering, 9* (2), p. 41-51.

Freedman, L.D., Dock, G.O. and Lang, G.G., (1992) "Antimony Compounds" in Kirk Othmer's Encyclopaedia of Chemical Technology*,* Vol. 3, pp. 381-404, 4th Ed., John Wiley and Sons, New York

Furches, B.J. (1993) "Plastics testing", in Kirk Othmer's Encyclopaedia of Chemical Technology, Vol. 19, p. 317-347, 4th Ed., John Wiley and Sons, New York.

Gann, R.G. (1993) "Flame retardants", in Kirk Othmer's Encyclopaedia of Chemical Technology, Vol. 10, p. 930-936, 4th Ed., John Wiley and Sons, New York.

Georlette, P., Simons, J. and Costa, L. (2000) "Halogen-Containing Fire-Retardant Compounds", in Fire Retardancy of Polymeric Materials, Chapter 8, p. 245-284, Wilkie, C.A. and Grand, A.F. (Editors), Marcel Dekker Inc., New York.

Gilman, J.W. and Kashiwagi, T. (1997) *Fire Science: NIST Research Shows Nanocomposites Can Take the Heat,* Biweekly capsule newsletter highlighting NIST activities, research and services, 14 October 1997, NIST, Gaitherburg, USA.

Gilman, J.W., Lomakin, S., Kashiwagi, T., VanderHart, D.L. and Nagy, V. (1997) "Characterisation of flame retarded polymer combustion char by solid-state ^{13}C and ^{29}Si NMR and EPR", *Polymer Preprints, 38* (1), p. 802-803.

Gordon, M.S. and Koob, R.D. (1973) "An INDO investigation of the structure and bonding of acetylacetone and trifluoroacetylacetone", *Journal of the American Chemical Society, 95* (18), p. 5863-5867.

Green, J. (1996) "Mechanism of flame retardancy and smoke suppression – A review", *Journal of Fire Science, 14,* Part 6, p. 426-442.

Green, J. (1997) "25 Years of flame retarding plastics", *Journal of Fire Science, 15,* Part 1, p. 52-67.

Green, J. (2000) "Phosphorous-Containing Flame Retardants", in Fire Retardancy of Polymeric Materials, Chapter 5, p. 147-170, Wilkie, C.A. and Grand, A.F. (Editors), Marcel Dekker Inc., New York.

Green, J.W. (1980) "Oxidative reactions and degradation" in THE CARBOHYDRATES Chemistry and Biochemistry, Vol. 1B, Chapter 24, pp. 1101-1166, 2nd Ed., Pigman, W. and Horton, D. (Editors), Academic Press, New York.

Hirschler, M.M. (2000) "Chemical aspects of thermal degradation", in Fire Retardancy of Polymeric Materials, Chapter 2, p. 27-79, Wilkie, C.A. and Grand, A.F. (Editors), Marcel Dekker Inc., New York.

Horacek, H and Grabner, R (1996) "Advantages of flame retardants based on nitrogen compounds", *Polymer Degradation and Stability, 54,* p. 205-215.

Horn Jr., W.E. (2000) "Inorganic Hydroxides and Hydroxycarbonates: Their Function and Use as Flame-Retardant Additives", in Fire Retardancy of Polymeric Materials, Chapter 9, p. 285-352, Wilkie, C.A. and Grand, A.F. (Editors), Marcel Dekker Inc., New York.

Hornsby, P.R. and Watson, C.L. (1986) "Magnesium hydroxide – a combined flame retardant and smoke suppressant filler for thermoplastics", *Plastics and Rubber Processing and Applications, 6* (2), p. 169-175.

Houben-Weyl quoted by Siegel, H. and Eggersdorfer, M. (1988) "Ketones" Ullman's Encyclopaedia of Industrial Chemistry, Vol. A15, p. 77-95, 5th Ed., Gerhartz, W. (Editor),VCH Verslag, Weinheim.

Howard, W.L. (1991) "Acetone" in Kirk Othmer's Encyclopaedia of Chemical Technology, Vol. 1, pp. 176-194, 4th Ed., John Wiley and Sons, New York.

Hustede, H., Haberstroh, H.J. and Schinzig, E. (1988) "Gluconic acid" in Ullman's Encyclopaedia of Industrial Chemistry, Vol. A12, p. 449-456, 5th Ed., Gerhartz, W. (Editor),VCH Verslag, Weinheim.

Incropera, F.P. and DeWitt D.P. (1996) *Introduction to Heat Transfer,* 3rd Ed., John Wiley & Sons, New York.

Innes, J.D. and Cox, A.W. (1997) "Smoke: Test standards, Mechanisms, Suppressants", *Journal of Fire Science, 15,* p. 227-239.

Kaneko K., Kanada K., Miyagi M., Saito N., Ozeki T., Yuasa H. and Kanaya Y. (1998) "Formation of water-insoluble gel in dry-coated tablets for the controlled release of theophylline", *Chemical and Pharmaceutical Bulletin, 46* (4) p. 728-729.

Kono K., Watanabe T., Dote T., Usuda K., Nishiura H., Tagawa T., Tominaga M., Higuchi Y. and Onnda M. (2000) "Successful treatments of lung injury and skin burn due to hydrofluoric acid exposure", *International Archives of Occupational and Environmental Health, 73,* Supplement: June 2000, p. S93-S97.

Kuma, K., Koyama, K., Fujita; N., Kagawa; T., Okisaki, F., Itabashi, K. (1999) "Flame retardant and flame retardant resin composition formulated with the same", *US Patent 5,994,435,* assigned to Tosoh Corporation, Japan.

Labuschagné, F.J.W.J. (1998) *Study of Possible Alternative Latent Base Flame Retardants,* Project Report, Department of Chemical Engineering, University of Pretoria, South Africa.

Le Bras, M., Camico G., Bourbigot S. and Delobel R. (Ed's) (1998) *Fire Retardancy of Polymers – The Use of Intumescence,* The Royal Society of Chemistry, Cambribge.

Levchik, S.V., Levchik, G.F., Balabanovich, A.I., Camino, G. and Costa, L. (1996) "Mechanistic study of combustion performance and thermal decomposition behaviour of nylon 6 with added halogen-free fire retardants", *Polymer Degradation and Stability, 54,* p. 217-222.

Li, T., Archer, G.F. and Carapella, S.C., (1992) "Antimony and Antimony alloys" in Kirk Othmer's Encyclopaedia of Chemical Technology, Vol. 3, pp. 366-380, 4th Ed., John Wiley and Sons, New York

Lowrey, A.H., George, C., Antonio, P.D. and Karle, J. (1971) "Structure of acetylacetone by electron diffraction", *Journal of the American Chemical Society, 93* (24), p. 6399-6402.

Lück, E. and Von Rymon Lipinski, G. (1988) "Food Additives" in Ullman's Encyclopaedia of Industrial Chemistry, Vol. A11, p. 561-581, 5th Ed., Gerhartz, W. (Editor), VCH Verslag, Weinheim.

Lyons, J.W. (1987) *The Chemistry and Uses of Fire Retardants,* Robert E. Krieger Publishing Company, Florida.

Merkblatt Wacker-Chemie, quoted by Siegel, H. and Eggersdorfer, M. (1988) "Ketones" Ullman's Encyclopaedia of Industrial Chemistry, Vol. A15, p. 77-95, 5th Ed., Gerhartz, W. (Editor),VCH Verslag, Weinheim.

Miller, B. (1996) "Intumescents, FR efficiency pace flame retardant gains", *Plastic World,* Dec. 1996, p. 44-59.

Moser L.R., Smythe M.A. and Tisdale J.E. (2000) "The use of calcium salts in the prevention and management of verapamil- induced hypotension", *Annals of Pharmacotherapy, 34* (5), p. 622-629.

Mount, R.A. (1992) "The three sisters of intumescence", *Proceedings of the FRCA Conference,* Orlando, Florida, US, p. 33-34.

Nelson, G.L. and Wilkie, C.A. (2001) "Fire Retardancy in 2001", in Fire and Polymers, Materials and Solutions for Hazard Prevention, Chapter 1, p. 1-6, Nelson, G.L. and Wilkie, C.A. (Editors), American Chemical Society, Washington DC.

Nimmo, W., Agnew, J., Hampartsoumian, E. and Jones, J.M. (1999) "Removal of H_2S by spray-calcinated calcium acetate", *Industrial and Engineering Chemistry Research, 38*, p. 2954-2962.

O'Rourke, J.F. (1974) "Use of intumescent coatings for fire protection of structural steel", *Loss Prevention, 8,* p. 69-72.

Oshima, Y., and Fukuda, Y. (1935) "Effect of Ash on Combustion Characteristics of Carbons", *Industrial and Engineering Chemistry,* 27(2), p. 212-217.

Paul, K. (1999) "Testing for fire" in Handbook of Polymer Testing – Physical Methods, p. 659-695, Brown, R. (Editor), Marcel Dekker Inc, New York.

Pearce, E.M. (1986) "Flame retardants for polymer systems", *Pure and Applied Chemistry, 58,* p. 925-930.

Pettigrew, A. (1993) "Halogenated flame retardants" in Kirk Othmer's Encyclopaedia of Chemical Technology, Vol. 10, pp. 954-976, 4th Ed., John Wiley and Sons, New York.

Pigman, W. (1957) "Structure and stereochemistry of sugars" in THE CARBOHYDRATES Chemistry, Biochemistry and Physiology, Chapter 1, pp. 1-76, 2nd Ed., Pigman, W. (Editor), Academic Press, New York.

Pigman, W. and Anet, E.F.L.J. (1972) "Mutarotations and actions of acids and bases" in THE CARBOHYDRATES Chemistry and Biochemistry, Vol. 1A, Chapter 4, pp. 165-194, 2nd Ed.,

Pigman, W. and Horton, D. (Editors), Academic Press, New York.

Rajendran, S., Apparao, B.V. and Palaniswamy, N. (1998) "Calcium gluconate as corrosion inhibitor for mild steel in low chloride media", *British Corrosion Journal, 33* (4), p. 315-317.

Rakszawski, J.F. and Parker, W.E. (1964) "The effect of group IIIA-VIIA elements and their oxides on graphite oxidation", *Carbon, 2,* p. 53-64.

Ramsbottom, J.E. (1947) *Fire-proofing of Fabrics,* His Majesties Stationary Office, London, England.

Reyes, J.D., Georlette, P., Finberg, I. and Reznick, G. (1999) "Flame retardants for enhanced properties in polyolefins", paper presented at *The Tenth Annual BCC Conference on Recent Advances in Flame Retardancy of Polymeric Materials*, 24-26 May, 1999, Stamford, Connecticut, USA.

Rhys, J.A. (1969) "Flame retarding of plastics materials", *Chemistry and Industry, (London), 7,* 15 February, p. 187-191.

Rizzoni, G. (1996) *Principles and Applications of Electrical Engineering,* 2nd Ed., Irwin, Chicago.

Roelle, W. (1991) "Extenders" as part of "Paints and coatings" in Ullman's Encyclopaedia of Industrial Chemistry*,* Vol. A18, p. 460-465, 5th Ed., Gerhartz, W. (Editor), VCH Verslag, Weinheim.

Rothon, R.N. (1995) *Particulate Filled Polymer Composites*, Chapter 67, Longman Scientific & Technical, Essex.

Rothon, R.N. and Hornsby, P.R. (1996) "Flame retardant effects of magnesium hydroxide", *Polymer Degradation and Stability, 54,* p. 383-385.

Sawyer, D.T. (1957) "Metal-gluconate complexes", *Chemical Review, 64* p. 633-643.

Sasaoka, E., Sada, N. and Uddin, M.A. (1998) "Preparation of macro porous lime from natural lime by swelling method with acetic acid for high-temperature desulphurisation", *Industrial and Engineering Chemistry Research, 37* (10), October 1998 p. 3943-3949.

Schmidt, W.G. (1965) "Flame retardant additives in plastics and recent patents", *Plastics Institute, (London), Transactions and Journal, 33* (108), Dec 1965, p. 247-255.

Shen, K.K. and Ferm, J. (1999) "Maximizing fire test performances of polyolefins with zinc borate", paper presented at *The Tenth Annual BCC Conference on Recent Advances in Flame Retardancy of Polymeric Materials*, 24-26 May, 1999, Stamford, Connecticut, USA.

Sheridan, R.L., Ryan, C.M., Quinby Jr, W.C., Blair, J., Tompkins, R.G. and Burke, J.F. (1995) "Emergency management of major hydrofluoric acid exposures", *Burns, 21* (1), February 1995, p. 62-64,

Shields, T.J. and Silcock, G.W.H. (1987) *Buildings and Fire*, Longman Scientific & Technical, Essex.

Siegel, H. and Eggersdorfer, M. (1988) "Ketones" Ullman's Encyclopaedia of Industrial Chemistry, Vol. A15, p. 77-95, 5th Ed., Gerhartz, W. (Editor),VCH Verslag, Weinheim.

Sievert. (*s.a.*) Sievert LP Gas Information, http://www.sievert.se/en/lp_gas_information.htm, Sievert AB, [2003, July 11].

Sifniades, S. (1985) "Acetone" in Ullman's Encyclopaedia of Industrial Chemistry, Vol. A1, p. 79-96, 5th Ed., Gerhartz, W. (Editor), VCH Verslag, Weinheim.

Smith, R.A. (1994) "Inorganic (Halogen) Fluorine compounds" in Kirk Othmer's Encyclopaedia of Chemical Technology, Vol. 11, pp. 355-376, 4th Ed., John Wiley and Sons, New York.

Sobolev, I. and Woycheshin, E.A. (1974) "Alumina hydrate as a flame retardant filler for thermoplastics", *Journal of Fire and Flammability/Fire Retardant Chemistry, 1,* p. 13-25.

Sowden, J.C. (1957) "Saccharinic acids", *Advances in Carbohydrate Chemistry, 12* p. 35-79.

Stern, S.G. and Horacek, H. (1994) "Melamine cyanurate, halogen and phosphorus free flame retardant", *International Journal of Polymeric Materials, 25* (3-4) p. 255-268.

Sutker, B.J. (1988) "Flame retardants" in Ullman's Encyclopaedia of Industrial Chemistry, Vol. A11, p. 123-140, 5th Ed., Gerhartz, W. (Editor), VCH Verslag, Weinheim.

Tang W.K. and Neill, W. K. (1964) "Effect of flame retardants on pyrolysis and combustion of α-cellulose", *Journal of Polymer Science: Part C, 6,* p. 65-81.

Taylor, C. Ralph, (1966) *Webster's Home University Dictionary*, Adams, L.M. (Editor), Books Inc., New York.

Theander, O. (1980) "Acids and other oxidation products" in THE CARBOHYDRATES Chemistry and Biochemistry, Vol. 1B, Chapter 23, pp. 1013-1099, 2nd Ed., Pigman, W. and Horton, D. (Editors), Academic Press, New York.

Troitzsch, J. (1990) *International Plastics Flammability Handbook – Principles – Regulations – Testing and Approvals*, 2nd Ed., Carl Hanser Verslag, New York.

Touval, I. (1993) "Antimony and other inorganic flame retardants" in Kirk Othmer's Encyclopaedia of Chemical Technology, Vol. 10, pp. 936-954, 4th Ed., John Wiley and Sons, New York.

Vandersall, H.L. (1970) "Intumescent coating systems, their development and chemistry", *Journal of Fire and Flammability, 1,* April 1970, p. 97-140.

Van der Walt, S. (2000), "'Capture' Data logging software", Personal Communication, Department of Chemistry, University of Pretoria, Pretoria, Retired, Tel no: +27 83 654 3660

Van Krevelen, D.W. (1975) "Flame resistance of polymeric materials", *Polymer, 16* (8), p. 615-620.

Van Krevelen, D.W. (1990) *Properties of Polymers,* 3rd Ed., Elsevier, Amsterdam.

Venter, G.A. (2000) "Chelating agents for calcium and iron", Masters student, Department of Chemical Engineering, University of Pretoria, Pretoria

Weil, E.D. (1992a) "Mechanisms of phosphorous-based flame retardants", *Proceedings of the FRCA Conference,* Orlando, Florida, US, p. 19-32.

Weil, E.D. (1992b) "What does oxygen index correlate to?", *Proceedings of the International Conference on Fire Safety, 17,* p. 353-377.

Weil, E.D. (1993) "Phosphorous flame retardants" in Kirk Othmer's Encyclopaedia of Chemical Technology, Vol. 10, pp. 976-998, 4th Ed., John Wiley and Sons, New York.

Weil, E.D. (2000) "Synergists, Adjuvants, and Antagonists in Flame-Retardant Systems", in Fire Retardancy of Polymeric Materials, Chapter 4, p. 115-145, Wilkie, C.A. and Grand, A.F. (Editors), Marcel Dekker Inc., New York.

Weinstein R. (1996) "Prevention of citrate reactions during therapeutic plasma exchange by constant infusion of calcium gluconate with the return fluid", *Journal of Clinical Apheresis, 11* (4) p. 204-210.

Wilkie, C.A. (1999) "Poly(sodium stryrenesulfonate): a self intumescent material", paper presented at *The Tenth Annual BCC Conference on Recent Advances in Flame Retardancy of Polymeric Materials*, 24-26 May, 1999, Stamford, Connecticut, USA.

Wills W.L. (1952) "textile treating compounds", *US Patent 2,607,729,* assigned to E.I. du Pont de Nemours & Company, US.

Wolf, R. and Lal Kaul, B. (1992) "Plastics, Additives" in Ullman's Encyclopaedia of Industrial Chemistry, Vol. A20, p. 459-507, 5th Ed., Gerhartz, W. (Editor), VCH Verslag, Weinheim.

Zaikov, G.E. and Lomakin, S.M. (1996) "New aspects of ecologically friendly polymer flame retardant systems", *Polymer Degradation and Stability, 54,* p. 223-233.

7.   Appendices

7.1.   Appendix A

7.1.1.   Processing temperatures for commercial polymers

Polymer	"Melt" Temperature	Processing Temperature	Mould Temperature
Poly(vinyl chloride) [PVC]	100	195	35
Polyoxymethylene [POM]	180	200	100
Polyurethane [PUR]	160	205	35
Polystyrene [PS]	100	225	45
Polyamide 11 [Nylon 11; PA 11]	175	230	60
Polyamide 12 [Nylon 12; PA 12]	175	230	60
Poly(methyl methacrylate) [PMMA]	100	245	70
Acrylonitrile-Butadiene-Styrene [ABS]	110	250	75
Polyethylene [PE]	140	250	25
Polyamide 6 [Nylon 6; PA 6]	220	250	90
Polyamide 6,10 [Nylon 6,10; PA 6,10]	215	250	90
Polypropylene [PP]	170	255	35
Poly(butylene terephthalate) [PBT]	225	255	35
Styrene-Acrylonitrile [SAN]	115	255	80
Poly(ethylene terephthalate) [PET]	225	280	140
Polyamide 6,6 [Nylon 6,6; PA 6,6]	255	285	90
Polycarbonate [PC]	150	300	90
Polyphenylene oxides [PPO]	120	300	80
Polysulphone [PSU]	200	315	150
Perfluoro(ethylene/propylene) [FEP]	275	315	150
Poly(phenylene sulphide) [PPS]	290	330	110
Polyethersulphone [PES]	230	350	150
Poly(amide imide) [PAI]	300	365	230
Poly(ester imide) [PEI]	215	370	100
Poly(ether ether ketone) [PEEK]	335	370	160
Liquid crystal polymers [LCP]	330	400	175
Units	°C	°C	°C

7.2.   Appendix B

7.2.1.   Limiting Oxygen Index for commercial polymers

(Van Krevelen, 1990; Lyons, 1987; Hirschler, 2000)

Polymer	LOI
Polyformaldehyde	0.15
Poly(ethylene oxide) [PEO]	0.15
Polyoxymethylene [POM]	0.15
Polyacetal	0.16
Kitchen candle	0.16
Poly(methyl methacrylate) [PMMA]	0.17
Styrene-Acrylonitrile [SAN]	0.18
Acrylonitrile-Butadiene-Styrene [ABS]	0.18
Polyacrylonitrile [PAN]	0.18
Polyethylene [PE]	0.18
Polypropylene [PP]	0.18
Polystyrene [PS]	0.19
Polyisoprene	0.19
Polybutadiene	0.19
Cellulose	0.19
Cotton	0.20
Poly(ethylene terephthalate) [PET]	0.21
Air	**0.21**
Poly(vinyl alcohol) [PVA]	0.22
Polyamide 6,6 [Nylon 6,6]	0.23
Penton [®]	0.23
Wool	0.25
Polyamide 6 [Nylon 6]	0.26
Polycarbonate [PC]	0.27
Nomex [®]	0.29
Polyphenylene oxides [PPO]	0.29
Polysulphone	0.30
Silicone rubber	0.32
Phenol-formaldehyde resin	0.35
Polyether-ether ketone	0.35
Neoprene [®]	0.40
Polybenzimidazole	0.42
Poly(vinyl chloride) [PVC]	0.42
Poly(vinylidene fluoride)	0.44
Polyphenylene sulphide	0.44
Poly(vinylidene chloride)	0.60
Carbon	0.60
Poly(tetrafluoroethylene) [PTFE, Teflon[®]]	0.95

7.3. Appendix C

7.3.1. List and structure of acids (and complexes) used

Compound	Aromatic	Acid groups	Carbons	Hydroxyl groups	Other
Acids					
α-Fufoic acid = 2-Furan carboxylic acid		1	5		
2-Ketoglutaric acid		2	5		
3,5-Diaminobenzoic acid	*	1	7		2 x NH$_2$
3-Picolinic acid = Nicotinic acid		1	6		Pyridine
4-*t*-Butylbenzoic acid	*	1	11		
Adipic acid		2	6		
Anisic acid = Methoxybenzoic acid	*	1	8		
Aspartic acid		2	4		NH$_2$
Azelaic acid		2	9		
Barbital = Barbitone = 5,5-Diethylbarbituric acid			8		2 x NH
Benzoic acid	*	1	7		
Butyric acid		1	4		
Citric acid		3	6	1	
Coumaric acid = 2-Hydroxicinnamic acid	*	1	9	1	
Cyanuric acid = *i*-Cyanuric acid			3	3	3 x N in ring
Decanoic acid = Capric acid		1	10		
Formic acid		1	1		
Galacturonic acid		1	6	4	
Gallic acid	*	1	7	3	
Gluconic acid		1	6	5	
Glutaric acid		2	5		
Glycine = Glycocoll = Aminoacetic acid		1	2		NH$_2$
Glycolic acid		1	2	1	
Glycolic acid ethyl ether = Ethoxyacetic acid		1	4		
Heptanoic acid = Enanthic acid		1	7		
Hexanoic acid = Caproic acid		1	6		
Homophthalic acid	*	2	9		
i-Butyric acid		1	4		
i-Phthalic acid	*	2	8		
Lauric acid		1	12		
Levukinic acid		1	5		
Maleic acid		2	4		
Malic acid		2	4	1	
Malonic acid		2	3		
Mandelic acid	*	1	8	1	

Compound	Aromatic	Acid groups	Carbons	Hydroxyl groups	Other
Mucic acid = Galactaric acid		2	6	4	
Myristic acid		1	14		
Nitrillo triacetic acid		3	6		N
Nonanoic acid = Pelargonic acid		1	9		
Octanoic acid = Caprylic acid		1	8		
Oxalic acid		2	2		
Palmitic acid		1	16		
Phenylacetic acid	*	1	8		
Phthalic acid = 1,2-Benzene dicarboxylic acid	*	2	8		
Phthalic anhydride	*	2	8		
Phytic acid		12	6		$6 \times H_2PO_4^-$
Pyrazinecarboxylic acid		1	5		Pyrazine
Pyrogallic acid = Pyrogallol	*		6	3	
Pyromellitic acid = 1,2,4,5-Benzene tertacarboxylic acid	*	4	10		
Sebacic acid = Decanedioic acid		2	10		
Sorbic acid		1	6		
Stearic acid		1	18		
Succinic acid		2	4		
Tartaric acid		2	4	2	
Tiglic acid		1	5		
Trimesic acid = 1,3,5-Benzene tricarboxylic acid	*	3	9		
Undecylenic acid		1	11		
Uric acid			5		$4 \times NH$
Sodium complexes					
di-Sodium fumarate		2	4		
di-Sodium oxalate		2	2		
di-Sodium tartrate		2	4	2	
Phenylpyruvic acid sodium salt	*	1	9		
Phytic acid deodeca sodium salt		12	6		$6 \times H_2PO_4^-$
Pyruvic acid sodium salt		1	3		
Sodium cyclamate		1	6		$NHSO_3^-$
Sodium glycolate		1	2	1	
Sodium tetraphenyl borate	*	1	24		B
tri-Sodium citrate		3	6	1	
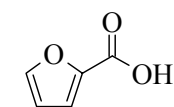
α-Furoic acid
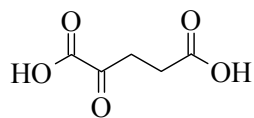
2-Ketoglutaric acid
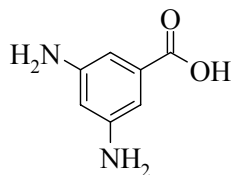
3,5-Diaminobenzoic acid
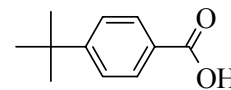
4-t-Butylbenzoic acid
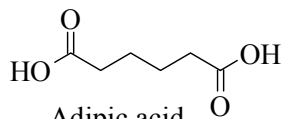
Adipic acid
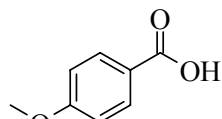
Anisic acid
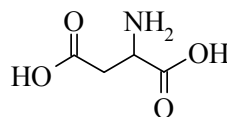
Aspartic acid
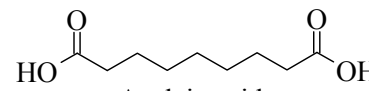
Azelaic acid
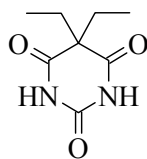
Barbital
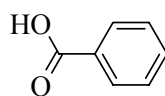
Benzoic acid
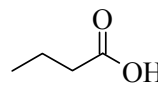
n-Butyric acid
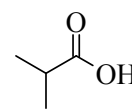
i-Butyric acid
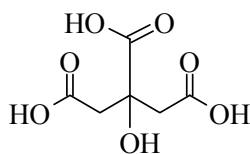
Citric acid
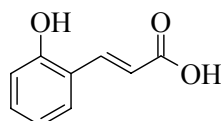
Coumaric acid
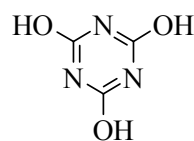
Cyanuric acid
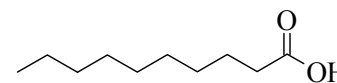
Decanoic acid
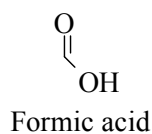
Formic acid
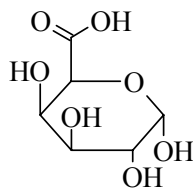
Galacturonic acid
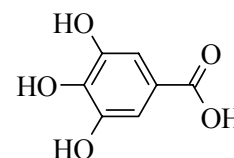
Gallic acid
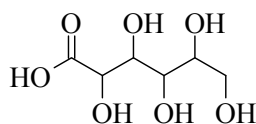
Gluconic acid
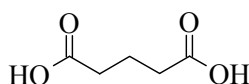
Glutaric
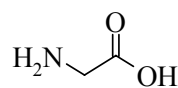
Glycine
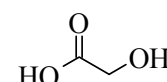
Glycolic acid
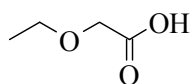
Glycolic acid ethyl ether
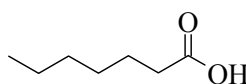
Heptanoic acid
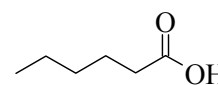
Hexanoic acid
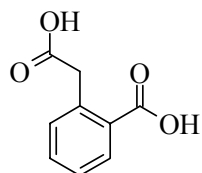
Homophthalic acid
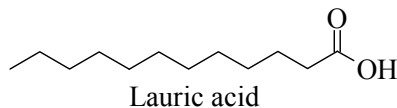
Lauric acid
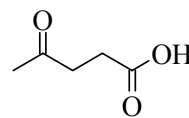
Levulinic acid
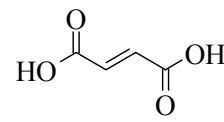
Maleic acid
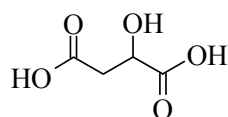
Malic acid
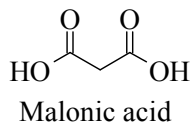
Malonic acid
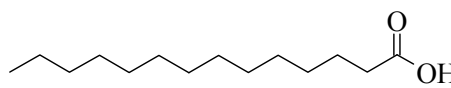
Myristic acid
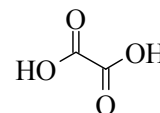
Oxalic acid
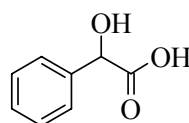
Mandelic acid
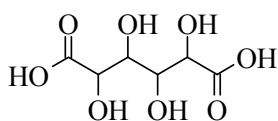
Mucic acid
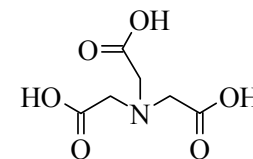
Nitrillo triacetic acid
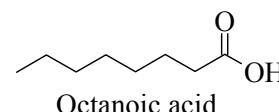
Octanoic acid
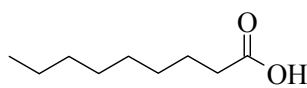
Pelargonic acid
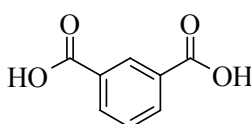
i-Phthalic acid
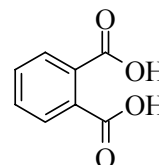
Phthalic acid
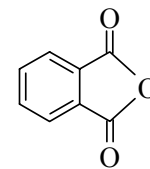
Phthalic anhydride
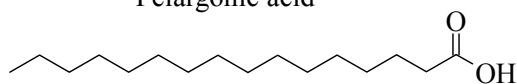
Palmitic acid
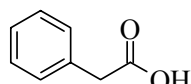
Phenylacetic acid

Picolinic acid

$R = -O-P=O$
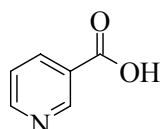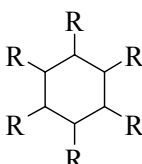
Phytic acid
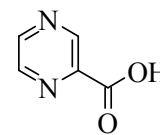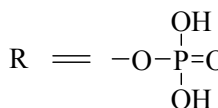
Pyrazinecarboxylic acid
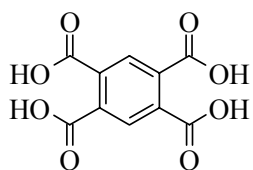
Pyromellitic acid
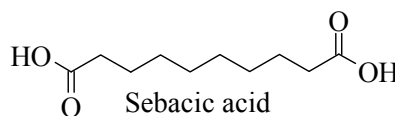
Sebacic acid
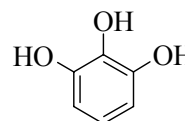
Pyrogallic acid
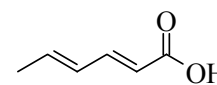
Sorbic acid
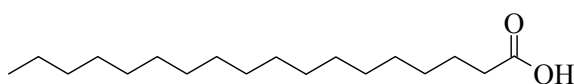
Stearic acid
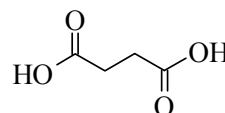
Succinic acid
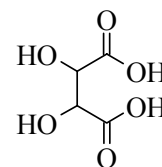
Tartaric acid
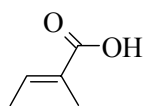
Tiglic acid
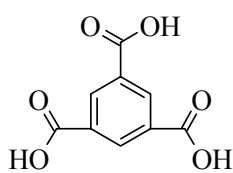
Trimesic acid
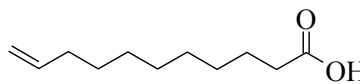
Undecylenic acid
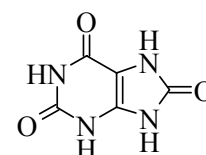
Uric acid
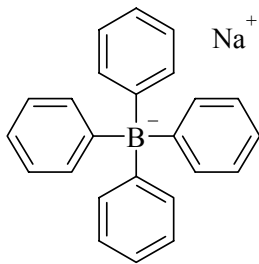
sodium tetraphenyl borate
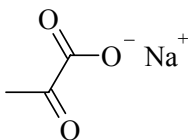
pyruvic acid sodium salt
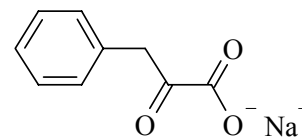
phenylpyruvic acid sodium salt
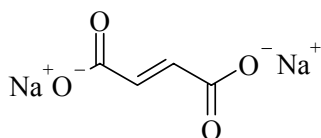
di-sodium fumarate
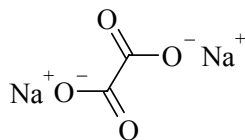
di-sodium oxalate
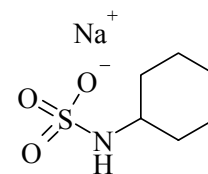
sodium cyclamate
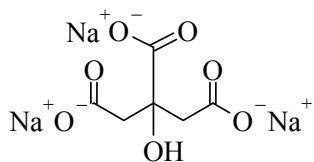
tri-sodium citrate
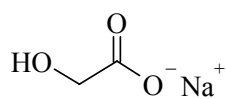
sodium glycolate
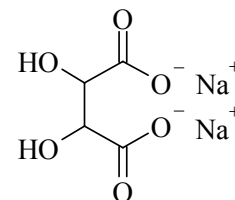
di-sodium tartrate

7.4. Appendix D

7.4.1. Acetylacetonate complexes used

Aluminium acetylacetonate

Calcium acetylacetonate

x calculated as 0.7

Copper (II) acetylacetonate

Iron (III) acetylacetonate

Magnesium acetylacetonate

Sodium acetylacetonate

Titanyl acetylacetonate

Vanadyl acetylacetonate

Zirconium acetylacetonate
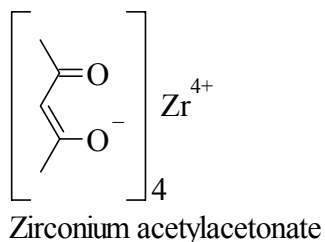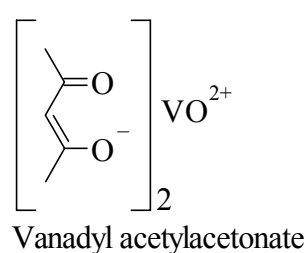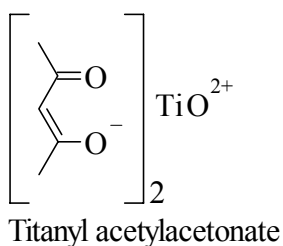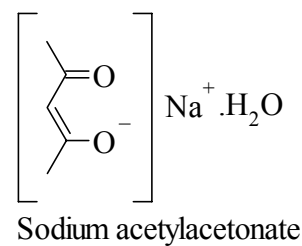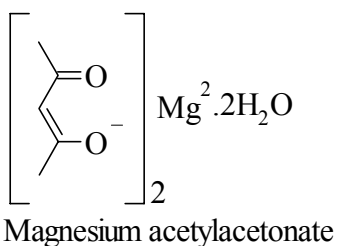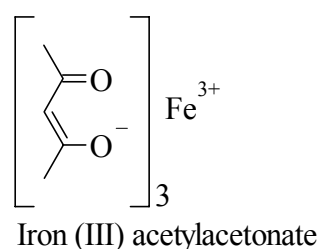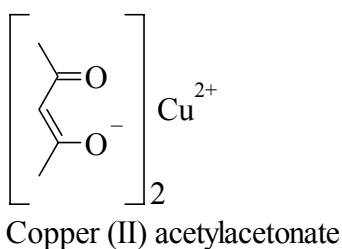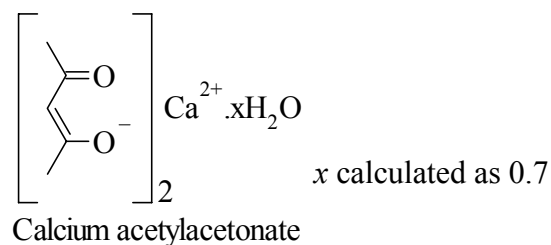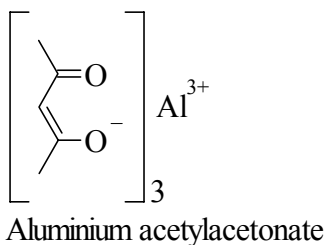
7.5.   Appendix E

7.5.1.   The commercial preparation of gluconic acid and its derivatives

Calcium gluconate is mass-produced by the neutralisation of gluconic acid with calcium carbonate. For the production of calcium gluconate, it is easiest to first produce gluconic acid and then neutralise with calcium carbonate (Green, 1980; Theander, 1980; Hustede *et al.,* 1988).

There are several ways to produce gluconic acid commercially. All have to do with the oxidation of glucose (dextrose) or glucose solutions to gluconic acid. **Chemical and electrochemical oxidation** has been used in industry before, but is costly and has relative low yields. Gluconic acid cannot be prepared through photochemical oxidation. The preferred method for the production of gluconic acid is through **biochemical oxidation** (Green, 1980; Theander, 1980; Hustede *et al.,* 1988).

The **catalytic oxidation** of glucose is being used in industry more readily in recent years. Glucose solutions of concentration of 1-2 mol/ℓ is oxidised with oxygen or air while the solution's pH is kept between 8 and 11 (preferably 9-10) with the continuous addition of an alkaline (calcium carbonate) solution. Normally highly purified glucose solutions should be used. The catalysts are platinum-group metals suspended on activated charcoal or aluminium oxide. The effectiveness of the catalysts can be improved by doping the platinum-group metals with lead, selenium, thallium or bismuth, with the preferred carrier being activated charcoal. Typical operation temperatures are 50°C. Catalyst activity, selectivity, lifetime and cost are the most important economical aspects (Green, 1980; Theander, 1980; Hustede *et al.,* 1988).

Chemical oxidation of D-glucose to D-gluconic acid with halogens (and especially chlorine) is known since the second half of the 19th century. Yields are relatively low but can be dramatically increased (up to ~ 96%) with the addition of a solid buffer. The gluconic acid is usually isolated as its calcium salt (Green, 1980).

The principal organisms employed for the **biochemical oxidation** are *Aspergillus niger* and *Gluconobacter suboxydans*, with the *Aspergillus niger* process being used most

regularly. For example, typical production parameters for the fermentative synthesis of sodium gluconate with *Aspergillus niger* are (Hustede *et al.,* 1988):

Typical substrate formulation: 250-300 g/ℓ glucose, 0.2-0.3 g/ℓ $MgSO_4.7H_2O$, 0.2-0.3 g/ℓ KH_2PO_4 and 0.4-0.5 g/ℓ $(NH_4)_2HPO_4$ or urea. The substrate must be sterilised. Sterilisation may be done either in batches at 110°C with a residence time of 45 min or continuously under conditions providing several minutes exposure to a temperature of 135-150°C. In the fermentation vessel, the pH is adjusted to 4.5-5.0 and inoculated with the cultured micro-organism. During the production phase, the temperature is maintained at 30-32°C and pH at 5.5-6.5 through continuous neutralisation. The optimum pH for the process is near 5.6. A 30-50% sodium hydroxide solution is used for the neutralisation. Fermentation continues for a period of 40-100 h, depending on the starting concentration. To ensure yields above 80%, an adequate oxygen supply (0.1 ℓ oxygen per ℓ solution per minute) must be maintained. Gas distribution within the fermentor must be optimised. The partial pressure of oxygen may be increased by using oxygen-enriched air or operating the fermentor at elevated pressures.

The cultured medium contains only about 100 g/ℓ glucose, but as much as twice the mentioned amounts of nutrient salts, an increased amount of nitrogen compounds and a 0.2-0.4 g/ℓ corn steep powder (a growth-stimulating additive). A lyophilized permanent culture is used to grow the conidia. The culture is first activated with a specific growth medium in culture tubes. After the production of several subcultures, the organism is introduced into a special medium that encourages the formation of conidia. The conidia are harvested after a 5-10 days incubation period and used to inoculate the preculture.

For the production of calcium gluconate, calcium carbonate may be used for neutralisation instead of sodium hydroxide. The micro-organisms are removed by filtration after fermentation. The product may be decolourised with activated carbon and then either evaporated or crystallised or spray dried.

7.6.   Appendix F

7.6.1.   Vitamin supplement label

Sport en aktie programme pl op die liggaam en vermoë om deur die dieët a: spesiale behoe 'n gebalansee aan hoë geha en 'n goedg dieëtaanvulling s Sport's Own a

Sport and active exercise programmes place heavy demands on the body's reserves and ability to replenish these reserves through dietary intake. These special needs should be catered for through a healthy balanced diet which includes a sufficient supply of high quality carbohydrates plus a well formulated dietary supplement such as Bettaway's Sport's Own.

Made in South Africa
BETTER NUTRITION (Pty) Ltd
PO Box 494, Bergvlei, 2012
1 Carey Street,
Wynberg, Sandton.
☎ (011) 444-6921
E-Mail: bettaway@pharma.co.za
6B8874/98

NUTRITIONAL INFORMATION		
Each tablet contains:		%RDA*
Vitamin A	1666 iu	50
Vitamin D	66.7 iu	33
Vitamin E	25 iu	168
Vitamin C	50 mg	83
Vitamin B1	10 mg	714
Vitamin B2	10 mg	625
Nicotinamide (B3)	20 mg	111
Vitamin B6	10 mg	500
Folic Acid	200 ug	100
Vitamin B12	5 ug	500
Biotin	25 ug	25
Calcium D		
Pantothenate	6.6 mg	101
Calcium (carbonate)	133.3 mg	17
Choline Bitartrate	4 mg	·
Copper (gluconate)	0.17 mg	·
Desiccated Liver	16.7 mg	·
Hesperidin Complex	4 mg	·
Inositol	6 mg	·
Iron (ferrous fumarate)	5 mg	36
Lecithin	20 mg	·
Lemon Bioflavonoid Complex	5 mg	·
Magnesium (oxide)	100 mg	33
Manganese (gluconate)	10 ug	·
Potassium (gluconate)	6.7 mg	·
Rutin	5 mg	·
Selenium (AAC)	30 ug	·
Zinc (gluconate)	5 mg	33
Iodine (kelp)	25 ug	17
L-Glutamic Acid	3.5 mg	·
L-Lysine	25 mg	·

* Recommended Daily Dietary
Allowance per tablet:
AAC = Amino Acid Chelate

CONTAINS NO ARTIFICIAL
COLOURS OR FLAVOURS,
PRESERVATIVES, LACTOSE,
YEAST OR SALT.

Bettaway
SPORT'S OWN

TIME RELEASE

Hi-Potency

CONTAINS **30** TABLETS

A multivitamin fit to keep any active person on their toes.

Directions:
One tablet to be taken once daily with food. Keep out of reach of children. Store below 25°C.

Aanwysings:
Neem een tablet daagliks met etes. Hou buite bereik van kinders. Bewaar benede 25°C.

7.7.   Appendix G

7.7.1.   Pictures of the burn test setup

Front view of the setup

Rear view of the setup (no thermocouples)

Flame nozzle
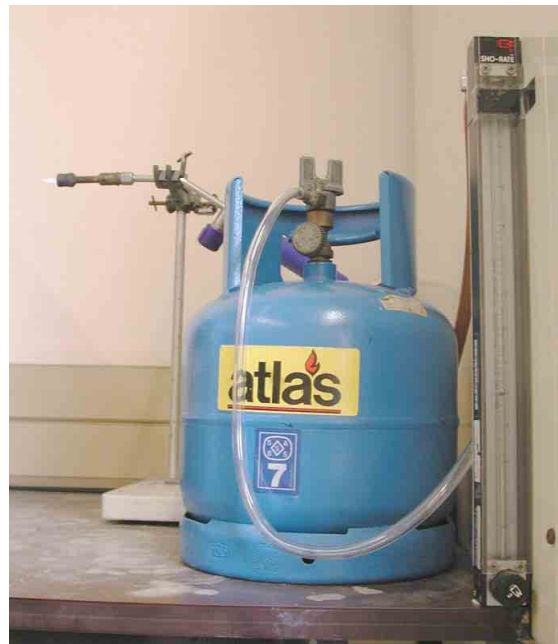
Gas bottle and rotameter

7.8.   Appendix H

7.8.1.   Screen grab of the data logging software, "Capture".
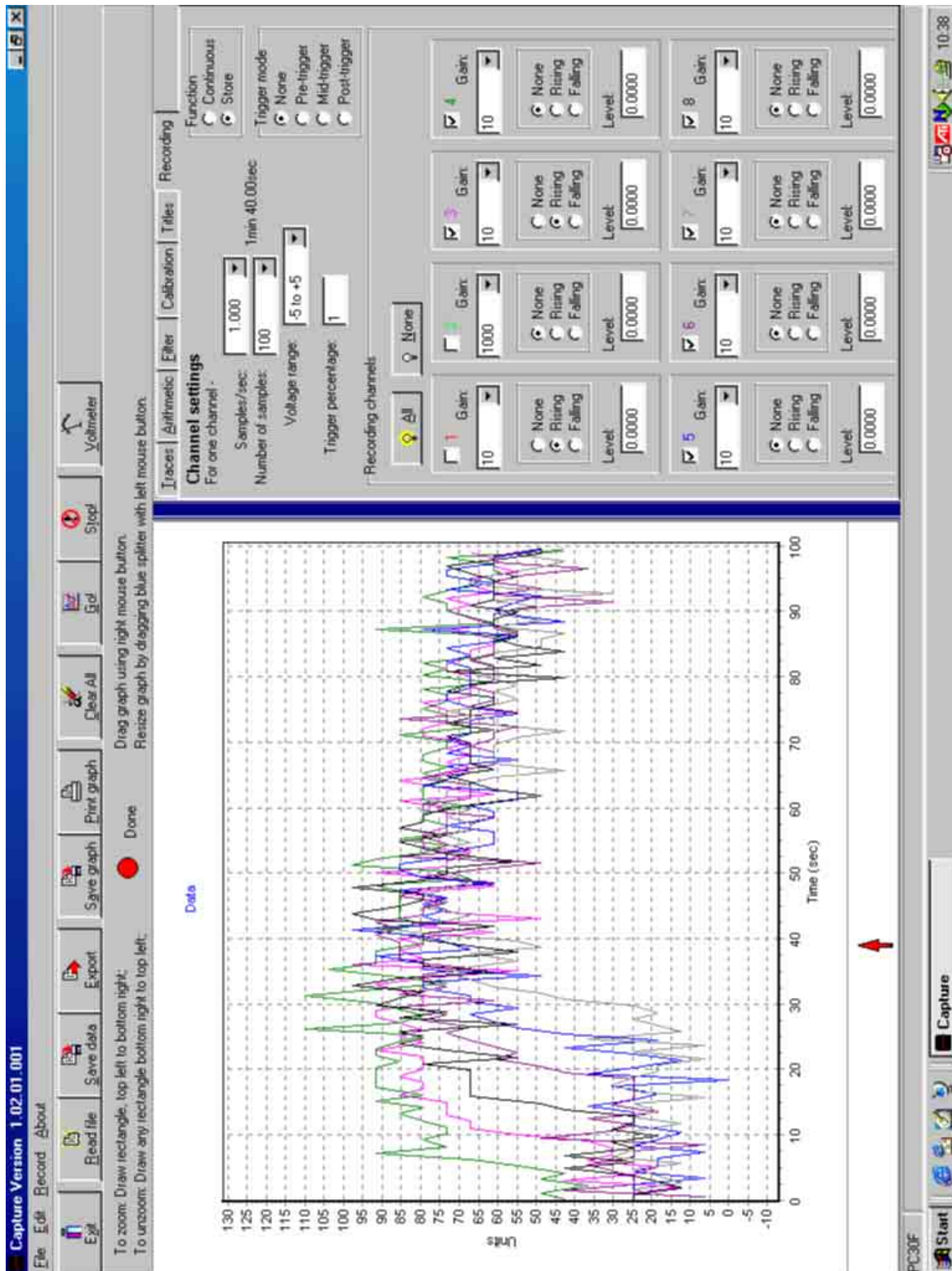
7.9. Appendix I

7.9.1. Photos of the cold finger used for the sublimation crystallisation

7.10. Appendix J

7.10.1. Elemental analysis of the leached SiO_2 from Foskor Pty. Ltd.

SET POINT LABORATORIES
INC. BERGSTRÖM & BAKKER, GOLDLABS AND ROCKLABS

SET POINT TECHNOLOGY

ANALYSIS REPORT

Attention: Mr Johan Labuschagne
Company: University of Pretoria
Order No: 163188/77
Address: Lynnwoodweg
Pretoria

SPL Report No: 0/1063
Date: 18/5/2000

SAMPLE NAME	Fe2O3 %	MnO %	Cr2O3 %	V2O5 %	TiO2 %	CaO %	K2O %	P2O5 %	SiO2 %	Al2O3 %	MgO %	Na2O %	CL %	M.CH %	S %
SiO2	1.36	0.03	0.02	0	0.15	3.54	1.01	0.06	72.3	1.2	2.7	0.1	0	-15	2.33

Dr CJ Rademeyer
(Divisional Director)

Margaret Farrell
(Analyst)

While every effort is made to provide analysis of the highest accuracy, the liability of Set Point Laboratories is restricted to the cost of the analysis

ANALYSTS AND CONSULTANTS
46 Chadwick Avenue, Wynberg, 2090
PO Box 447, Bergvlei, 2012
Tel: +27 (0)11 786 0215
Fax: +27 (0)11 786 7317
E-mail: info@rl.setpoint.co.za
Internet: www.setpoint.co.za

A division of Set Point Industrial Technology (Pty) Ltd
Reg No 89/00291/07
Directors: RJ Smith, GP Bruwershoek
JL Martin Ph D
Company Secretary: LR Goosman
Divisional Director: CJ Rademeyer Pr B

7.11. Appendix K

7.11.1. Preparation of CaDex (Venter, 2000)

METHOD OF PREPARATION OF CADEX

REACTANTS.

(a) 50.00 g of dextrose monohydrate
(b) 75.00 g of distilled water
(c) 13.84 g of calcium hydroxide powder

METHOD:

1. On a heater/stirrer prepare a solution of the dextrose monohydrate in the water. The water has to be heated slightly. (Time necessary: ± 20 minutes).

2. Put this solution in a 250 ml round bottom flask with three openings. Add about 10 glass boiling stones. Fit a thermometer in one of the openings. Fit two running water coolers, one on top of the other one, to the central opening. Close the third opening with a glass stopper. Heat the solution on a water bath to 60°C.

3. When the solution has reached 60°C add the calcium hydroxide powder through the free opening in the flask with the aid of a funnel.

4. Keep the reaction mixture at 60°C for 20 minutes. Stir the round bottom flask from time to time. The solution immediately turns yellow brown, and later red brown.

5. After twenty minutes remove the round bottom flask from the water bath, and filter the solution with a Buchner filter.

6. The brown liquid filtrate (Cadex) should be stored.

7. Determination of the calcium content of the liquid (Cadex): Add 1 mole of oxalic acid per mole of calcium hydroxide used initially (± 17 g) to 10g of concentrated Cadex solution, as well as about 400 g of distilled water. Stir the solution for about 30 minutes on a heater/stirrer. Filter the suspension (calcium oxalate) through a Buchner filter. Dry the dry filtrate on the filter paper in an oven at about 60°C. Determine the mass of the dry calcium oxalate. Burn 1.00g of calcium oxalate in an oven at 1050°C for about 12 hours. Determine the mass of the resulting calcium oxide powder. Correct the calcium content of the concentrated Cadex solution. (It should contain more or less 4% - 5% calcium.)

8. Add the required amount of distilled water to the concentrated solution

of Cadex to adjust the calcium concentration to the required level (usually about 1%).

METHOD OF PREPARATION OF CAFOR

REACTANTS:

(a) 1.00 g of dextrose monohydrate
(b) 124.00 g of 37% aqueous formaldehyde solution
(c) 13.84 g of calcium hydroxide powder

METHOD:

Follow the same procedure as for preparing Cadex. The starting solution will have 1.00g of dextrose monohydrate and 124.00g of 37% aqueous formaldehyde solution. Work in a fume cupboard when heating the solution. Before the condensation reaction begins there will be an induction period of 5 to 6 minutes during which the temperature of the reaction mixture will rise to about 75°C to 80°C. Make sure that the two Liebig coolers function! The rest of the procedure is as described above.

NB: During each reaction period one obtains about 130 g of product. The reaction has to be repeated several times to prepare bigger amounts of the product.

7.12. Appendix L

7.12.1. Tabulated results for the pyrolysis of the sodium compounds and the synthesis and pyrolysis of the sodium salts

Synthesis	No	A2	A3	A4	A5	A6	B1	B2	B3	B4	B5	
Acid H		1	2	1	1	12	2	2	1	1	3	mole
% Na in product		11.261	34.313	6.718	20.892	29.863	19.984	28.730	11.425	13.283	26.725	%
Tube mass	Before	8.860	8.880	8.970	7.210	8.970	7.050	7.240	7.150	7.070	6.880	g
Sample mass		0.200	0.670	0.200	0.120	0.340	0.100	0.150	0.160	0.100	0.100	g
Height powder		20	15	12	5	12	3	5	6	4	3	mm
Mass Na in		0.023	0.230	0.013	0.025	0.102	0.020	0.043	0.018	0.013	0.027	g
Total mass	After	8.970	9.500	9.100	7.280	9.210	7.100	7.360	7.220	7.130	6.950	g
Height char		41	17	12	61	38	17	27	7	14	40	mm
Mass left (total)		0.110	0.620	0.130	0.070	0.240	0.050	0.120	0.070	0.060	0.070	g
Mass left (Na)		0.023	0.230	0.013	0.025	0.102	0.020	0.043	0.018	0.013	0.027	g
Mass left (Na_2CO_3)		0.052	0.530	0.031	0.058	0.234	0.046	0.099	0.042	0.031	0.062	g
Mass left (carbon)		0.058	0.090	0.099	0.012	0.006	0.004	0.021	0.028	0.029	0.008	g
% carbon left		52.804	14.524	76.176	17.440	2.479	7.867	17.216	39.801	48.969	11.992	%
Height change		21	2	0	56	26	14	22	1	10	37	mm

Synthesis				Na₂CO₃	1	2	3	47	4	5	6	7	29	8	9	10	
	No				1	2	3	47	4	5	6	7	29	8	9	10	
	Acid			Na₂CO₃	Octanoic	n-Heptanoic	Pelargonic	Nonanoic	Formic	i-Butyric	2-Furoic	Oxalic	Oxalic	Citric	Decanoic	Lauric	
		M_w		105.99	144.22	130.19	158.23	158.24	46.03	88.11	112.09	126.07	126.07	210.14	172.27	200.32	g/mol
		Calculated	Mass acid		2.00	2.00	2.00	2.00	0.85	1.00	2.00	2.00	2.00	2.00	2.00	2.00	g
			Mole acid		0.014	0.015	0.013	0.013	0.018	0.011	0.018	0.016	0.016	0.010	0.012	0.010	mole
			Acid H		1	1	1	1	1	1	1	2	2	3	1	1	mole
			Mass Na₂CO₃		1.470	1.628	1.340	1.340	1.957	1.203	1.891	1.681	1.681	1.009	1.231	1.058	g
			Mole Na₂CO₃		0.014	0.015	0.013	0.013	0.018	0.011	0.018	0.016	0.016	0.010	0.012	0.010	mole
		In	Mass acid		2.020	2.000	2.020	2.020	1.010	1.000	2.010	2.000	2.010	2.010	2.020	2.010	g
			Mole acid		0.014	0.015	0.013	0.013	0.022	0.011	0.018	0.016	0.016	0.010	0.012	0.010	mole
			Mass Na₂CO₃ (sol)		29.440	32.560	26.810	26.820	39.450	24.060	37.830	33.650	33.640	20.180	24.620	21.170	g
			Mass Na₂CO₃		1.472	1.628	1.341	1.341	1.973	1.203	1.892	1.683	1.682	1.009	1.231	1.059	g
			Mole Na₂CO₃		0.014	0.015	0.013	0.013	0.019	0.011	0.018	0.016	0.016	0.010	0.012	0.010	mole
			Mole Na		0.028	0.031	0.025	0.025	0.037	0.023	0.036	0.032	0.032	0.019	0.023	0.020	mole
			Mass Na		0.639	0.706	0.582	0.582	0.856	0.522	0.821	0.730	0.730	0.438	0.534	0.459	g
	Product		Mass expected		3.058	3.152	2.965	2.965	2.302	1.851	3.345	2.699	2.698	2.426	2.887	2.757	g
		Out	Mass obtained		3.730	3.100	3.570	3.220	2.730	2.120	4.710	1.970	2.050	2.390	3.540	2.910	g
			Percentage yield		121.990	98.363	120.421	108.596	118.592	114.531	140.791	73.003	75.982	98.527	122.604	105.537	%
			% Na in product	43.381	17.120	22.782	16.289	18.067	31.344	24.617	17.422	37.050	35.594	18.315	15.085	15.780	%

Synthesis		units	11	12	13	14	61	15	16	17	18	19	20	21	22
No	Acid		Myristic	Palmitic	Trimesic	Mucic	Mucic	Phenylacetic	Anisic	Adipic	Uric	Coumaric	i-Cyanuric	i-Phthalic	Malonic
	M_w	g/mol	228.38	256.43	210.14	210.14	210.14	136.14	152.15	146.14	168.11	140.10	129.08	166.13	104.07
Mass acid	*Calculated*	g	2.00	2.00	2.00	2.00	2.00	2.00	2.00	2.00	2.00	2.00	2.00	2.00	2.00
Mole acid		mole	0.009	0.008	0.010	0.010	0.010	0.015	0.013	0.014	0.012	0.014	0.015	0.012	0.019
Acid H	*In*	mole	1	1	3	2	2	1	1	2	3	1	3	2	2
Mass Na$_2$CO$_3$		g	0.928	0.827	1.009	1.009	1.009	1.557	1.393	1.451	1.261	1.513	1.642	1.276	2.037
Mole Na$_2$CO$_3$		mole	0.009	0.008	0.010	0.010	0.010	0.015	0.013	0.014	0.012	0.014	0.015	0.012	0.019
Mass acid		g	2.010	2.020	2.010	2.010	1.960	2.000	2.010	2.010	2.000	2.000	2.010	2.020	2.010
Mole acid		mole	0.009	0.008	0.010	0.010	0.009	0.015	0.013	0.014	0.012	0.014	0.016	0.012	0.019
Mass Na$_2$CO$_3$ (sol)		g	18.580	16.560	20.190	20.180	5.940	31.160	27.870	29.000	25.230	30.260	32.850	25.540	40.760
Mass Na$_2$CO$_3$		g	0.929	0.828	1.010	1.009	0.990	1.558	1.394	1.450	1.262	1.513	1.643	1.277	2.038
Mole Na$_2$CO$_3$		mole	0.009	0.008	0.010	0.010	0.009	0.015	0.013	0.014	0.012	0.014	0.015	0.012	0.019
Mole Na		mole	0.018	0.016	0.019	0.019	0.019	0.029	0.026	0.027	0.024	0.029	0.031	0.024	0.038
Mass Na		g	0.403	0.359	0.438	0.438	0.429	0.676	0.605	0.629	0.547	0.656	0.713	0.554	0.884
Mass expected	**Product**	g	2.666	2.604	2.426	2.426	2.371	3.102	2.994	2.607	2.524	3.070	2.687	2.543	2.850
Mass obtained	*Out*	g	3.100	2.950	2.890	2.400	2.594	3.500	3.180	3.400	3.220	2.820	3.350	2.900	2.690
Percentage yield		%	116.277	113.300	119.115	98.939	109.383	112.816	106.219	130.422	127.596	91.848	124.690	114.046	94.386
% Na in product		%	13.000	12.176	15.153	18.238	16.557	19.311	19.010	18.501	16.996	23.275	21.270	19.103	32.867

Synthesis		Units	23	24	25	26	27	28	30	31	32	33	34	35
No	Acid		Stearic	Azeloic	Pyrogallic	Malic	Keto Glutaric	Picolinic	Barbitone	Glycocoll	Phthalic Anhydride	Butyl benzoic	Tiglic	Pyrazine carboxylic
M_w	Calculated	g/mol	284.48	188.22	126.11	134.09	146.10	123.11	184.20	75.07	148.12	178.23	100.12	124.10
Mass acid		g	2.00	2.00	2.00	2.00	2.00	2.00	2.00	1.00	2.00	2.00	2.00	2.00
Mole acid		mole	0.007	0.011	0.016	0.015	0.014	0.016	0.011	0.013	0.014	0.011	0.020	0.016
Acid H		mole	1	2	3	2	2	1	2	1	2	1	1	1
Mass Na$_2$CO$_3$		g	0.745	1.126	1.681	1.581	1.451	1.722	1.151	1.412	1.431	1.189	2.117	1.708
Mole Na$_2$CO$_3$		mole	0.007	0.011	0.016	0.015	0.014	0.016	0.011	0.013	0.014	0.011	0.020	0.016
Mass acid	In	g	2.020	2.000	2.020	2.000	2.000	2.010	2.000	1.010	2.000	2.010	2.010	2.000
Mole acid		mole	0.007	0.011	0.016	0.015	0.014	0.016	0.011	0.013	0.014	0.011	0.020	0.016
Mass Na$_2$CO$_3$ (sol)		g	14.920	22.530	33.620	31.650	29.040	34.440	23.020	28.250	28.640	23.810	42.480	34.170
Mass Na$_2$CO$_3$		g	0.746	1.127	1.681	1.583	1.452	1.722	1.151	1.413	1.432	1.191	2.124	1.709
Mole Na$_2$CO$_3$		mole	0.007	0.011	0.016	0.015	0.014	0.016	0.011	0.013	0.014	0.011	0.020	0.016
Mole Na	Product	mole	0.014	0.021	0.032	0.030	0.027	0.032	0.022	0.027	0.027	0.022	0.040	0.032
Mass Na		g	0.324	0.489	0.729	0.687	0.630	0.747	0.499	0.613	0.621	0.516	0.921	0.741
Mass expected		g	2.546	2.467	2.707	2.657	2.603	3.226	2.478	2.005	2.595	2.851	3.511	3.209
Mass obtained	Out	g	2.690	2.560	3.970	2.590	2.910	3.650	2.880	2.200	3.580	2.910	4.050	3.350
Percentage yield		%	105.665	103.752	146.630	97.465	111.797	113.155	116.244	109.712	137.984	102.078	115.339	104.404
% Na in product		%	12.031	19.090	18.369	26.506	21.646	20.467	17.338	27.853	17.353	17.748	22.751	22.125

Synthesis		Units	36	37	38	39	40	41	42	43	44	45	46	48
No			36	37	38	39	40	41	42	43	44	45	46	48
Acid			Sebacic	Homophthalic	Mandelic	Maleic	Pyromellitic	Tartaric	Diamino-benzoic	Galacturonic	Glutaric	Succinic	Sorbic	Levulinic
M_w		g/mol	202.24	180.16	152.15	116.07	254.16	150.09	152.15	212.20	132.11	118.09	112.13	116.11
Mass acid	Calculated	g	2.00	2.00	2.00	2.00	2.25	2.00	2.00	2.00	2.00	2.00	2.00	2.00
Mole acid		mole	0.010	0.011	0.013	0.017	0.009	0.013	0.013	0.009	0.015	0.017	0.018	0.017
Acid H		mole	2	2	1	2	4	2	1	1	2	2	1	1
Mass Na_2CO_3		g	1.048	1.177	1.393	1.826	0.938	1.412	1.393	0.999	1.605	1.795	1.890	1.826
Mole Na_2CO_3		mole	0.010	0.011	0.013	0.017	0.009	0.013	0.013	0.009	0.015	0.017	0.018	0.017
Mass acid	In	g	2.000	2.000	2.010	2.010	2.258	2.010	2.010	2.010	2.000	2.000	2.010	2.000
Mole acid		mole	0.010	0.011	0.013	0.017	0.009	0.013	0.013	0.009	0.015	0.017	0.018	0.017
Mass Na_2CO_3 (sol)		g	20.980	23.540	27.870	36.550	18.770	28.270	27.880	19.990	32.100	35.900	37.830	36.520
Mass Na_2CO_3		g	1.049	1.177	1.394	1.828	0.939	1.414	1.394	1.000	1.605	1.795	1.892	1.826
Mole Na_2CO_3		mole	0.010	0.011	0.013	0.017	0.009	0.013	0.013	0.009	0.015	0.017	0.018	0.017
Mole Na		mole	0.020	0.022	0.026	0.034	0.018	0.027	0.026	0.019	0.030	0.034	0.036	0.034
Mass Na		g	0.455	0.511	0.605	0.793	0.407	0.613	0.605	0.434	0.696	0.779	0.821	0.792
Mass expected	Product	g	2.436	2.488	2.994	2.763	2.645	2.593	2.994	2.716	2.666	2.745	3.346	3.292
Mass obtained	Out	g	2.380	2.350	3.120	3.200	2.990	2.830	3.310	2.530	2.390	4.510	4.030	3.600
Percentage yield		%	97.716	94.436	104.215	115.799	113.040	109.146	110.543	93.160	89.647	164.327	120.457	109.362
% Na in product		%	19.121	21.728	19.376	24.775	13.617	21.668	18.270	17.138	29.133	17.266	20.361	22.004

Synthesis		Units	49	50	51	52	53	54	55	56	57	58	59	60
No / Acid			Gluconic	Glycollic	Phytic	Nit.triacetic	Undecylenic	Hexanoic	Ethoxy acetic	Phthalic	n-Butyric	Aspartic	Benzoic	Gallic
M_w		g/mol	196.16	76.05	660.04	191.14	182.26	116.16	104.11	166.13	88.11	133.10	122.12	188.12
Mass acid	*Calculated*	g	1.50	1.32	1.60	2.00	2.00	2.00	2.00	2.00	1.00	2.00	2.00	2.00
Mole acid		mole	0.008	0.017	0.002	0.010	0.011	0.017	0.019	0.012	0.011	0.015	0.016	0.011
Acid H	*In*	mole	1	1	12	3	1	1	1	2	1	2	1	1
Mass Na$_2$CO$_3$		g	0.810	1.840	0.257	1.109	1.163	1.825	2.036	1.276	1.203	1.593	1.736	1.127
Mole Na$_2$CO$_3$		mole	0.008	0.017	0.002	0.010	0.011	0.017	0.019	0.012	0.011	0.015	0.016	0.011
Mass acid	*In*	g	1.495	1.320	1.600	2.000	2.020	2.000	2.000	2.010	0.980	2.010	2.000	2.000
Mole acid		mole	0.008	0.017	0.002	0.010	0.011	0.017	0.019	0.012	0.011	0.015	0.016	0.011
Mass Na$_2$CO$_3$ (sol)		g	16.220	36.790	5.120	22.180	23.260	36.520	40.730	25.520	24.080	31.860		
Mass Na$_2$CO$_3$		g	0.811	1.840	0.256	1.109	1.163	1.826	2.037	1.276	1.204	1.593	1.736	1.130
Mole Na$_2$CO$_3$		mole	0.008	0.017	0.002	0.010	0.011	0.017	0.019	0.012	0.011	0.015	0.016	0.011
Mole Na	*Product*	mole	0.015	0.035	0.005	0.021	0.022	0.034	0.038	0.024	0.023	0.030	0.033	0.021
Mass Na		g	0.352	0.798	0.111	0.481	0.505	0.792	0.883	0.554	0.522	0.691	0.753	0.490
Mass expected		g	2.070	2.621	1.706	2.460	2.839	3.292	3.441	2.536	1.839	2.666	3.228	2.800
Mass obtained	*Out*	g	2.240	2.990		3.800	3.270	3.540	3.720	3.070	2.040		3.449	2.756
Percentage yield		%	108.231	114.069		154.472	115.170	107.532	108.116	121.078	110.926		106.843	98.418
% Na in product		%	15.706	26.689		12.661	15.429	22.377	23.749	18.031	25.604		21.835	17.787

No	Acid	Bubbled	Dissolved	Colour	State	Other
	Pure Na$_2$CO$_3$	-	Yes	White	Powder	-
1	Octanoic	Yes	Yes	White	Pieces	-
2	n-Heptanoic	Yes	Yes	White	Pieces	-
3	Pelargonic	Little	No	White	Pieces	Gelled
47	Nonanoic	Little	No	White	Pieces	Gelled
4	Formic	Yes	Yes	White	Crystals	-
5	i-Butyric	Yes	Yes	White	Crystals	-
6	2-Furoic	Yes	Yes	Yellow	Crystals	-
7	Oxalic	Yes	Yes	White	Crystals	-
29	Oxalic	Yes	Yes	White	Crystals	-
8	Citric	Yes	Yes	Cream	Pieces	-
9	Decanoic	Little	Little	White	Pieces	Add water
10	Lauric	No	No	White	Wax	Gelled
11	Myristic	Little	Little	White	Wax	Gelled, Add water
12	Palmitic	Little	Little	White	Wax	Add water
13	Trimesic	Yes	Yes	White	Crystals	-
14	Mucic	Yes	Yes	White	Powder	-
61	Mucic	Yes	Yes	White	Powder	-
15	Phenylacetic	Yes	Yes	White	Crystals	-
16	Anisic	Yes	Yes	White	Crystals	-
17	Adipic	Yes	Yes	White	Pieces	-
18	Uric	Little	Little	White	Pieces	Add water
19	Coumaric	Yes	Yes	Brown	Pieces	-
20	i-Cyanuric	Little	Little	White	Powder	-
21	i-Phthalic	Yes	Yes	White	Crystals	-
22	Malonic	Yes	Yes	White	Crystals	-
23	Stearic	Little	Little	White	Wax	Add water
24	Azeloic	Yes	Yes	White	Powder	-
25	Pyrogallic	No	Yes	Black	Pieces	-
26	Malic	Yes	Yes	Cream	Pieces	-
27	2-Ketoglutaric	Yes	Yes	Cream	Powder	-
28	Picolinic	Yes	Yes	White	Pieces	-
30	Barbitone	Little	Slow	White	Powder	-
31	Glycocoll	No	Yes	White	Pieces	-
32	Phthalic Anhy	Slow	Slow	Cream	Crystals	-
33	Butyl benzoic	Little	Slow	White	Crystals	-
34	Tiglic	Little	Slow	White	Crystals	-
35	Pyr.carboxylic	Yes	Yes	White	Crystals	-
36	Sebacic	Slow	Slow	White	Powder	-
37	Homophthalic	Yes	Yes	Cream	Powder	-
38	Mandelic	Yes	Yes	White	Powder	-
39	Maleic	Yes	Yes	White	Crystals	-
40	Pyromellitic	Yes	Yes	Yellow	Powder	-
41	Tartaric	Yes	Yes	White	Crystals	-
42	Diam.benzoic	Yes	Yes	Black	Crystals	-
43	Galacturonic	Yes	Yes	Brown	Pieces	-
44	Glutaric	Yes	Yes	Cream	Pieces	-
45	Succinic	Yes	Yes	White	Crystals	-
46	Sorbic	Little	Yes	Yellow	Wax	-
48	Levulinic	Little	No	White	Wax	Gelled
49	Gluconic	Yes	Yes	Brown	Pieces	-

No	Acid	Bubbled	Dissolved	Colour	State	Other
50	Glycollic	Yes	Yes	White	Crystals	-
51	Phytic	Little	Yes	-	-	-
52	Nit.triacetic	Yes	Yes	White	Pieces	-
53	Undecylenic	Little	Slow	Cream	Wax	-
54	n-Hexanoic	Little	Yes	Cream	Wax	-
55	Ethoxy acetic	Yes	Yes	White	Crystals	-
56	Phthalic	Yes	Yes	White	Crystals	-
57	n-Butyric	Yes	Yes	White	Powder	-
58	Aspartic	Yes	Slow	-	-	-
59	Benzoic	Yes	Yes	White	Crystals	-
60	Gallic	Yes	Yes	White	Pieces	-

Pyrolysis	No		Na₂CO₃	1	2	3	47	4	5	6	7	29	8	9	10	
	Acid			Octanoic	n-Heptanoic	Pelargonic	Nonanoic	Formic	i-Butyric	2-Furoic	Oxalic	Oxalic	Citric	Decanoic	Lauric	
Tube mass	Before		8.970	8.985	9.248	8.816	8.852	8.958	8.954	8.841	8.924	8.792	8.914	8.541	8.844	g
Sample mass			0.130	0.132	0.114	0.155	0.142	0.246	0.132	0.350	0.213	0.214	0.085	0.119	0.136	g
Effective mass			0.130	0.108	0.114	0.129	0.131	0.207	0.115	0.249	0.213	0.214	0.085	0.097	0.129	g
Height powder			4	5	4	6	6	7	9	10	5	5	2	5	7	mm
Mass Na in			0.056	0.019	0.026	0.021	0.024	0.065	0.028	0.043	0.079	0.076	0.016	0.015	0.020	g
Total mass	After		9.100	9.044	9.306	8.886	8.916	9.148	9.024	9.025	9.132	9.000	8.953	8.583	8.896	g
Height char			4	2	2	3	1	14	1	1	5	6	6	1	1	mm
Mass left (total)			0.130	0.059	0.058	0.070	0.064	0.190	0.070	0.184	0.208	0.208	0.039	0.042	0.052	g
Mass left (Na)			0.056	0.019	0.026	0.021	0.024	0.065	0.028	0.043	0.079	0.076	0.016	0.015	0.020	g
Mass left (Na₂CO₃)			0.130	0.043	0.060	0.048	0.054	0.150	0.065	0.100	0.182	0.176	0.036	0.034	0.047	g
Mass left (carbon)			0.000	0.016	-0.002	0.022	0.010	0.040	0.005	0.084	0.026	0.032	0.003	0.008	0.005	g
% carbon left			0.000	27.624	-3.221	30.956	14.912	21.117	6.571	45.742	12.541	15.584	7.987	19.638	9.858	%
Height change			0	-3	-2	-3	-5	7	-8	-9	0	1	4	-4	-6	mm

Pyrolysis	No	11	12	13	14	61	15	16	17	18	19	20	21	22	
	Acid	Myristic	Palmitic	Trimesic	Mucic	Mucic	Phenylacetic	Anisic	Adipic	Uric	Coumaric	i-Cyanuric	i-Phthalic	Malonic	
Tube mass	Before	8.607	8.896	8.780	8.721	11.043	8.630	8.946	8.821	9.129	9.205	9.176	8.805	9.150	g
Sample mass		0.112	0.137	0.153	0.153	0.411	0.118	0.083	0.110	0.161	0.170	0.139	0.126	0.265	g
Effective mass		0.096	0.121	0.128	0.153	0.376	0.105	0.078	0.084	0.126	0.170	0.111	0.110	0.265	g
Height powder		7	9	5	6	12	7	6	4	8	5	7	6	7	mm
Mass Na in		0.013	0.015	0.019	0.028	0.062	0.020	0.015	0.016	0.021	0.040	0.024	0.021	0.087	g
Total mass	After	8.645	8.938	8.870	8.803	11.247	8.682	8.988	8.893	9.212	9.326	9.285	8.915	9.359	g
Height char		1	1	8	6	14	1	2	1	10	6	9	6	4	mm
Mass left (total)		0.038	0.042	0.090	0.082	0.204	0.052	0.042	0.072	0.083	0.121	0.109	0.110	0.209	g
Mass left (Na)		0.013	0.015	0.019	0.028	0.062	0.020	0.015	0.016	0.021	0.040	0.024	0.021	0.087	g
Mass left (Na$_2$CO$_3$)		0.029	0.034	0.045	0.064	0.143	0.047	0.034	0.036	0.049	0.091	0.055	0.049	0.201	g
Mass left (carbon)		0.009	0.008	0.045	0.018	0.061	0.005	0.008	0.036	0.034	0.030	0.054	0.061	0.008	g
% carbon left		24.038	19.193	50.147	21.556	29.705	10.462	18.472	50.043	40.442	24.620	49.856	55.773	3.938	%
Height change		-6	-8	3	0	2	-6	-4	-3	2	1	2	0	-3	mm

Pyrolysis	No		23	24	25	26	27	28	30	31	32	33	34	35	
	Acid		Stearic	Azeloic	Pyrogallic	Malic	Keto Glutaric	Picolinic	Barbitone	Glycocoll	Phthalic Anhydride	Butyl benzoic	Tiglic	Pyrazine carboxylic	
Tube mass		*Before*	9.099	9.007	8.920	9.023	8.445	9.096	9.176	9.298	8.853	8.731	8.904	9.023	g
Sample mass			0.124	0.156	0.141	0.152	0.138	0.203	0.217	0.166	0.205	0.126	0.172	0.143	g
Effective mass			0.117	0.150	0.096	0.152	0.123	0.179	0.187	0.151	0.149	0.123	0.149	0.137	g
Height powder			9	7	5	5	5	8	7	6	9	15	8	7	mm
Mass Na in			0.014	0.029	0.018	0.040	0.027	0.037	0.032	0.042	0.026	0.022	0.034	0.030	g
Total mass		*After*	9.141	9.100	9.020	9.127	8.531	9.220	9.266	9.415	9.007	8.844	8.997	9.116	g
Height char			1	1	8	16	7	1	7	8	32	1	1	38	mm
Mass left (total)			0.042	0.093	0.100	0.104	0.086	0.124	0.090	0.117	0.154	0.113	0.093	0.093	g
Mass left (Na)			0.014	0.029	0.018	0.040	0.027	0.037	0.032	0.042	0.026	0.022	0.034	0.030	g
Mass left (Na$_2$CO$_3$)			0.033	0.066	0.041	0.093	0.062	0.085	0.075	0.097	0.059	0.050	0.078	0.070	g
Mass left (carbon)			0.009	0.027	0.059	0.011	0.024	0.039	0.015	0.020	0.095	0.063	0.015	0.023	g
% carbon left			22.513	28.856	59.283	10.699	28.382	31.744	17.105	16.970	61.411	55.312	15.905	24.888	%
Height change			-8	-6	3	11	2	-7	0	2	23	-14	-7	31	mm

Pyrolysis		No	36	37	38	39	40	41	42	43	44	45	46	48	
		Acid	Sebatic	Homophthalic	Mandelic	Maleic	Pyromellitic	Tartaric	Diamino benzoic	Galacturonic	Glutaric	Succinic	Sorbic	Levulinic	
Tube mass	*Before*		9.280	9.111	8.895	9.191	9.146	9.054	9.162	9.055	9.008	8.950	8.914	8.677	g
Sample mass			0.191	0.154	0.188	0.174	0.185	0.234	0.143	0.222	0.188	0.267	0.235	0.203	g
Effective mass			0.191	0.154	0.180	0.150	0.164	0.214	0.129	0.222	0.188	0.162	0.195	0.186	g
Height powder			7	5	9	8	8	5	6	7	6	9	10	9	mm
Mass Na in			0.037	0.033	0.035	0.037	0.022	0.046	0.024	0.038	0.055	0.028	0.040	0.041	g
Total mass	*After*		9.389	9.242	8.982	9.308	9.252	9.175	9.258	9.163	9.139	9.061	9.038	8.793	g
Height char			1	1	7	20	9	9	10	2	1	9	10	2	mm
Mass left (total)			0.109	0.131	0.087	0.117	0.106	0.121	0.096	0.108	0.131	0.111	0.124	0.116	g
Mass left (Na)			0.037	0.033	0.035	0.037	0.022	0.046	0.024	0.038	0.055	0.028	0.040	0.041	g
Mass left (Na$_2$CO$_3$)			0.084	0.077	0.081	0.086	0.051	0.107	0.054	0.088	0.126	0.065	0.092	0.094	g
Mass left (carbon)			0.025	0.054	0.006	0.031	0.055	0.014	0.042	0.020	0.005	0.046	0.032	0.022	g
% carbon left			22.767	41.121	7.390	26.656	51.539	11.502	43.250	18.793	3.625	41.740	26.156	18.835	%
Height change			-6	-4	-2	12	1	4	4	-5	-5	0	0	-7	mm

Pyrolysis	No	49	50	51	52	53	54	55	56	57	58	59	60	
	Acid	Gluconic	Glycollic	Phytic	Nit.triacetic	Undecylenic	n-Hexanoic	Ethoxy acetic	Phthalic	n-Butyric	Aspartic	Benzoic	Gallic	
Tube mass	Before	9.193	9.083		9.300	9.050	8.767	9.018	8.585	9.181		10.324	10.436	g
Sample mass		0.125	0.224		0.230	0.197	0.191	0.188	0.150	0.131		0.206	0.221	g
Effective mass		0.115	0.196		0.149	0.171	0.178	0.174	0.124	0.118		0.193	0.221	g
Height powder		6	8		7	7	10	8	5	7		7	6	mm
Mass Na in		0.018	0.052		0.019	0.026	0.040	0.041	0.022	0.030		0.042	0.039	g
Total mass	After	9.257	9.220		9.444	9.136	8.870	9.119	8.711	9.265		10.478	10.567	g
Height char		6	9		10	1	41	28	27	2		0	52	mm
Mass left (total)		0.064	0.137		0.144	0.086	0.103	0.101	0.126	0.084		0.154	0.131	g
Mass left (Na)		0.018	0.052		0.019	0.026	0.040	0.041	0.022	0.030		0.042	0.039	g
Mass left (Na$_2$CO$_3$)		0.042	0.121		0.043	0.061	0.092	0.095	0.051	0.070		0.097	0.091	g
Mass left (carbon)		0.022	0.016		0.101	0.025	0.011	0.006	0.075	0.014		0.057	0.040	g
% carbon left		34.664	11.816		69.824	29.261	11.048	5.749	59.133	17.023		36.983	30.830	%
Height change		0	1		3	-6	31	20	22	-5		-7	46	mm

7.13. Appendix M

7.13.1. Summarised results for the gluconate synthesis.

Tabulated results of the standardisation of the synthesised gluconates

Metal	Theoretical ratio metal to gluconate	Calculated% metal in gluconate	Calculated ratio metal to gluconate (inc. water)
Al	1:3	9.10	1:1.38
Na	1:1	8.52	1:1.27
Sb	1:3	22.13	1:2.20
Zn	1:2	13.06	1:2.22
Zr	1:2[#]	29.97	1:1.09
Ca*	1:2	6.57	1:2.92
Cu*	1:2	13.42	1:2.10
Fe*	1:2	9.44	1:2.74
Mg*	1:2	4.13	1:2.22

* commercial material

[#] basic Zr salt (ZrO^{2-})

7.13.2. Thermal analysis of pentaerythritol, the acetylacetonates and acetylacetonate/pentaerythritol mixtures.

All DCS/TGA scans were done at a scan rate of 10°C from room temperature to 1000°C in air, unless indicated otherwise.
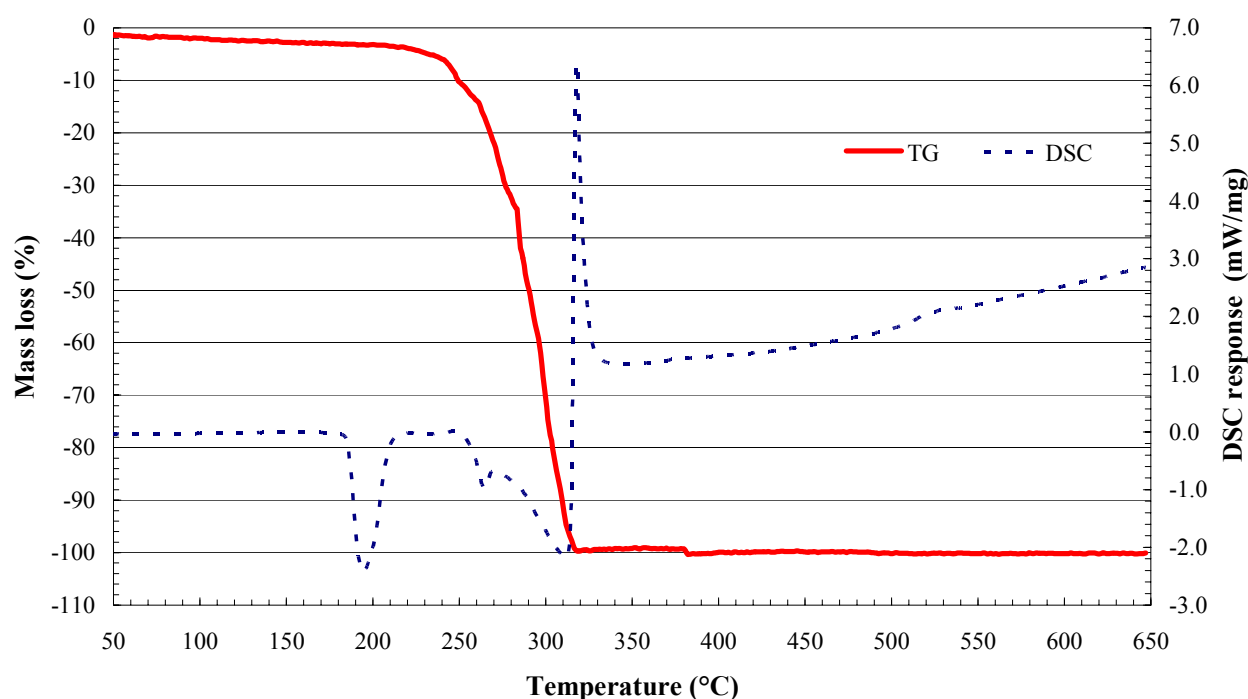
DSC/TGA scan of Pentaerythritol
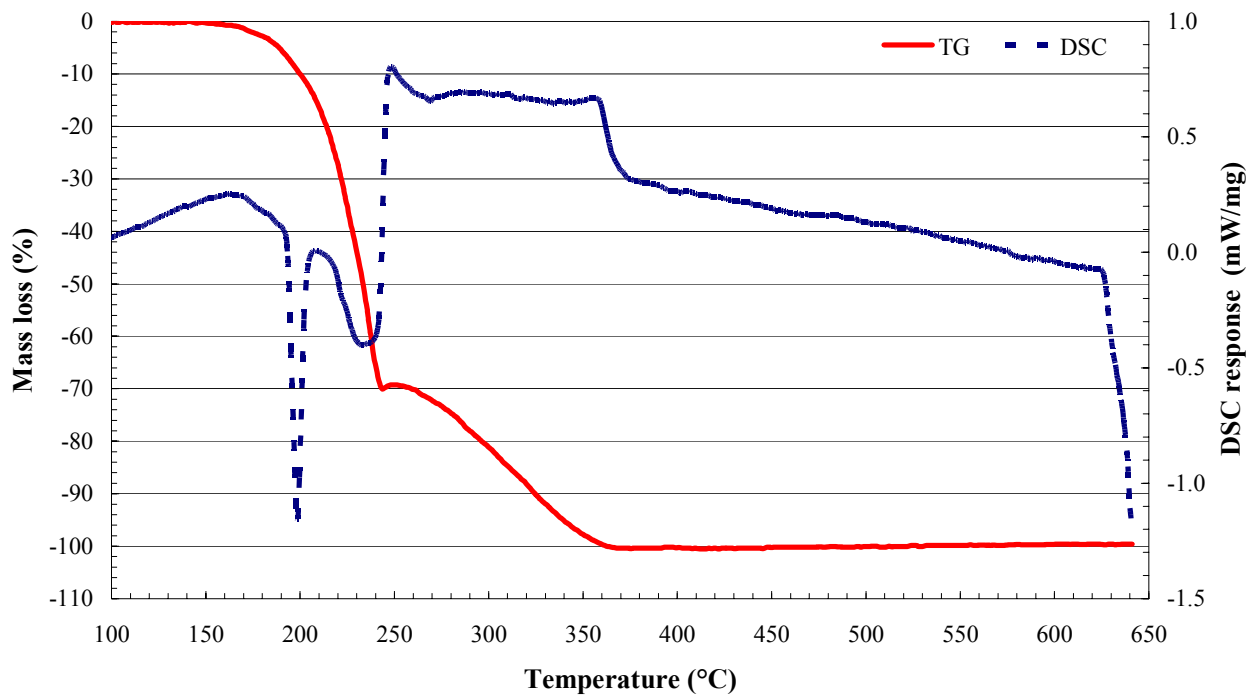
DSC/TGA scan of Al acetylacetonate
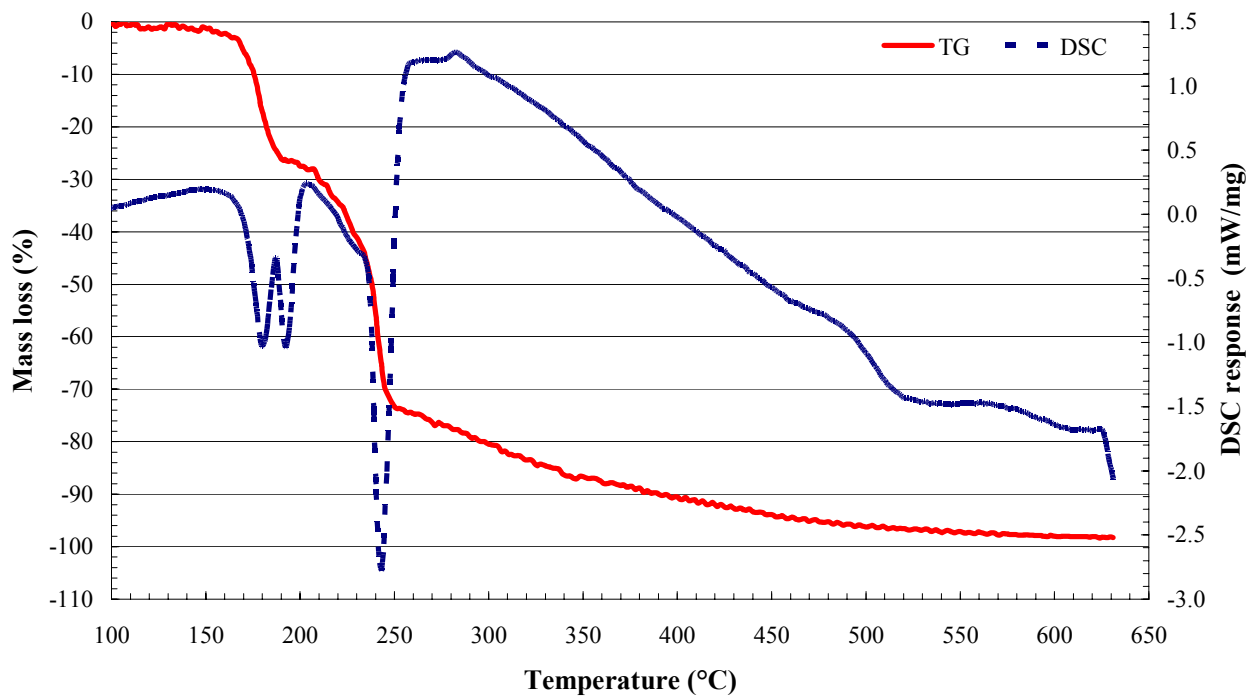
DSC/TGA scan of Al acetylacetonate/pentaerythritol mixture
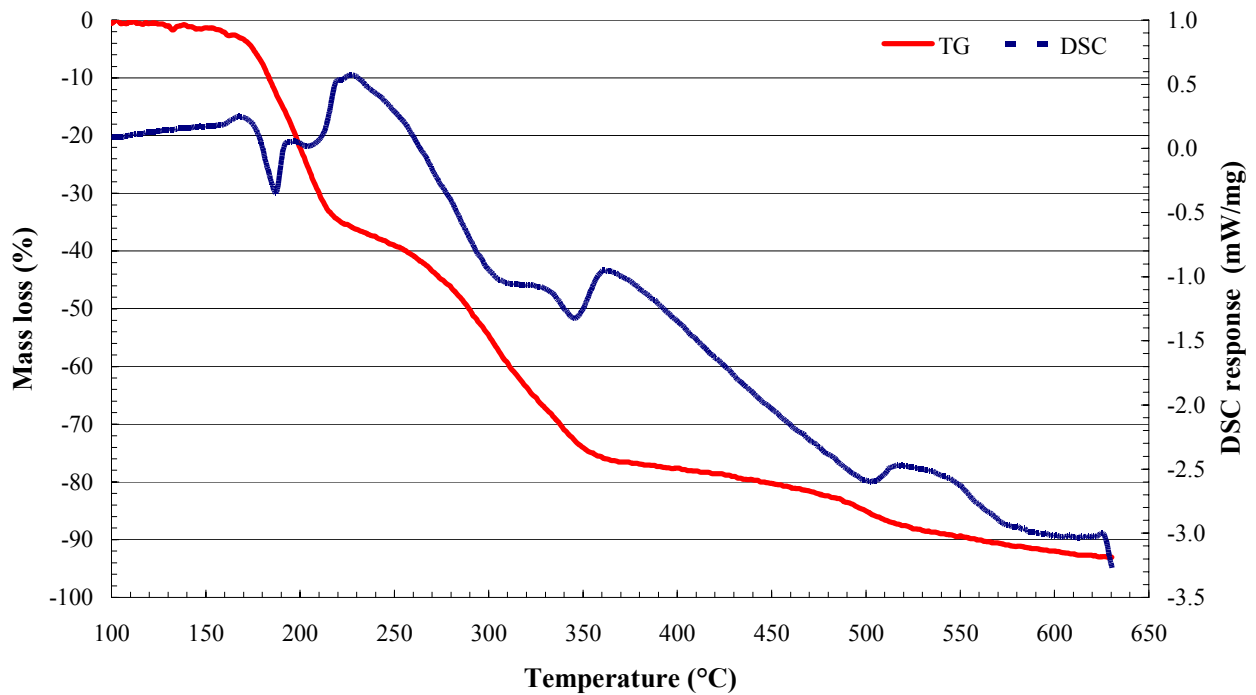
DSC/TGA scan of Al acetylacetonate/fumaric acid mixture
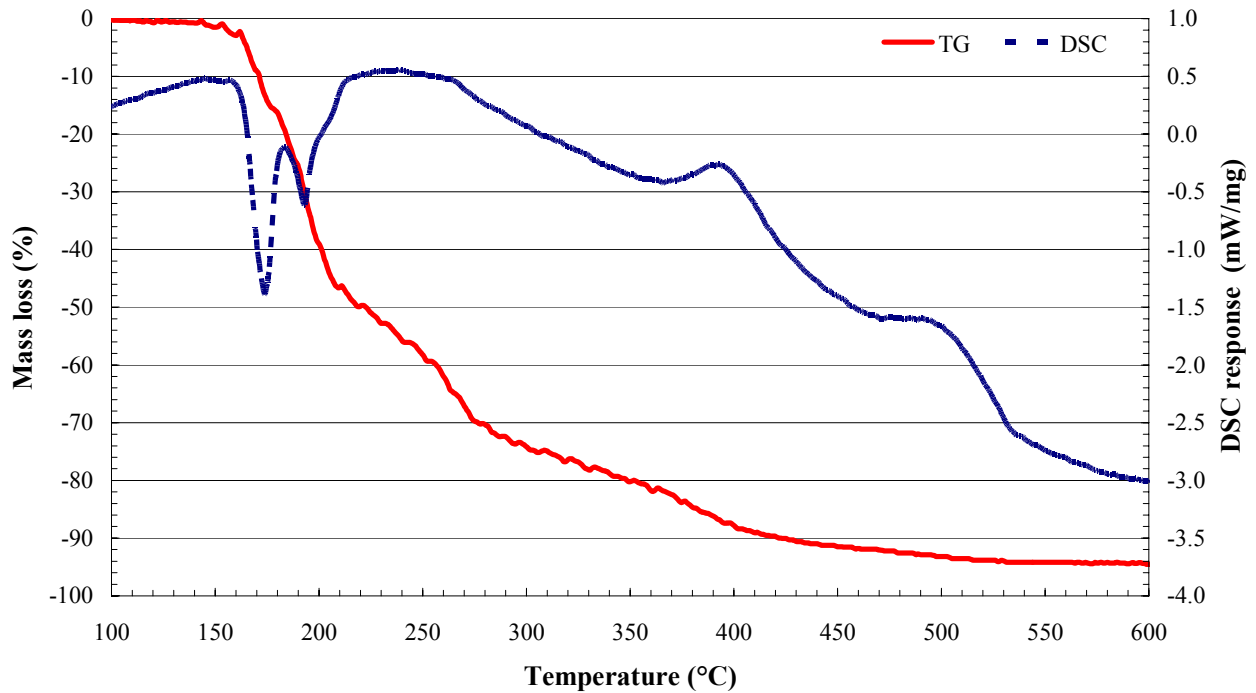
DSC/TGA scan of Al acetylacetonate/tartaric acid mixture
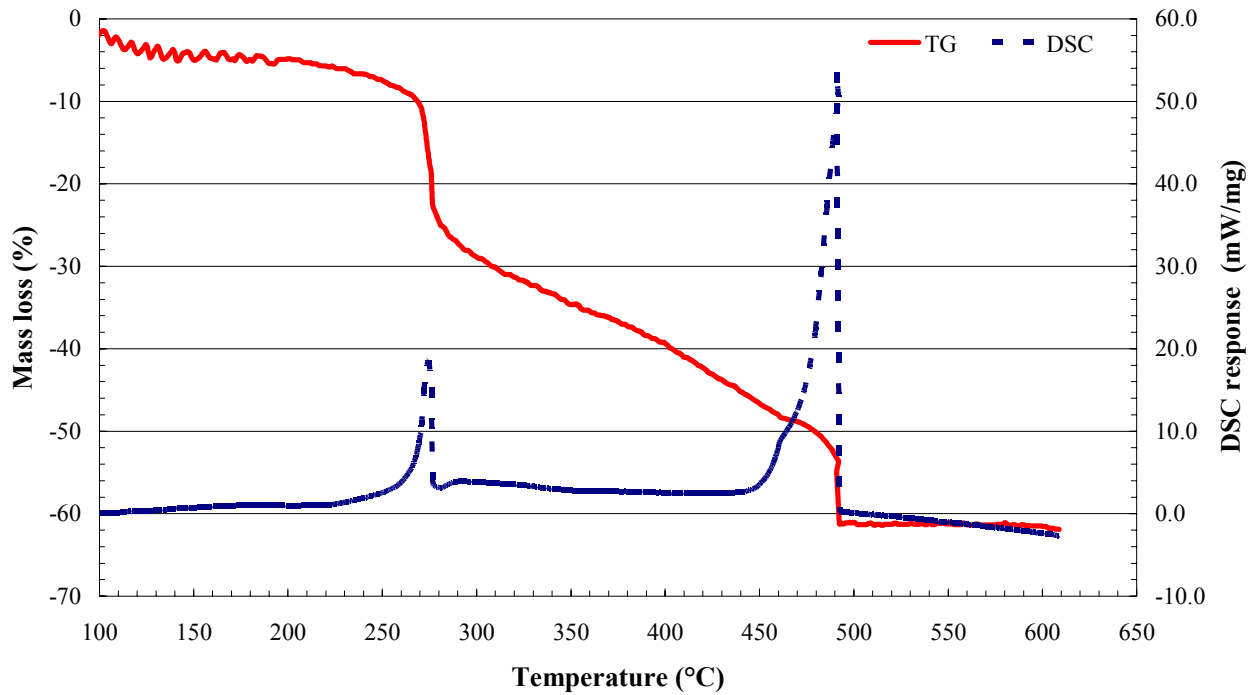
DSC/TGA scan of Ca acetylacetonate
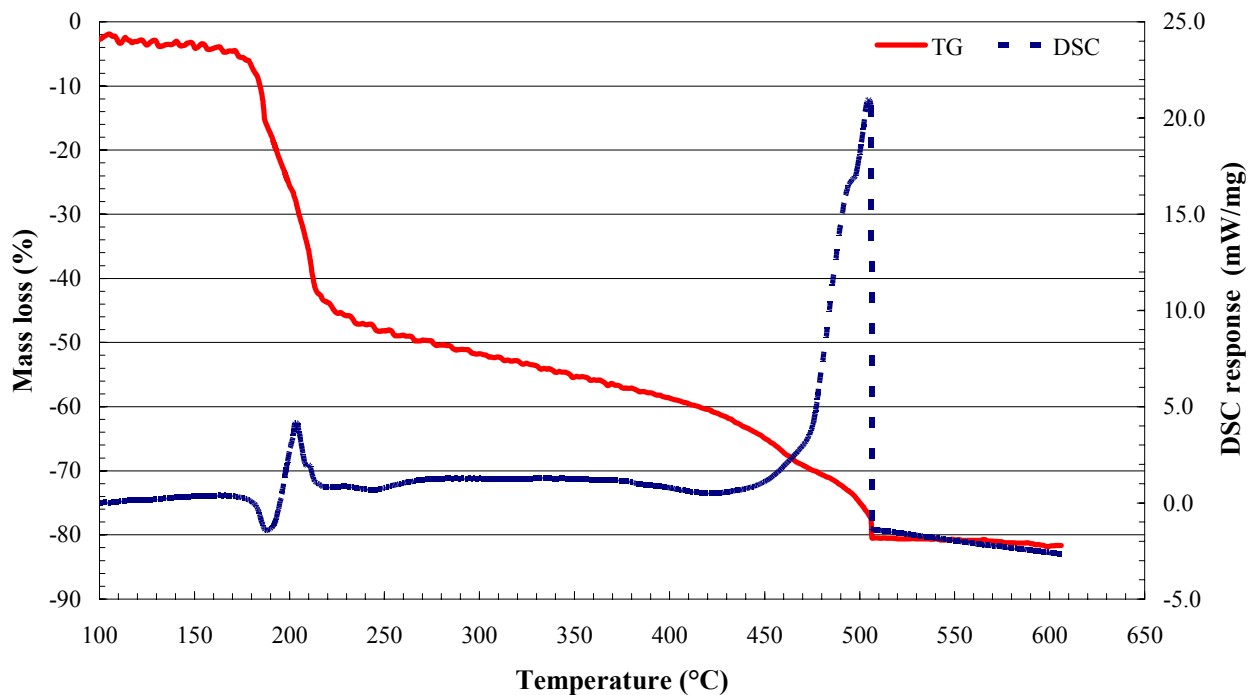
DSC/TGA scan of Ca acetylacetonate/pentaerythritol mixture
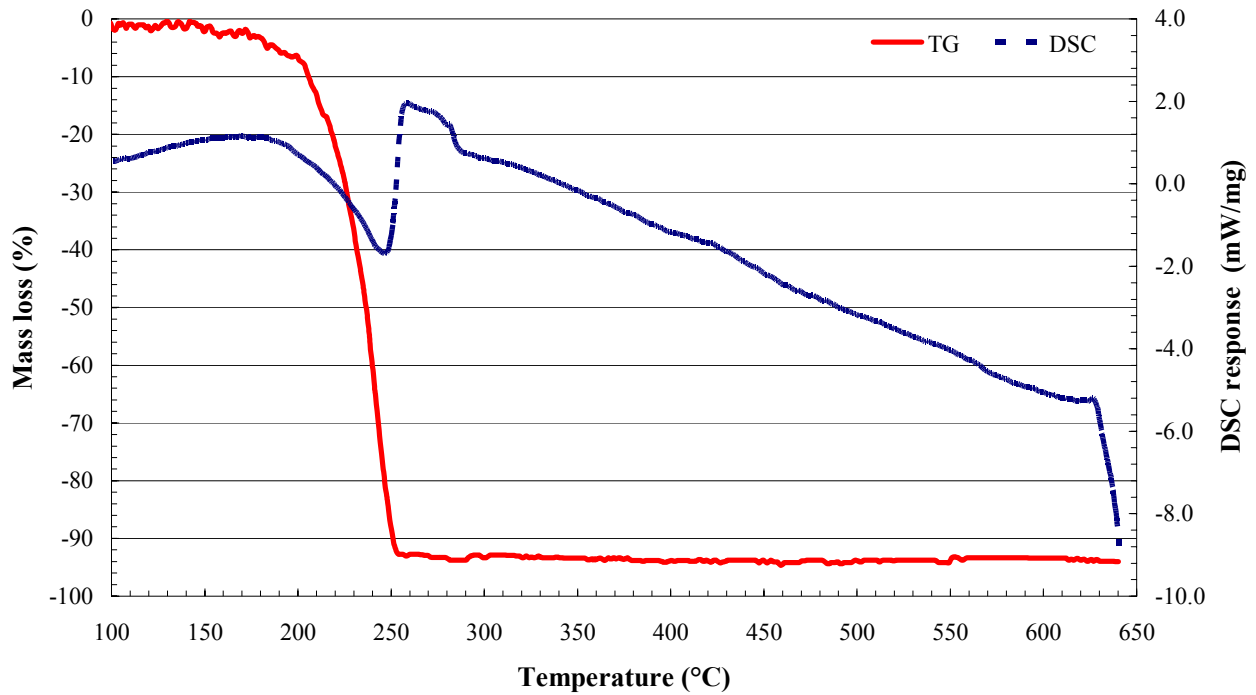
DSC/TGA scan of Cu acetylacetonate
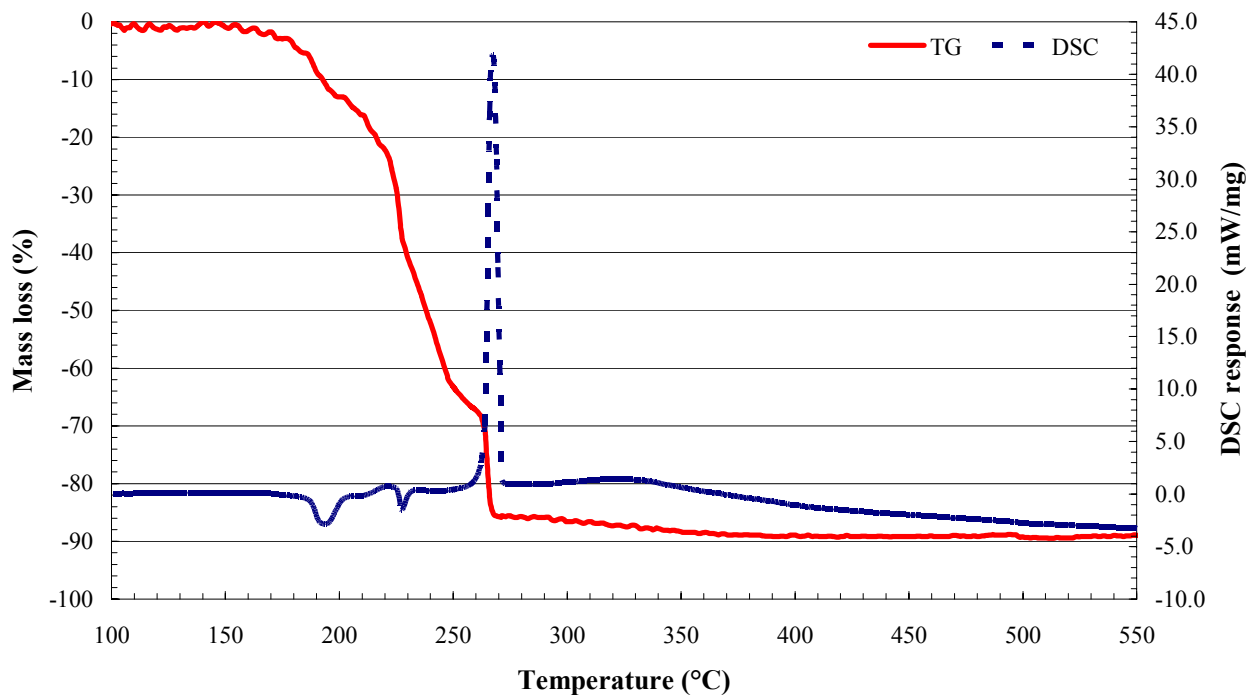
DSC/TGA scan of Cu acetylacetonate/pentaerythritol mixture
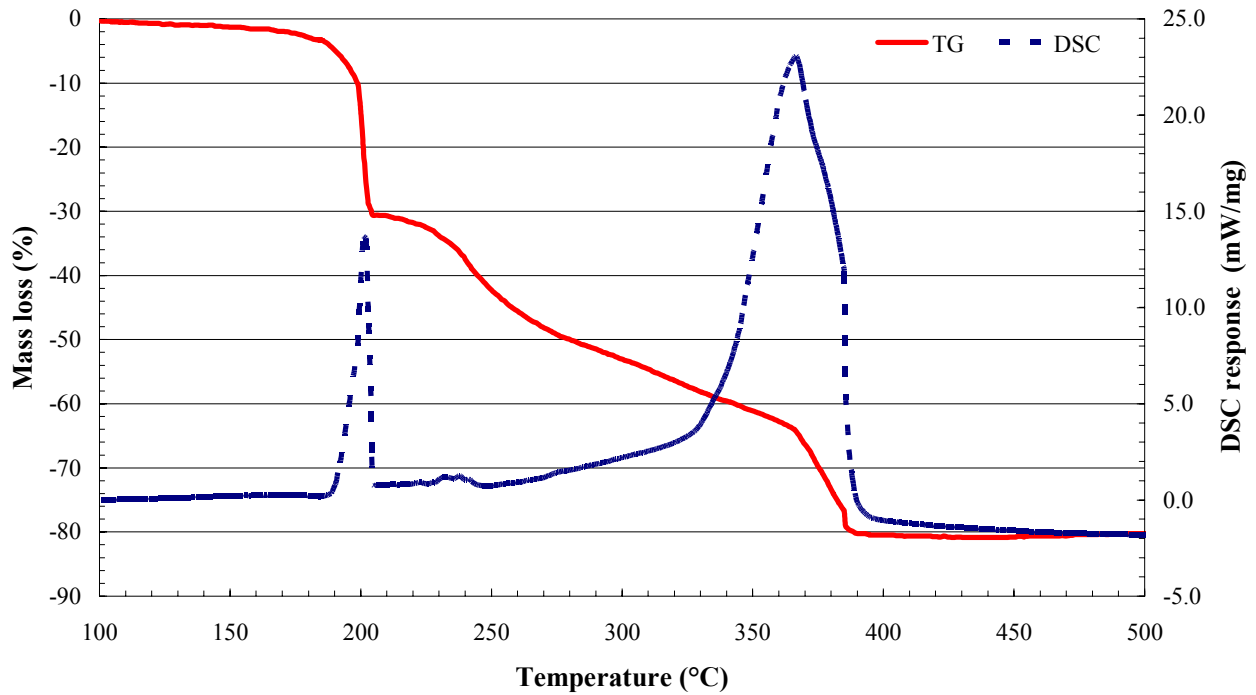
DSC/TGA scan of Fe acetylacetonate
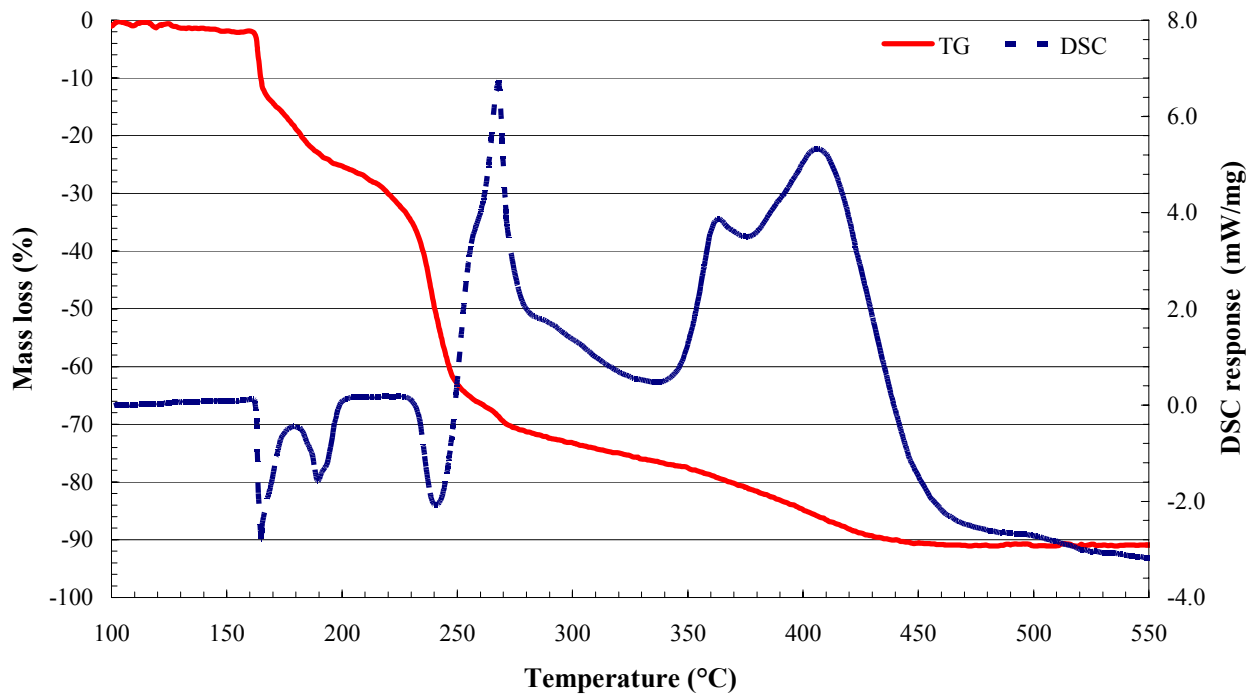
DSC/TGA scan of Fe acetylacetonate/pentaerythritol mixture
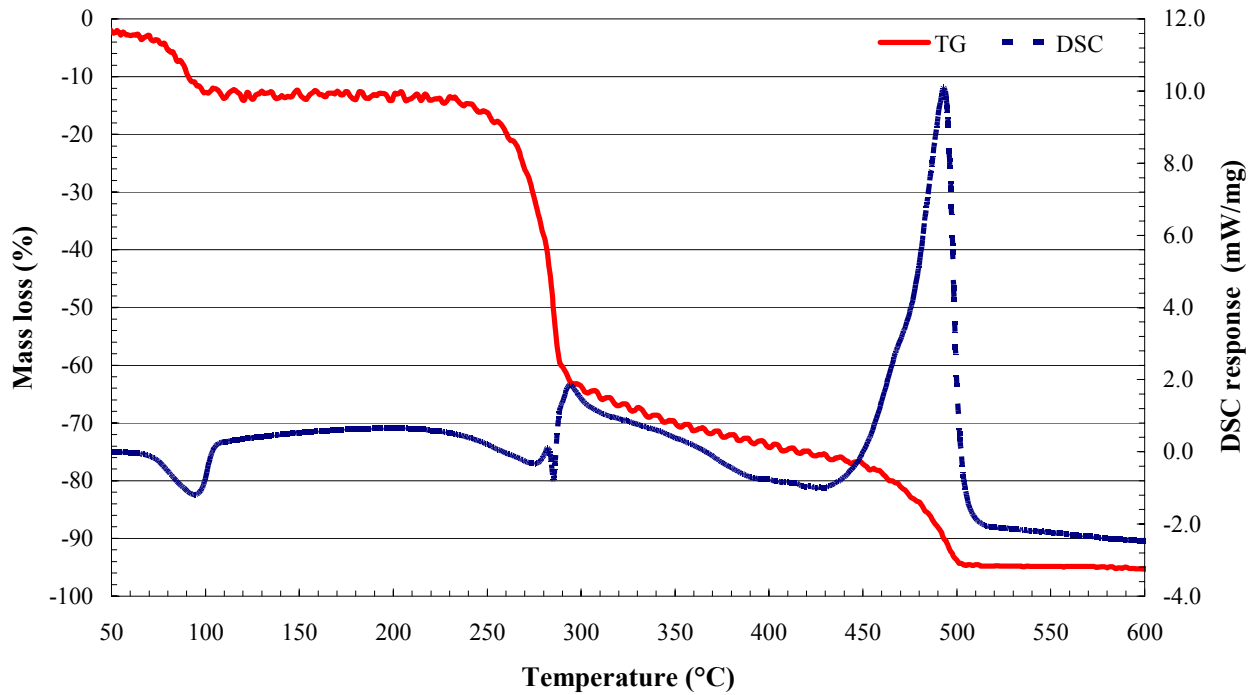
DSC/TGA scan of Mg acetylacetonate
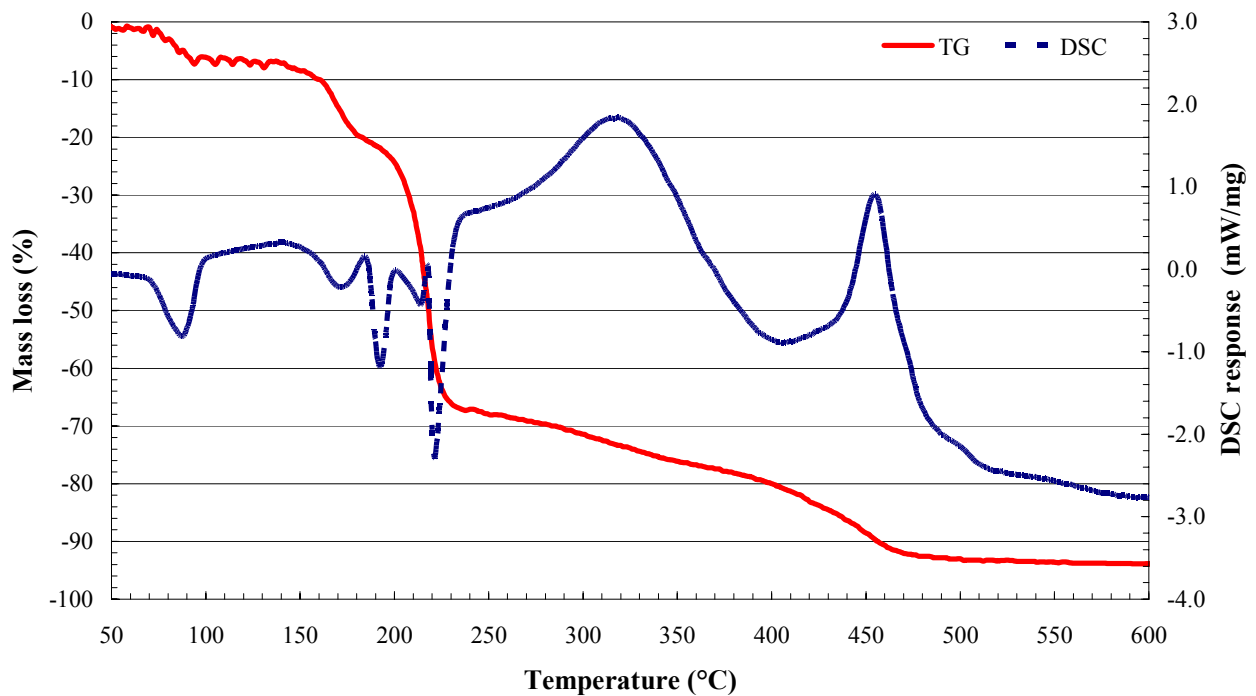
DSC/TGA scan of Mg acetylacetonate/pentaerythritol mixture
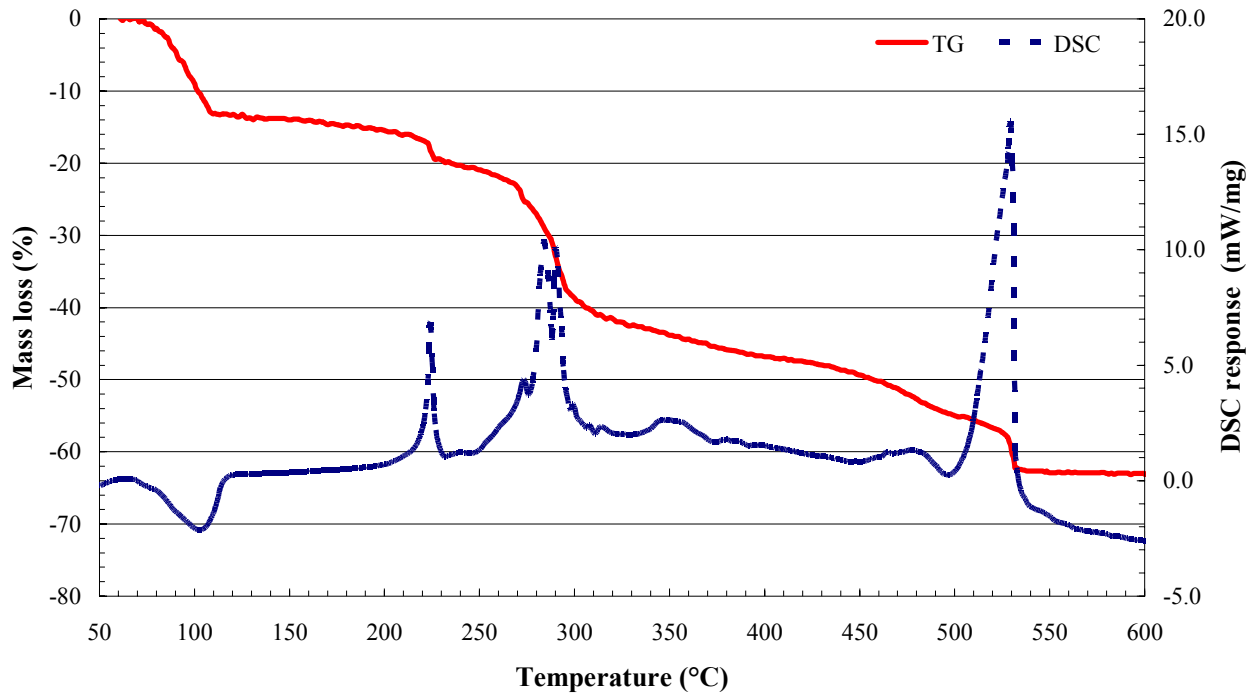
DSC/TGA scan of Na acetylacetonate
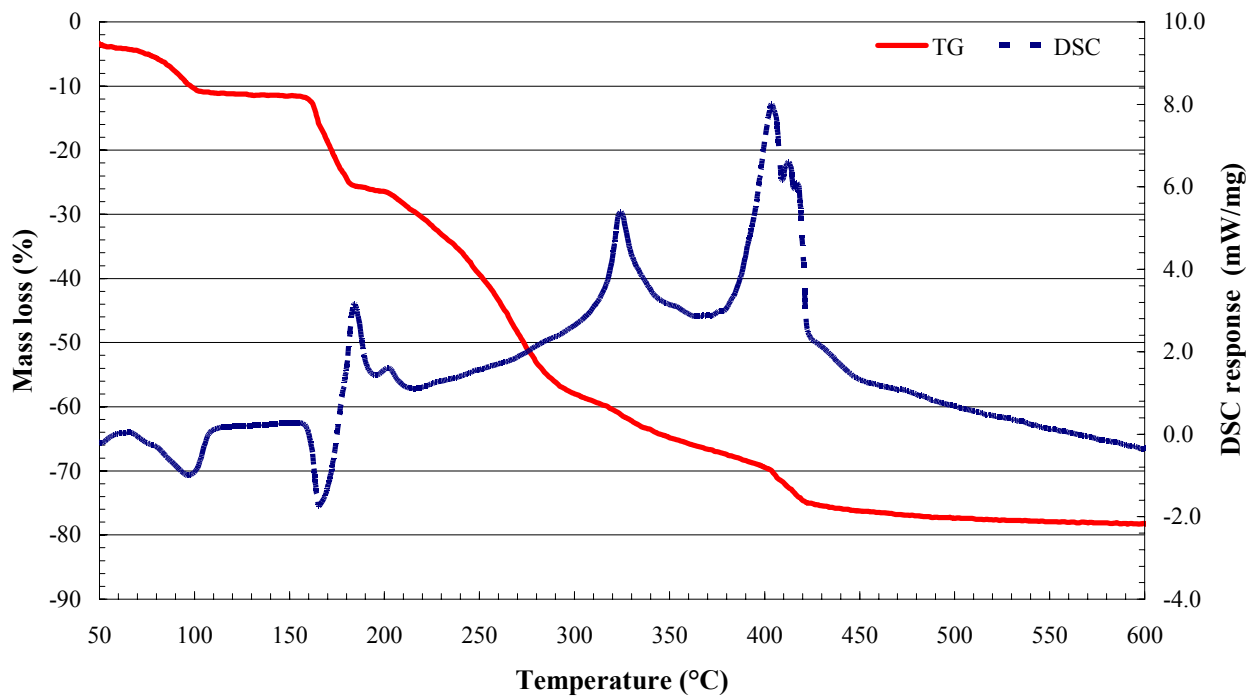
DSC/TGA scan of Na acetylacetonate/pentaerythritol mixture
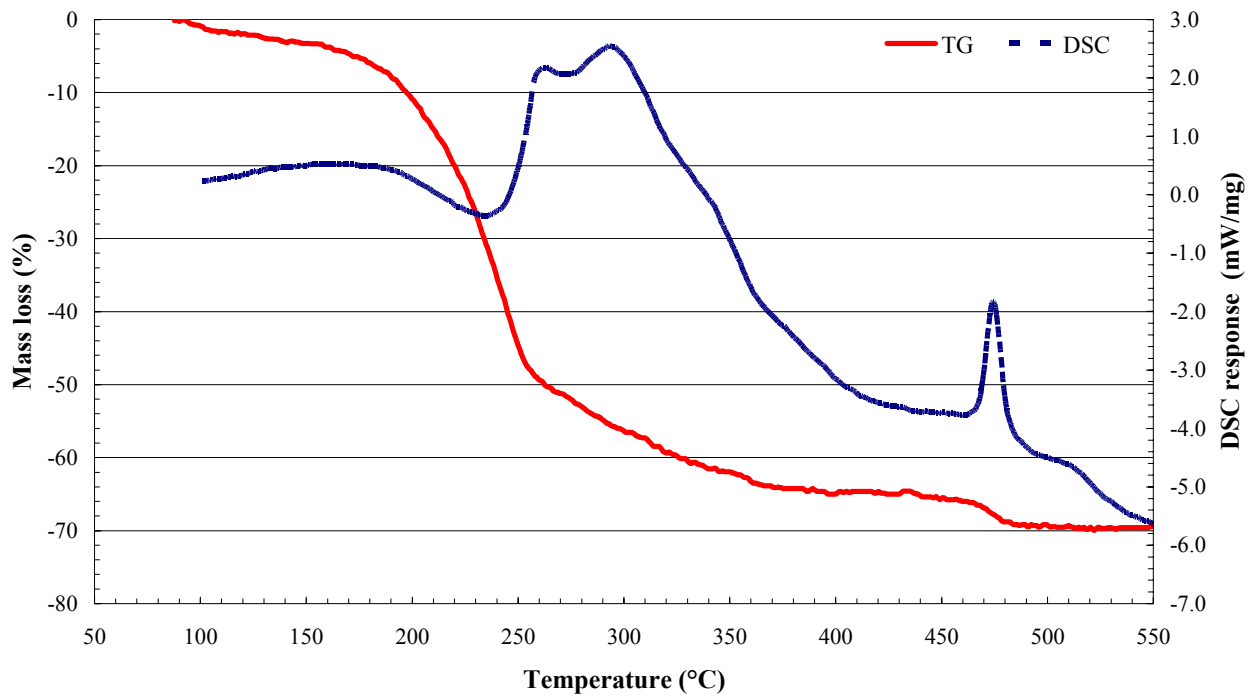
DSC/TGA scan of Ti acetylacetonate
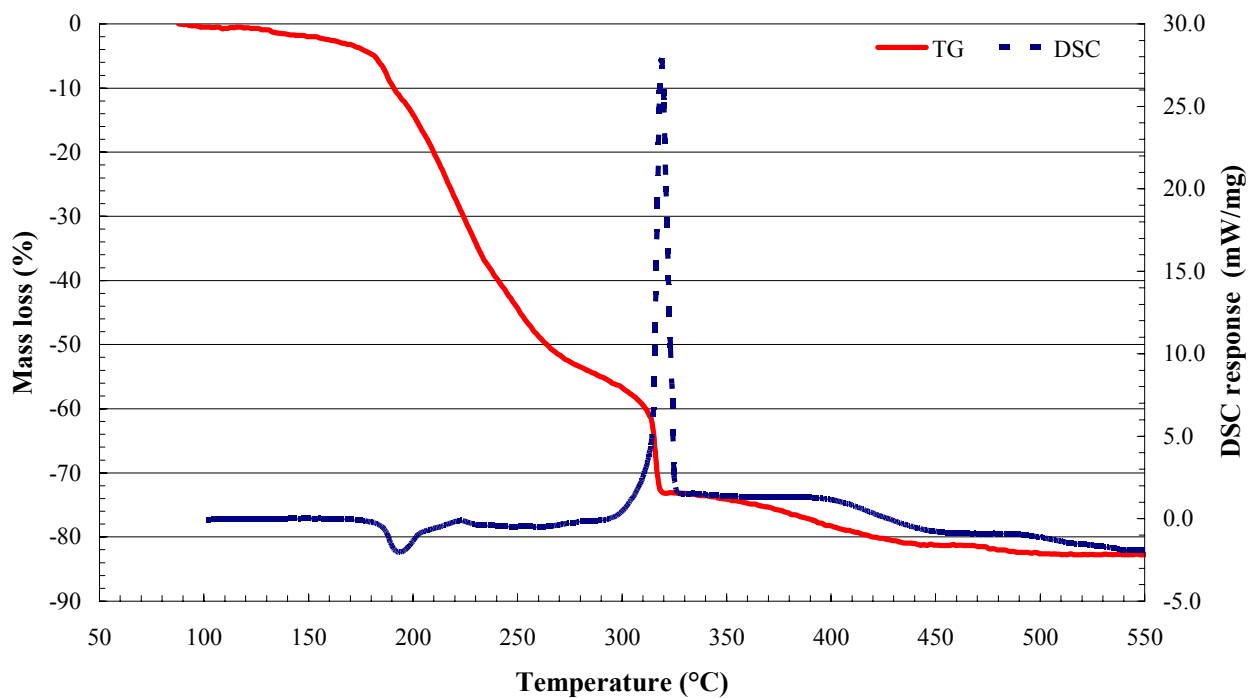
DSC/TGA scan of Ti acetylacetonate/pentaerythritol mixture
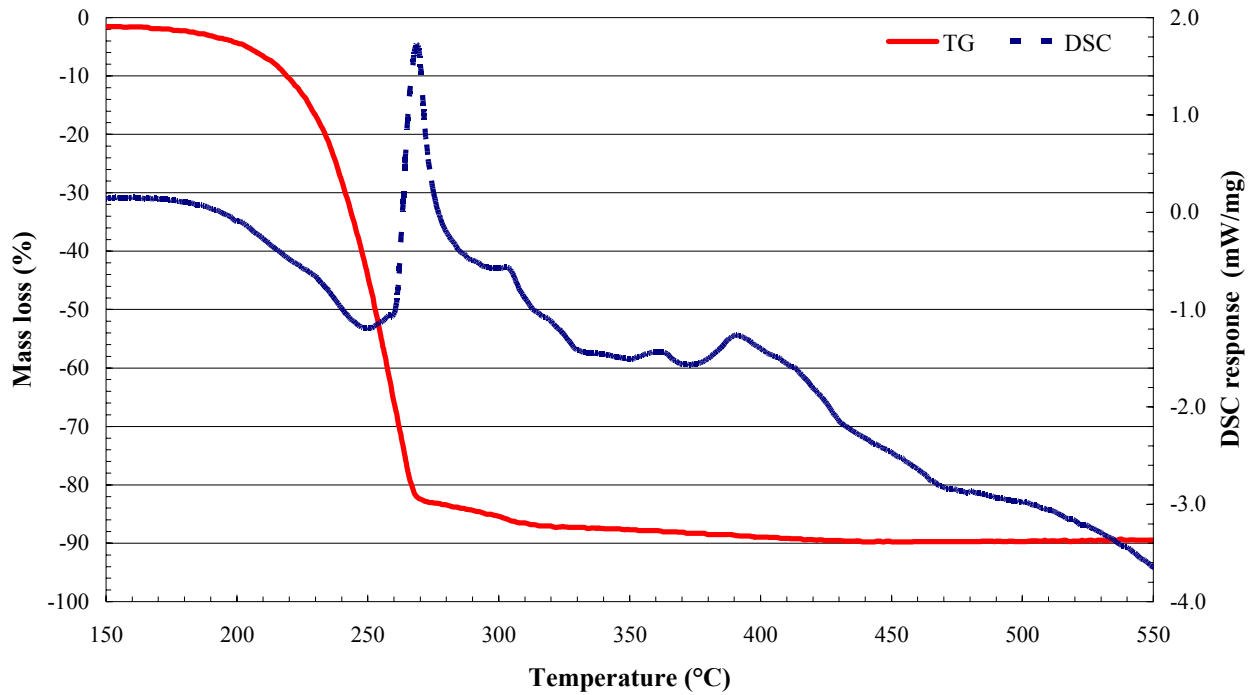
DSC/TGA scan of V acetylacetonate
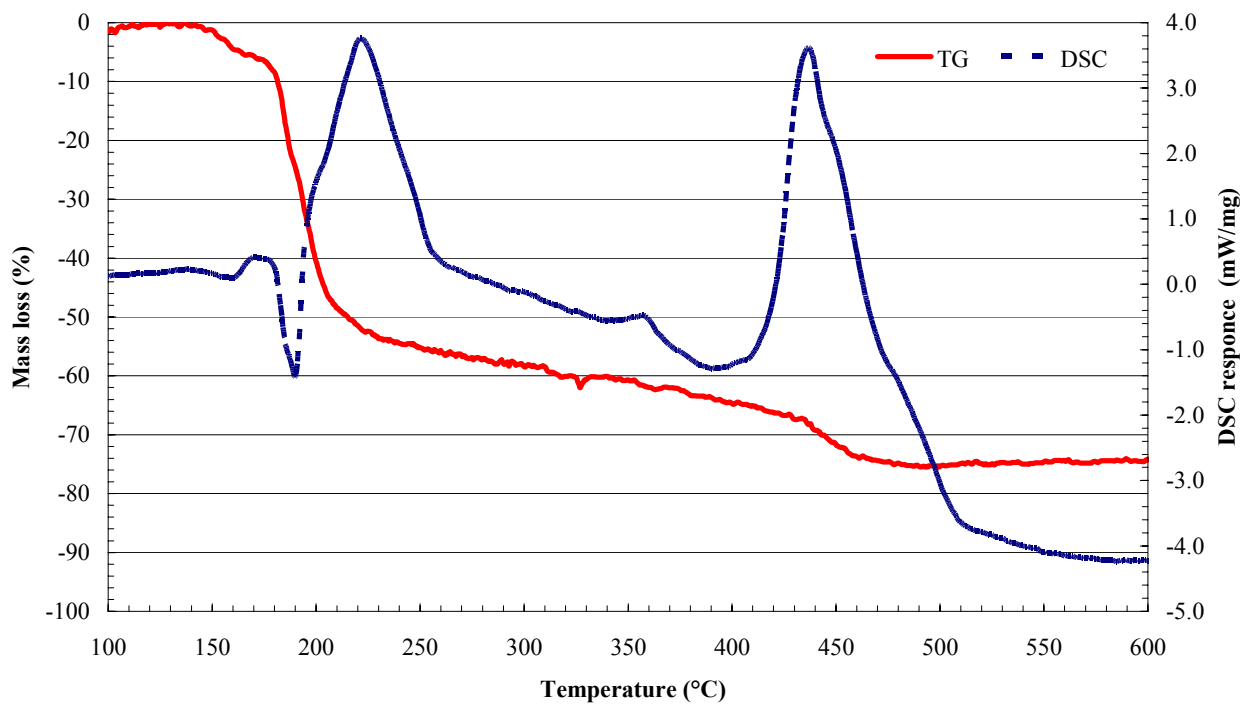
DSC/TGA of V acetylacetonate/pentaerythritol mixture
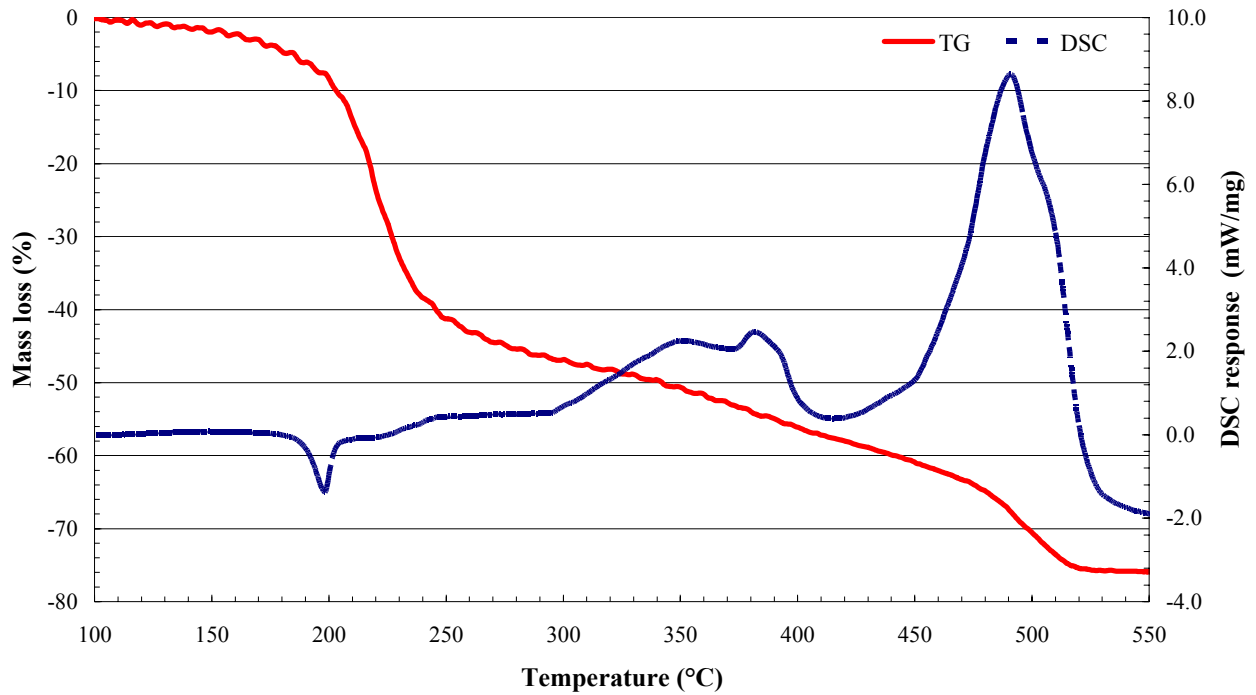
DSC/TGA scan of Zr acetylacetonate
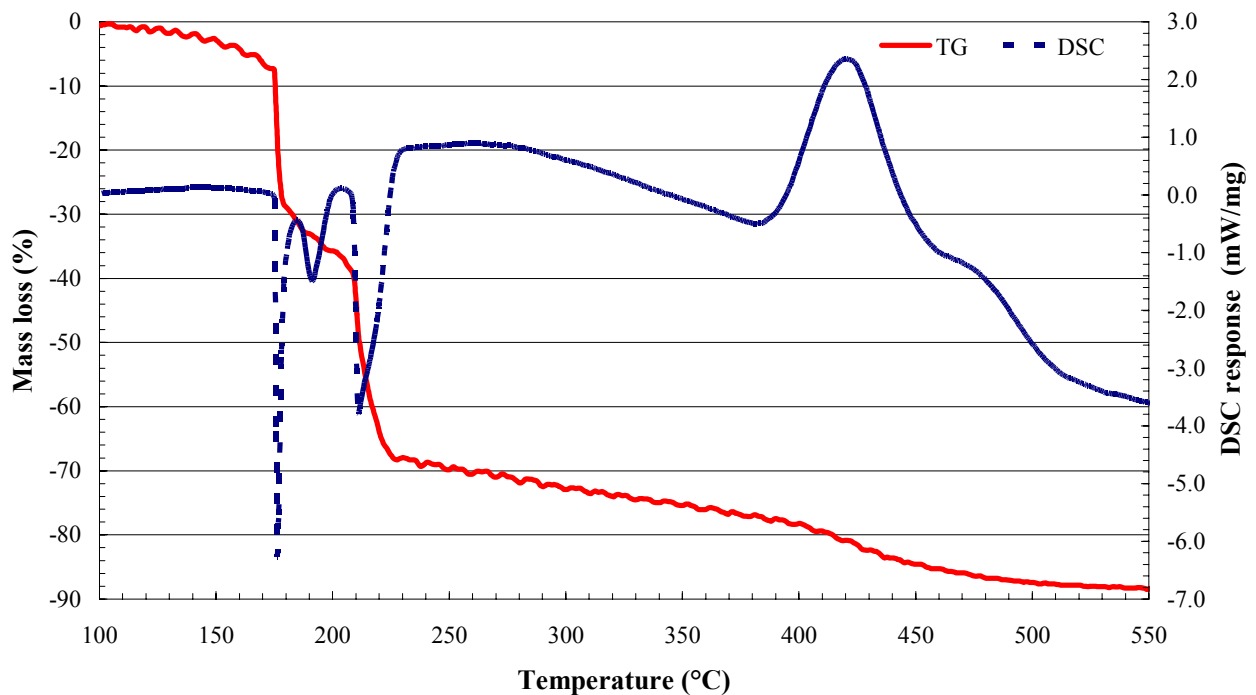
DSC/TGA scan of Zr acetylacetonate/pentaerythritol mixture

7.13.3. Thermal analysis of the gluconates.
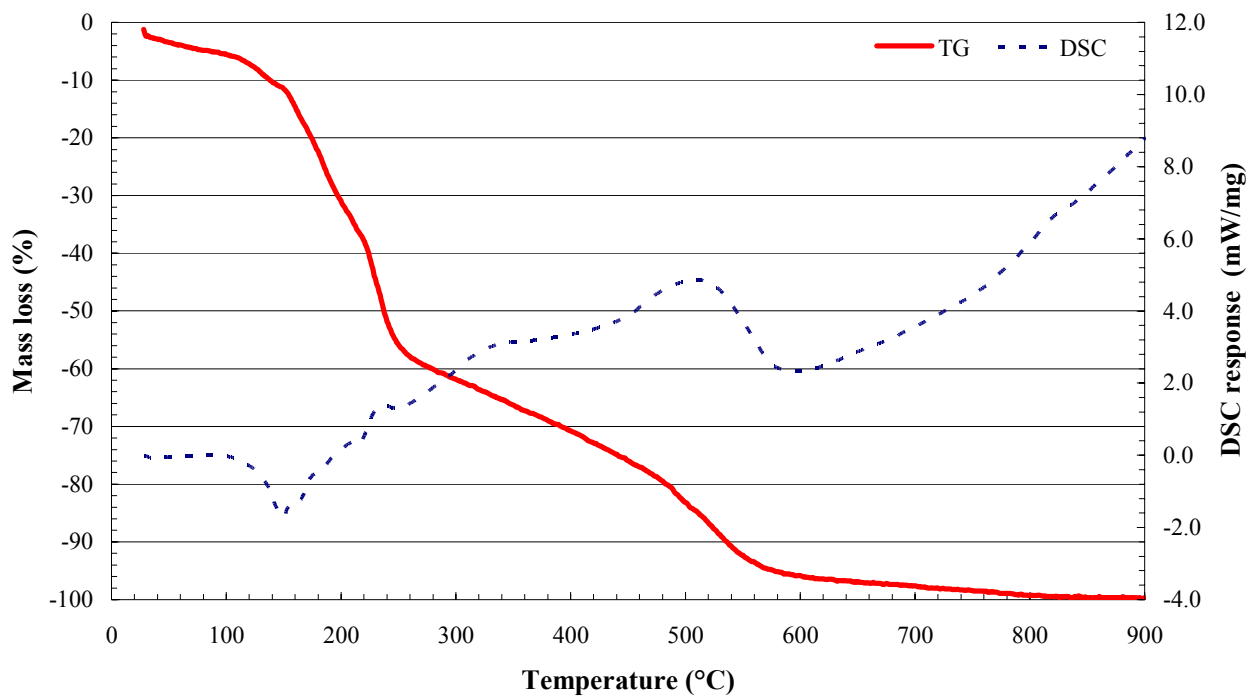
DSC/TGA scan of NH$_4$ gluconate
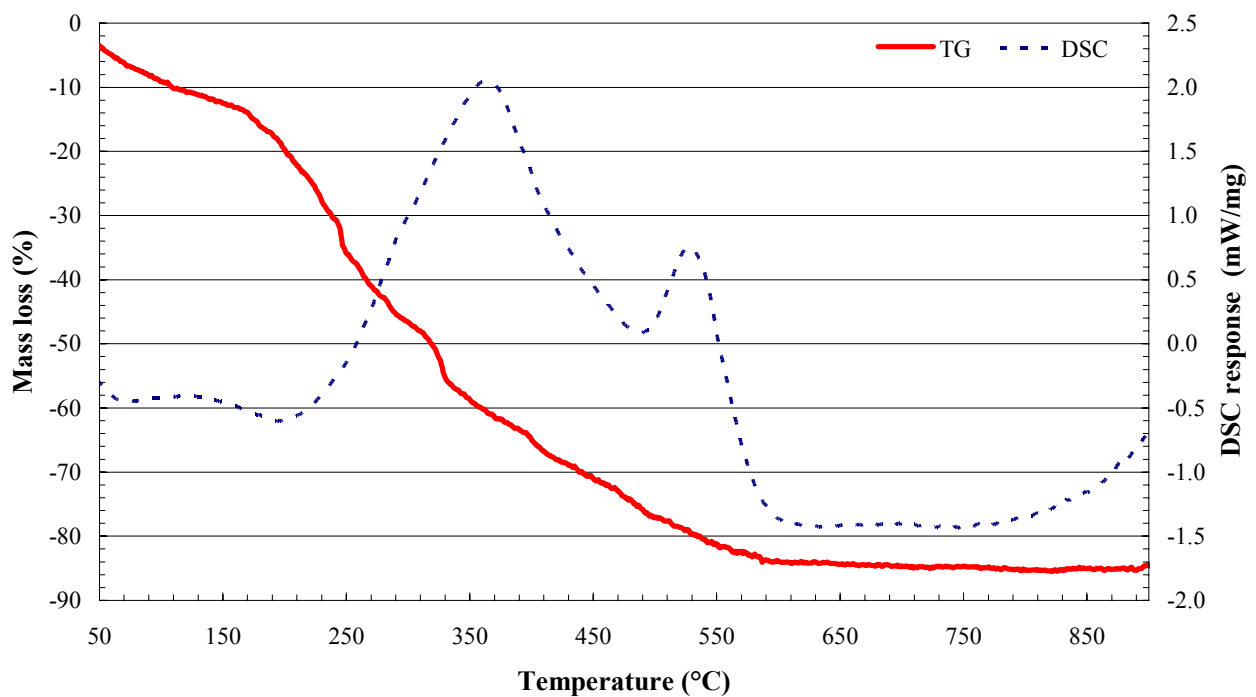
DSC/TGA scan of Al gluconate
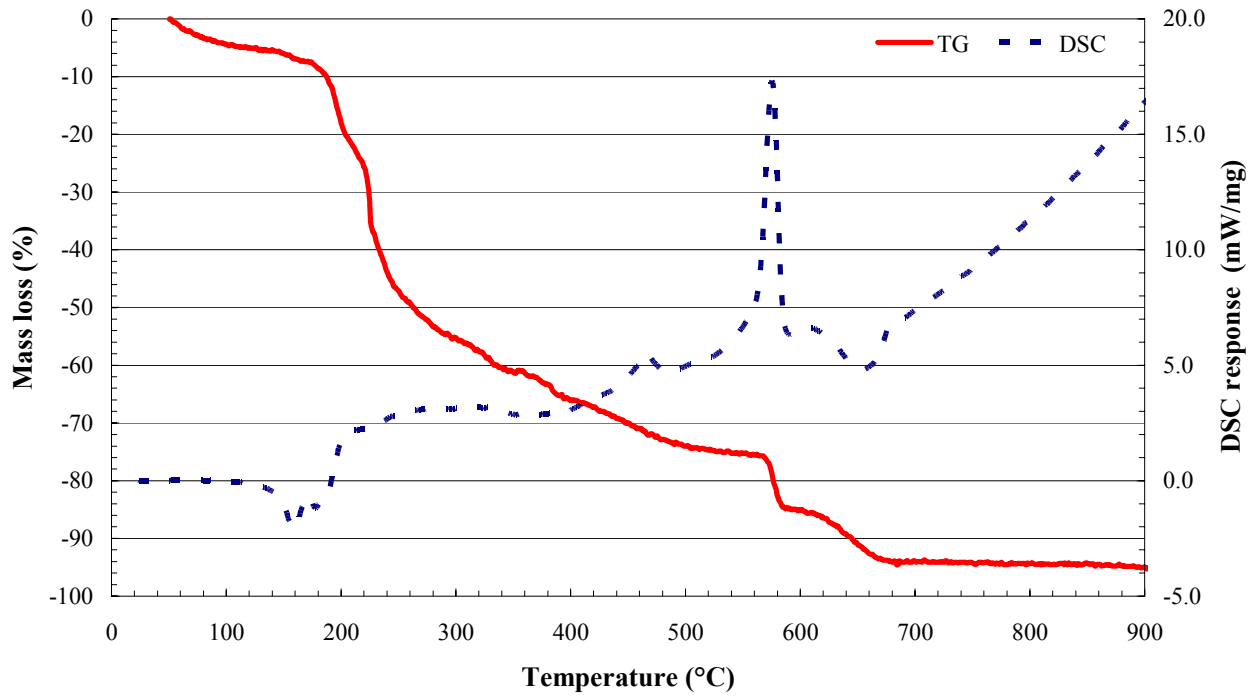
DSC/TGA scan of Ca gluconate
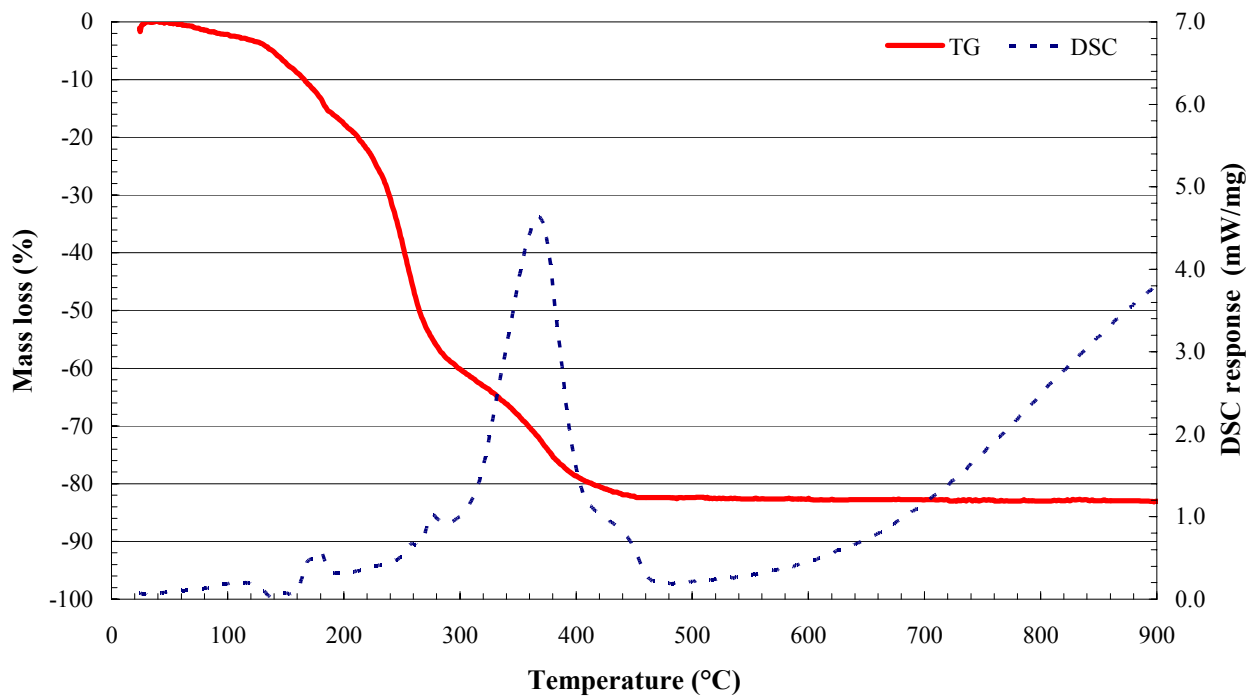
DSC/TGA scan of Cu gluconate
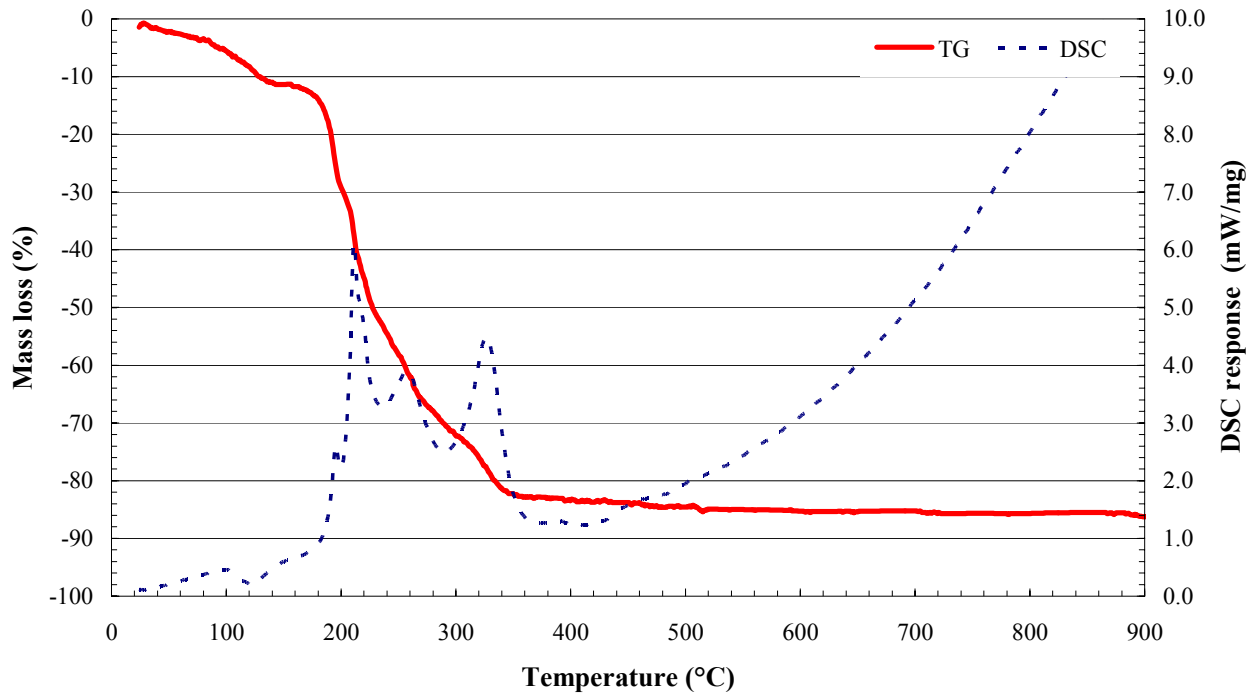
DSC/TGA scan of Fe gluconate
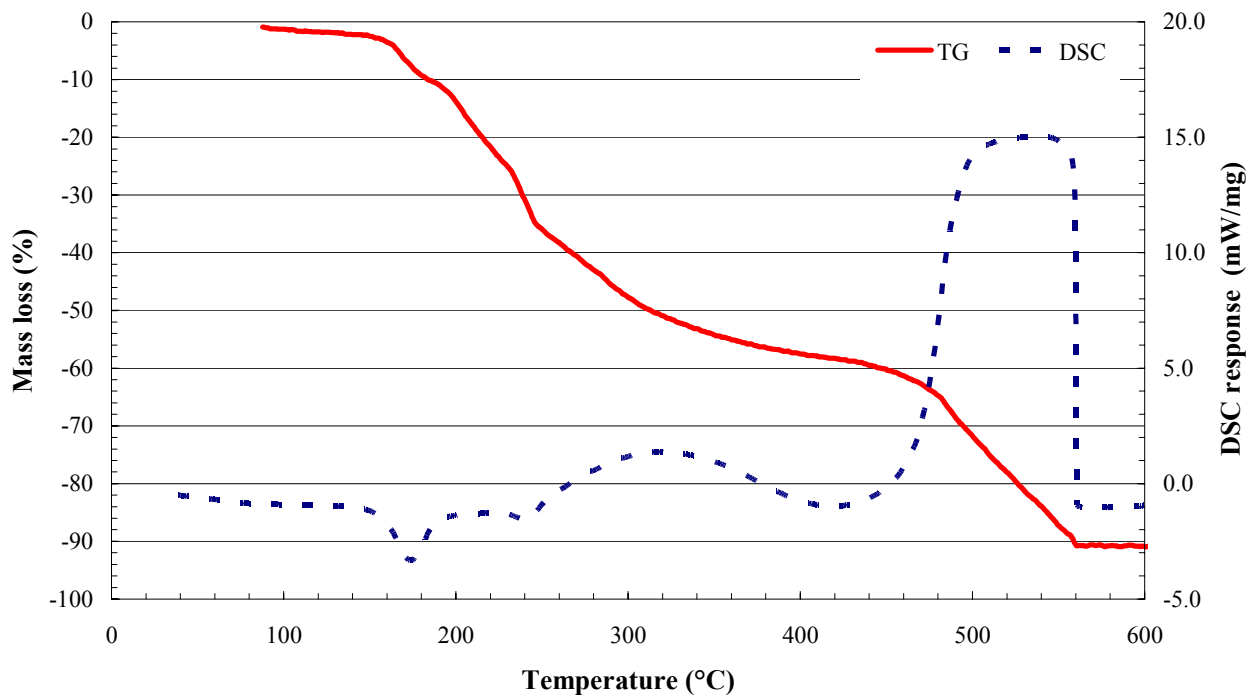
DSC/TGA scan of Mg gluconate
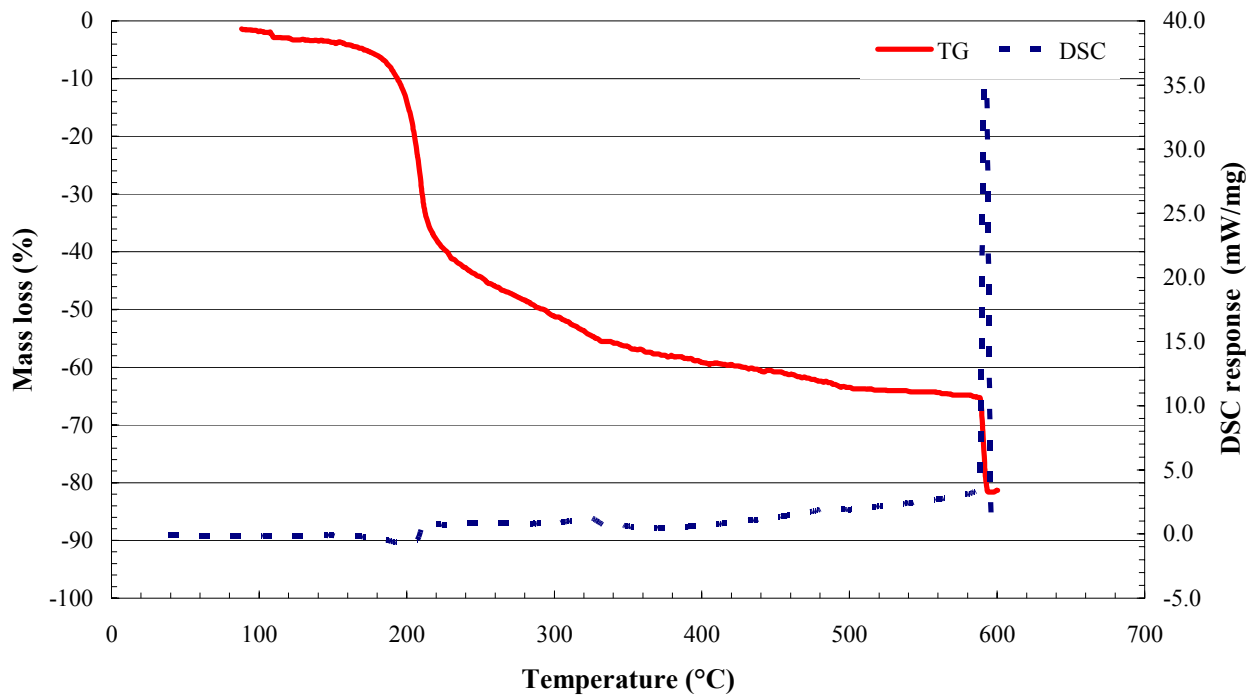
DSC/TGA scan of Na gluconate
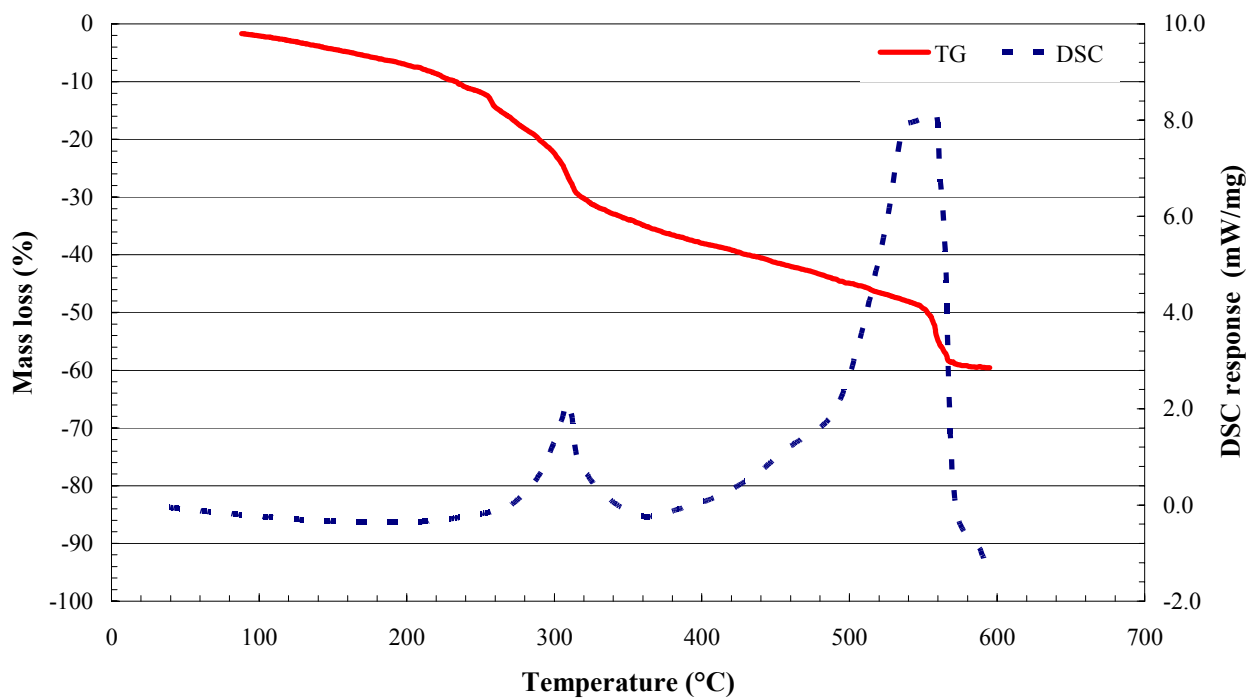
DSC/TGA scan of Sb gluconate
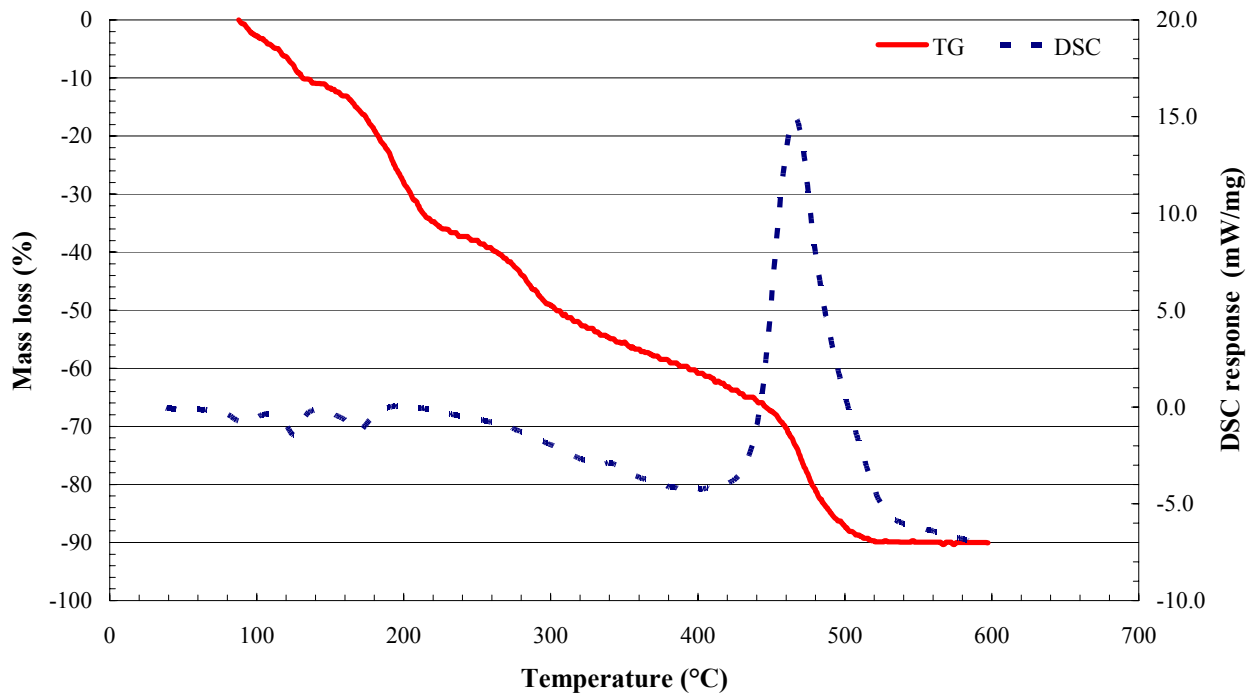
DSC/TGA scan of Zn gluconate
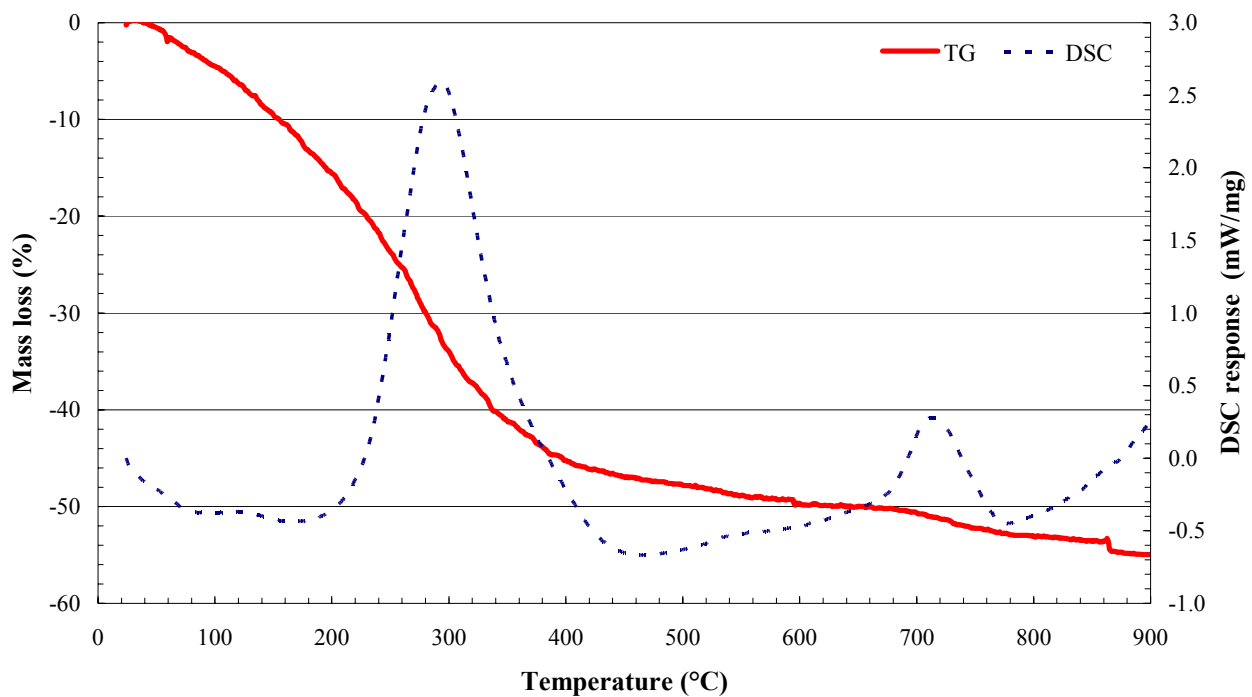
DSC/TGA scan of Zr gluconate

7.14. Appendix N

7.14.1. SEM images of calcium gluconate monohydrate powder (crystals).
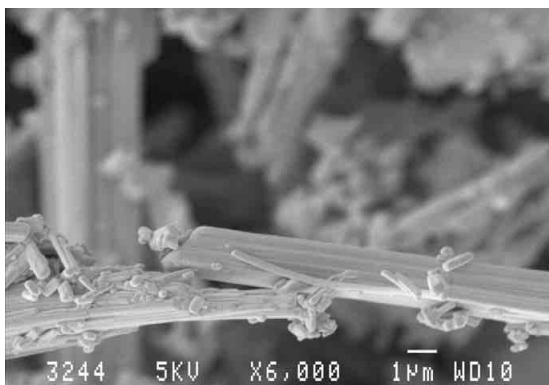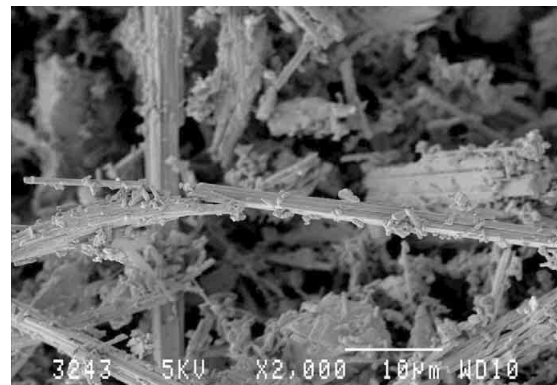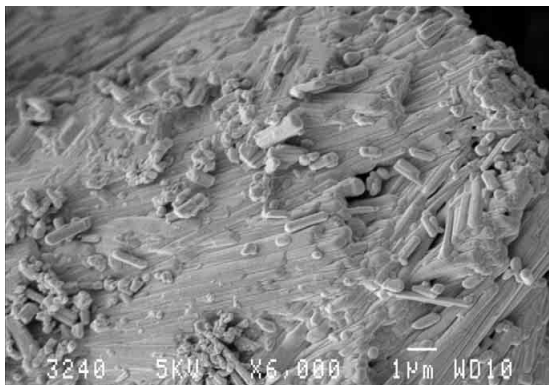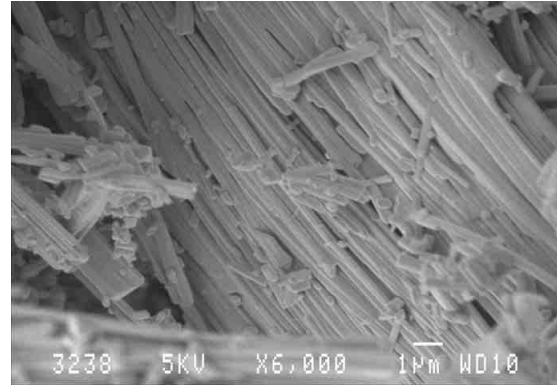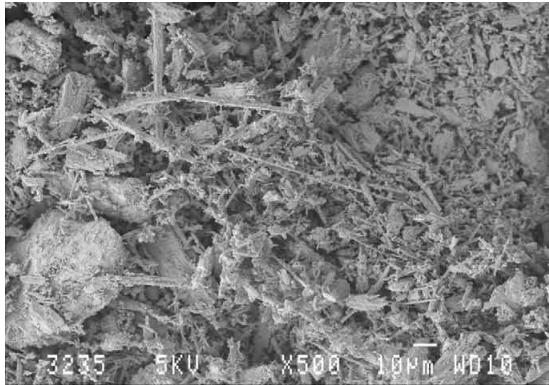
7.14.2. SEM images of ammonium gluconate hydrate (crystals).
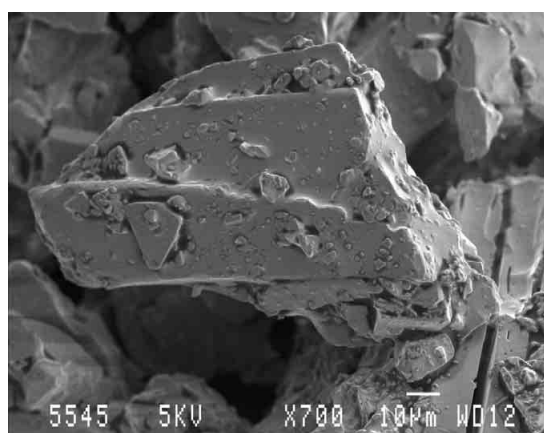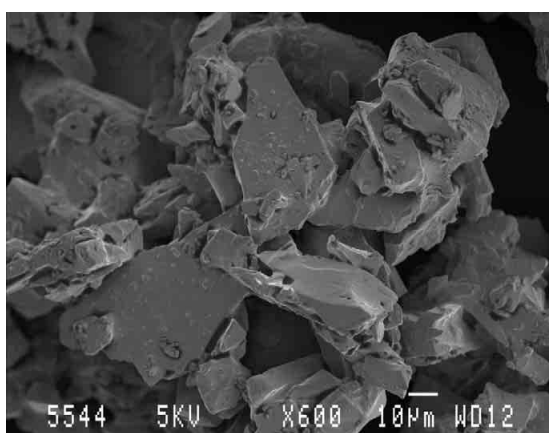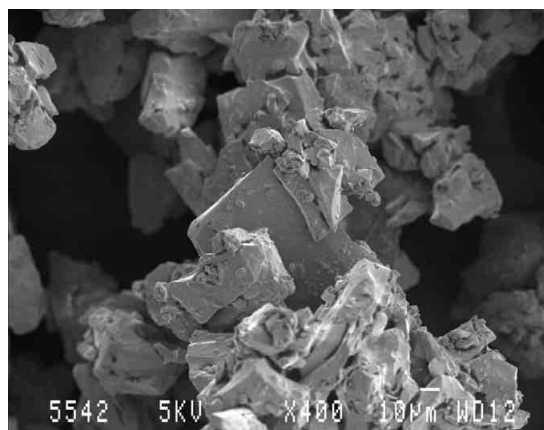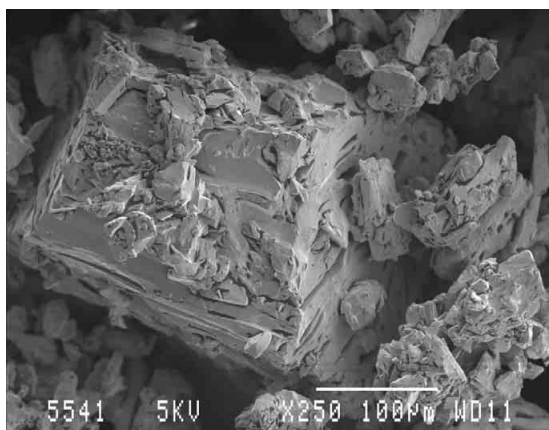
7.14.3. SEM images of the plate like leached SiO_2
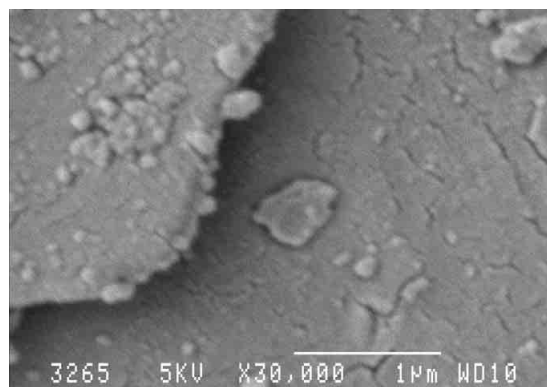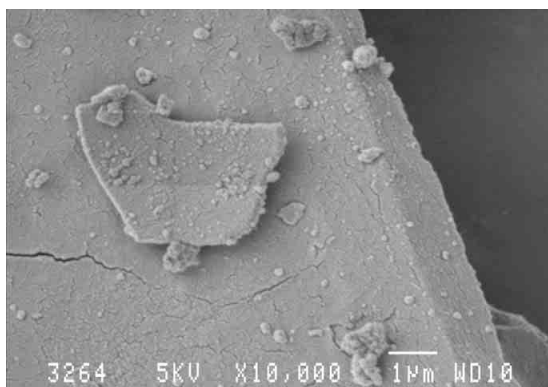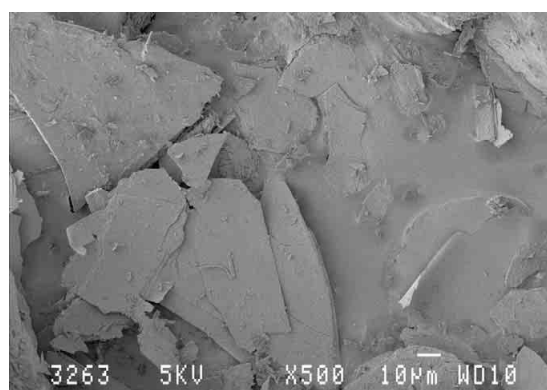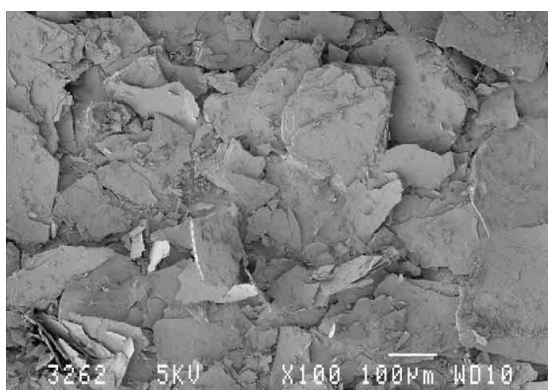
7.14.4. SEM images of calcium gluconate pyrolysed in air at selected temperatures

Calcium gluconate pyrolysed in air at 200 °C
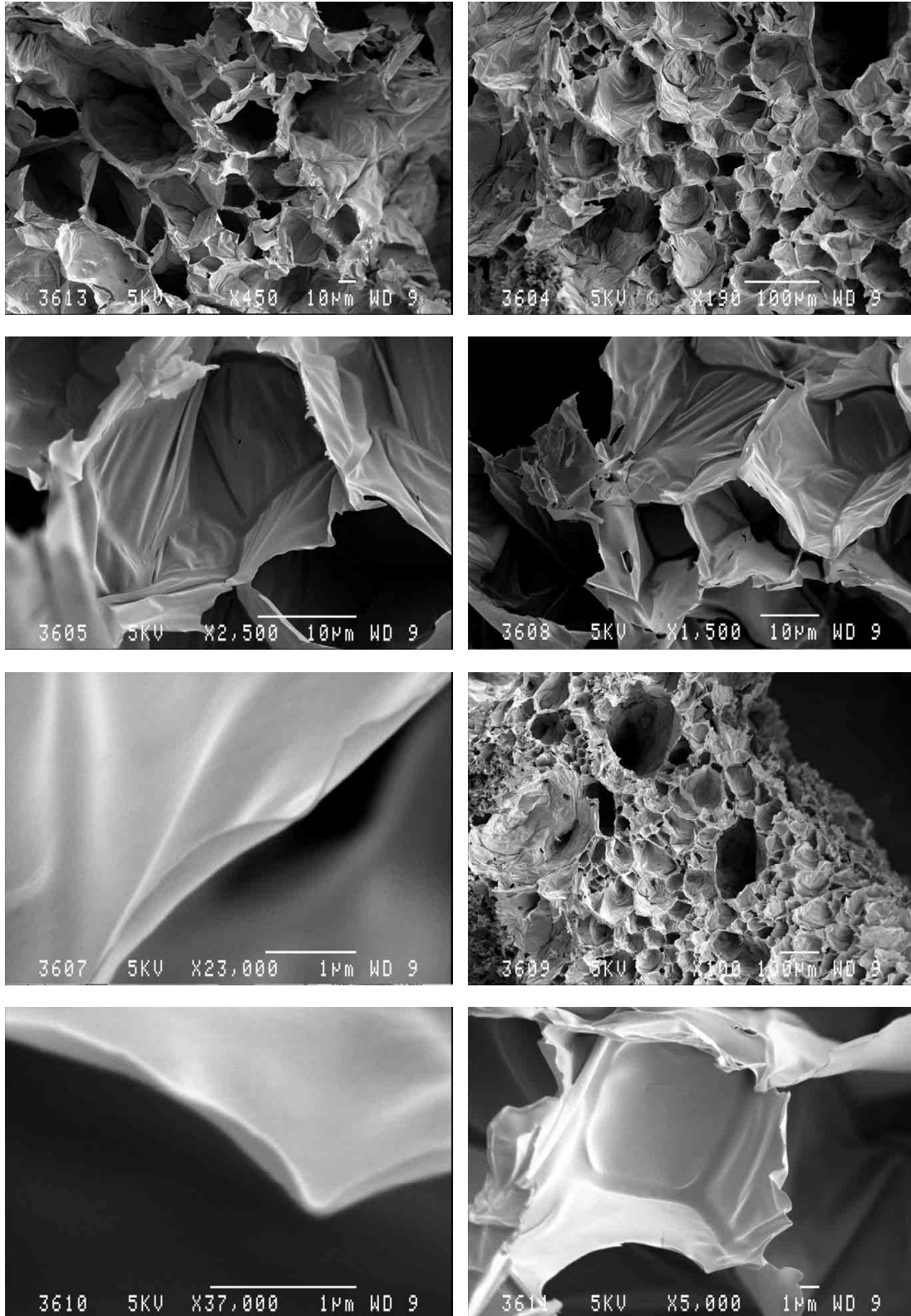
Calcium gluconate pyrolysed in air at 300 °C
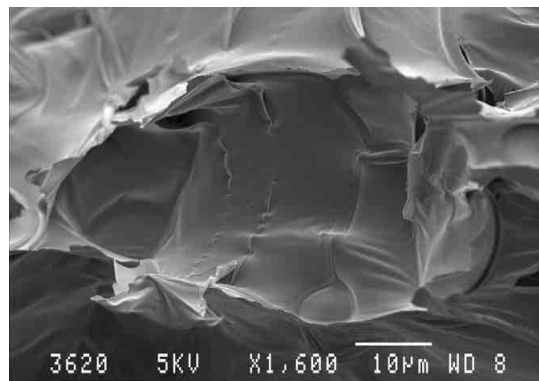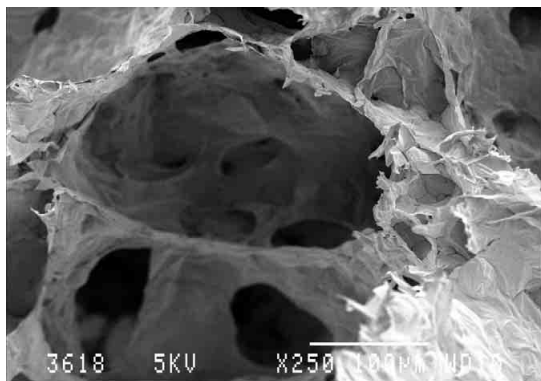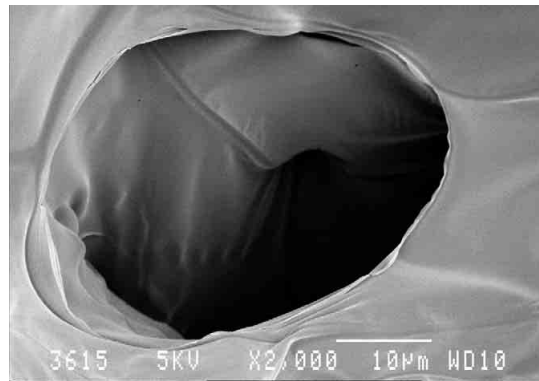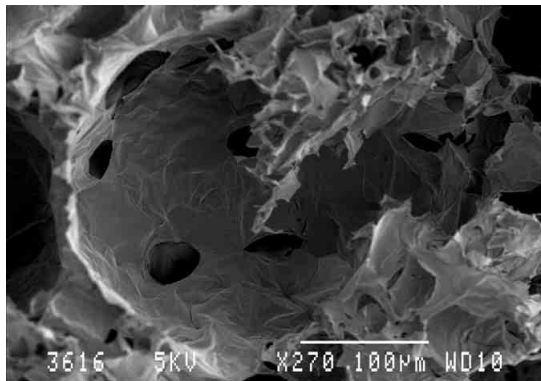
Calcium gluconate pyrolysed in air at 400 °C
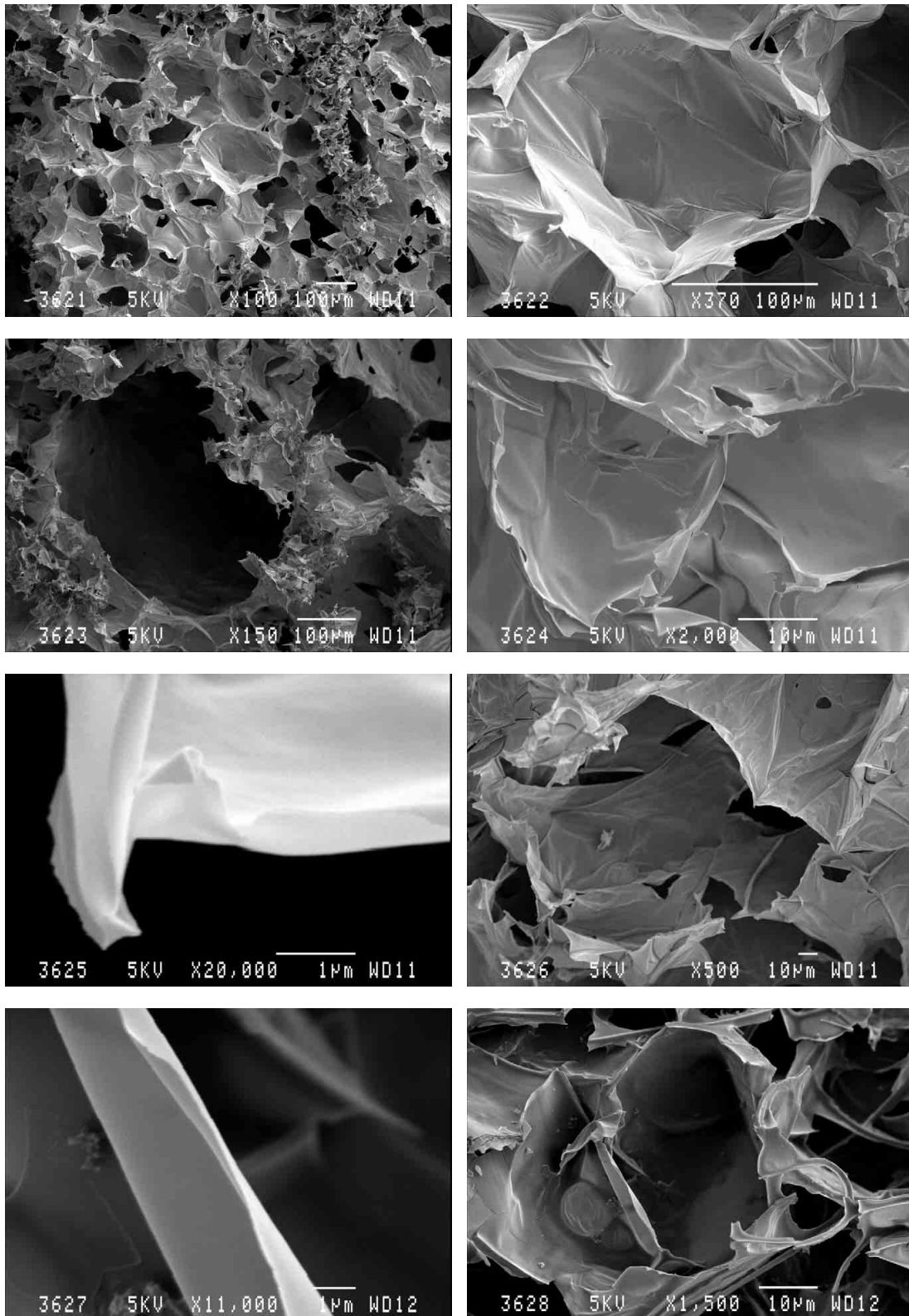
Calcium gluconate pyrolysed in air at 500 °C
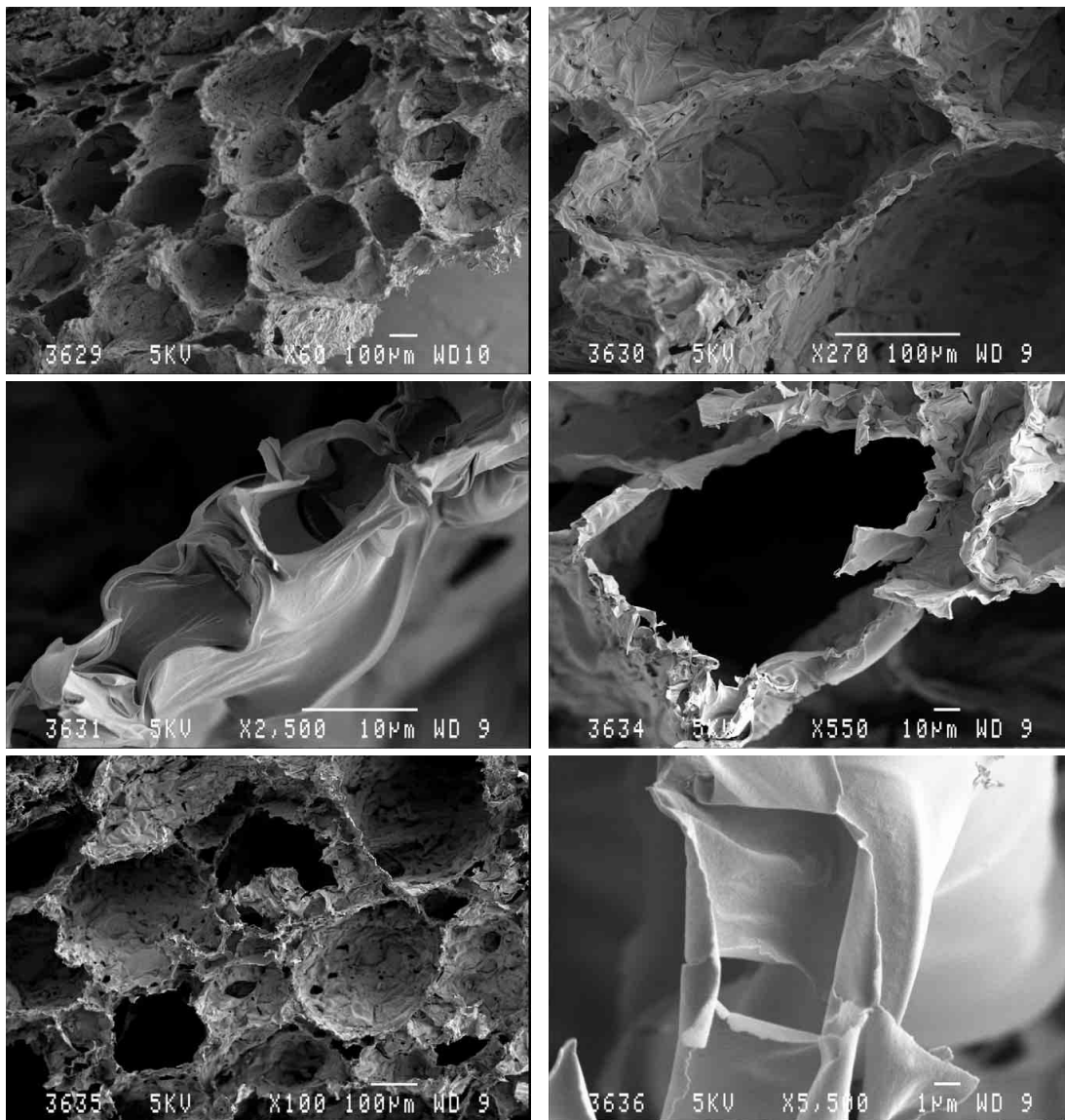
Calcium gluconate pyrolysed in air at 600 °C
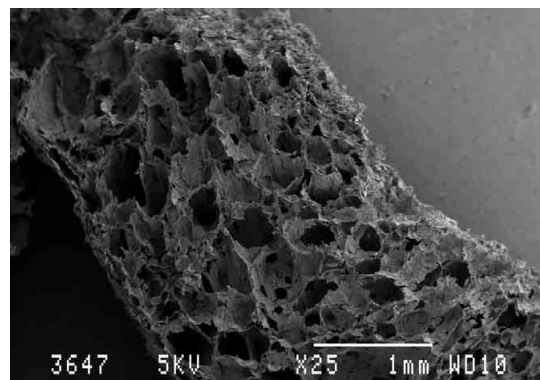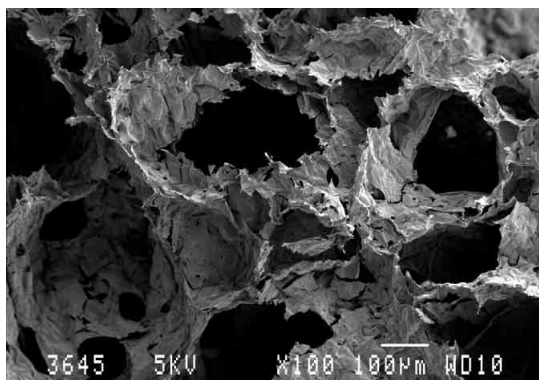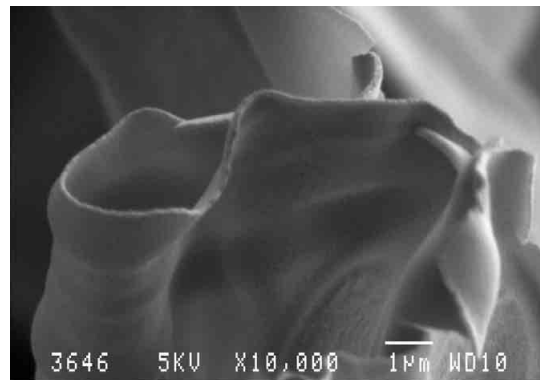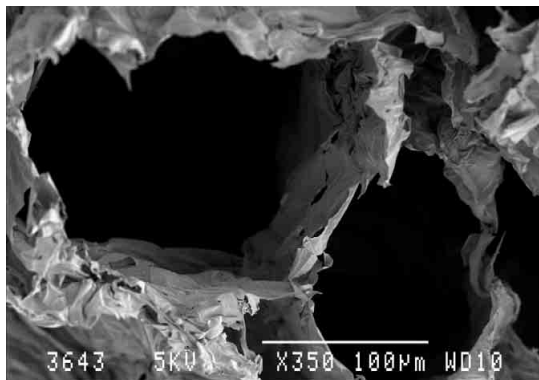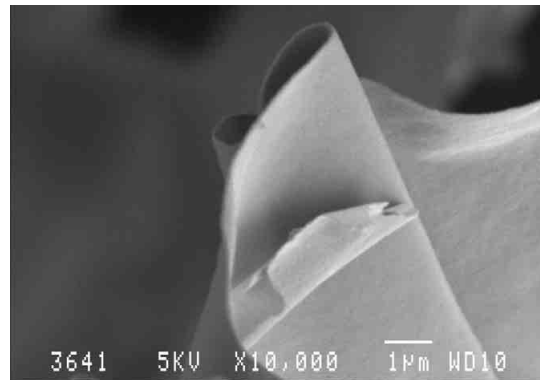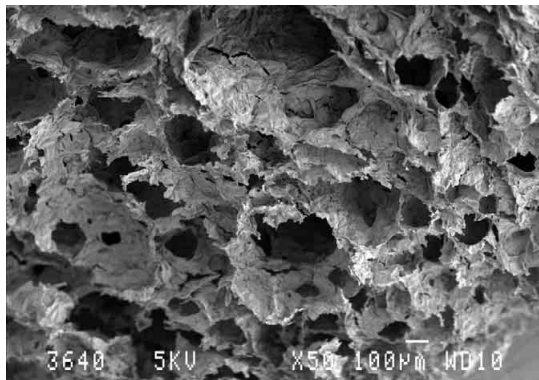
Calcium gluconate pyrolysed in air at 700 °C
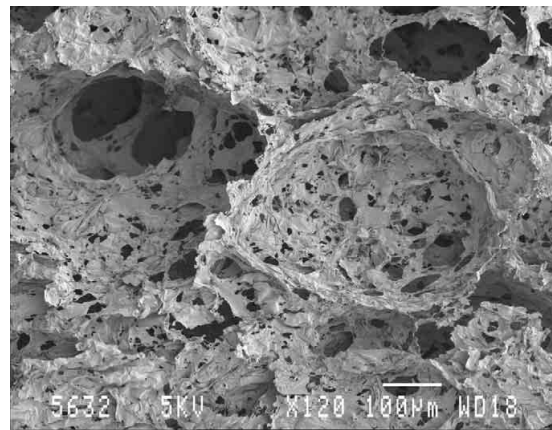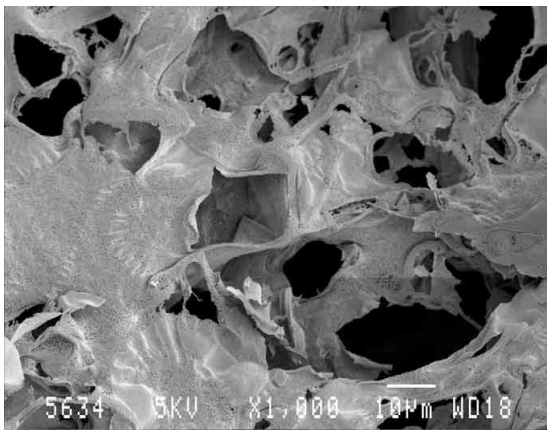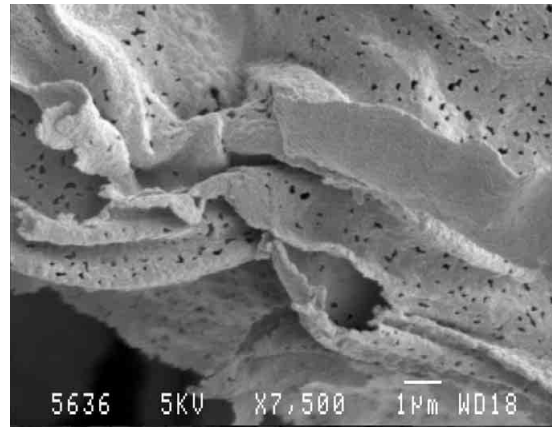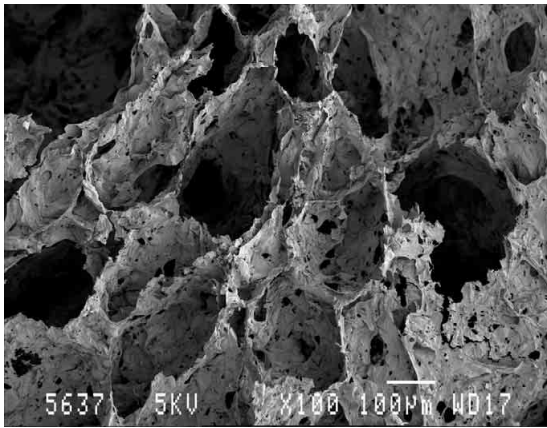
Calcium gluconate pyrolysed in air at 800 °C
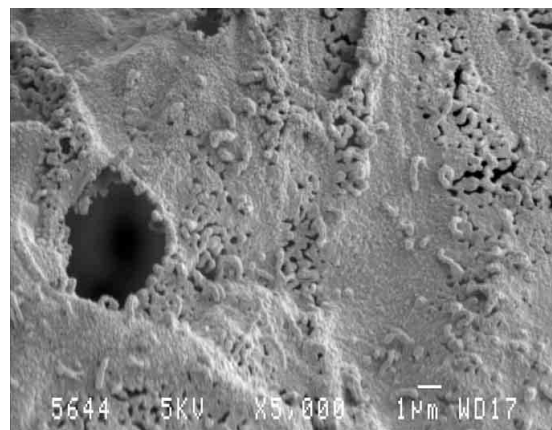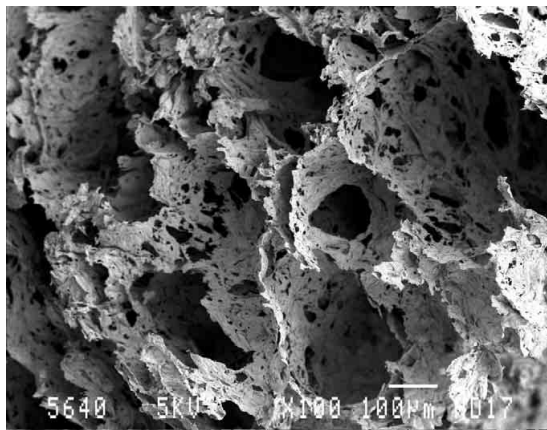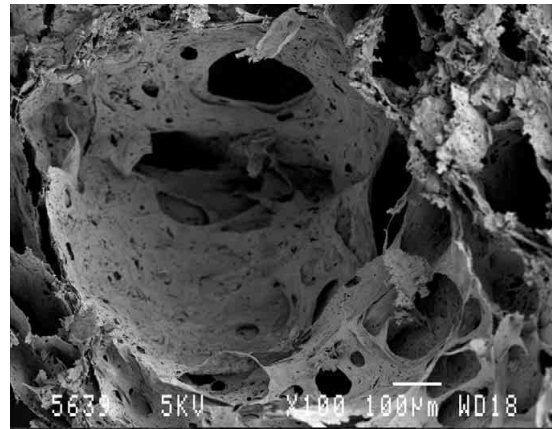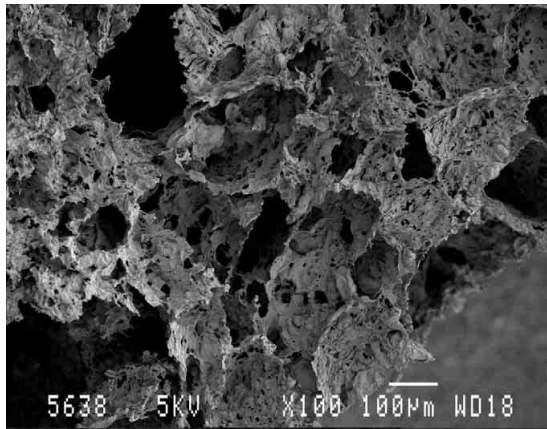
Calcium gluconate pyrolysed in air at 1000 °C
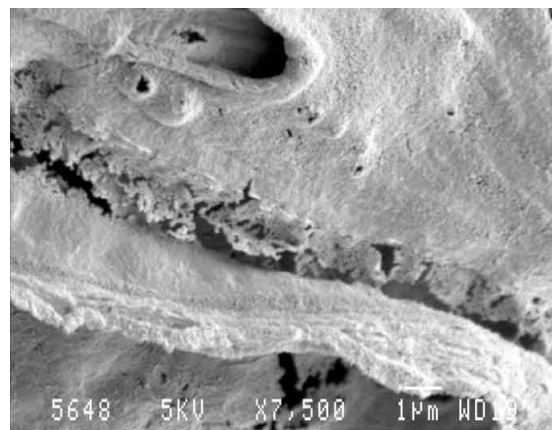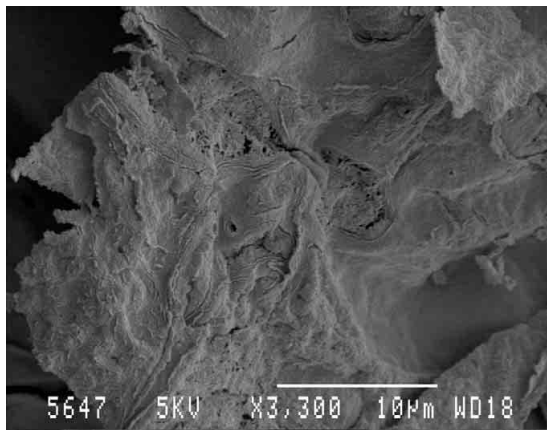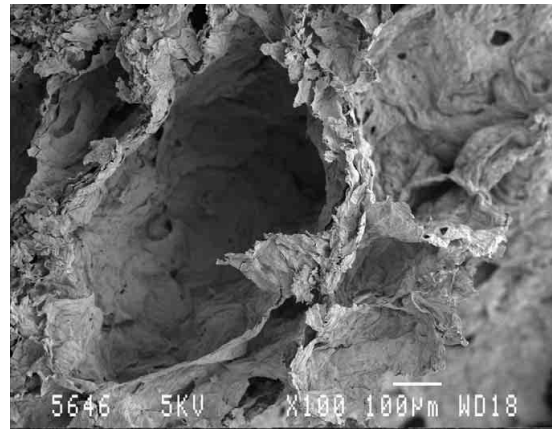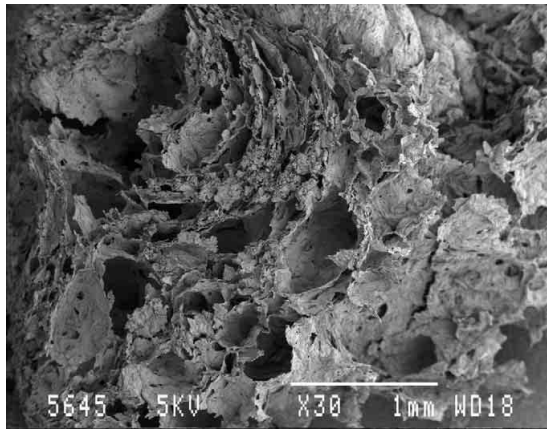
7.14.5. SEM images of calcium gluconate monohydrate pyrolysed in nitrogen at selected temperatures

Calcium gluconate pyrolysed in nitrogen at 200 °C
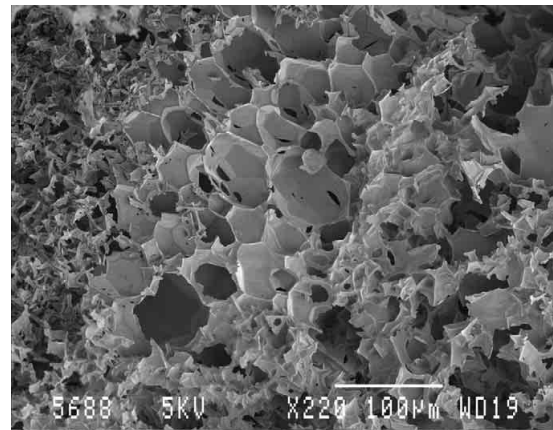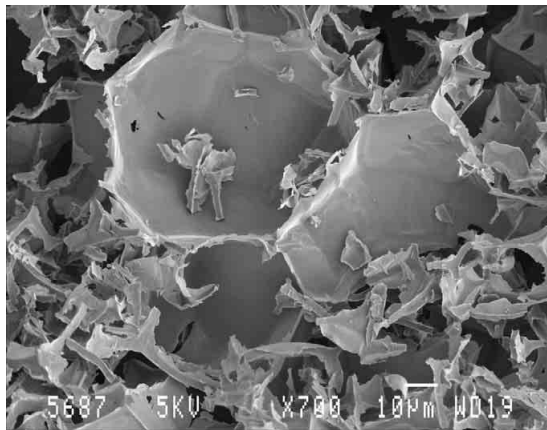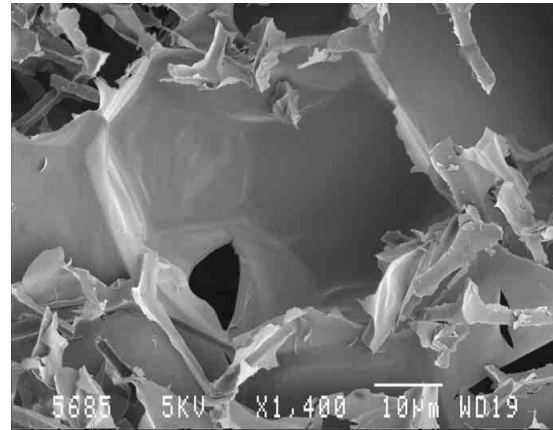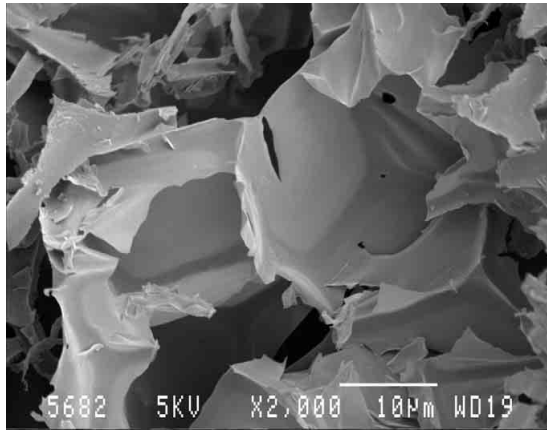
Calcium gluconate pyrolysed in nitrogen at 300 °C
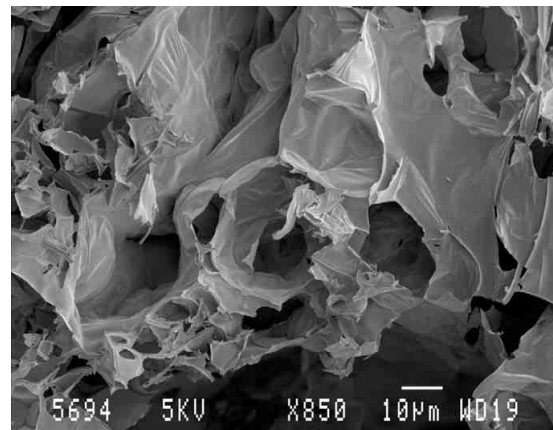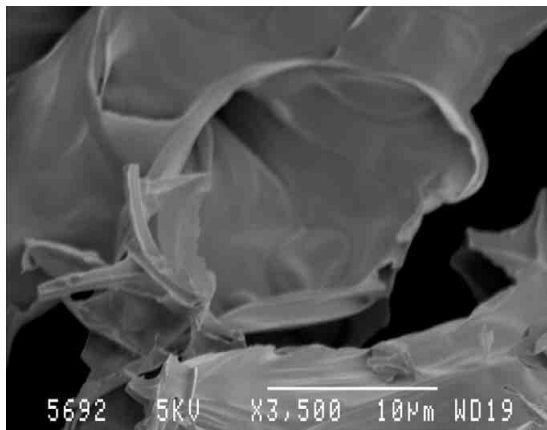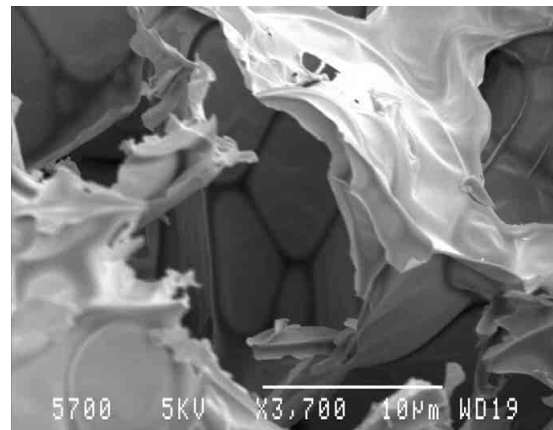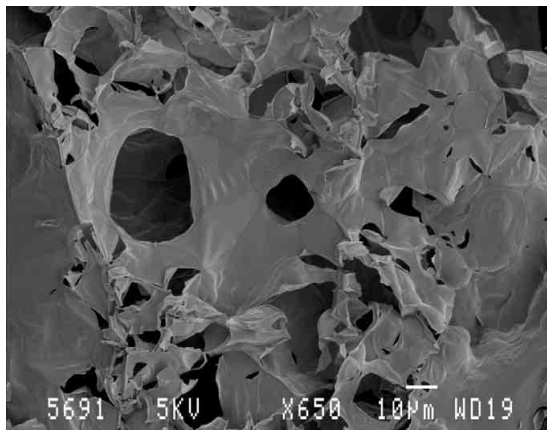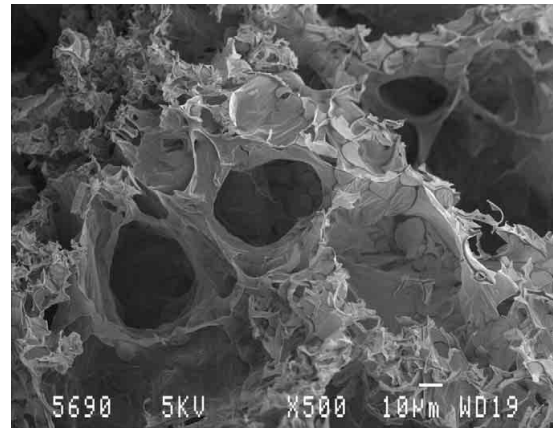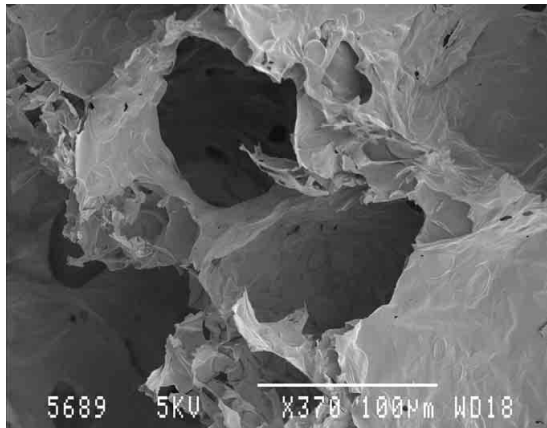
Calcium gluconate pyrolysed in nitrogen at 400 °C
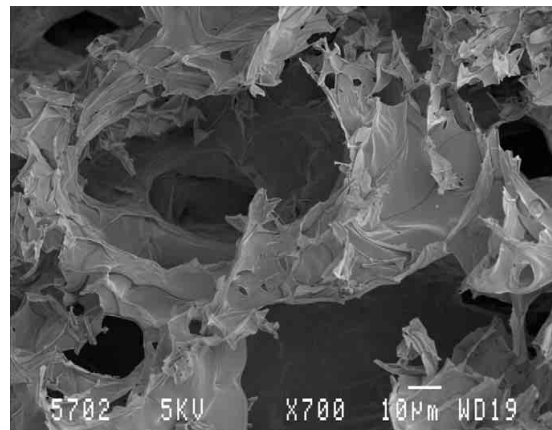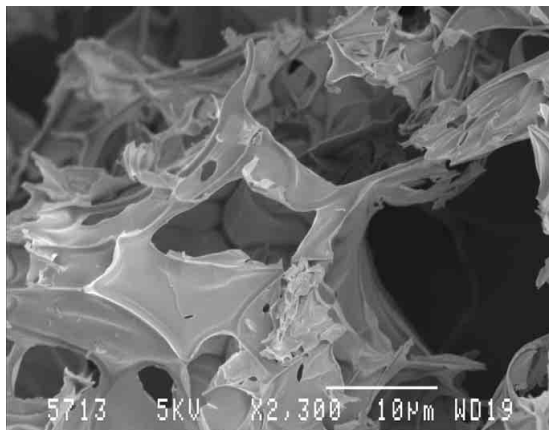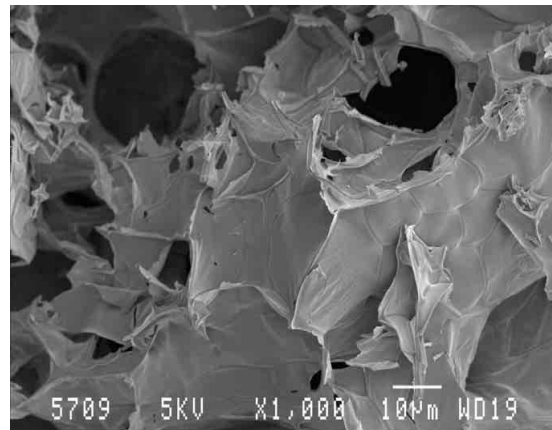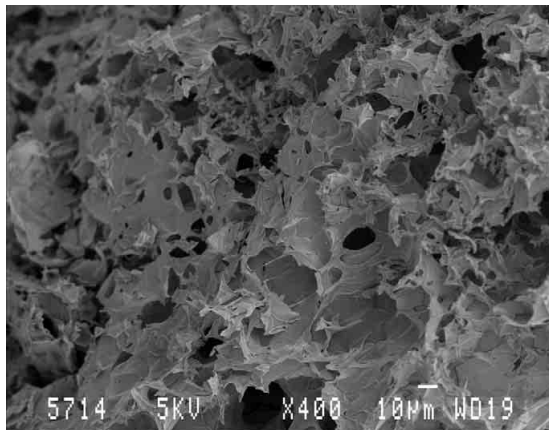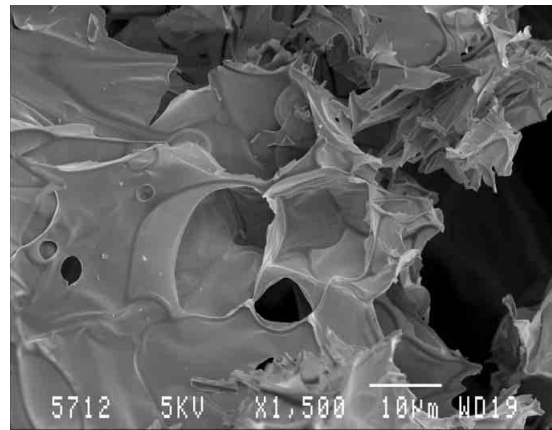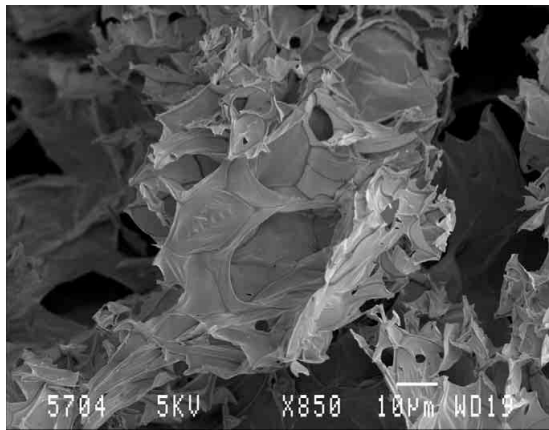
Wall thickness of calcium gluconate heated at 300°C
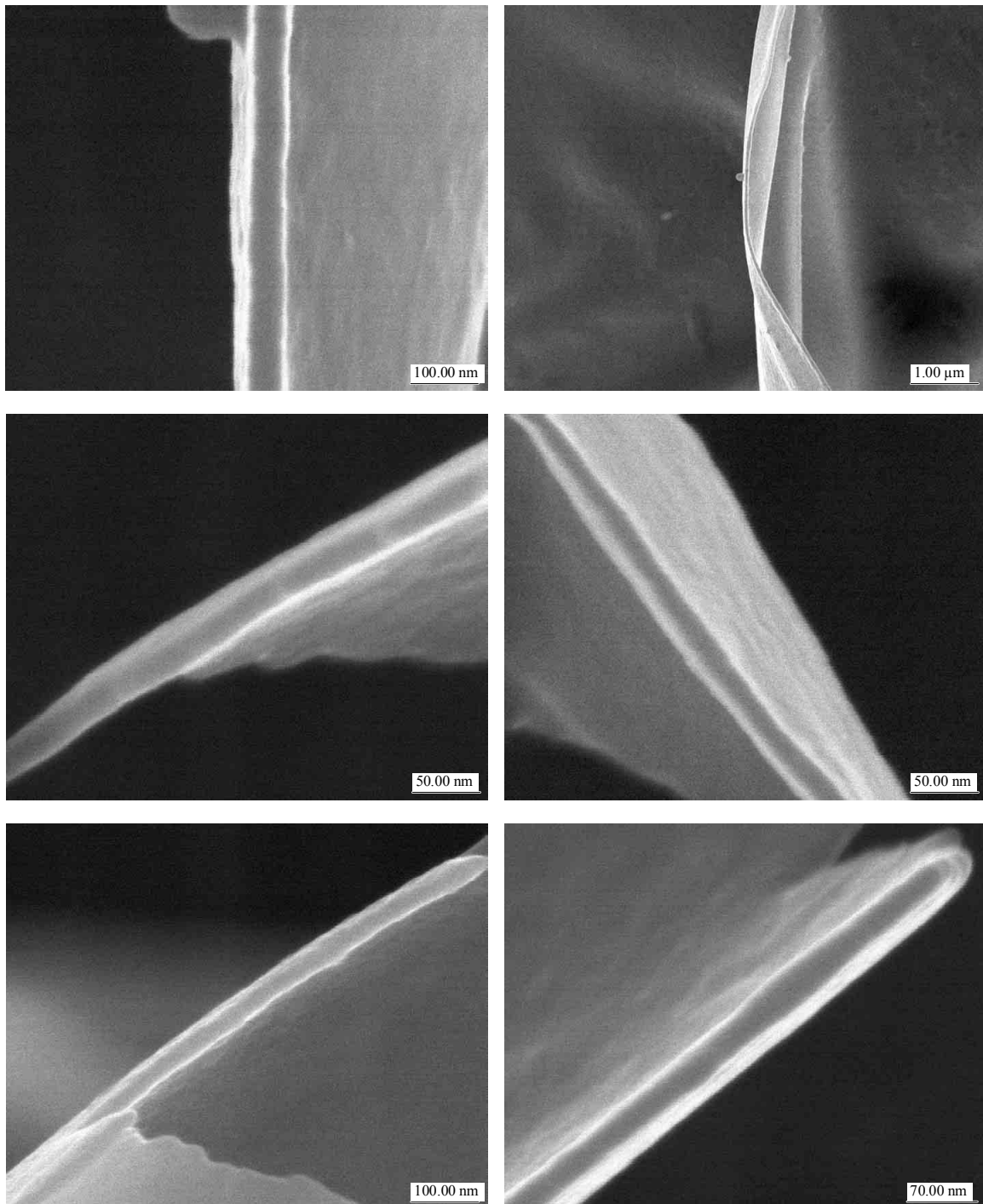
7.14.6. SEM images of calcium gluconate monohydrate and leached silica mixtures pyrolysed in air

4:1 mole ratio (gluconate: silica) heated at 400°C
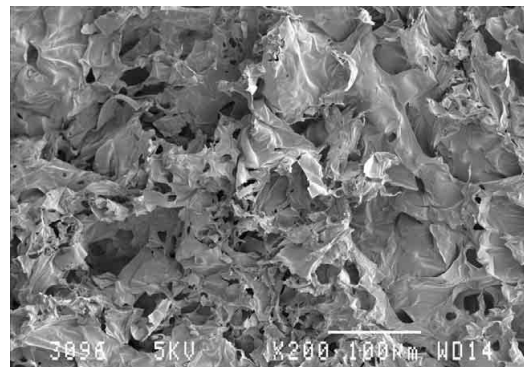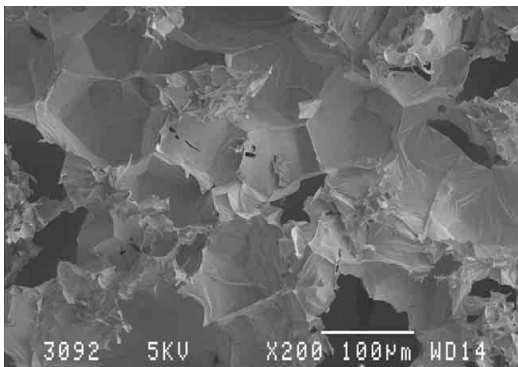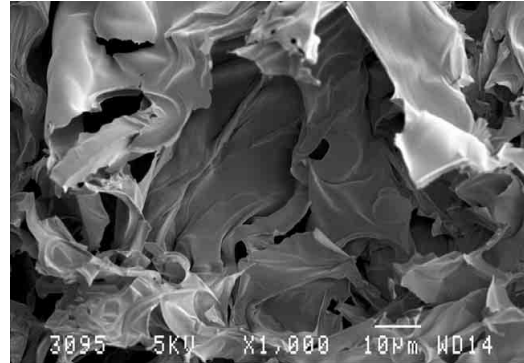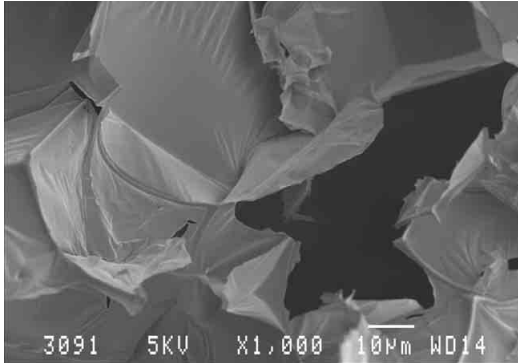
4:1 mole ratio (gluconate: silica) heated at 600°C
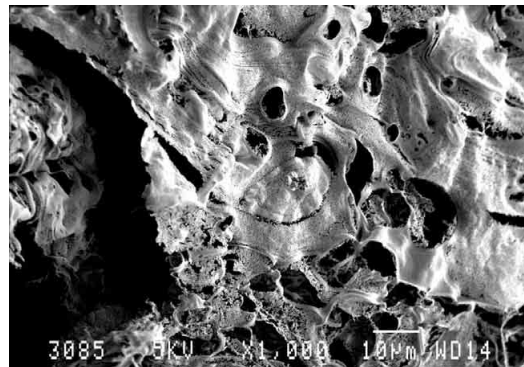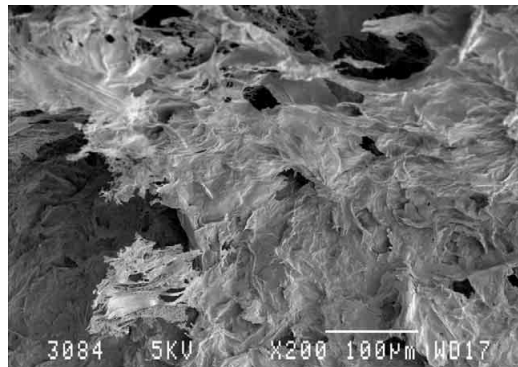
4:1 mole ratio (gluconate: silica) heated at 1000°C
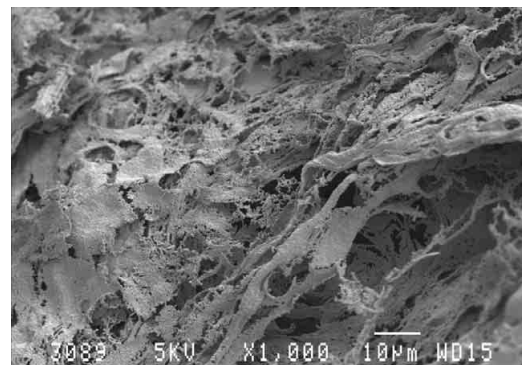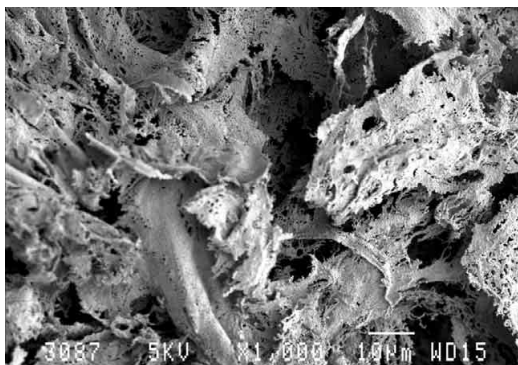
2:1 mole ratio (gluconate: silica) heated at 600°C
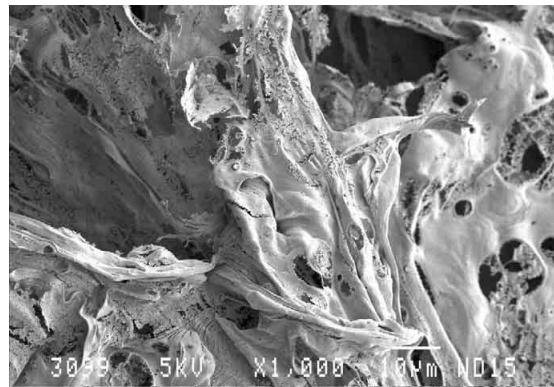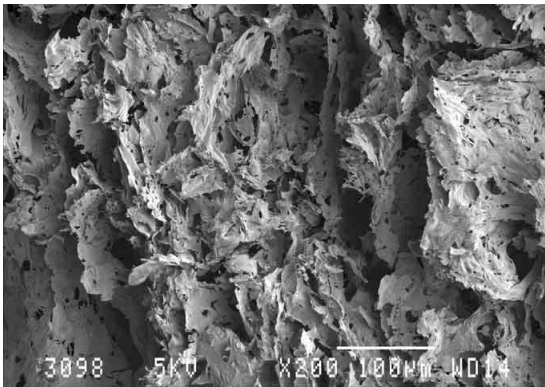
1:1 mass ratio (gluconate: silica) heated at 600°C
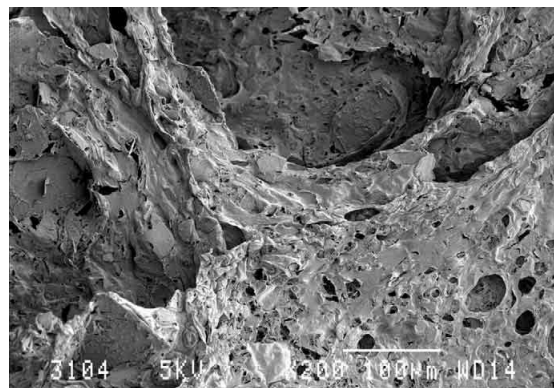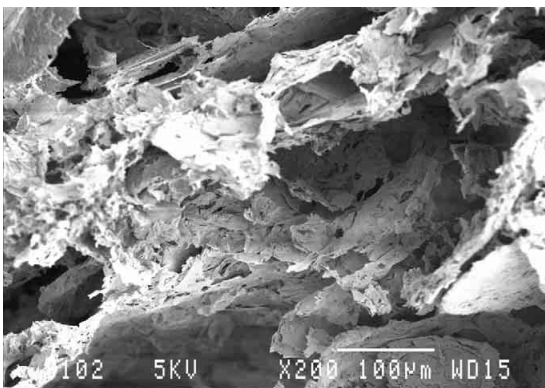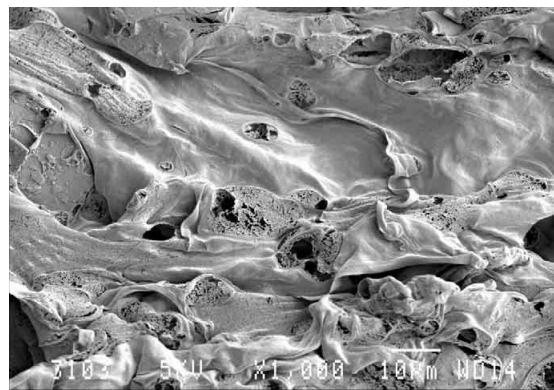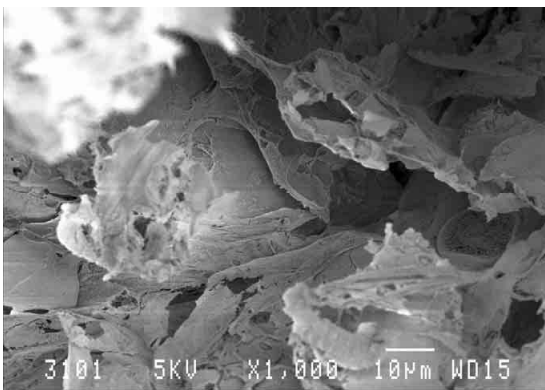
7.14.7. SEM images of ammonium gluconate hydrate pyrolysed in air at selected temperatures

Ammonium gluconate pyrolysed in air at 300 °C
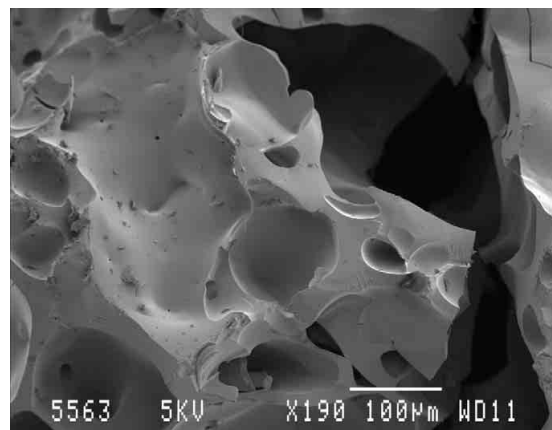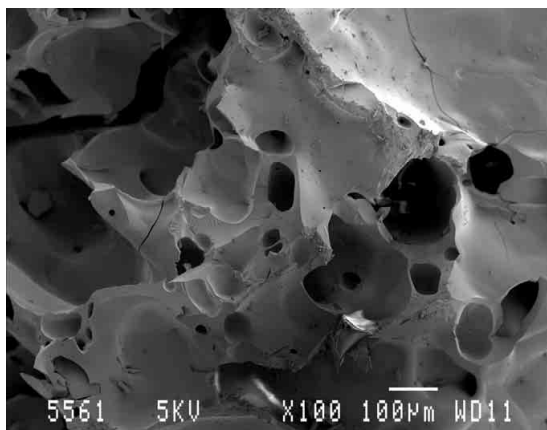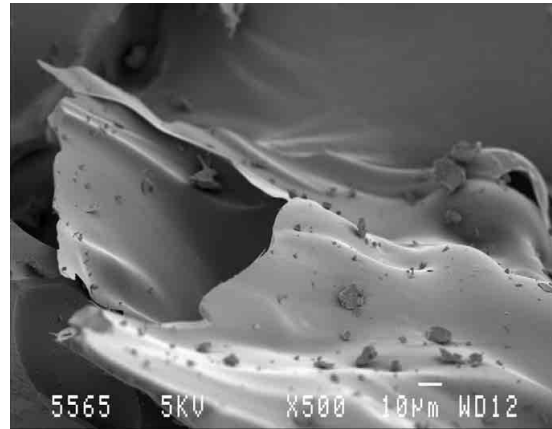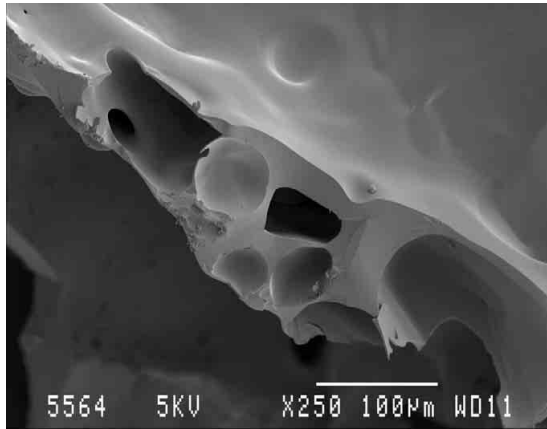
Ammonium gluconate pyrolysed in air at 400 °C
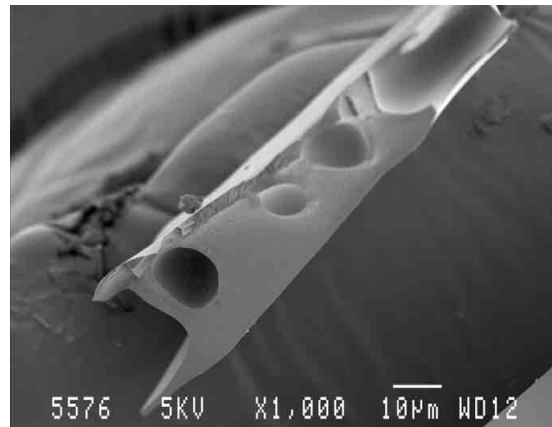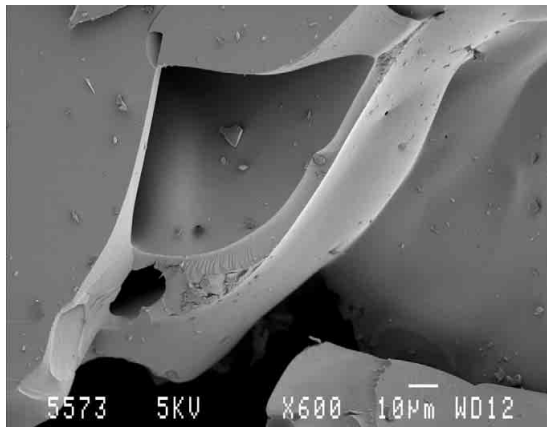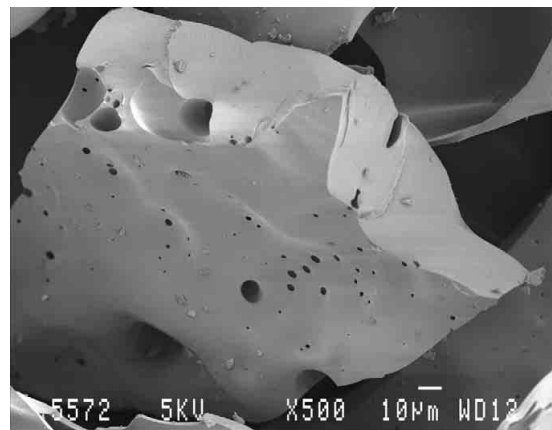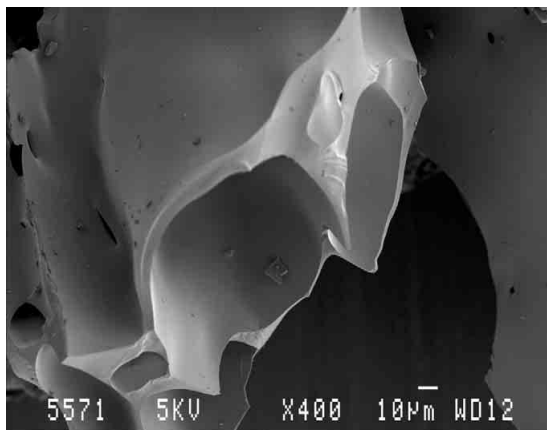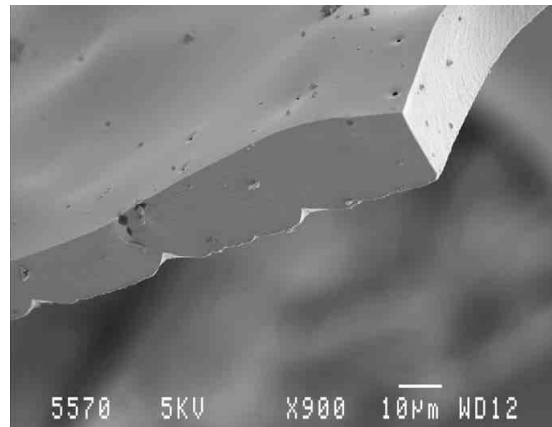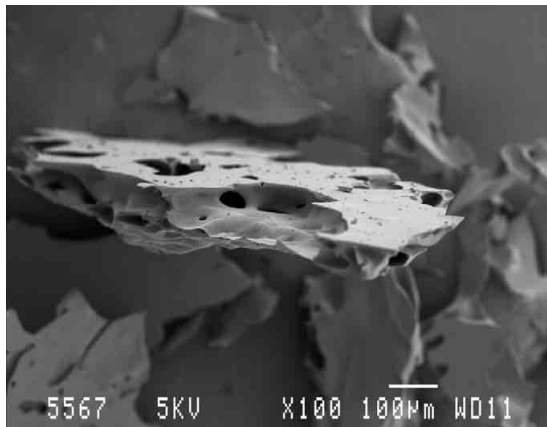
7.14.8. SEM images of ammonium gluconate hydrate pyrolysed in nitrogen at selected temperatures

Ammonium gluconate pyrolysed in nitrogen at 300 °C
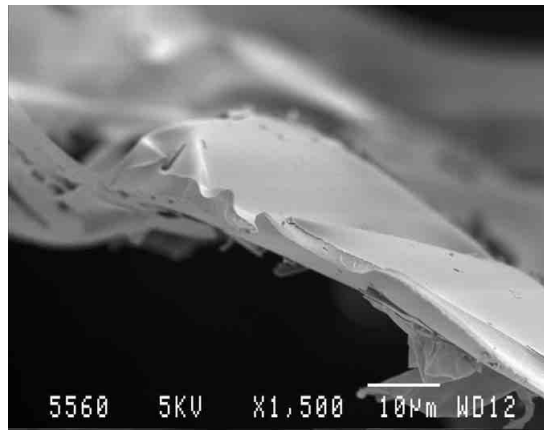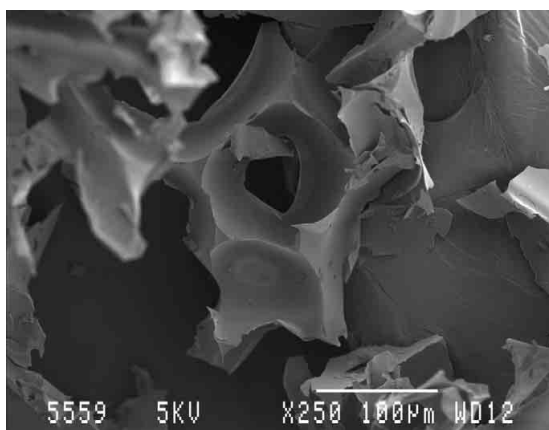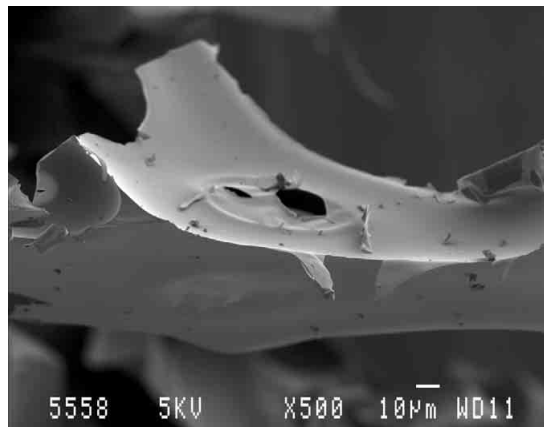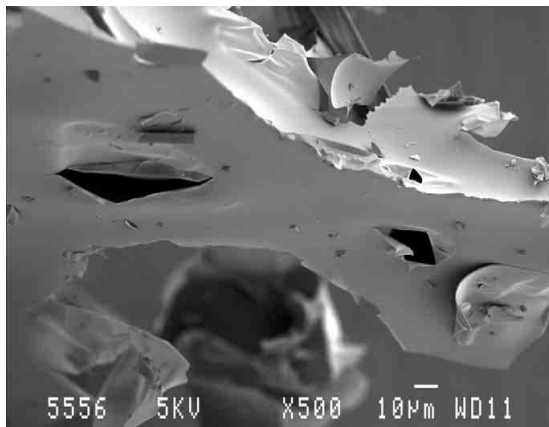
Ammonium gluconate pyrolysed in nitrogen at 400 °C
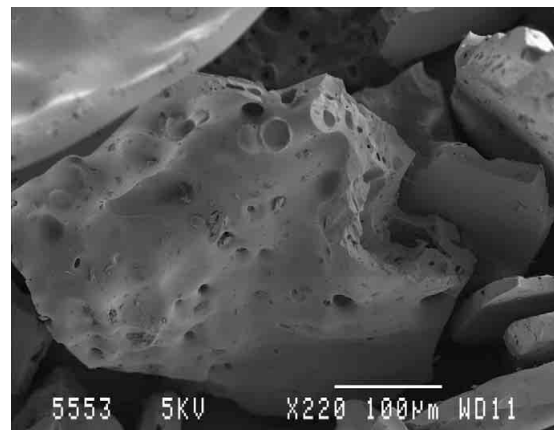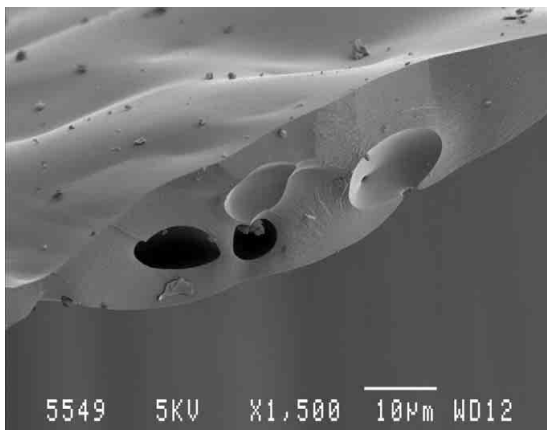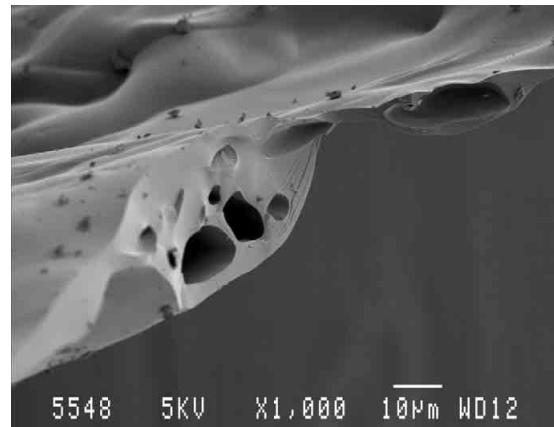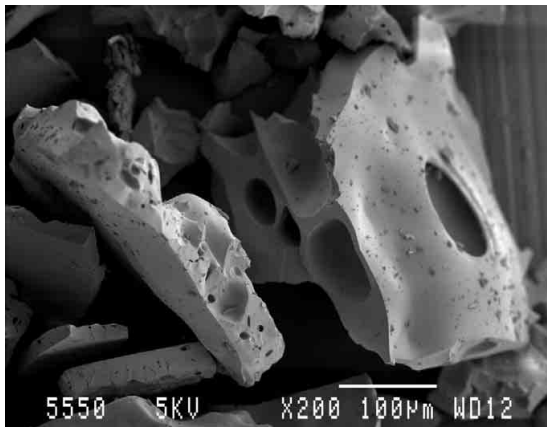
Wall thickness of ammonium gluconate heated at 300°C
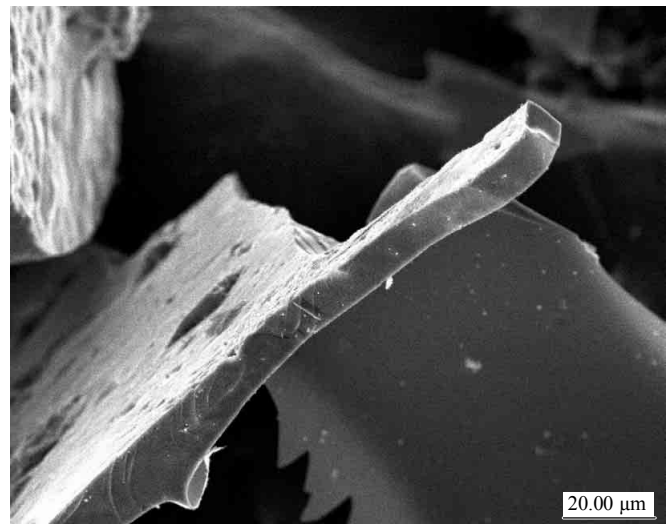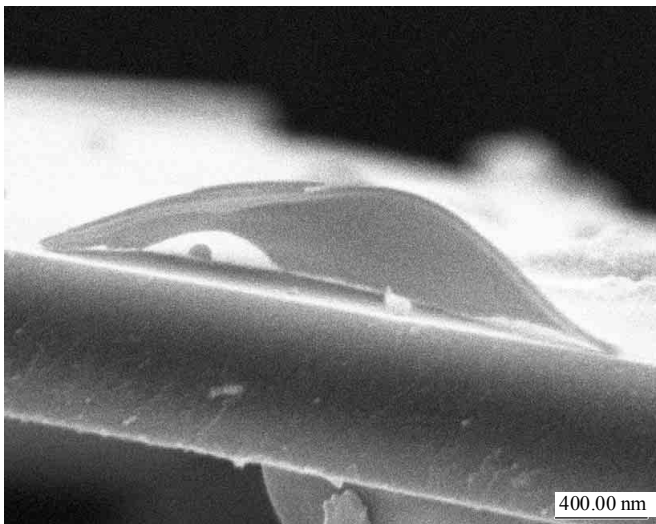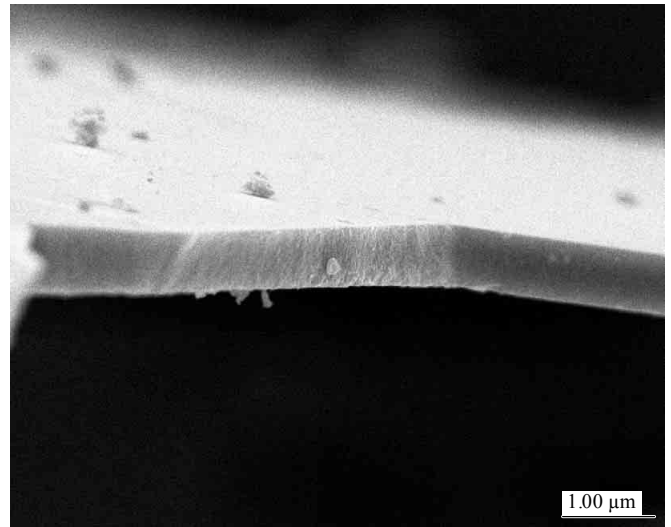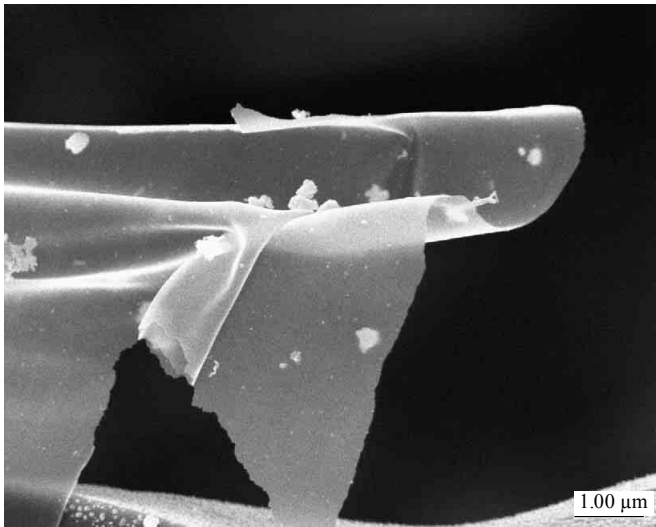
7.14.9. SEM images of AP750 pyrolysed in air at 400 °C
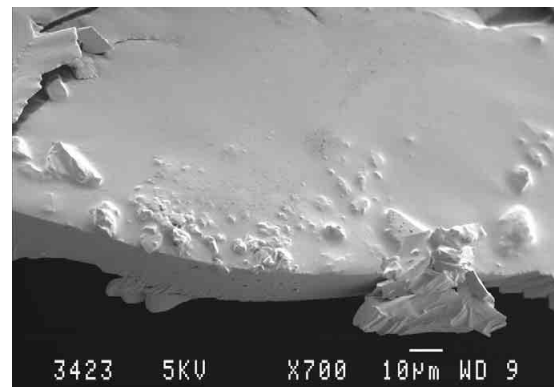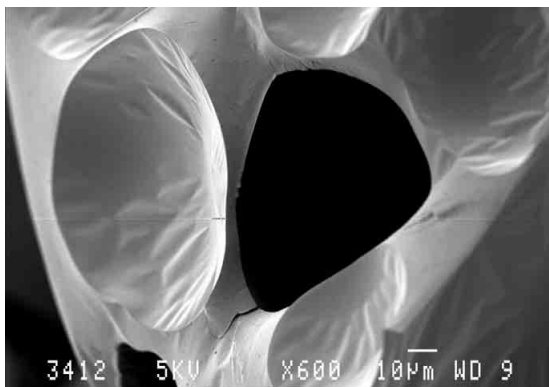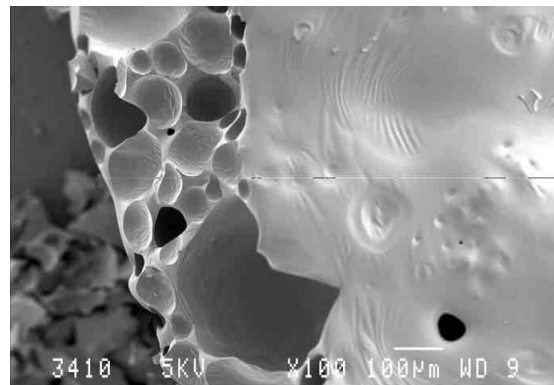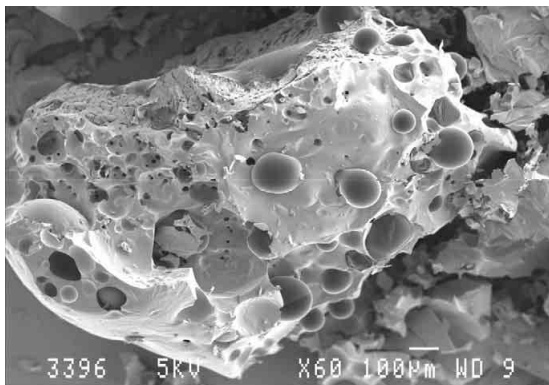
7.14.10.   SEM images of PEN pyrolysed in air at 400 °C
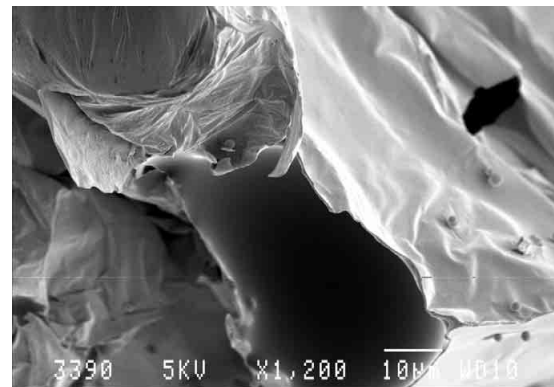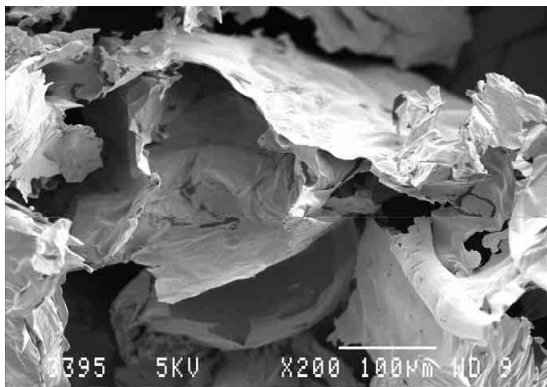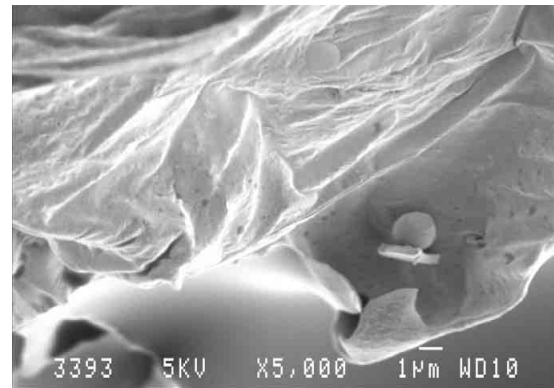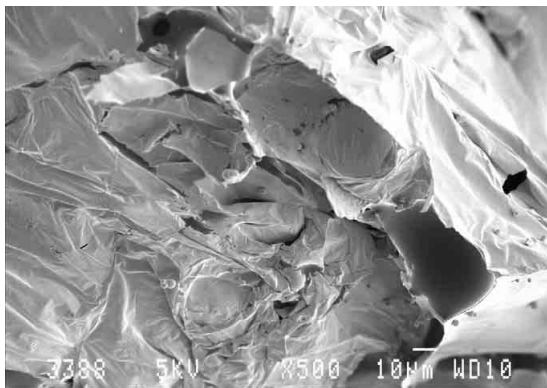
7.15. Appendix O

7.15.1. Thermal decomposition analysis of gluconic acid
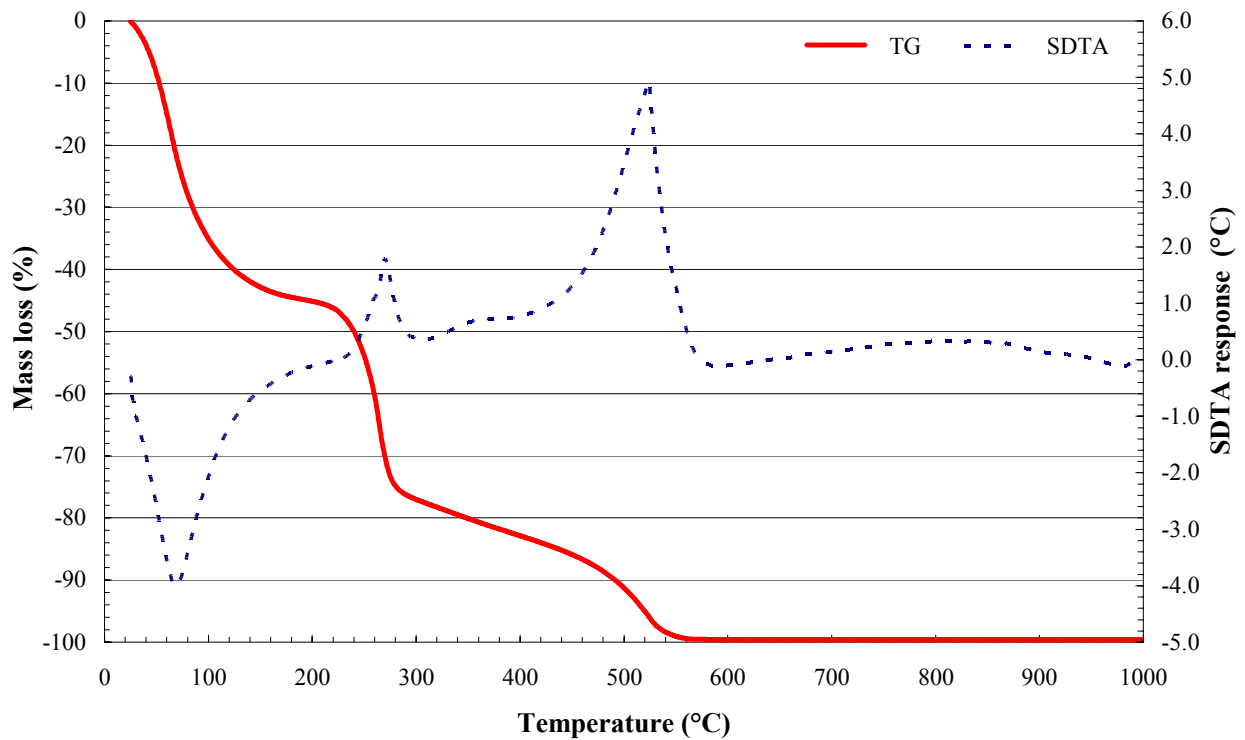
SDTA/TGA analysis of gluconic acid solution in water (50%) in air
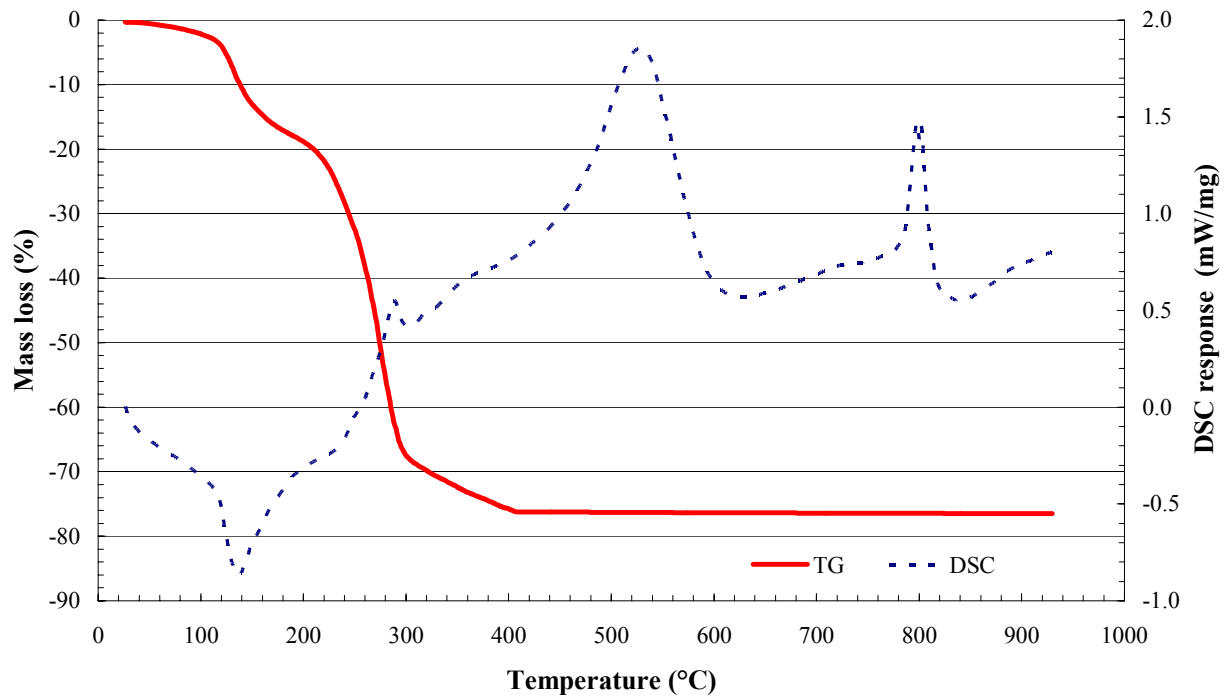
DSC/TGA analysis of gluconic acid solution in water (50%) in air

7.15.2. Thermal decomposition analysis of calcium gluconate monohydrate
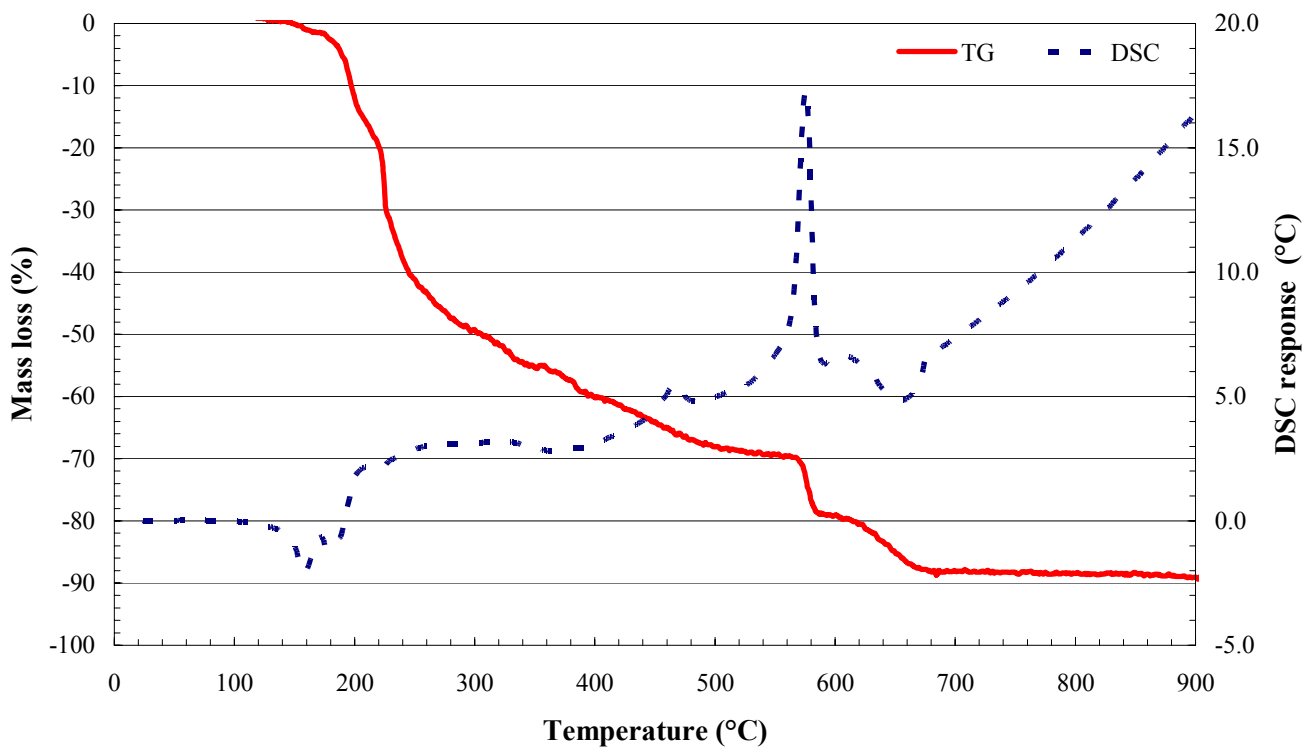
DSC/TGA analysis of calcium gluconate monohydrate in air
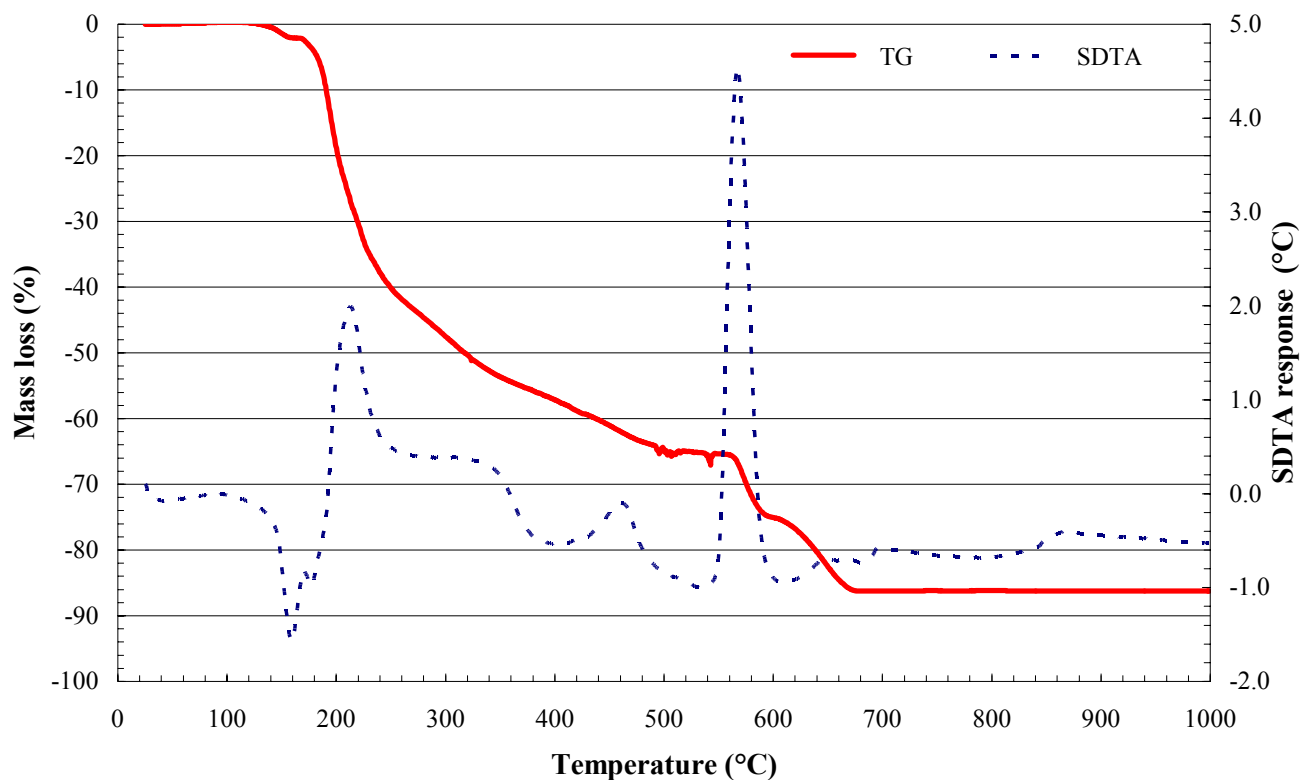
SDTA/TGA analysis of calcium gluconate monohydrate in air
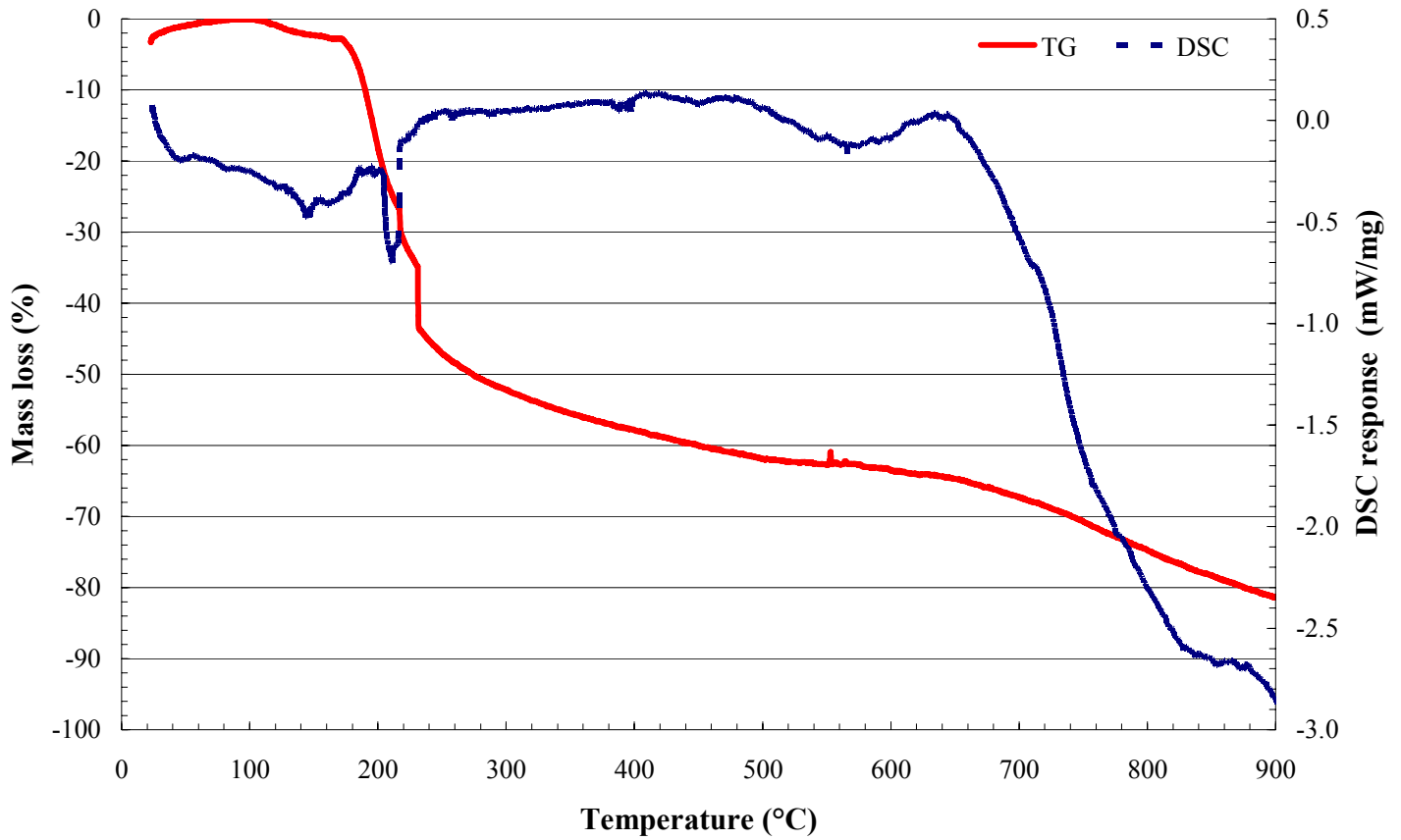
DSC/TGA analysis of calcium gluconate monohydrate in argon

7.15.3. Thermal decomposition analysis of ammonium gluconate hydrate
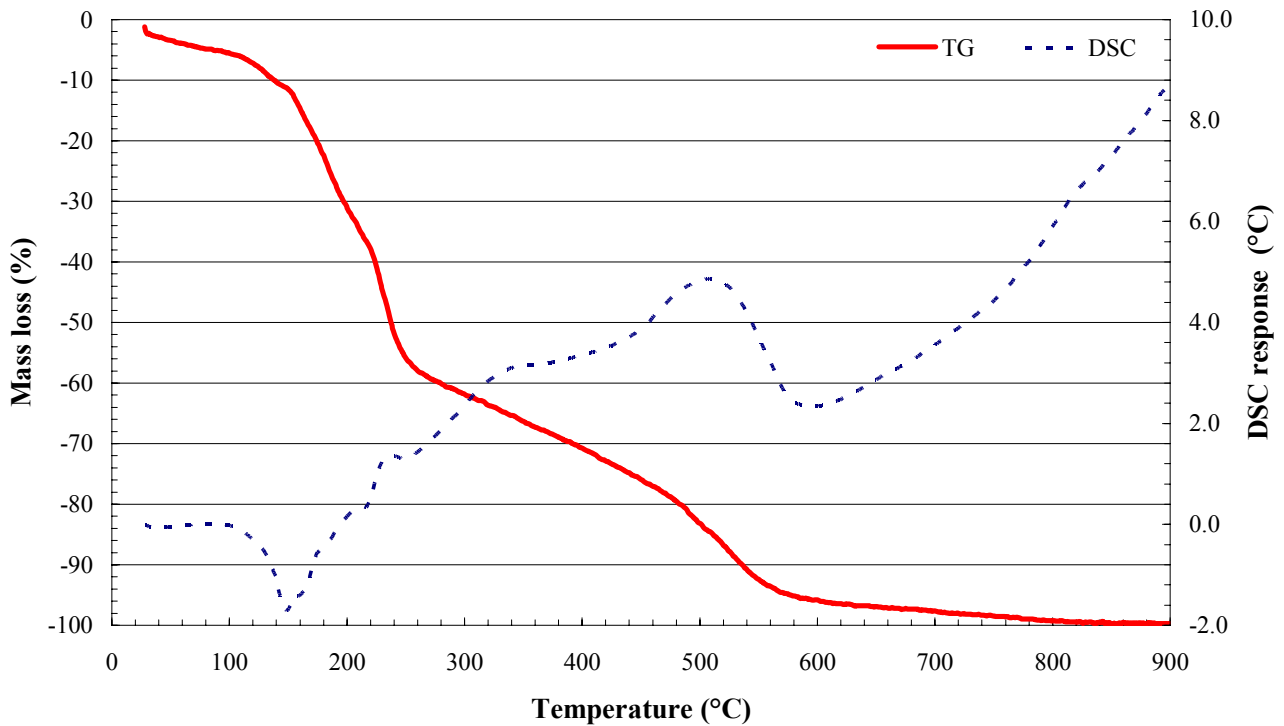
DSC/TGA analysis of ammonium gluconate hydrate in air
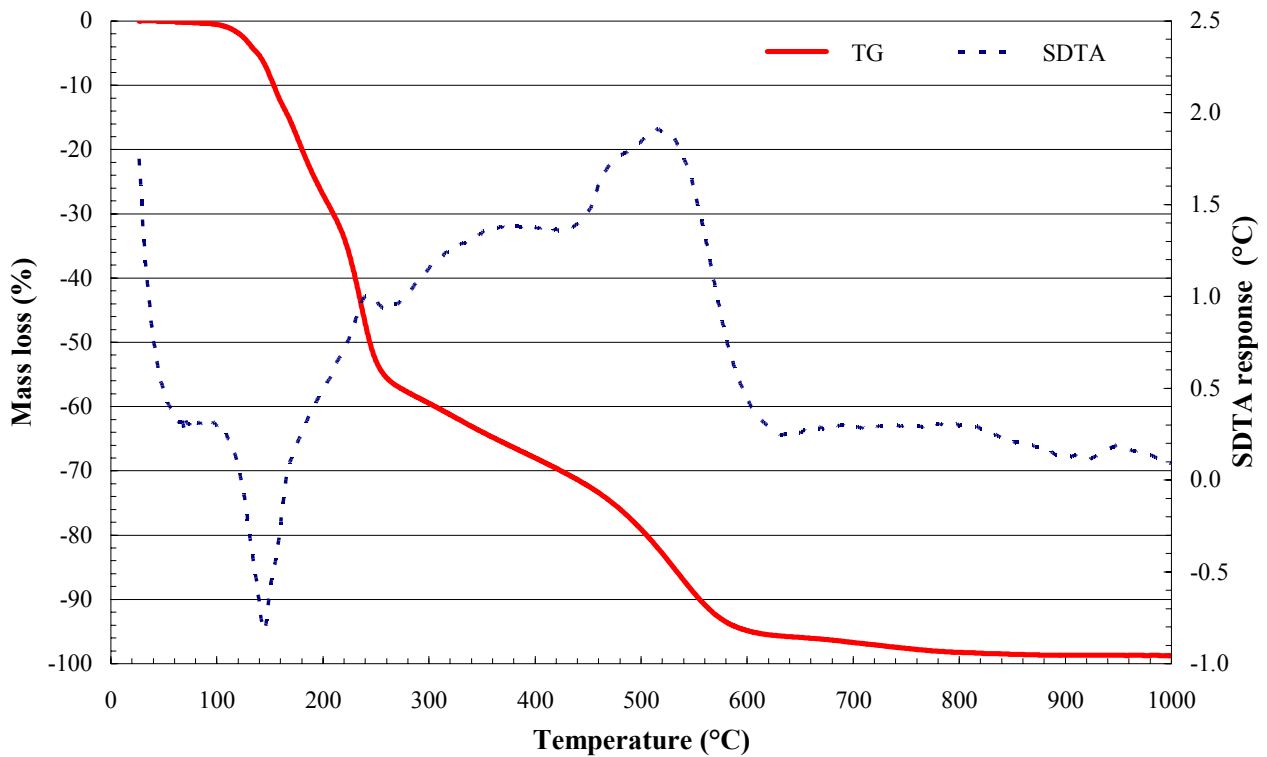
SDTA/TGA analysis of ammonium gluconate hydrate in air
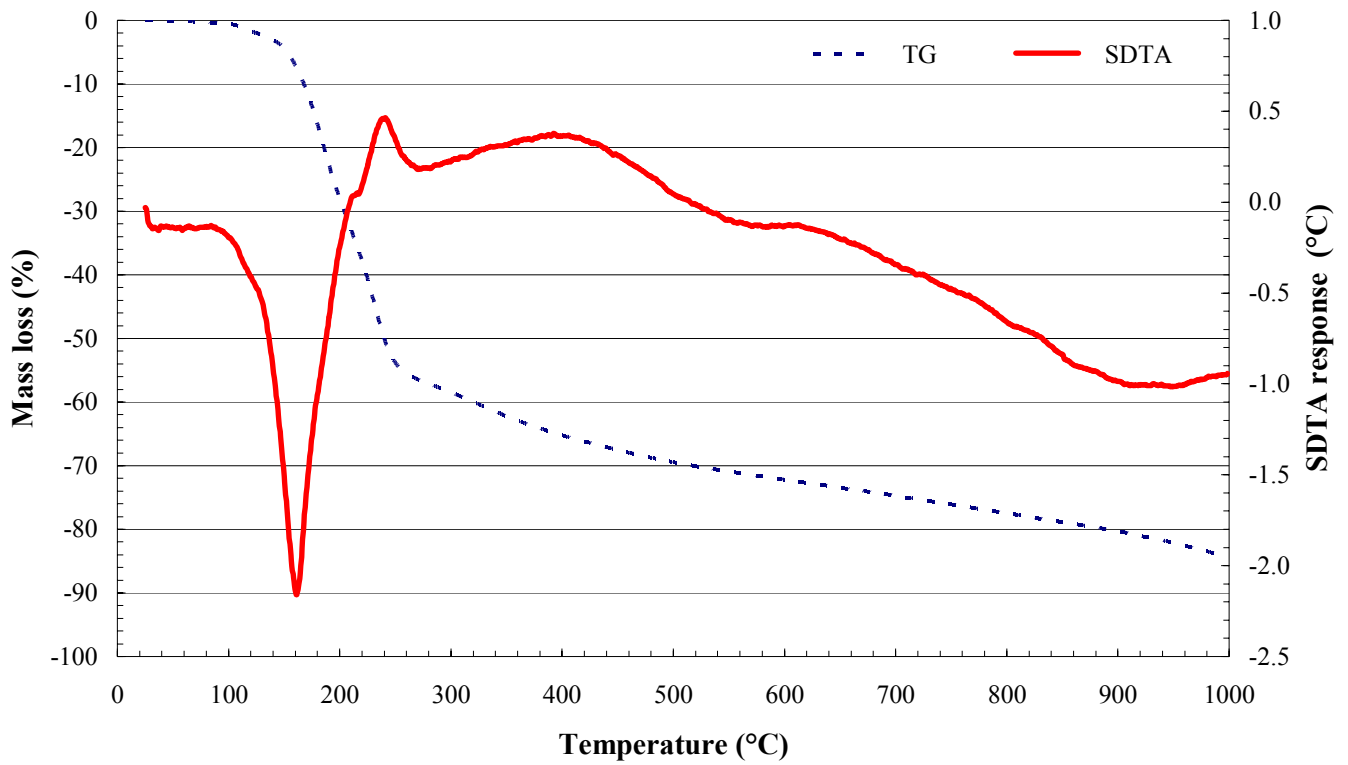
SDTA/TGA analysis of ammonium gluconate hydrate in nitrogen

7.15.4. Thermal decomposition analysis of the leached silica (ex Foskor)
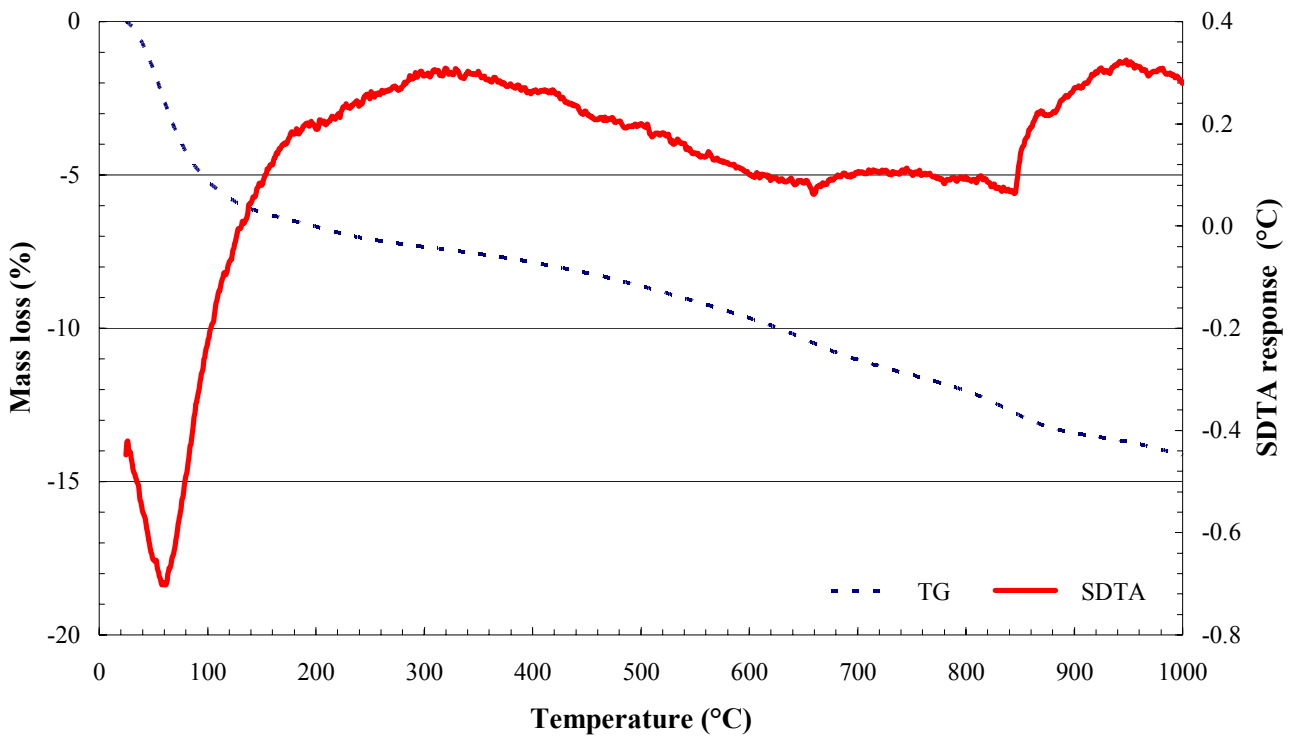
SDTA/TGA analysis of the leached silica in air

7.15.5. Thermal decomposition analysis of the expandable graphite (ex Fedmis)
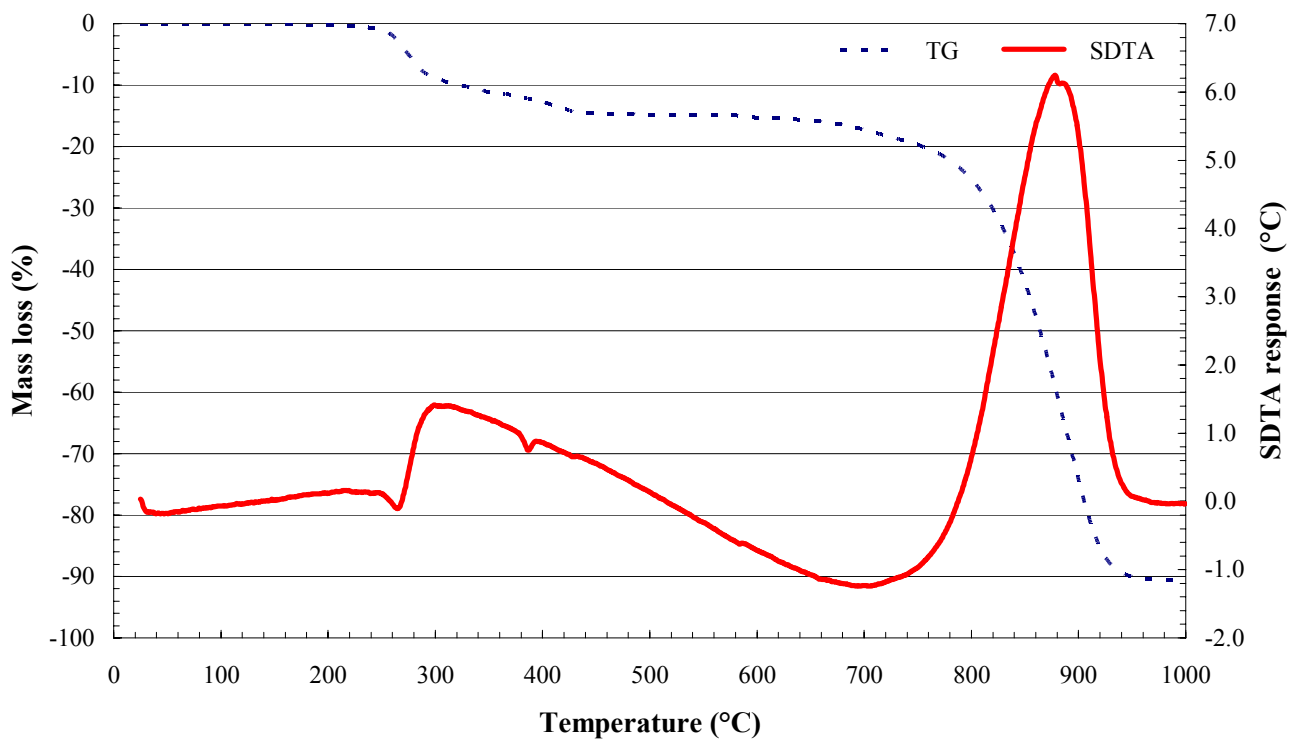
SDTA/TGA analysis of the expandable graphite in air

7.16. Appendix P

7.16.1. XRD pattern of calcium gluconate monohydrate
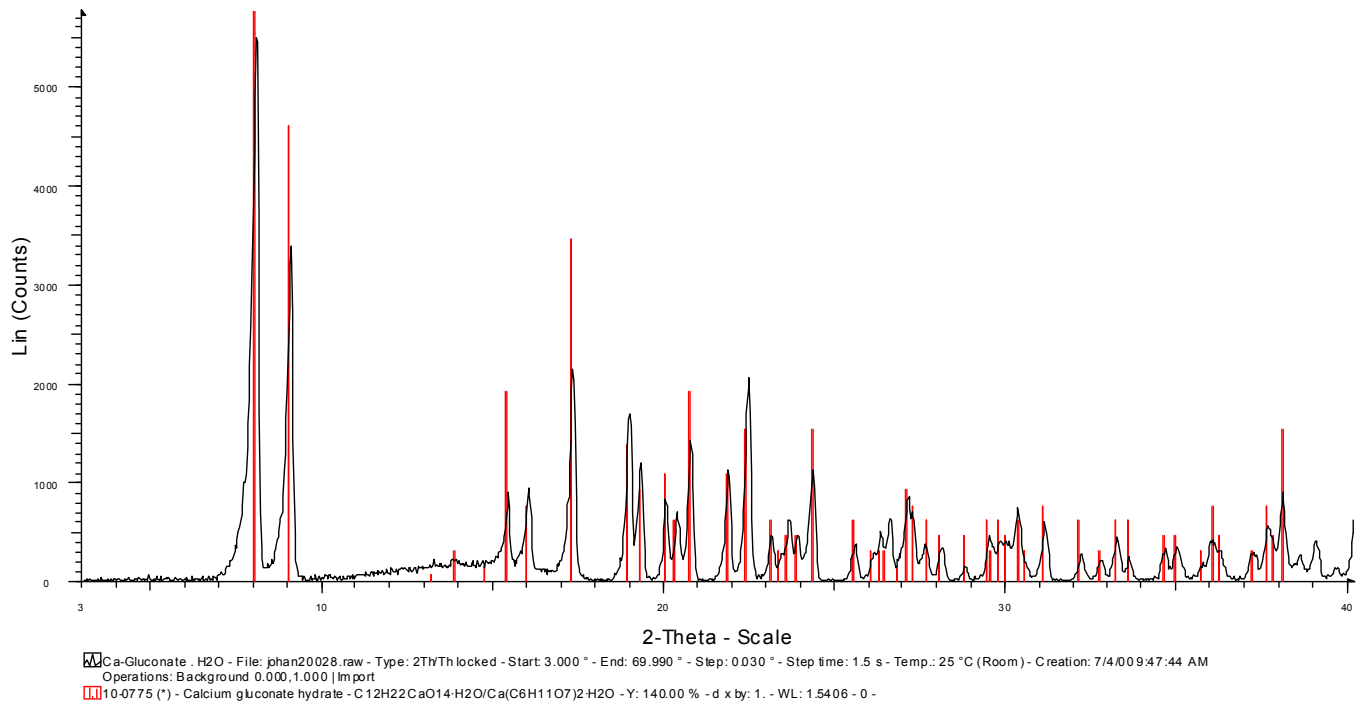
XRD spectrum of calcium gluconate monohydrate

7.16.2. XRD pattern of ammonium gluconate hydrate
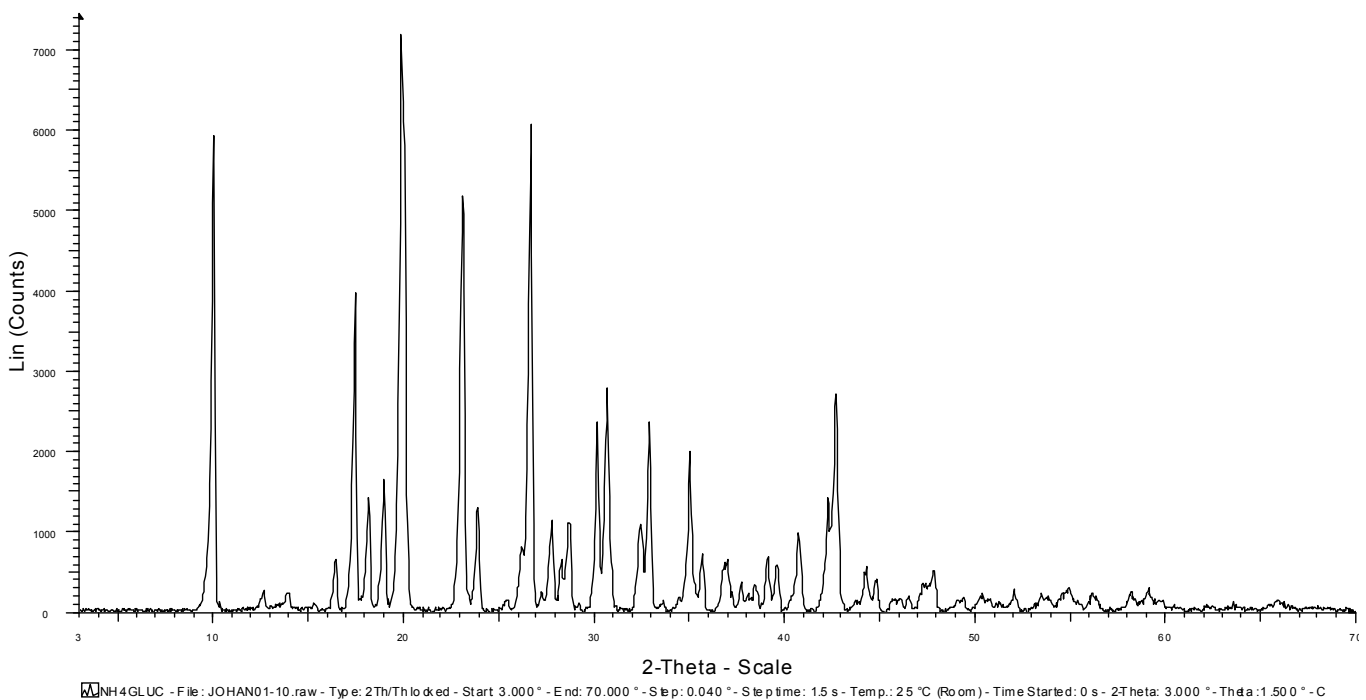
XRD spectrum of ammonium gluconate

7.16.3. XRD pattern of Leached silica from Foskor Pty. Ltd.

SiO2 - File: johan2009.raw - Type: 2Th/Th locked - Start: 3.000 ° - End: 69.990 ° - Step: 0.030 ° - Step time: 1.5 s - Temp.: 25 °C (Room) - Creation: 5/17/00 11:44:07 AM
Operations: Background 0.000,1.000 | Import
33-1161 (*) - Quartz, syn - SiO2 - Y: 89.58 % - d x by: 1. - WL: 1.5406 - 0 -
26-0911 (I) - Illite-2M1 - (K,H3O)Al2Si3AlO10(OH)2 - Y: 50.00 % - d x by: 1. - WL: 1.5406 - 0 -
10-0357 (N) - Sanidine, potassian, disordered, syn - (Na,K)(Si3Al)O8 - Y: 18.75 % - d x by: 1. - WL: 1.5406 - 0 -
41-1370 (*) - Diopside - Ca(Mg,Al)(Si,Al)2O6 - Y: 25.00 % - d x by: 1. - WL: 1.5406 - 0 -
21-0683 (N) - Potassium Sulfate - K2S2O7 - Y: 27.08 % - d x by: 1. - WL: 1.5406 - 0 -

XRD spectrum of Leached silica from Foskor Pty. Ltd.

7.16.4. XRD pattern of calcium gluconate monohydrate pyrolised in air

@ 100 - File: JOHAN01-32.raw - Type: 2Th/Th locked - Start: 3.000 ° - End: 70.040 ° - Step: 0.040 ° - Step time: 1.5 s - Temp.: 25 ℃ (Room) - Time Started: 0 s - 2-Theta: 3.000 ° - Theta: 1.500 ° - Chi: 0.
10-0775 (*) - Calcium gluconate hydrate - C12H22CaO14·H2O/Ca(C6H11O7)2·H2O - Y: 100.00 % - d x by: 1. - WL: 1.5406 - Orthorhombic -
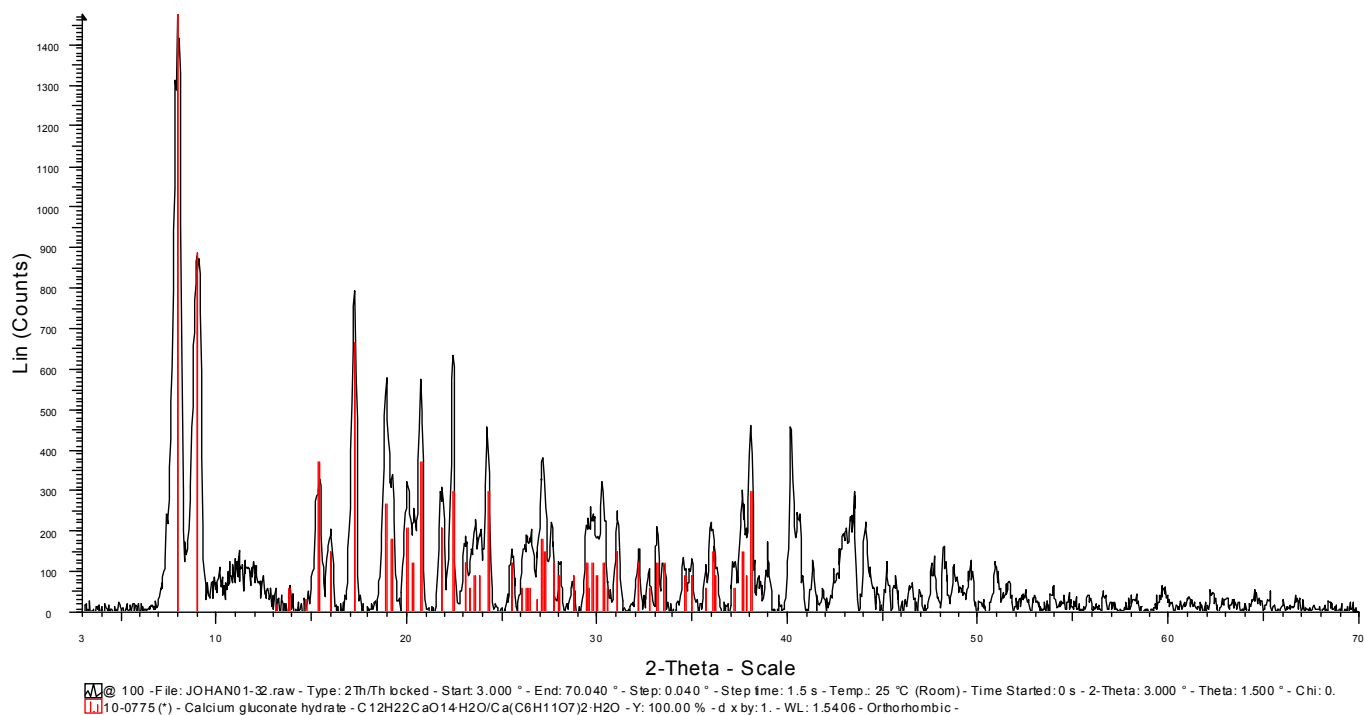
XRD spectrum of calcium gluconate pyrolysed at 100°C for 5 min in air.

Ca GLUC 150C - File: JOHAN01-15.raw - Type: 2Th/Th locked - Start: 3.000 ° - End: 70.000 ° - Step: 0.040 ° - Step time: 1.5 s - Temp.: 25 ℃ (Room) - Time Started: 0 s - 2-Theta: 3.000 ° - Theta: 1.500
10-0774 (Q) - Calcium gluconate - C12H22CaO14/Ca(C6H11O7)2 - Y: 20.14 % - d x by: 1. - WL: 1.5406 - 0 -
10-0775 (*) - Calcium gluconate hydrate - C12H22CaO14·H2O/Ca(C6H11O7)2·H2O - Y: 136.10 % - d x by: 1. - WL: 1.5406 - 0 -
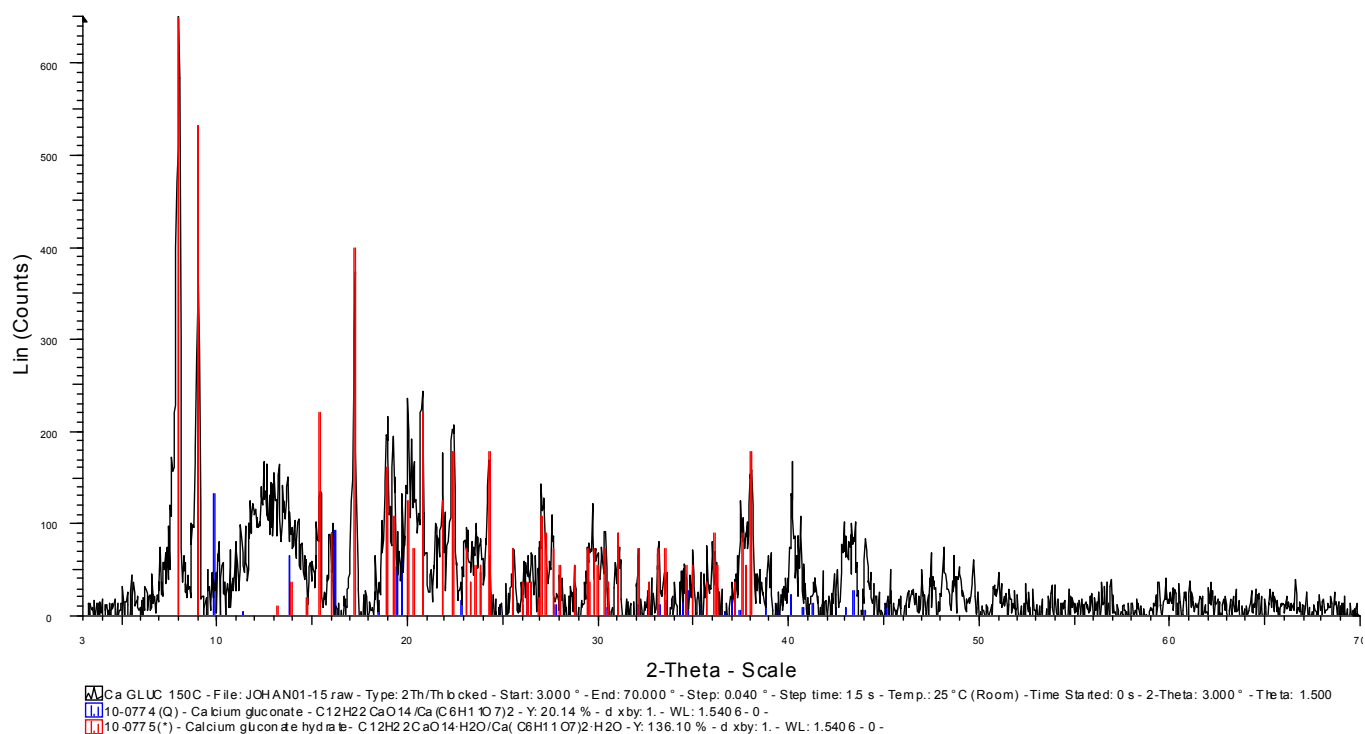
XRD spectrum of calcium gluconate pyrolysed at 150°C for 5 min in air
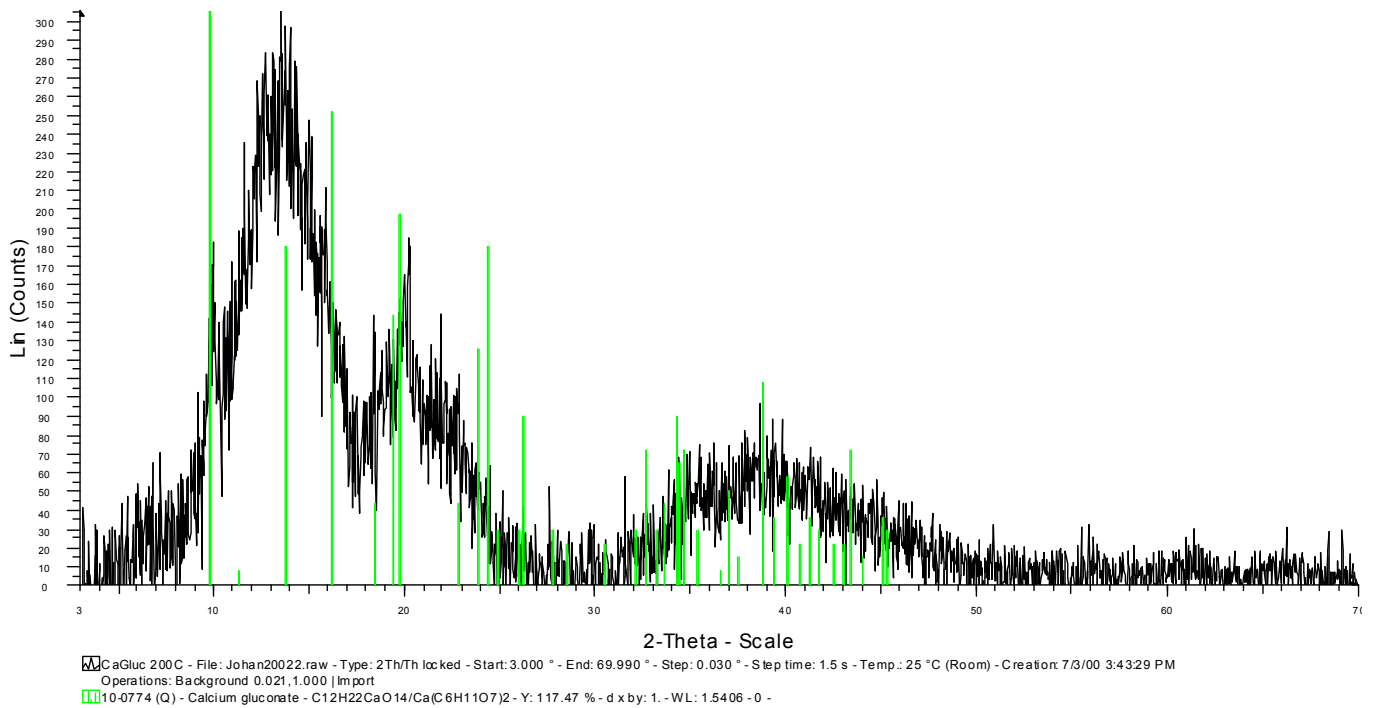
CaGluc 200C - File: Johan20022.raw - Type: 2Th/Th locked - Start: 3.000 ° - End: 69.990 ° - Step: 0.030 ° - Step time: 1.5 s - Temp.: 25 °C (Room) - Creation: 7/3/00 3:43:29 PM
Operations: Background 0.021,1.000 | Import
10-0774 (Q) - Calcium gluconate - C12H22CaO14/Ca(C6H11O7)2 - Y: 117.47 % - d x by: 1. - WL: 1.5406 - 0 -

XRD spectrum of calcium gluconate pyrolysed at 200°C for 5 min in air

CAGLUC@250C - File: JOHAN01-2.raw - Type: 2Th/Th locked - Start: 3.000 ° - End: 70.000 ° - Step: 0.040 ° - Step time: 1.5 s - Temp.: 25 °C (Room) - Time Started: 0 s - 2-Theta: 3.000 ° - Theta: 1.500
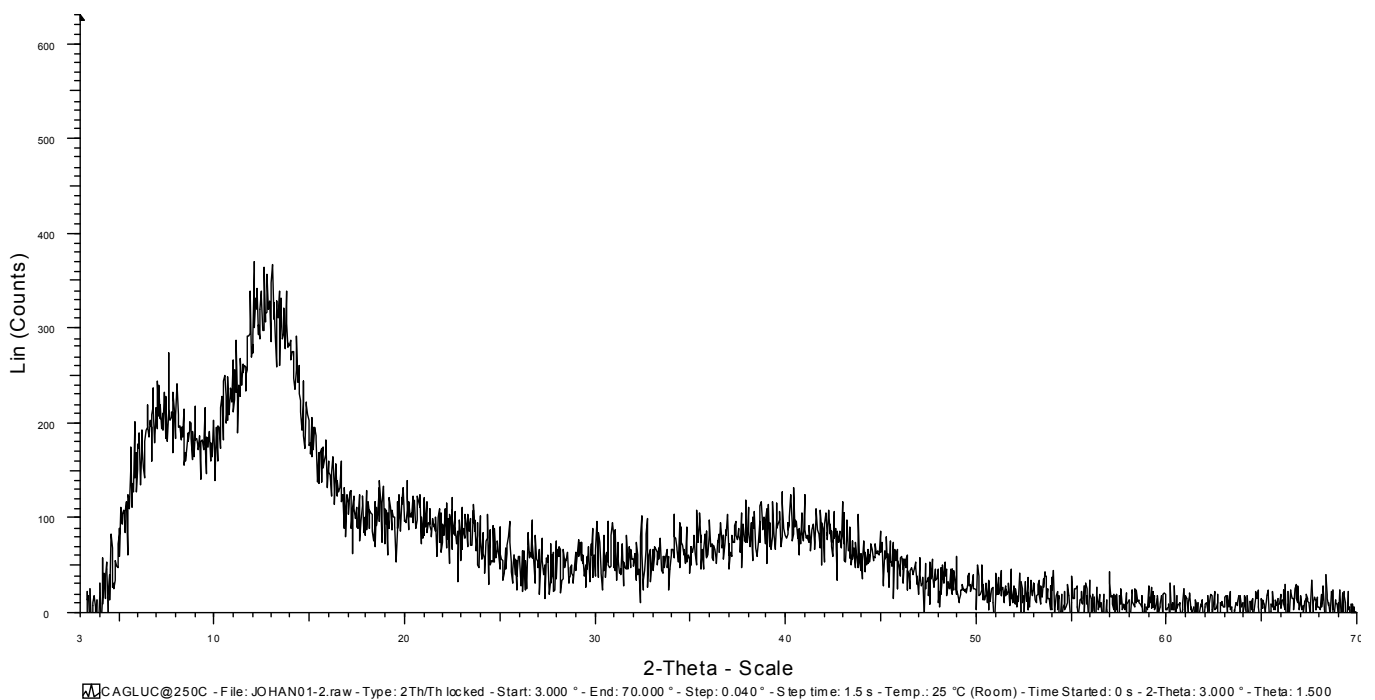
XRD spectrum of calcium gluconate pyrolysed at 250°C for 5 min in air
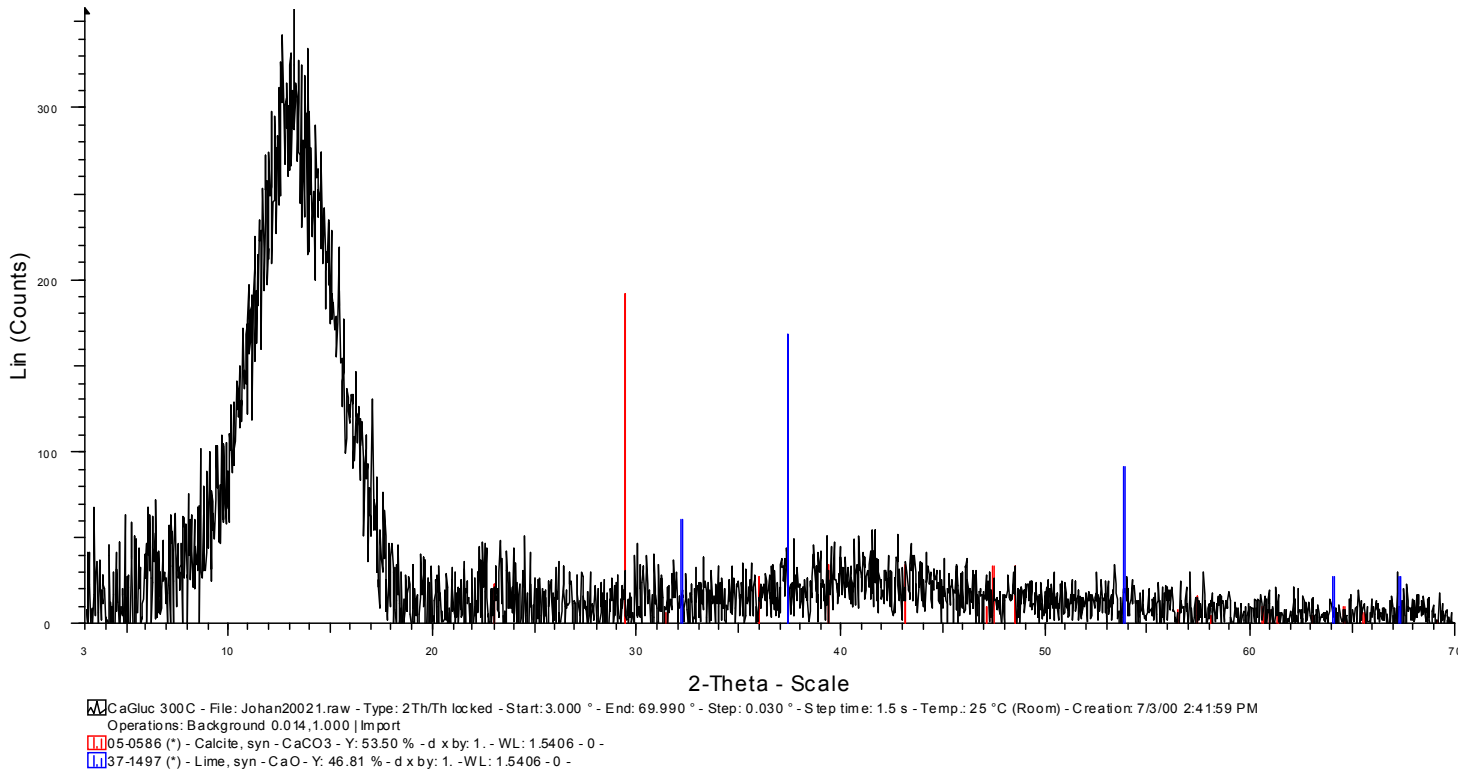
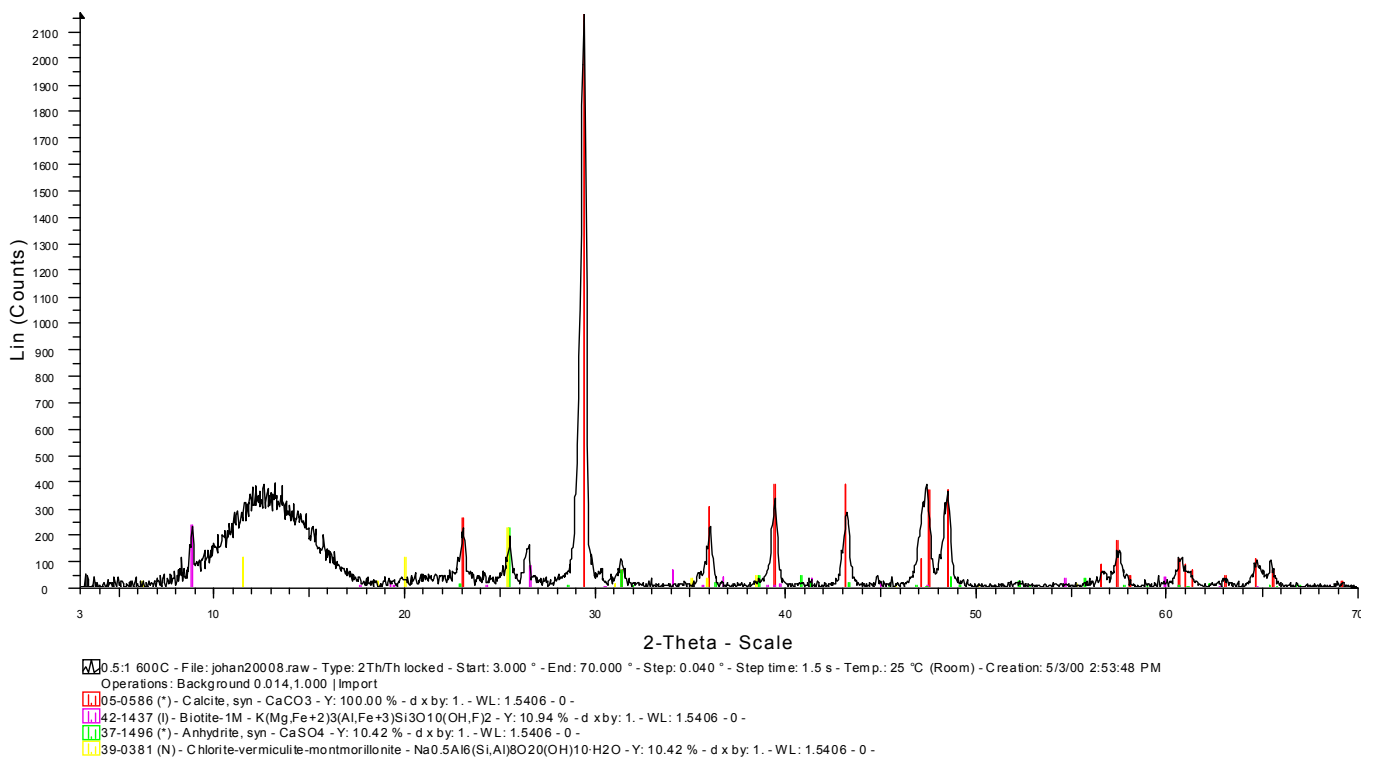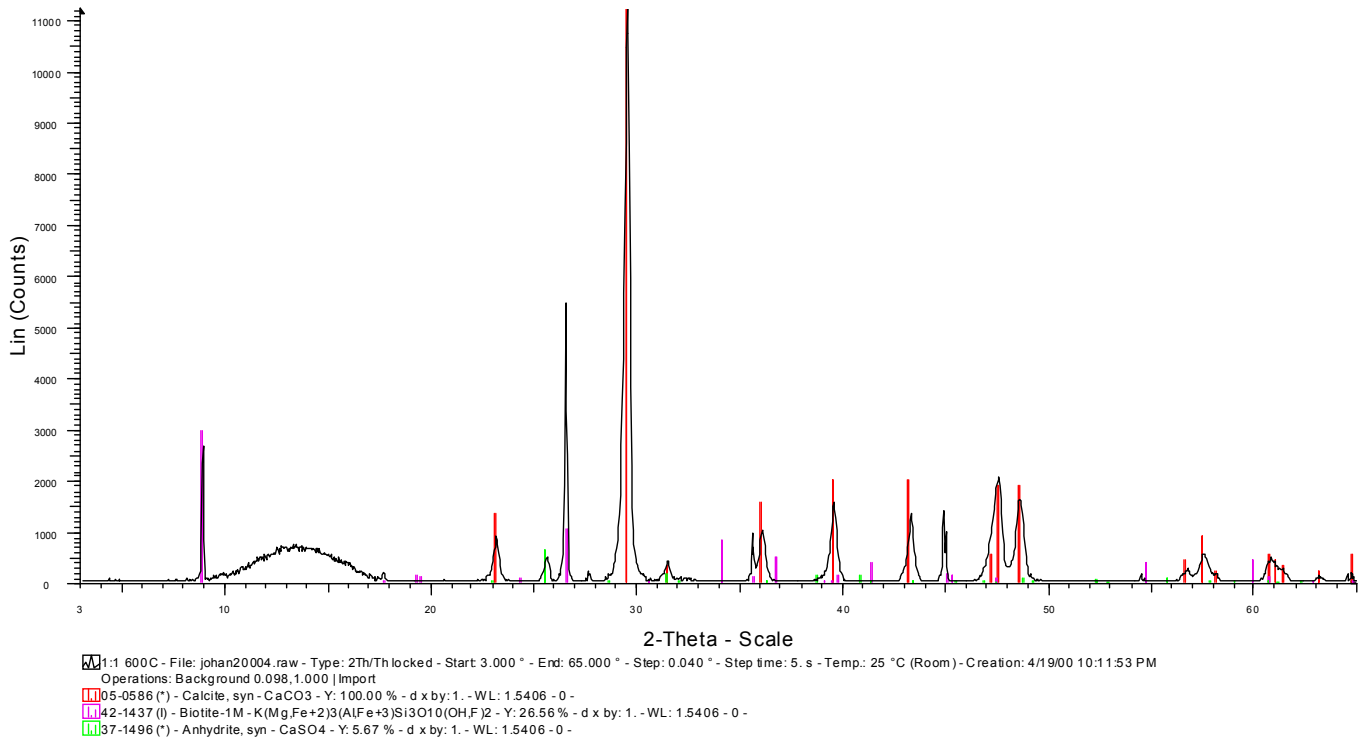XRD spectrum of calcium gluconate pyrolysed at 300°C for 5 min in air
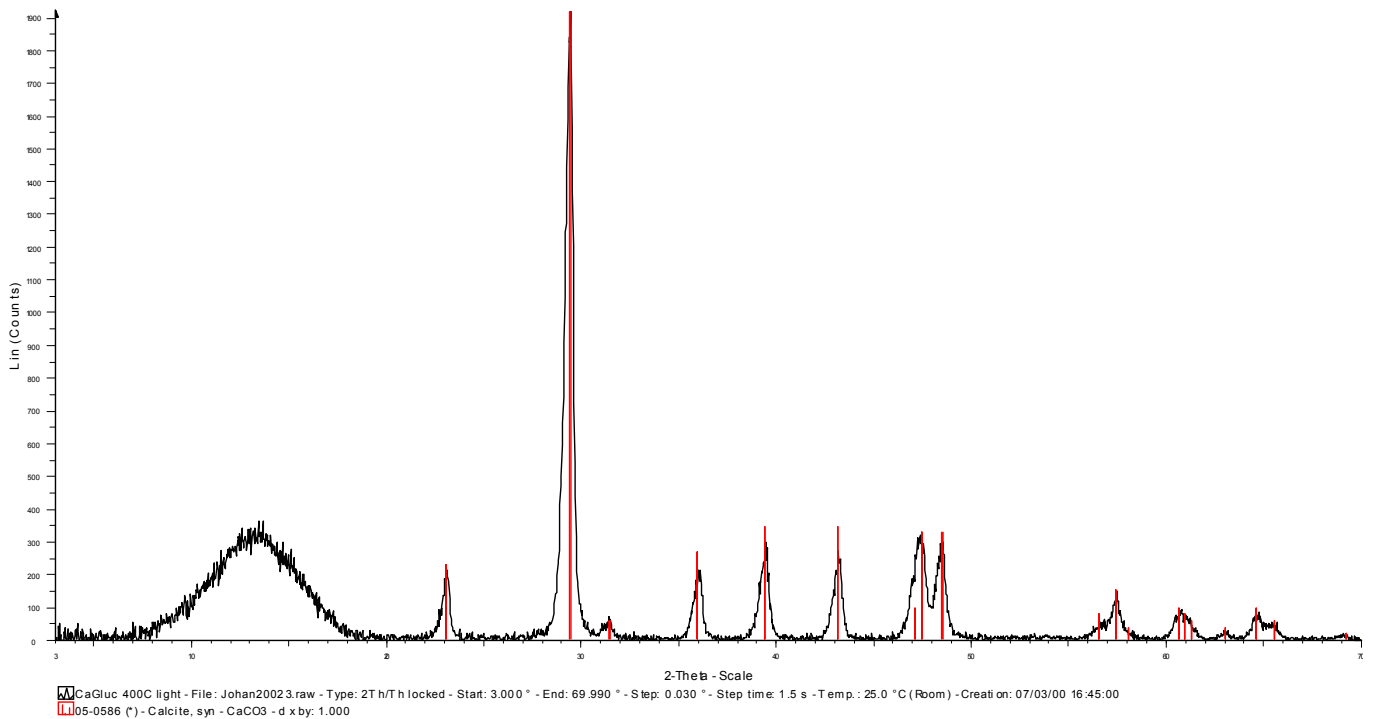
XRD spectrum of calcium gluconate pyrolysed at 400°C for 5 min in air – light material (top of polytop™)
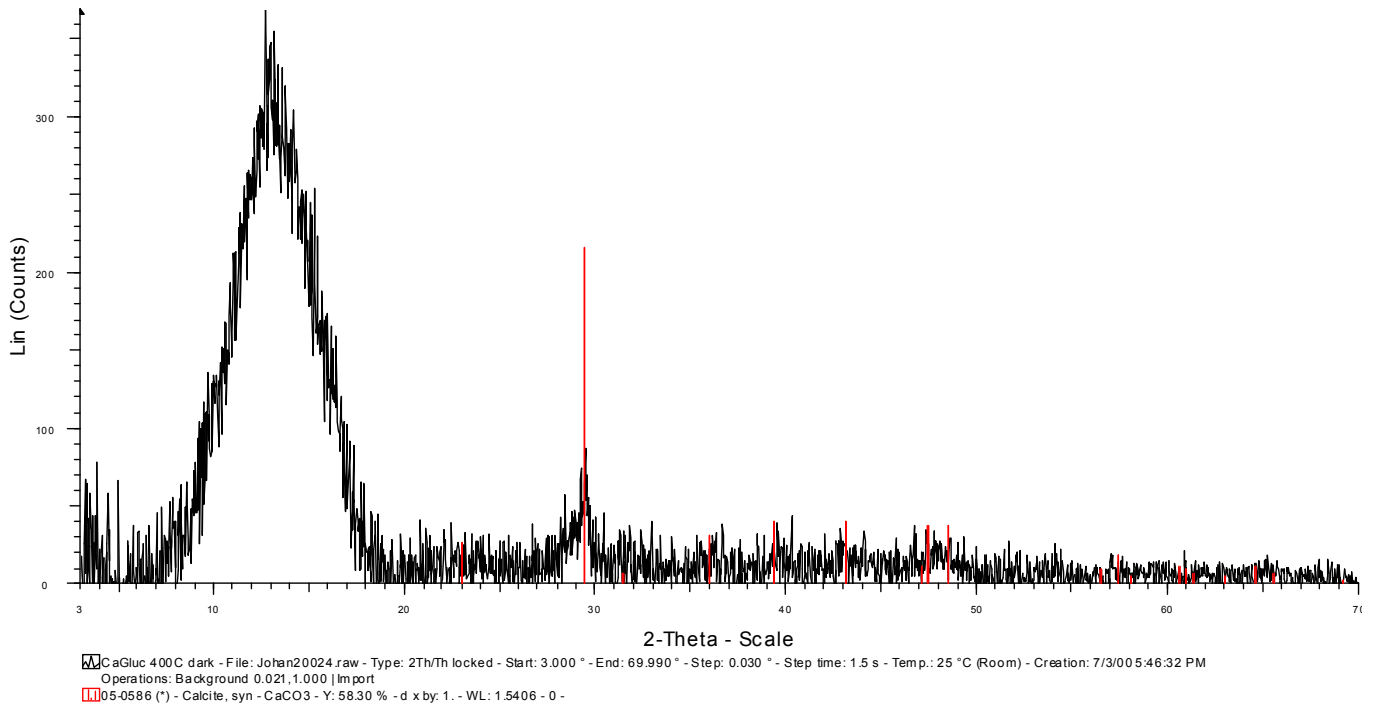
XRD spectrum of calcium gluconate pyrolysed at 400°C for 5 min in air – dark material (bottom of polytop™)

XRD spectrum of calcium gluconate pyrolysed at 500°C for 5 min in air – light material (top of polytop™)

CaGluc 400C dark - File: Johan20024.raw - Type: 2Th/Th locked - Start: 3.000 ° - End: 69.990 ° - Step: 0.030 ° - Step time: 1.5 s - Temp.: 25 °C (Room) - Creation: 7/3/00 5:46:32 PM
Operations: Background 0.021,1.000 | Import
05-0586 (*) - Calcite, syn - CaCO3 - Y: 58.30 % - d x by: 1. - WL: 1.5406 - 0 -

XRD spectrum of calcium gluconate pyrolysed at 500°C for 5 min in air – dark material (bottom of polytop™)

CaGluc 600C light - File: Johan20020.raw - Type: 2Th/Th locked - Start: 3.000 ° - End: 69.990 ° - Step: 0.030 ° - Step time: 1.5 s - Temp.: 25.0 °C (Room) - Creation: 07/03/00 13:40:18
05-0586 (*) - Calcite, syn - CaCO3 - d x by: 1.000
10-0775 (*) - Calcium gluconate hydrate - C12H22CaO14·H2O/Ca(C6H11O7)2·H2O - d x by: 1.000

XRD spectrum of calcium gluconate pyrolysed at 600°C for 5 min in air – light material (top of polytop™)

CaGluc 600C dark - File: Johan20027.raw - Type: 2Th/Th locked - Start: 3.000 ° - End: 69.990 ° - Step: 0.030 ° - Step time: 1.5 s - Temp.: 25.0 °C (Room) - Creation: 07/03/00 20:51:08
05-0586 (*) - Calcite, syn - CaCO3 - d x by: 1.000

XRD spectrum of calcium gluconate pyrolysed at 600°C for 5 min in air – dark material (bottom of polytop™)

CA GLUE@700 - File: JOHAN01-36.raw - Type: 2Th/Th locked - Start: 3.095 ° - End: 70.118 ° - Step: 0.040 ° - Step time: 1.5 s - Temp.: 25 °C (Room) - Time Started: 0 s - 2-Theta: 3.095 ° - Theta: 1.500
05-0586 (*) - Calcite, syn - CaCO3 - Y: 98.55 % - d x by: 1. - WL: 1.5406 - Rhombohedral - I/Ic PDF 2. -

XRD spectrum of calcium gluconate pyrolysed at 700°C for 5 min in air

CA GLUE @ 750 - File: JOHAN01-31.raw - Type: 2Th/Th locked - Start: 3.000 ° - End: 70.040 ° - Step: 0.040 ° - Step time: 1.5 s - Temp.: 25 °C (Room) - Time Started: 0 s - 2-Theta: 3.000 ° - Theta: 1.50
04-0733 (I) - Portlandite, syn - Ca(OH)2 - Y: 90.00 % - d x by: 1. - WL: 1.5406 - Hexagonal - I/Ic PDF 1.4 -
05-0586 (*) - Calcite, syn - CaCO3 - Y: 100.00 % - d x by: 1. - WL: 1.5406 - Rhombohedral - I/Ic PDF 2. -
37-1497 (*) - Lime, syn - CaO - Y: 49.32 % - d x by: 1. - WL: 1.5406 - Cubic -

XRD spectrum of calcium gluconate pyrolysed at 750°C for 5 min in air

CA GLUE @ 800 - File: JOHAN01-30.raw - Type: 2Th/Th locked - Start: 3.000 ° - End: 70.040 ° - Step: 0.040 ° - Step time: 1.5 s - Temp.: 25 °C (Room) - Time Started: 0 s - 2-Theta: 3.000 ° - Theta: 1.500
37-1497 (*) - Lime, syn - CaO - Y: 97.92 % - d x by: 1. - WL: 1.5406 - Cubic -
44-1481 (*) - Portlandite, syn - Ca(OH)2 - Y: 37.50 % - d x by: 1. - WL: 1.5406 - Hexagonal - I/Ic PDF 2.9 -

XRD spectrum of calcium gluconate pyrolysed at 800°C for 5 min in air

NH4 GLUE @ 300 IN N2 - File: JOHAN01-39.raw - Type: 2Th/Th locked - Start: 3.000 ° - End: 70.040 ° - Step: 0.040 ° - Step time: 1.5 s - Temp.: 25 °C (Room) - Time Started: 0 s - 2-Theta: 3.000 ° - Thet
04-0733 (I) - Portlandite, syn - Ca(OH)2 - Y: 58.85 % - d x by: 1. - WL: 1.5406 - Hexagonal - I/Ic PDF 1.4 -
37-1497 (*) - Lime, syn - CaO - Y: 98.90 % - d x by: 1. - WL: 1.5406 - Cubic -

XRD spectrum of calcium gluconate pyrolysed at 1000°C for 5 min in air

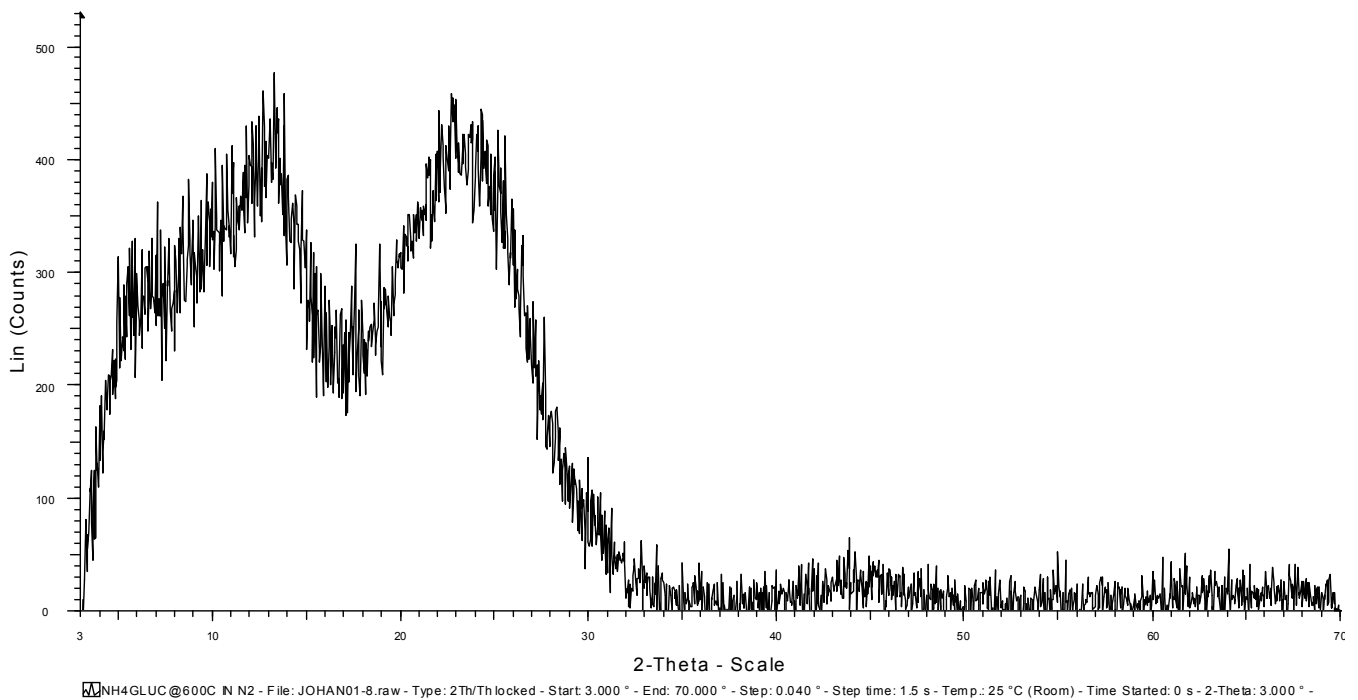### 7.16.5. XRD pattern of calcium gluconate pyrolised in nitrogen

Ca-Gluc 200C N2 - File: johan20029.raw - Type: 2Th/Th locked - Start: 3.000 ° - End: 69.990 ° - Step: 0.030 ° - Step time: 1.5 s - Temp.: 25.0 °C (Room) - Creation: 07/06/00 17:35:51
10-0774 (Q) - Calcium gluconate - C12H22CaO14/Ca(C6H11O7)2 - d x by: 1.000

XRD spectrum of calcium gluconate pyrolysed at 200°C for 5 min in nitrogen

Ca-Gluc 300C N2 - File: johan20031.raw - Type: 2Th/Th locked - Start: 3.000 ° - End: 69.990 ° - Step: 0.030 ° - Step time: 1.5 s - Temp.: 25.0 °C (Room) - Creation: 07/06/00 19:38:56

XRD spectrum of calcium gluconate pyrolysed at 300°C for 5 min in nitrogen

Ca-Gluc 400C N2 - File: johan20032.raw - Type: 2Th/Th locked - Start: 3.000 ° - End: 69.990 ° - Step: 0.030 ° - Step time: 1.5 s - Temp.: 25.0 °C (Room) - Creation: 07/06/00 20:40:28

XRD spectrum of calcium gluconate pyrolysed at 400°C for 5 min in nitrogen

CA GLUE -N2 - 500 - File: JOHAN01-33.raw - Type: 2Th/Th locked - Start: 3.000 ° - End: 70.040 ° - Step: 0.040 ° - Step time: 1.5 s - Temp.: 25 °C (Room) - Time Started: 0 s - 2-Theta: 3.000 ° - Theta: 1.5
Operations: Background 0.000,1.000 | Import

XRD spectrum of calcium gluconate pyrolysed at 500°C for 5 min in nitrogen

CAGLUC@600C IN N2 - File: JOHAN01-4.raw - Type: 2Th/Th locked - Start: 3.000 ° - End: 70.000 ° - Step: 0.040 ° - Step time: 1.5 s - Temp.: 25 ℃ (Room) - Time Started: 0 s - 2-Theta: 3.000 ° - Theta:

XRD spectrum of calcium gluconate pyrolysed at 600°C for 5 min in nitrogen

CAGLUC@700C IN N2 - File: JOHAN01-3.raw - Type: 2Th/Th locked - Start: 3.000 ° - End: 70.000 ° - Step: 0.040 ° - Step time: 1.5 s - Temp.: 25 ℃ (Room) - Time Started: 0 s - 2-Theta: 3.000 ° - Theta:
05-0586 (*) - Calcite, syn - CaCO3 - Y: 119.21 % - d x by: 1. - WL: 1.5406 - 0 -

XRD spectrum of calcium gluconate pyrolysed at 700°C for 5 min in nitrogen

XRD spectrum of calcium gluconate pyrolysed at 850°C for 5 min in nitrogen

XRD spectrum of calcium gluconate pyrolysed at 1000°C for 5 min in nitrogen

7.16.6. XRD pattern of calcium gluconate monohydrate – leached silica mixtures pyrolised in air
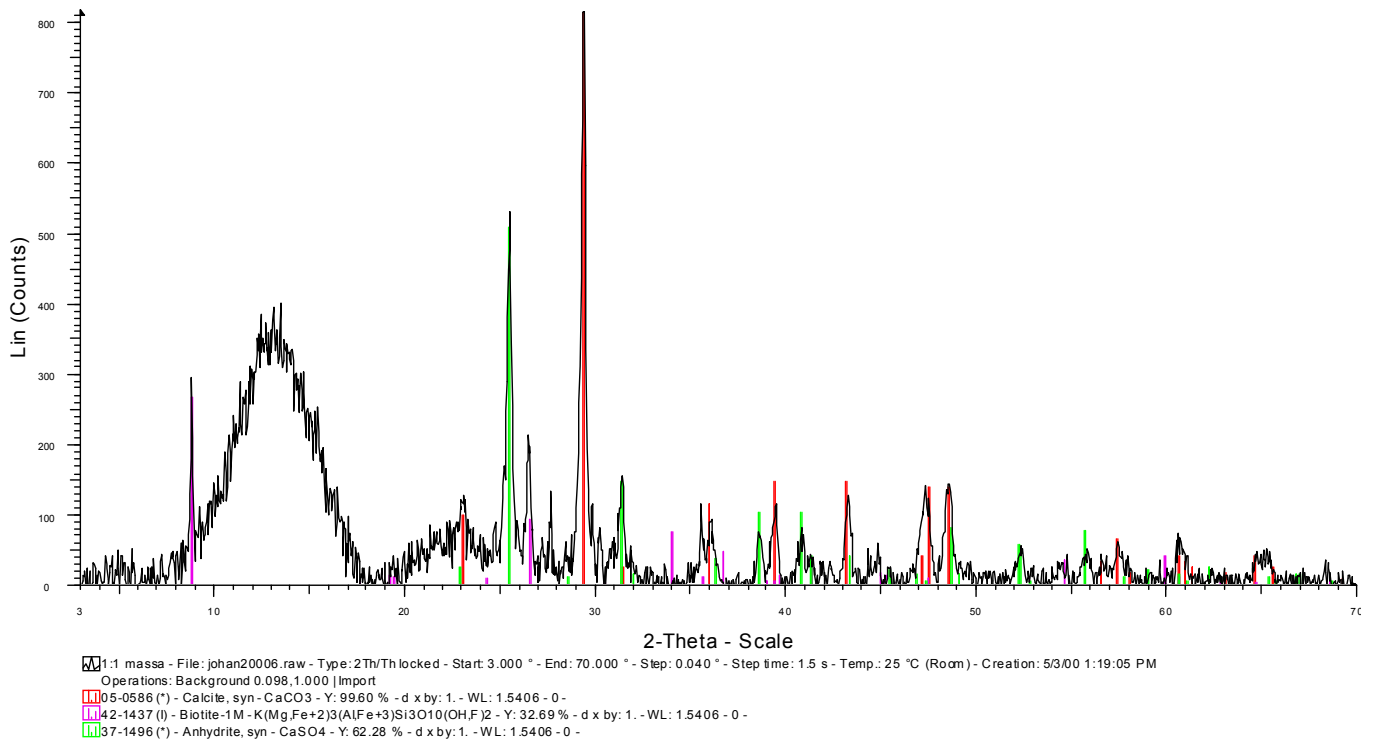
XRD spectrum of 1:1 mass ratio calcium gluconate and leached silica pyrolysed at 600°C for 5 min in air

XRD spectrum of 0.5:1 mole ratio calcium gluconate and leached silica pyrolysed at 600°C for 5 min in air

1:1 600C - File: johan20004.raw - Type: 2Th/Th locked - Start: 3.000 ° - End: 65.000 ° - Step: 0.040 ° - Step time: 5. s - Temp.: 25 °C (Room) - Creation: 4/19/00 10:11:53 PM
Operations: Background 0.098,1.000 | Import
05-0586 (*) - Calcite, syn - CaCO3 - Y: 100.00 % - d x by: 1. - WL: 1.5406 - 0 -
42-1437 (I) - Biotite-1M - K(Mg,Fe+2)3(Al,Fe+3)Si3O10(OH,F)2 - Y: 26.56 % - d x by: 1. - WL: 1.5406 - 0 -
37-1496 (*) - Anhydrite, syn - CaSO4 - Y: 5.67 % - d x by: 1. - WL: 1.5406 - 0 -

XRD spectrum of 1:1 mole ratio calcium gluconate and leached silica pyrolysed at 600°C for 5 min in air

2:1 600C - File: johan20003.raw - Type: 2Th/Th locked - Start: 3.000 ° - End: 65.000 ° - Step: 0.040 ° - Step time: 5. s - Temp.: 25 °C (Room) - Creation: 4/19/00 7:57:26 PM
Operations: Background 0.098,1.000 | Import
05-0586 (*) - Calcite, syn - CaCO3 - Y: 103.14 % - d x by: 1. - WL: 1.5406 - 0 -
42-1437 (I) - Biotite-1M - K(Mg,Fe+2)3(Al,Fe+3)Si3O10(OH,F)2 - Y: 6.44 % - d x by: 1. - WL: 1.5406 - 0 -
37-1496 (*) - Anhydrite, syn - CaSO4 - Y: 3.07 % - d x by: 1. - WL: 1.5406 - 0 -
39-0381 (N) - Chlorite-vermiculite-montmorillonite - Na0.5Al6(Si,Al)8O20(OH)10·H2O - Y: 3.07 % - d x by: 1. - WL: 1.5406 - 0 -
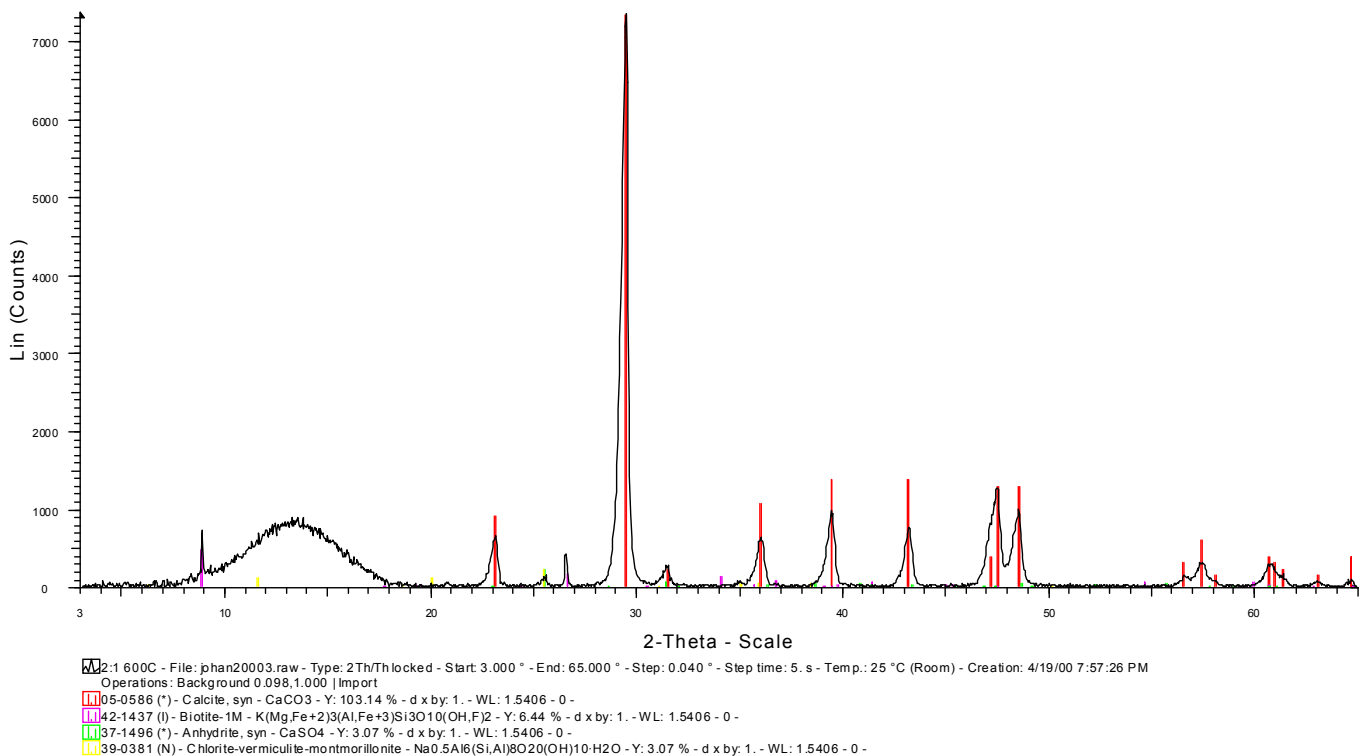
XRD spectrum of 2:1 mole ratio calcium gluconate and leached silica pyrolysed at 600°C for 5 min in air

3:1 600C - File: johan20007.raw - Type: 2Th/Th locked - Start: 3.000 ° - End: 70.000 ° - Step: 0.040 ° - Step time: 1.5 s - Temp.: 25 °C (Room) - Creation: 5/3/00 2:06:27 PM
Operations: Background 0.091,1.000 | Import
05-0586 (*) - Calcite, syn - CaCO3 - Y: 102.99 % - d x by: 1. - WL: 1.5406 - 0 -
42-1437 (I) - Biotite-1M - K(Mg,Fe+2)3(Al,Fe+3)Si3O10(OH,F)2 - Y: 1.15 % - d x by: 1. - WL: 1.5406 - 0 -
37-1496 (*) - Anhydrite, syn - CaSO4 - Y: 0.82 % - d x by: 1. - WL: 1.5406 - 0 -
39-0381 (N) - Chlorite-vermiculite-montmorillonite - Na0.5Al6(Si,Al)8O20(OH)10·H2O - Y: 1.10 % - d x by: 1. - WL: 1.5406 - 0 -
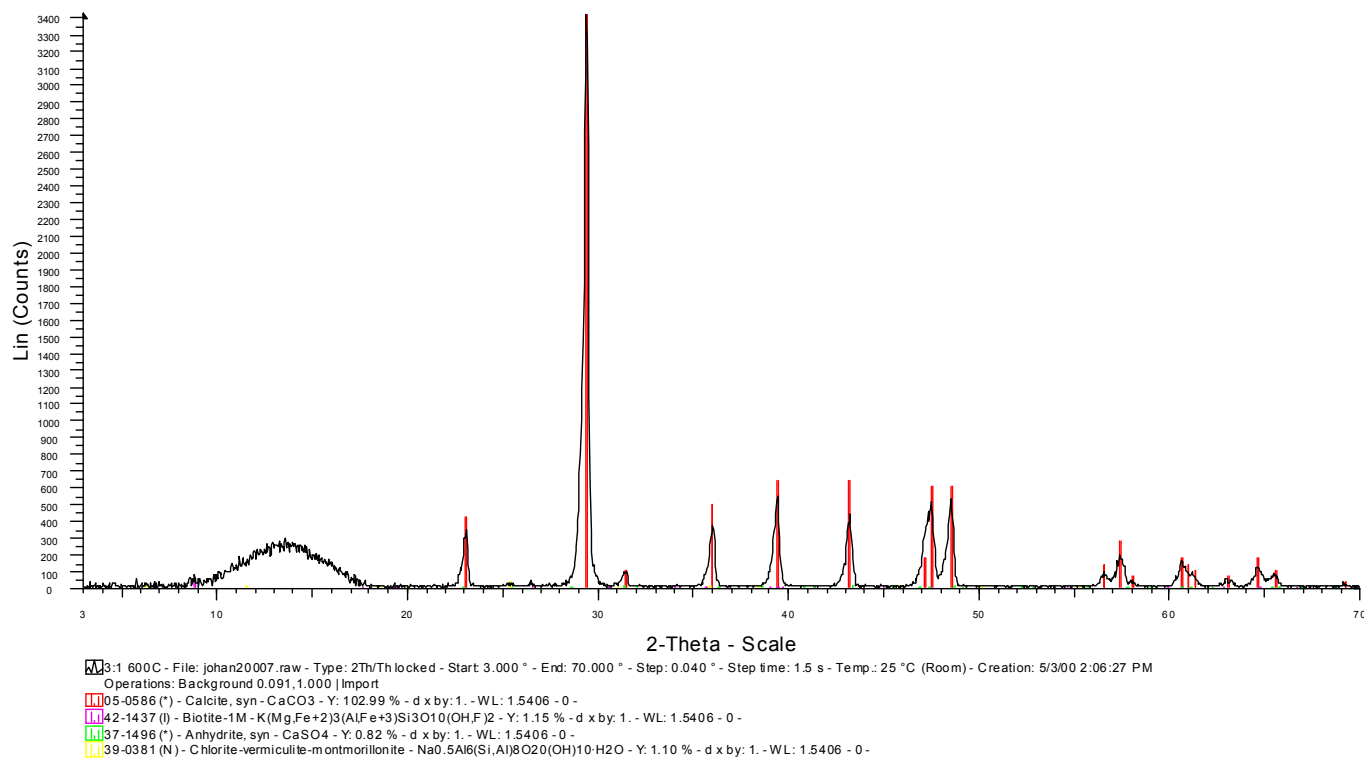
XRD spectrum of 3:1 mole ratio calcium gluconate and leached silica pyrolysed at 600°C for 5 min in air

4:1 600C - File: johan20001.raw - Type: 2Th/Th locked - Start: 3.000 ° - End: 65.000 ° - Step: 0.040 ° - Step time: 5. s - Temp.: 25 °C (Room) - Creation: 4/19/00 3:28:25 PM
Operations: Background 0.000,1.000 | Import
05-0586 (*) - Calcite, syn - CaCO3 - Y: 123.56 % - d x by: 1. - WL: 1.5406 - 0 -
42-1437 (I) - Biotite-1M - K(Mg,Fe+2)3(Al,Fe+3)Si3O10(OH,F)2 - Y: 4.16 % - d x by: 1. - WL: 1.5406 - 0 -
37-1496 (*) - Anhydrite, syn - CaSO4 - Y: 1.98 % - d x by: 1. - WL: 1.5406 - 0 -
39-0381 (N) - Chlorite-vermiculite-montmorillonite - Na0.5Al6(Si,Al)8O20(OH)10·H2O - Y: 1.98 % - d x by: 1. - WL: 1.5406 - 0 -

XRD spectrum of 4:1 mole ratio calcium gluconate and leached silica pyrolysed at 600°C for 5 min in air

4:1 400C - File: johan20002.raw - Type: 2Th/Th locked - Start: 3.000 ° - End: 65.000 ° - Step: 0.040 ° - Step time: 5. s - Temp.: 25 °C (Room) - Creation: 4/19/00 5:42:54 PM
Operations: Background 0.000,1.000 | Import
05-0586 (*) - Calcite, syn - CaCO3 - Y: 139.74 % - d x by: 1. - WL: 1.5406 - 0 -

XRD spectrum of 4:1 mole ratio calcium gluconate and leached silica pyrolysed at 400°C for 5 min in air

4:1 1000C - File: johan20005.raw - Type: 2Th/Th locked - Start: 3.000 ° - End: 70.000 ° - Step: 0.0   DF - 4:1 1000C - johan20005.dif - Y: 5.64 % - d x by: 1. - WL: 1.5406 - 0 -
Operations: Background 0.098,1.000 | Import
05-0586 (*) - Calcite, syn - CaCO3 - Y: 4.57 % - d x by: 1. - WL: 1.5406 - 0 -
42-1437 (I) - Biotite-1M - K(Mg,Fe+2)3(Al,Fe+3)Si3O10(OH,F)2 - Y: 3.00 % - d x by: 1. - WL: 1.54
37-1496 (*) - Anhydrite, syn - CaSO4 - Y: 110.50 % - d x by: 1. - WL: 1.5406 - 0 -
37-1497 (*) - Lime, syn - CaO - Y: 60.42 % - d x by: 1. - WL: 1.5406 - 0 -
04-0733 (I) - Portlandite, syn - Ca(OH)2 - Y: 20.83 % - d x by: 1. - WL: 1.5406 - 0 -
39-1425 (*) - Cristobalite, syn - SiO2 - Y: 4.17 % - d x by: 1. - WL: 1.5406 - 0 -

XRD spectrum of 4:1 mole ratio calcium gluconate and leached silica pyrolysed at 1000°C for 5 min in air

7.16.7. XRD pattern of ammonium gluconate hydrate pyrolised in air
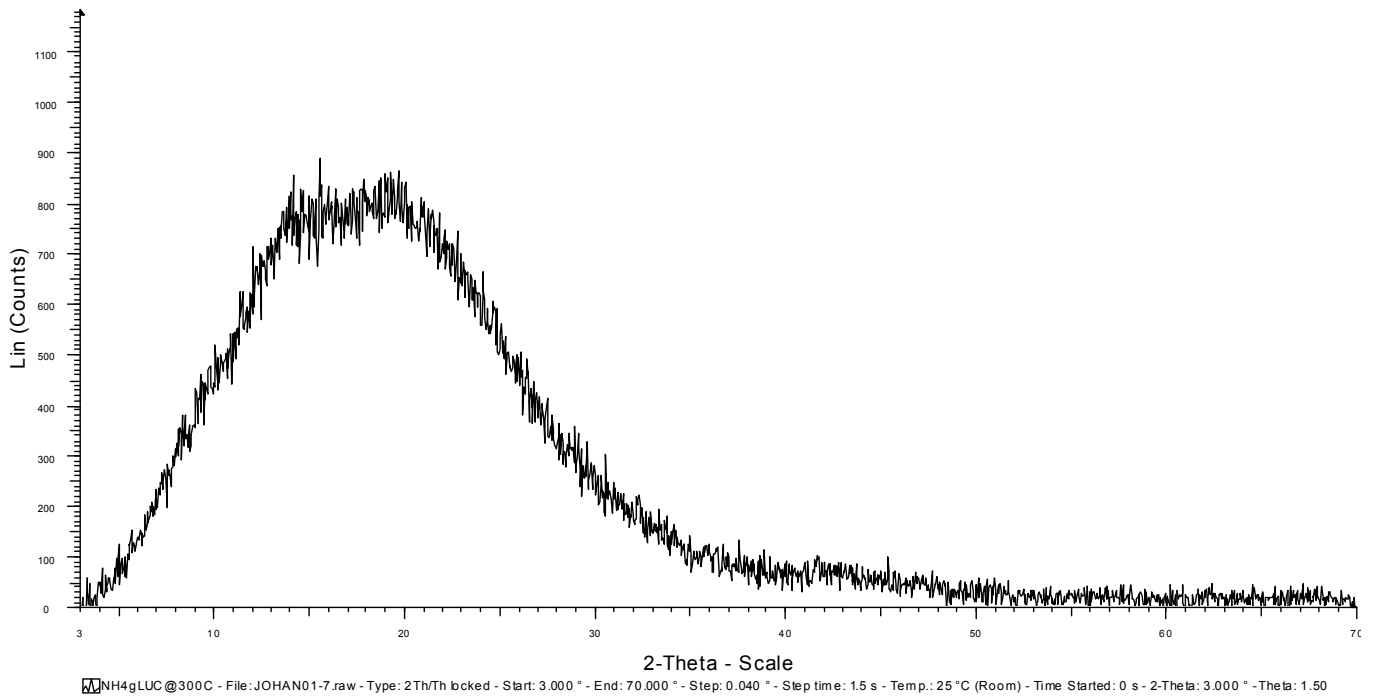
XRD spectrum of ammonium gluconate pyrolysed at 300°C for 5 min in air

XRD spectrum of ammonium gluconate pyrolysed at 400°C for 5 min in air

XRD spectrum of ammonium gluconate pyrolysed at 500°C for 5 min in air

XRD spectrum of ammonium gluconate pyrolysed at 600°C for 5 min in air

NH4 GLUC 700C - File: JOHAN01-41.raw - Type: 2Th/Th locked - Start: 3.000 ° - End: 70.040 ° - Step: 0.040 ° - Step time: 1.5 s - Temp.: 25 °C (Room) - Time Started: 0 s - 2-Theta: 3.000 ° - Theta: 1.500
Operations: Background 0.000,1.000 | Import

XRD spectrum of ammonium gluconate pyrolysed at 700°C for 5 min in air

NH4GLUC 800C - File: JOHAN121.raw - Type: 2Th/Th locked - Start: 3.000 ° - End: 70.000 ° - Step: 0.040 ° - Step time: 1.5 s - Temp.: 25 °C (Room) - Time Started: 0 s - 2-Theta: 3.000 ° - Theta: 1.500 °

XRD spectrum of ammonium gluconate pyrolysed at 800°C for 5 min in air

NH4 @ 1000 - File: JOHAN01-35.raw - Type: 2Th/Th locked - Start: 3.000 ° - End: 70.040 ° - Step: 0.040 ° - Step time: 1.5 s - Temp.: 25 °C (Room) - Time Started: 0 s - 2-Theta: 3.000 ° - Theta: 1.500 ° -
Operations: Background 0.000,1.000 | Import
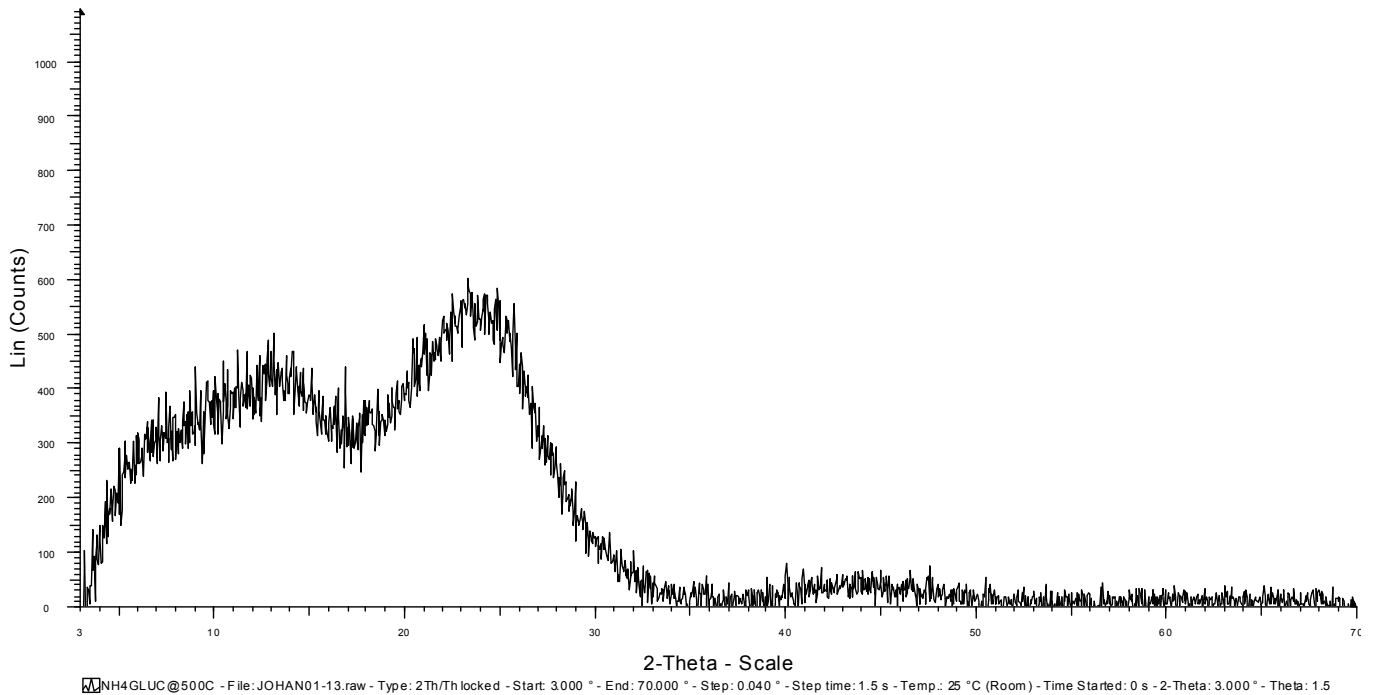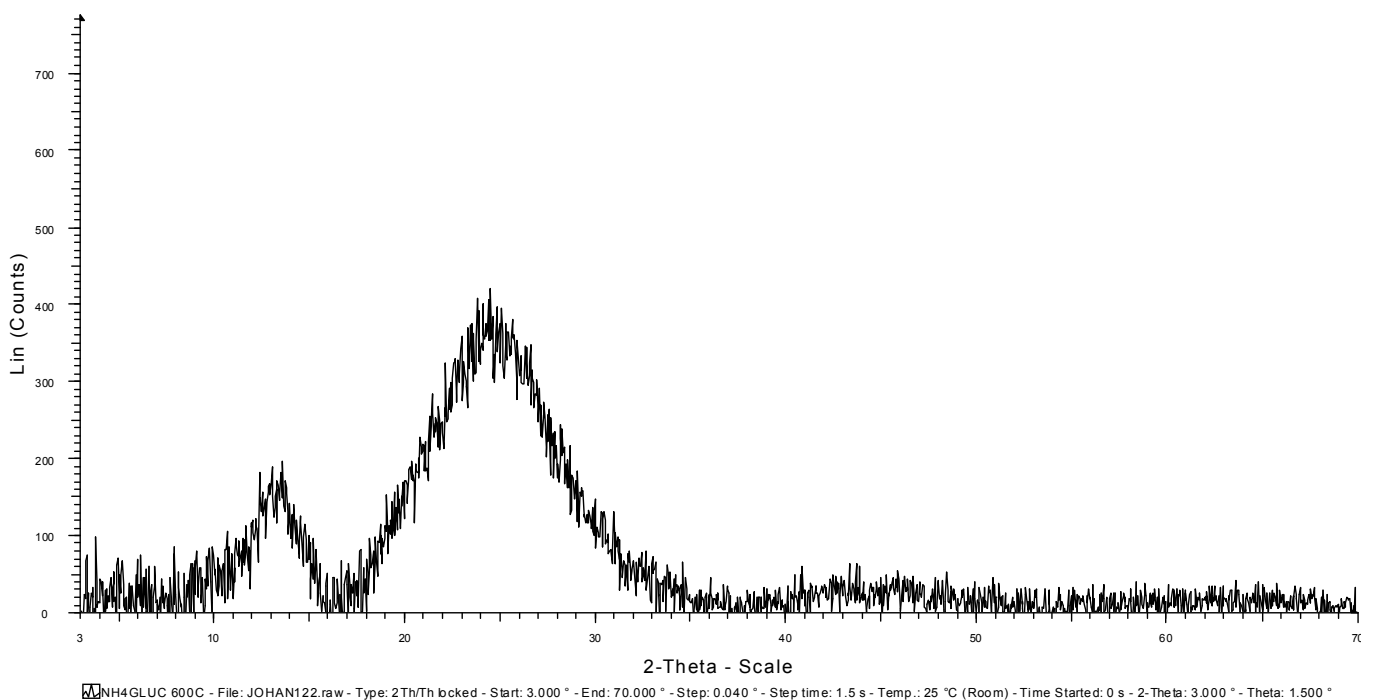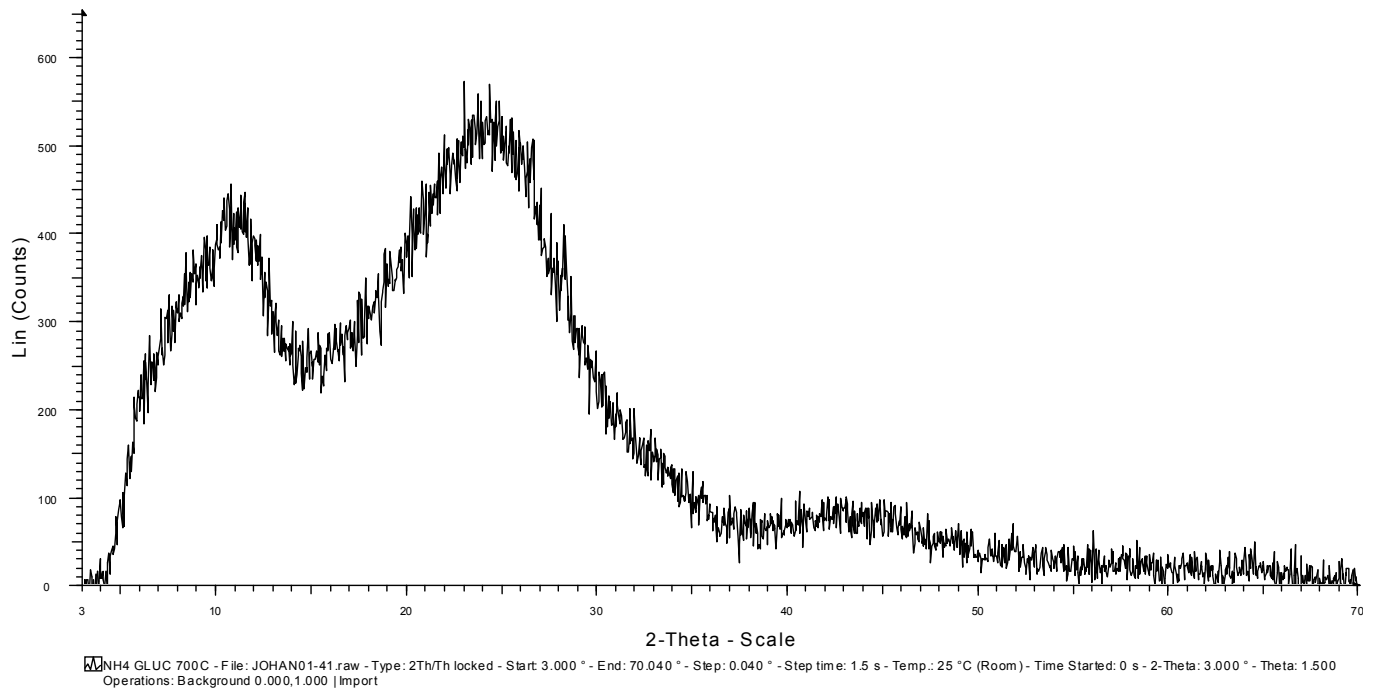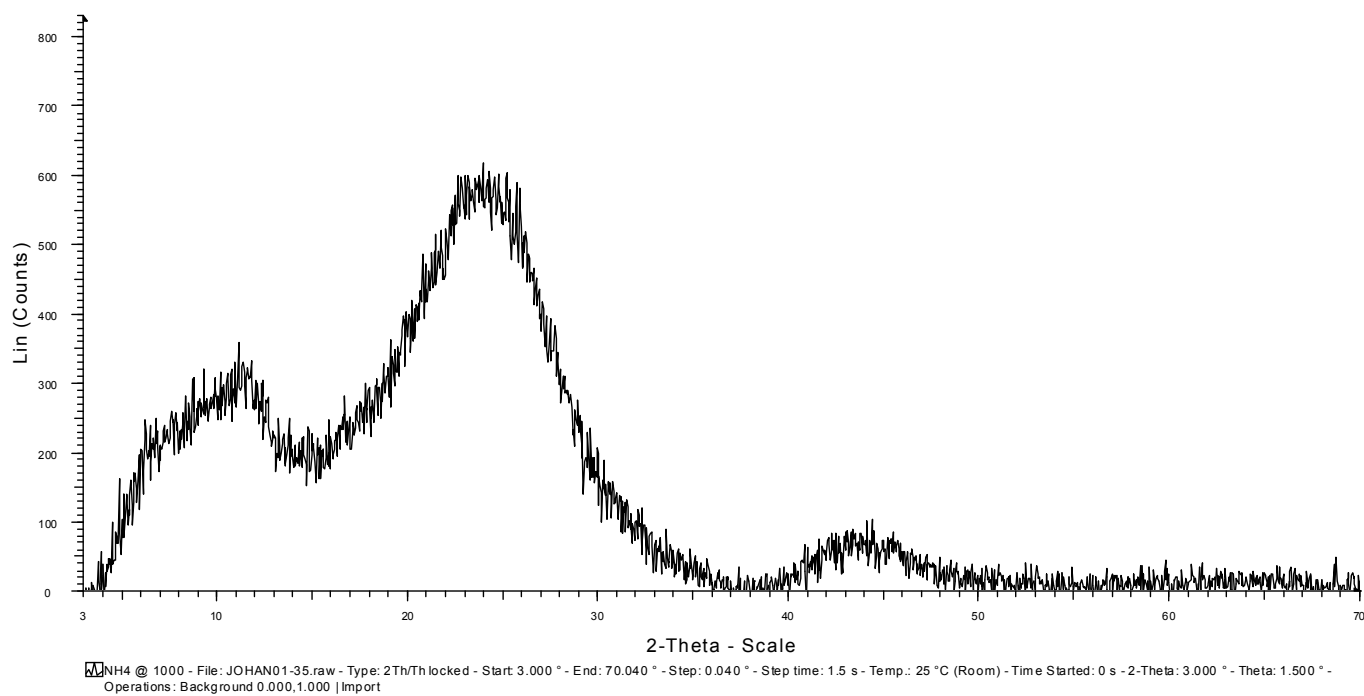
XRD spectrum of ammonium gluconate pyrolysed at 1000°C for 5 min in air

7.16.8. XRD pattern of ammonium gluconate pyrolised in nitrogen

NH4 GLUE @ 500 N2 - File: JOHAN01-40.raw - Type: 2Th/Th locked - Start: 3.000 ° - End: 70.040 ° - Step: 0.040 ° - Step time: 1.5 s - Temp.: 25 °C (Room) - Time Started: 0 s - 2-Theta: 3.000 ° - Theta:
Operations: Background 0.000,1.000 | Import

XRD spectrum of ammonium gluconate pyrolysed at 300°C for 5 min in nitrogen

NH4GLUC@400C IN N2 - File: JOHAN01-1.raw - Type: 2Th/Th locked - Start: 3.000 ° - End: 70.000 ° - Step: 0.040 ° - Step time: 1.5 s - Temp.: 25 °C (Room) - Time Started: 0 s - 2-Theta: 3.000 ° - Theta
Operations: Background 0.000,1.000 | Import

XRD spectrum of ammonium gluconate pyrolysed at 400°C for 5 min in nitrogen

NH4 GLUC 500C - File: JOHAN01-44.raw - Type: 2Th/Th locked - Start: 3.000 ° - End: 70.040 ° - Step: 0.040 ° - Step time: 1.5 s - Temp.: 25 °C (Room) - Time Started: 0 s - 2-Theta: 3.000 ° - Theta: 1.500
Operations: Background 0.000,1.000 | Import

XRD spectrum of ammonium gluconate pyrolysed at 500°C for 5 min in nitrogen

NH4GLUC@600C IN N2 - File: JOHAN01-8.raw - Type: 2Th/Th locked - Start: 3.000 ° - End: 70.000 ° - Step: 0.040 ° - Step time: 1.5 s - Temp.: 25 °C (Room) - Time Started: 0 s - 2-Theta: 3.000 ° -

XRD spectrum of ammonium gluconate pyrolysed at 600°C for 5 min in nitrogen

NH4 GLUC 850 IN N2 - File: JOHAN01-19.raw - Type: 2Th/Th locked - Start: 3.000 ° - End: 70.000 ° - Step: 0.040 ° - Step time: 1.5 s - Temp.: 25 °C (Room) - Time Started: 0 s - 2-Theta: 3.000 ° - Theta:

XRD spectrum of ammonium gluconate pyrolysed at 850°C for 5 min in nitrogen

NH4 GLUC 1000C IN N2 - File: JOHAN01-17.raw - Type: 2Th/Th locked - Start: 3.000 ° - End: 70.000 ° - Step: 0.040 ° - Step time: 1.5 s - Temp.: 25 °C (Room) - Time Started: 0 s - 2-Theta: 3.000 ° - Thet

XRD spectrum of ammonium gluconate pyrolysed at 1000°C for 5 min in nitrogen

7.16.9. IR spectra of calcium gluconate monohydrate pyrolised in air
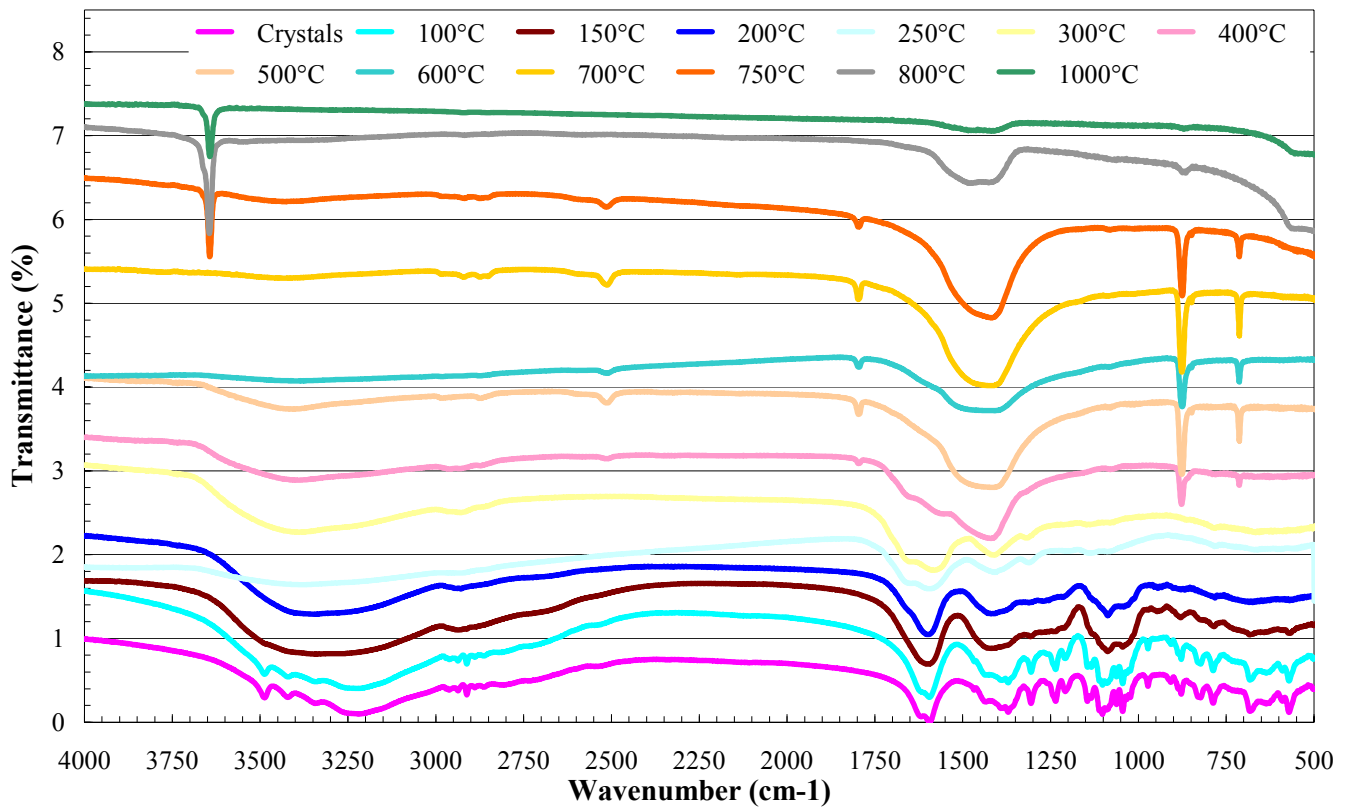
7.16.10.   IR spectra of calcium gluconate pyrolised in nitrogen
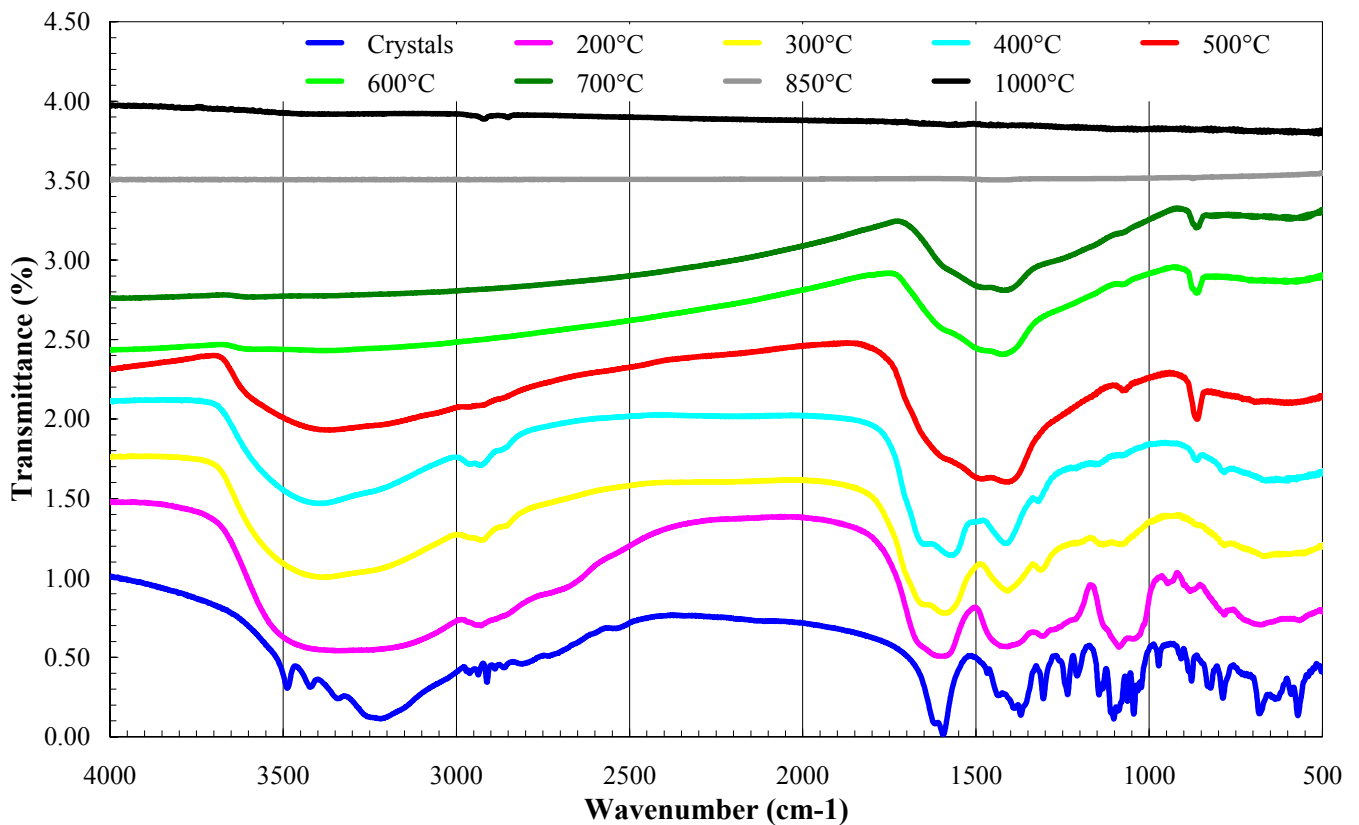
7.16.11.   IR spectra of ammonium gluconate hydrate pyrolised in air
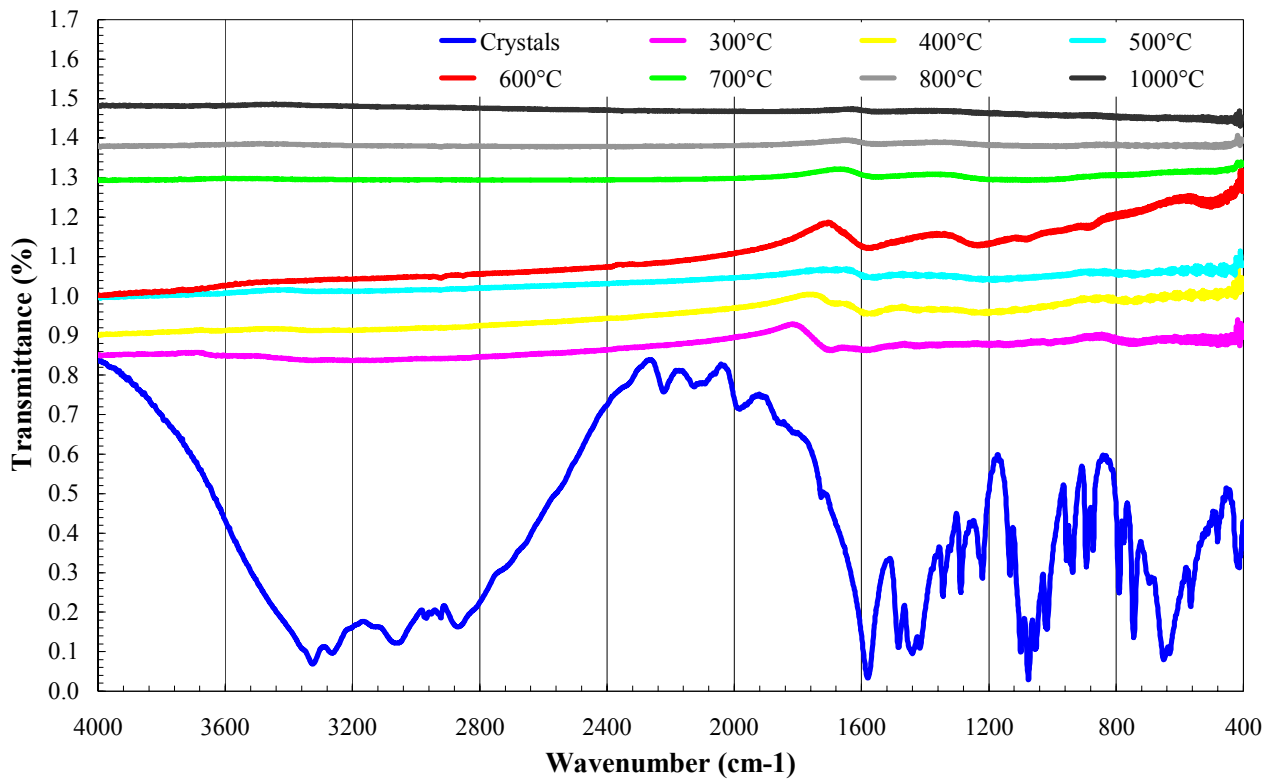
7.16.12.   IR spectra of ammonium gluconate pyrolised in nitrogen
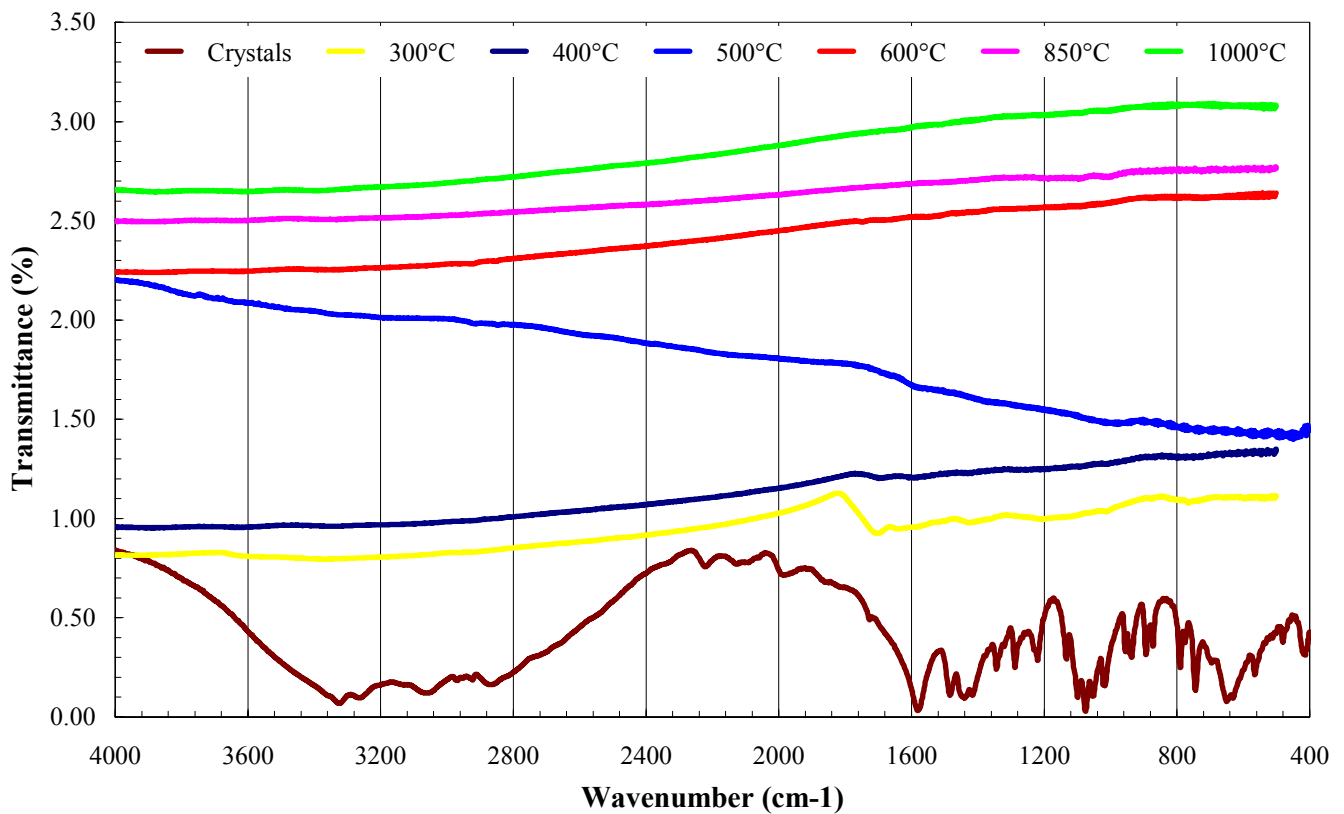
7.16.13   Decomposition products of calcium gluconate monohydrate
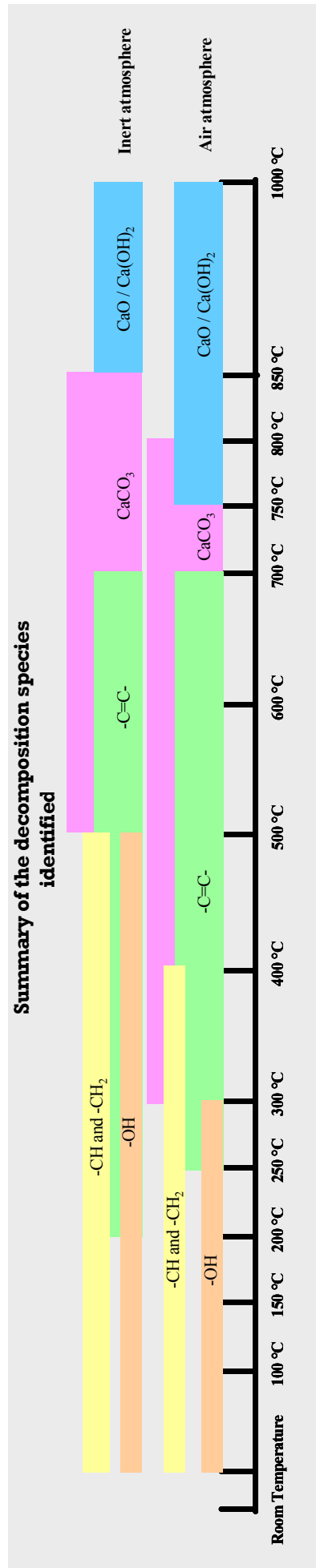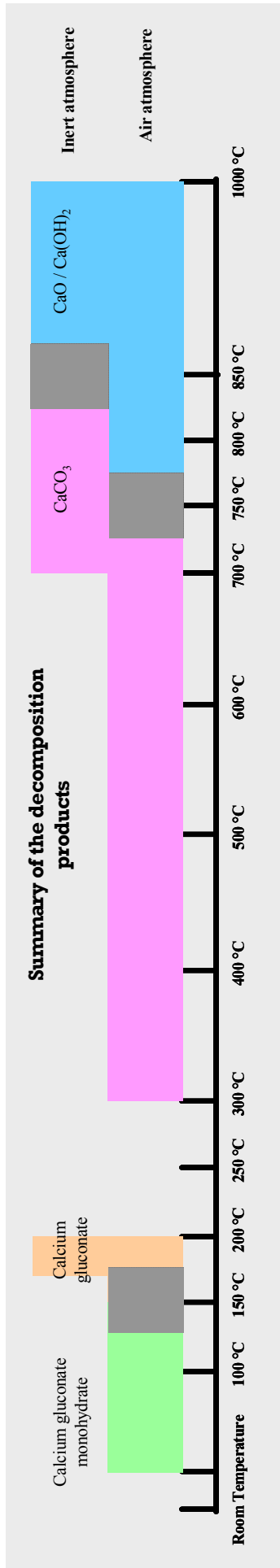
Graphic summary of the solid decomposition products of calcium gluconate monohydrate as identified with XRD and IR spectroscopy

7.17. Appendix Q

7.17.1. Thermal conductivity results from the SABS

```
Friday, September 29, 2000, Time 08:28

WinTherm32 Version 2.11
Instrument Program Version 38
Instrument Serial Number: 288


Sample Name: TKUP!
Sample Thickness: 5.025cm
         [ Polystyrene sample ]
Sample Thickness obtained   :   from instrument

TEST RUN

Calibration used   :  1450b
Calibration read from instrument

Number of transdusers per plate:        1
Number of transdusers used per plate:   1

Number of Setpoints: 2

Block Averages for setpoint 1 in SI units

Tupper  Tlower  Qupper  Qlower  Lambda
 [°C]    [°C]    [µV]    [µV]    [W/mK]
 10.01   35.01   -1676    1930   0.04023
 10.01   35.02   -1670    1935   0.04021
 10.01   35.02   -1669    1931   0.04015
 10.01   35.02   -1669    1928   0.04012
 10.01   35.02   -1669    1927   0.04010
 10.01   35.02   -1669    1924   0.04007
 10.01   35.02   -1668    1923   0.04004
 10.01   35.02   -1667    1922   0.04003
 10.01   35.02   -1666    1922   0.04002
 10.01   35.02   -1665    1921   0.03999

Friday, September 29, 2000, Time 09:24

Setpoint No.    1
 Setpoint Upper:        10.00 °C
 Setpoint Lower:        35.00 °C
   Temperature Upper:  10.01 °C
   Results Upper:            0.04006 W/mK
   Temperature Lower:  35.02 °C
   Results Lower:            0.04001 W/mK
   Percent Difference: 0.12%


      Experiment's Criteria:
      Temperature Equilibrium:        0.20
      Between Block HFM Equil.:        70
      HFM Percent Change:      2.00
      Min Number of Blocks:    10
      Calculation Blocks:              5

Block Averages for setpoint 2 in SI units

Tupper  Tlower  Qupper  Qlower  Lambda
 [°C]    [°C]    [µV]    [µV]    [W/mK]
 30.02   50.02   -1428    1700   0.04252
 30.03   50.03   -1439    1687   0.04250
 30.02   50.02   -1444    1682   0.04253
 30.02   50.01   -1443    1686   0.04257
 30.02   50.03   -1443    1687   0.04256
 30.02   50.02   -1446    1680   0.04252
 30.02   50.01   -1446    1681   0.04256
 30.02   50.02   -1447    1678   0.04252
 30.02   50.02   -1446    1681   0.04255
 30.02   50.01   -1446    1677   0.04251

Friday, September 29, 2000, Time 10:24

Setpoint No.    2
 Setpoint Upper:        30.00 °C
 Setpoint Lower:        50.00 °C
   Temperature Upper:  30.02 °C
   Results Upper:            0.04230 W/mK
   Temperature Lower:  50.02 °C
   Results Lower:            0.04276 W/mK
   Percent Difference: 1.08%


      Experiment's Criteria:
      Temperature Equilibrium:        0.20
      Between Block HFM Equil.:        70
      HFM Percent Change:      2.00
      Min Number of Blocks:    10
      Calculation Blocks:              5

Results Table -- SI Units

Mean Temp     Upper Cond     Lower Cond     Average Cond
22.52         0.04006        0.04001        0.04003
40.02         0.04230        0.04276        0.04253
```

```
Friday, September 29, 2000, Time 11:09

WinTherm32 Version 2.11
Instrument Program Version 38
Instrument Serial Number: 288


Sample Name: TKUP2
Sample Thickness: 5.027cm
        [ Polystyrene sample with sample in the middle
Sample Thickness obtained    :   from instrument

TEST RUN

Calibration used   :   1450b
Calibration read from instrument

Number of transdusers per plate:        1
Number of transdusers used per plate:   1

Number of Setpoints: 2

Block Averages for setpoint 1 in SI units

Tupper   Tlower   Qupper   Qlower   Lambda
 [°C]     [°C]     [µV]     [µV]     [W/mK]
10.00    35.01    -1741    1960    0.04132
10.01    35.02    -1725    1959    0.04112
10.01    35.02    -1715    1948    0.04088
10.01    35.02    -1708    1943    0.04074
10.01    35.02    -1700    1933    0.04055
10.01    35.02    -1699    1921    0.04041
10.01    35.02    -1695    1918    0.04034
10.00    35.02    -1682    1919    0.04019
10.02    35.02    -1674    1919    0.04010
10.02    35.03    -1675    1916    0.04007

Friday, September 29, 2000, Time 12:09

Setpoint No.     1
  Setpoint Upper:        10.00 °C
  Setpoint Lower:        35.00 °C
    Temperature Upper:  10.01 °C
    Results Upper:              0.04050 W/mK
    Temperature Lower:  35.02 °C
    Results Lower:              0.03994 W/mK
    Percent Difference: 1.39%


        Experiment's Criteria:
        Temperature Equilibrium:        0.20
        Between Block HFM Equil.:       70
        HFM Percent Change:     2.00
        Min Number of Blocks:   10
        Calculation Blocks:             5

Block Averages for setpoint 2 in SI units

Tupper   Tlower   Qupper   Qlower   Lambda
 [°C]     [°C]     [µV]     [µV]     [W/mK]
30.02    50.01    -1462    1706    0.04311
30.02    50.03    -1460    1711    0.04313
30.02    50.03    -1461    1687    0.04283
30.02    50.02    -1458    1677    0.04267
30.02    50.03    -1455    1675    0.04259
30.02    50.03    -1451    1668    0.04246
30.02    50.02    -1450    1664    0.04240
30.02    50.04    -1448    1668    0.04239
30.02    50.03    -1446    1651    0.04216
30.02    50.02    -1444    1649    0.04214

Friday, September 29, 2000, Time 13:09

Setpoint No.     2
  Setpoint Upper:        30.00 °C
  Setpoint Lower:        50.00 °C
    Temperature Upper:  30.02 °C
    Results Upper:              0.04235 W/mK
    Temperature Lower:  50.03 °C
    Results Lower:              0.04227 W/mK
    Percent Difference: 0.19%


        Experiment's Criteria:
        Temperature Equilibrium:        0.20
        Between Block HFM Equil.:       70
        HFM Percent Change:     2.00
        Min Number of Blocks:   10
        Calculation Blocks:             5

Results Table -- SI Units

Mean Temp       Upper Cond      Lower Cond      Average Cond
22.52           0.04050         0.03994         0.04022
40.02           0.04235         0.04227         0.04231
```

7.18. Appendix R

7.18.1. Electric conductivity for the pyrolysed ammonium gluconate

$y = 7E+06x$

$R^2 = 0.9838$
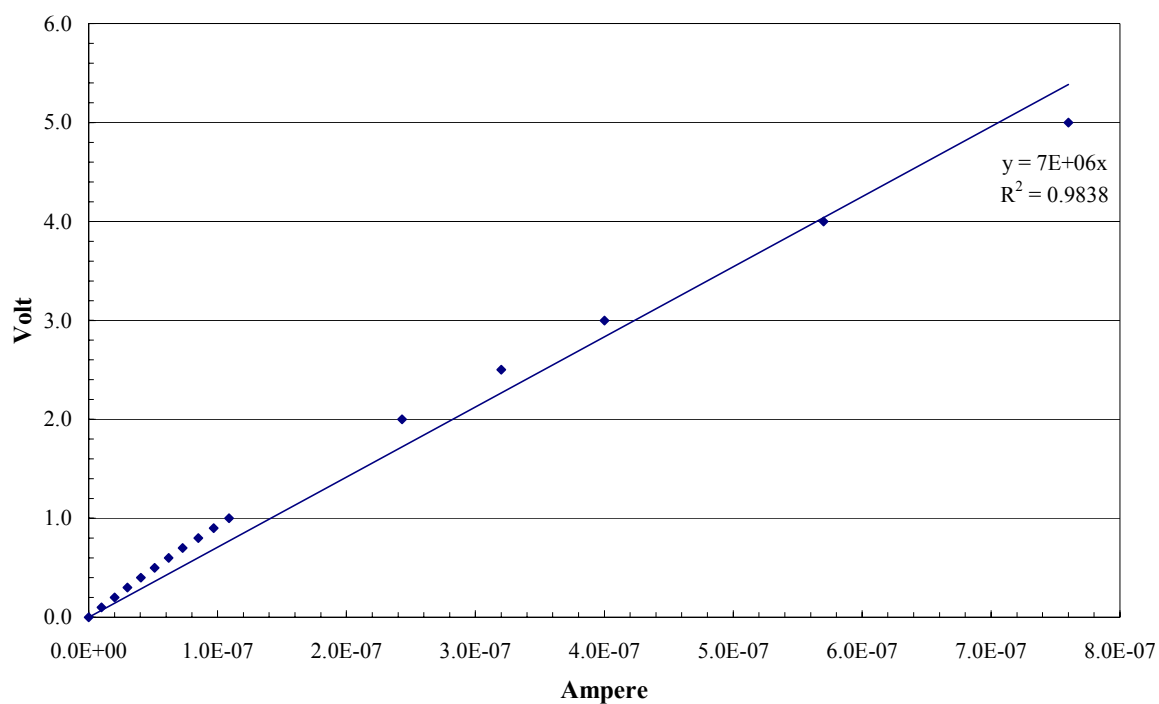
7.19. Appendix S

7.19.1. Burn through tests for the painted balsa wood planks – Graphs
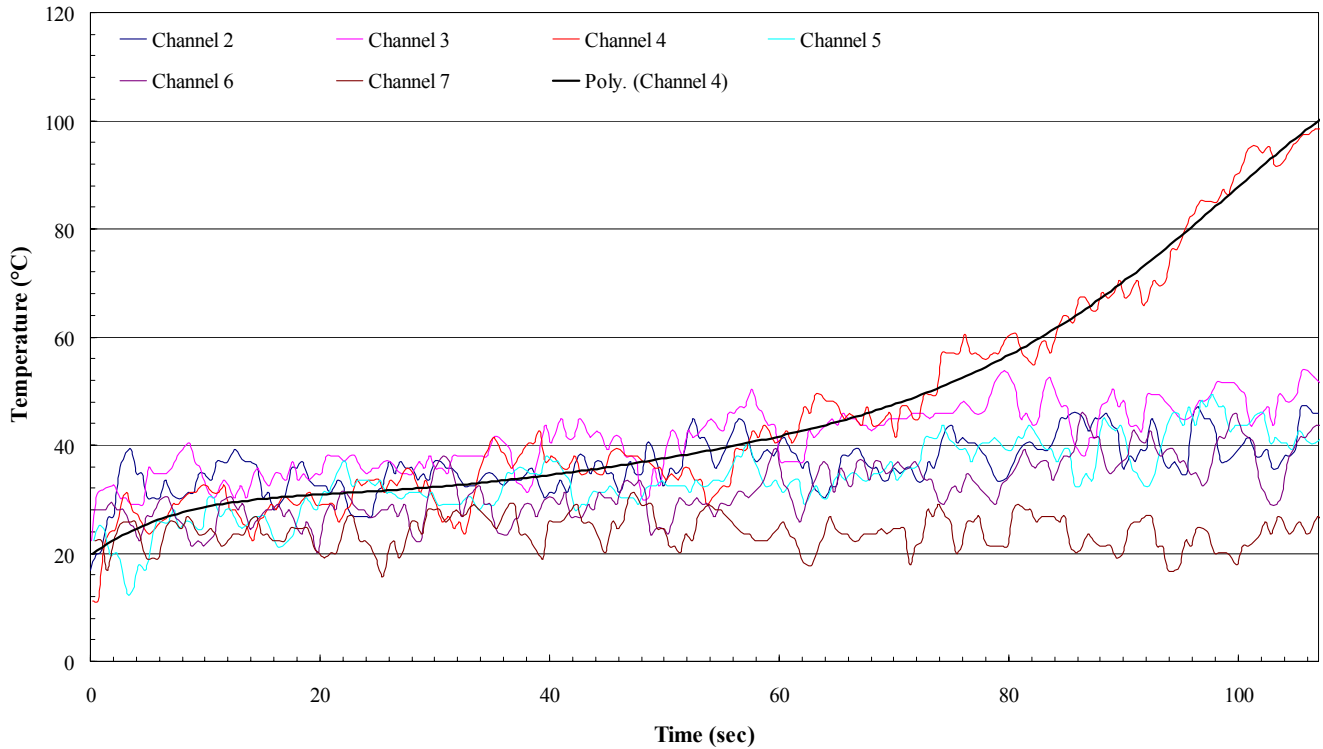
Balsa wood plank not painted (control)
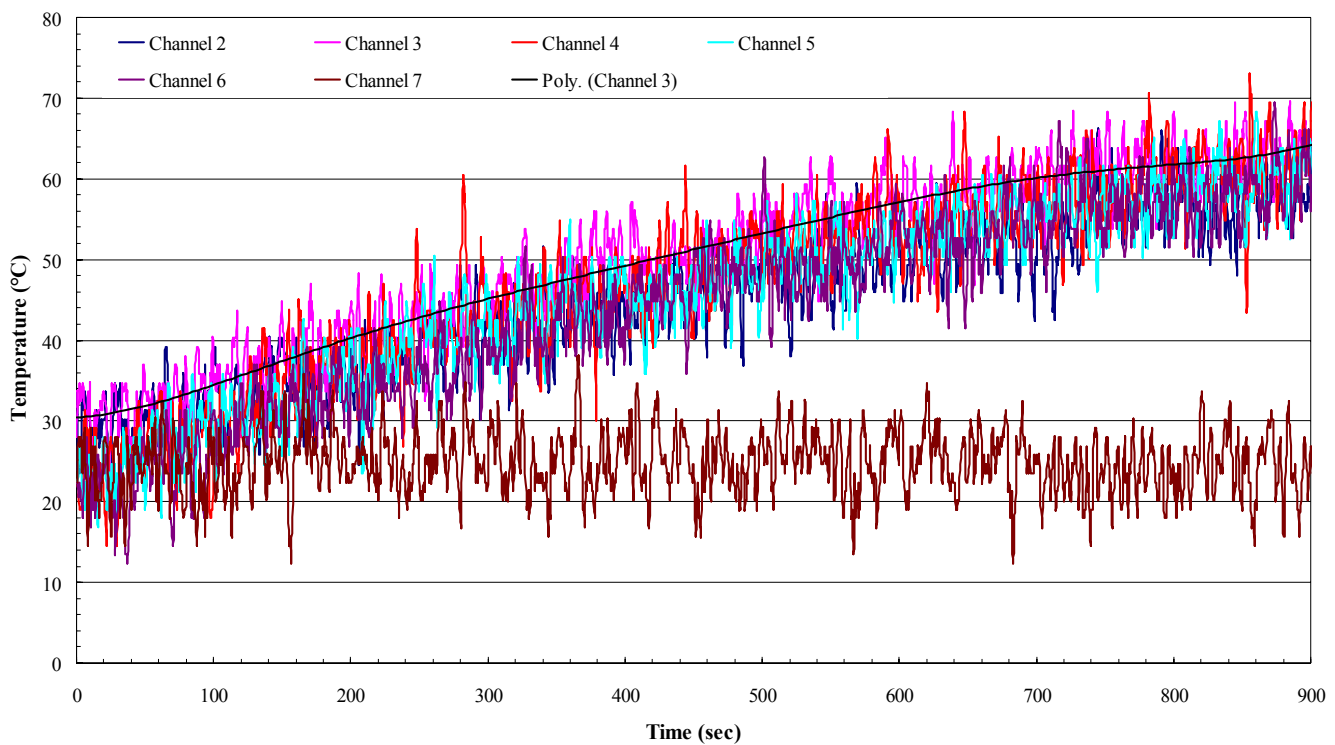
Balsa wood plank painted with AP750
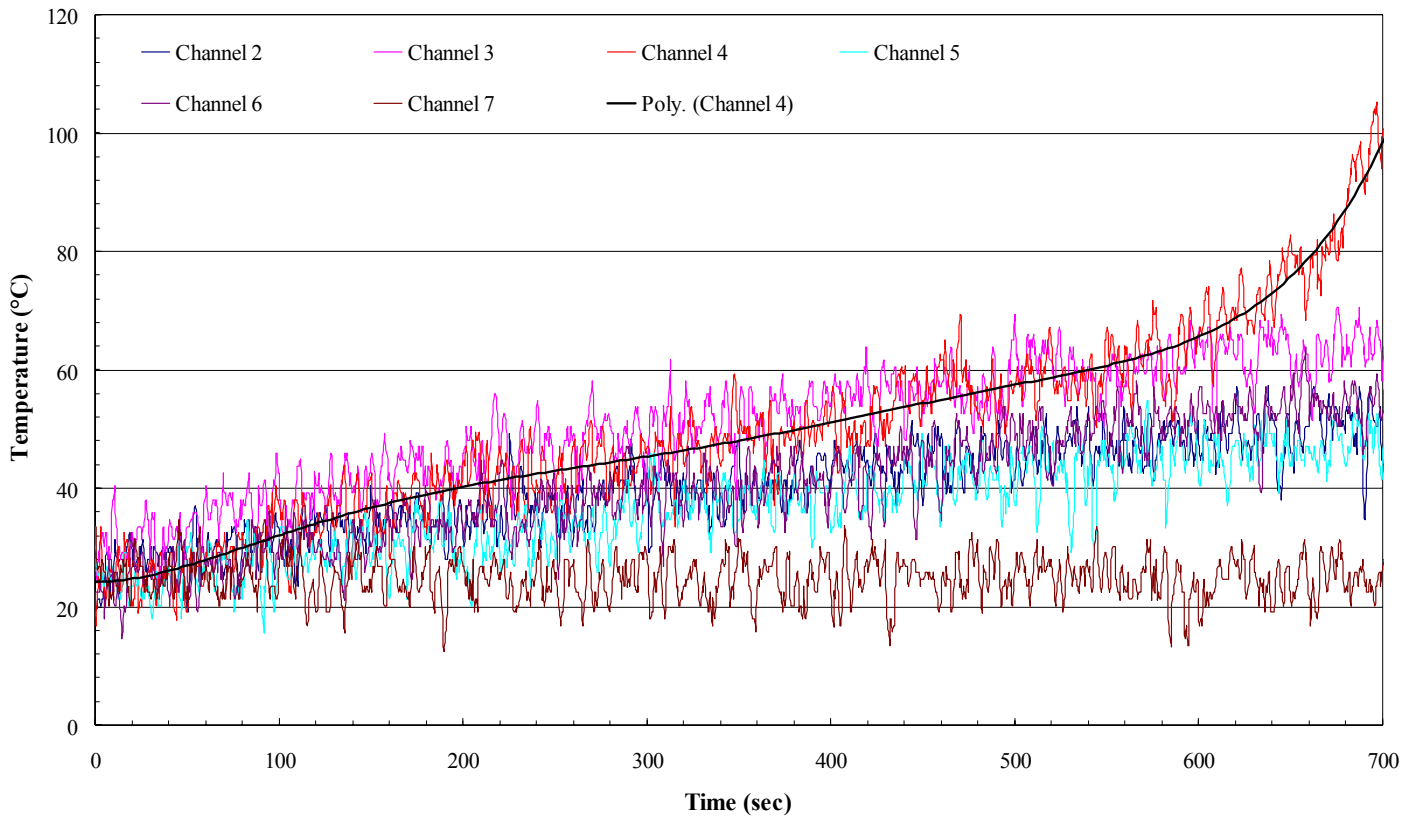
Balsa wood plank painted with PEN
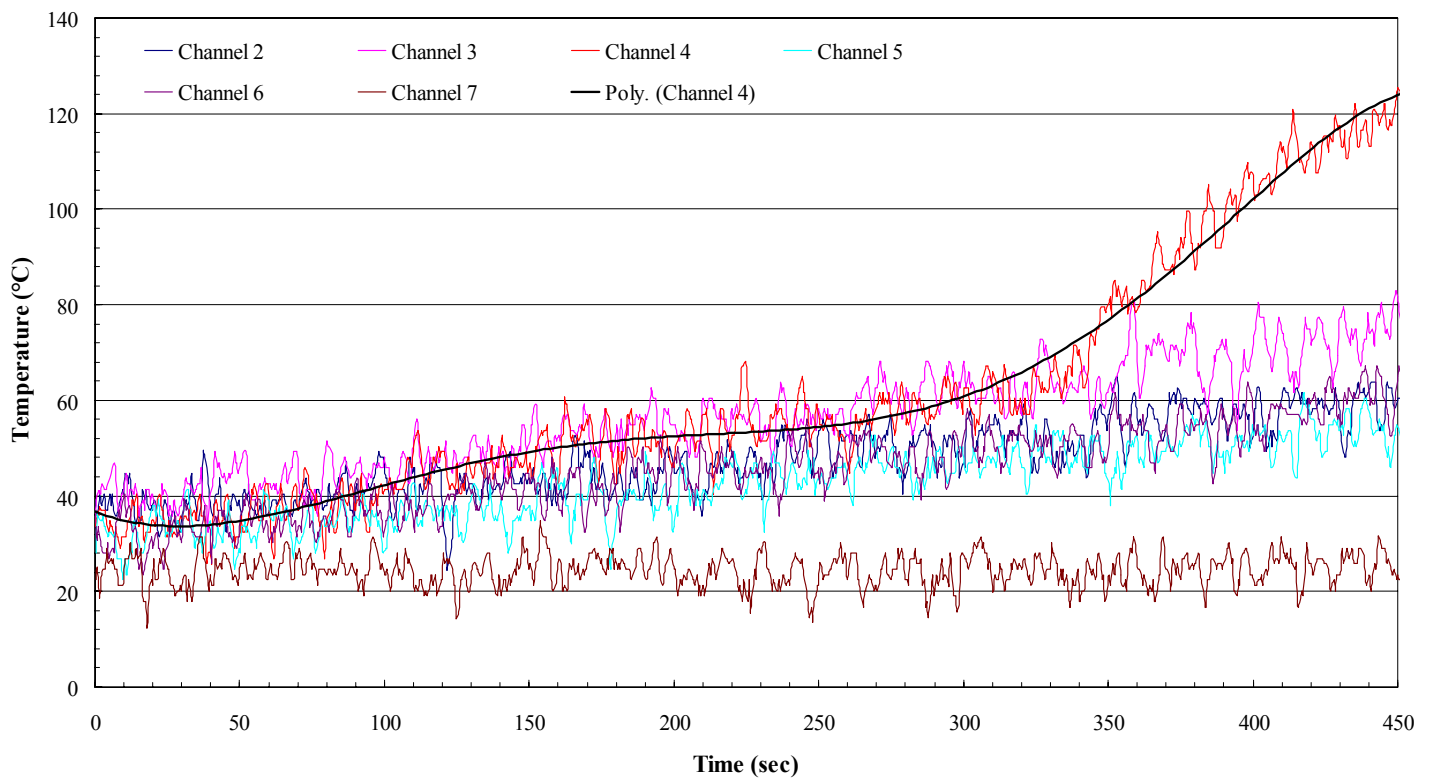
Balsa wood plank painted with Calcium gluconate
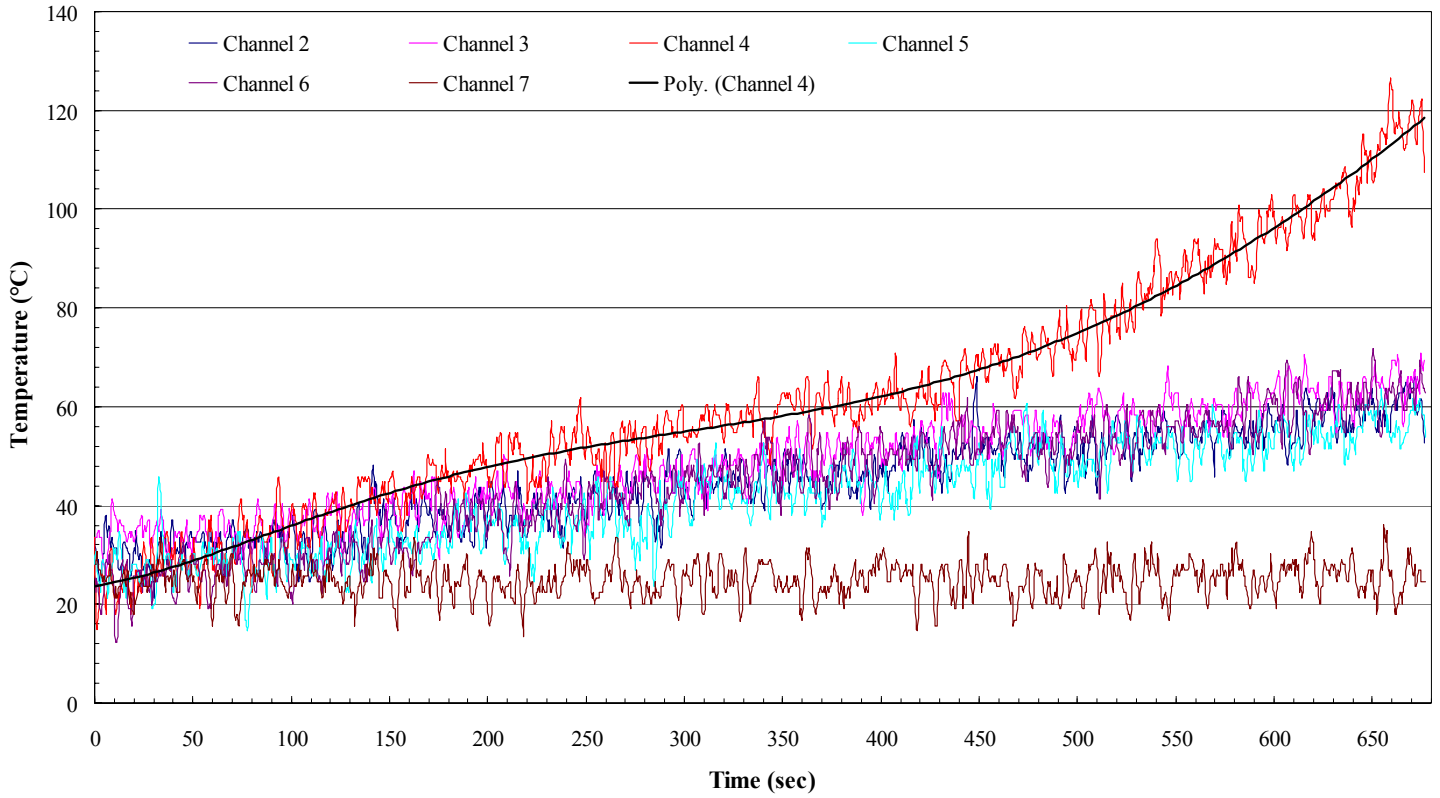
Balsa wood plank painted with Calcium gluconate and leached SiO$_2$
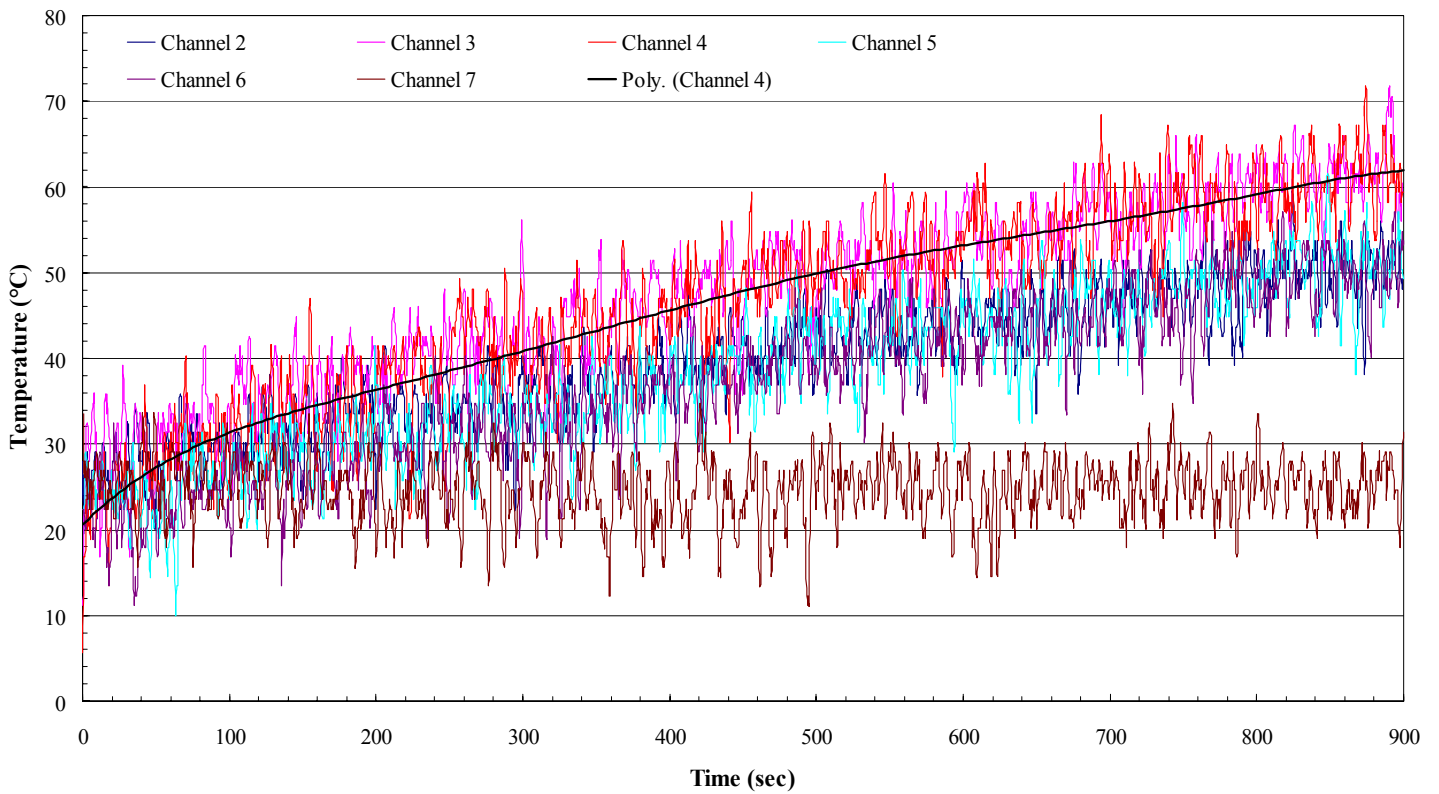
Balsa wood plank painted with Calcium gluconate and Expandable graphite
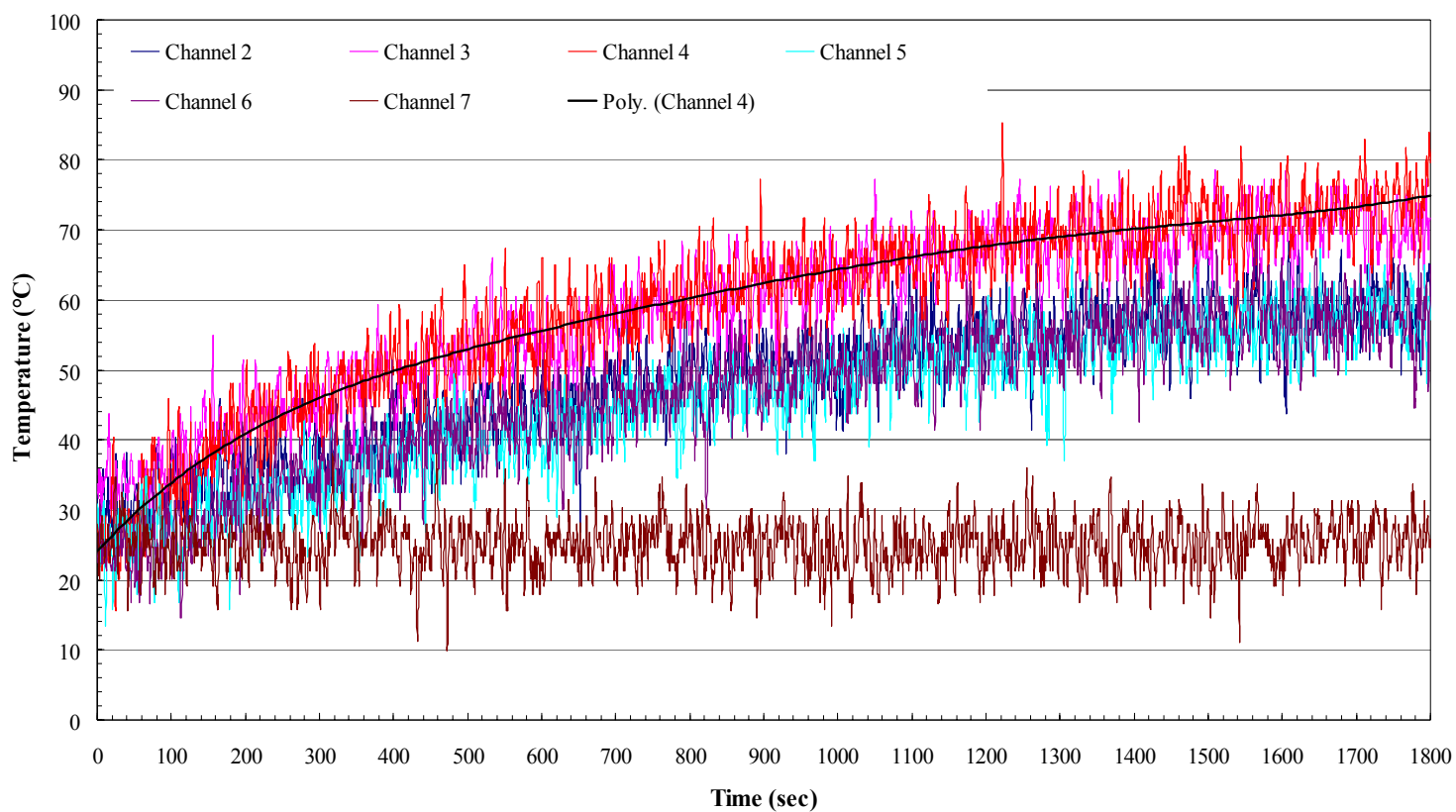
Balsa wood plank painted with Calcium gluconate, Leached SiO₂ and Expandable graphite

7.19.2. Burn through tests for the painted balsa wood planks – Pictures

With no coating: Left top – 30 sec exposure   Right top – 50 sec exposure

Left and right bottom – 80 sec exposure

With AP750 coating: Left top – 60 sec exposure   Right top – 180 sec exposure

Left and right bottom – 960 sec exposure
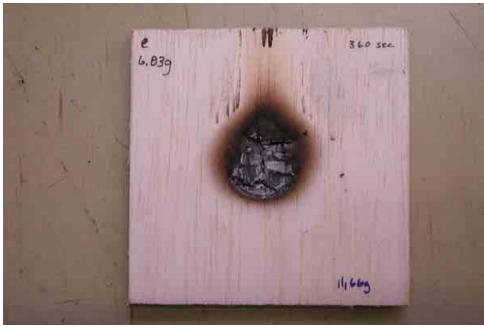
With Gluconate/silica/graphite coating: Left top – 60 sec exposure

Right top – 270 sec exposure   Left and right bottom – 360 sec exposure

With PEN coating: Left top – 30 sec exposure   Right top – 150 sec exposure

Left and right bottom – 180 sec exposure

7.19.3. Burn through tests for the painted aluminium plates – Graphs
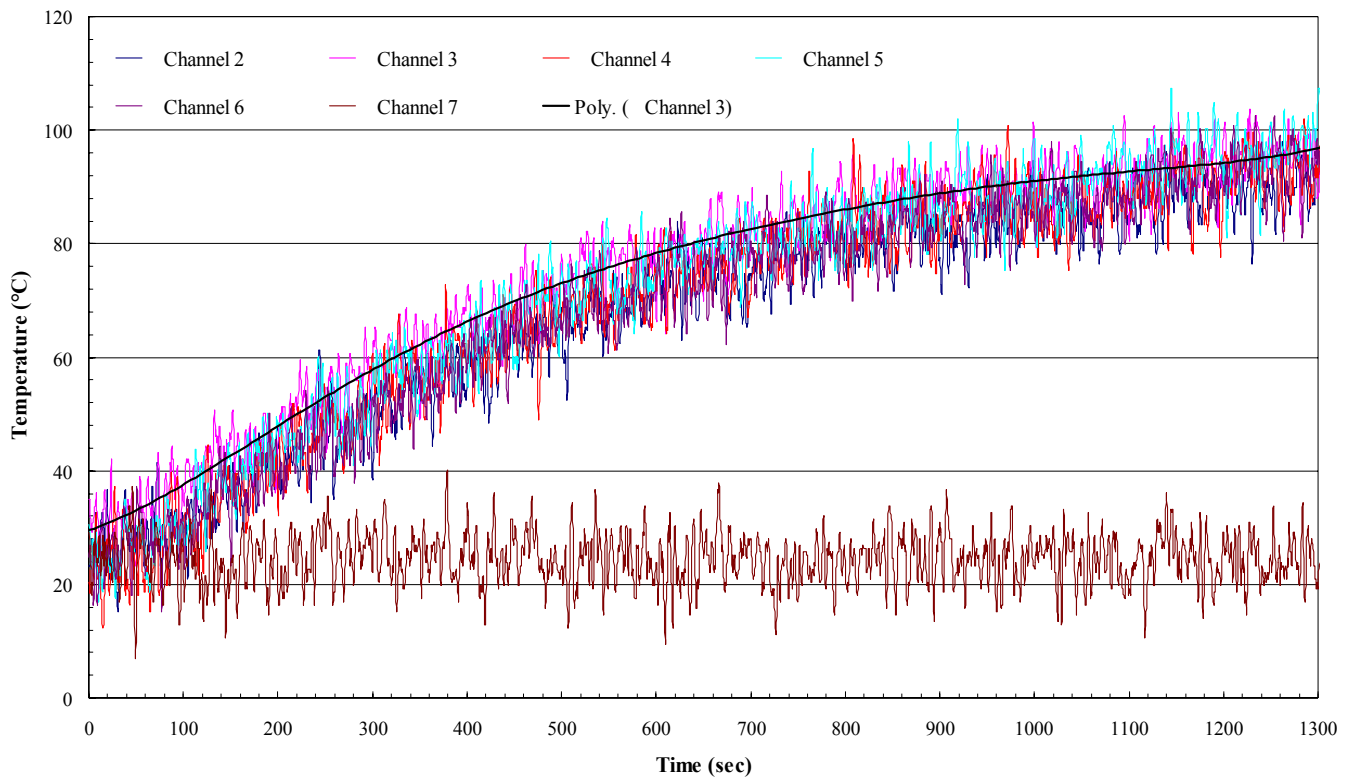
Aluminium plate not painted (control)
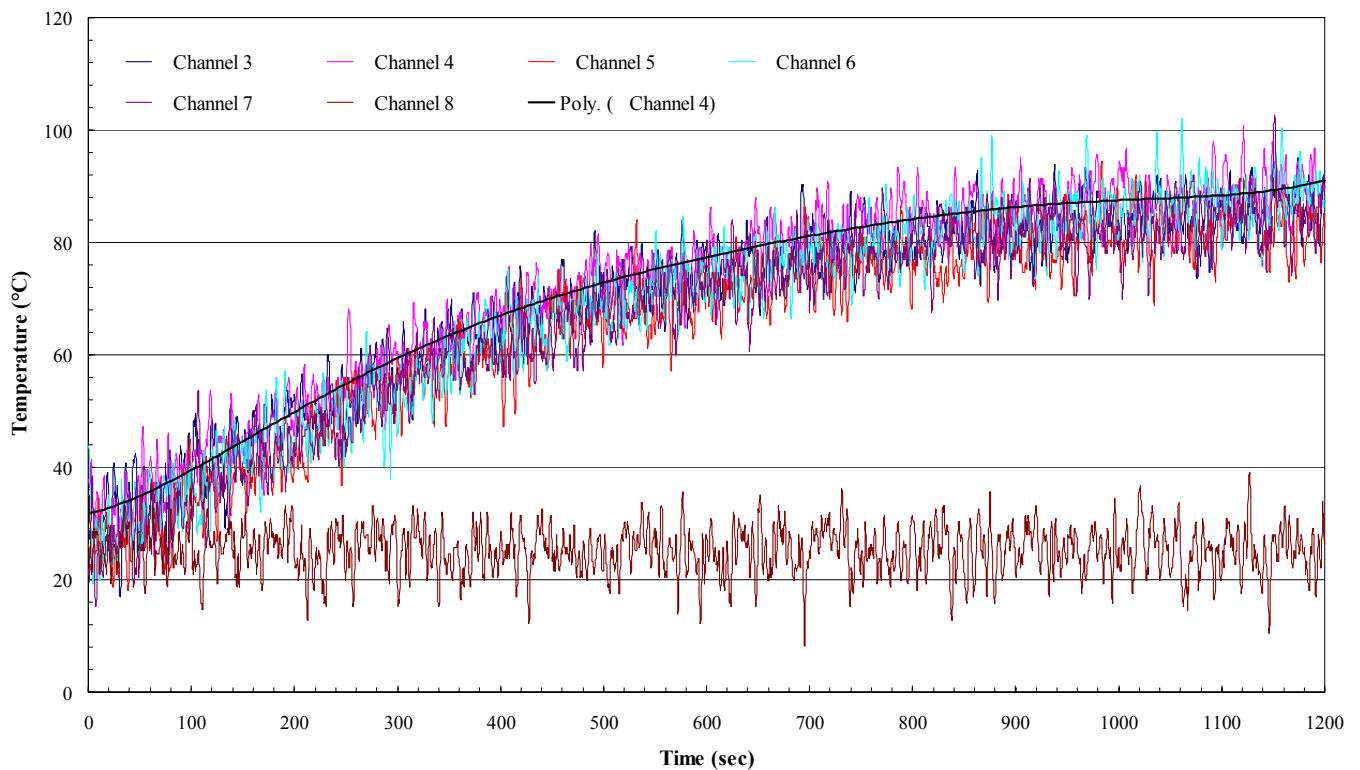
Aluminium plate painted with AP750
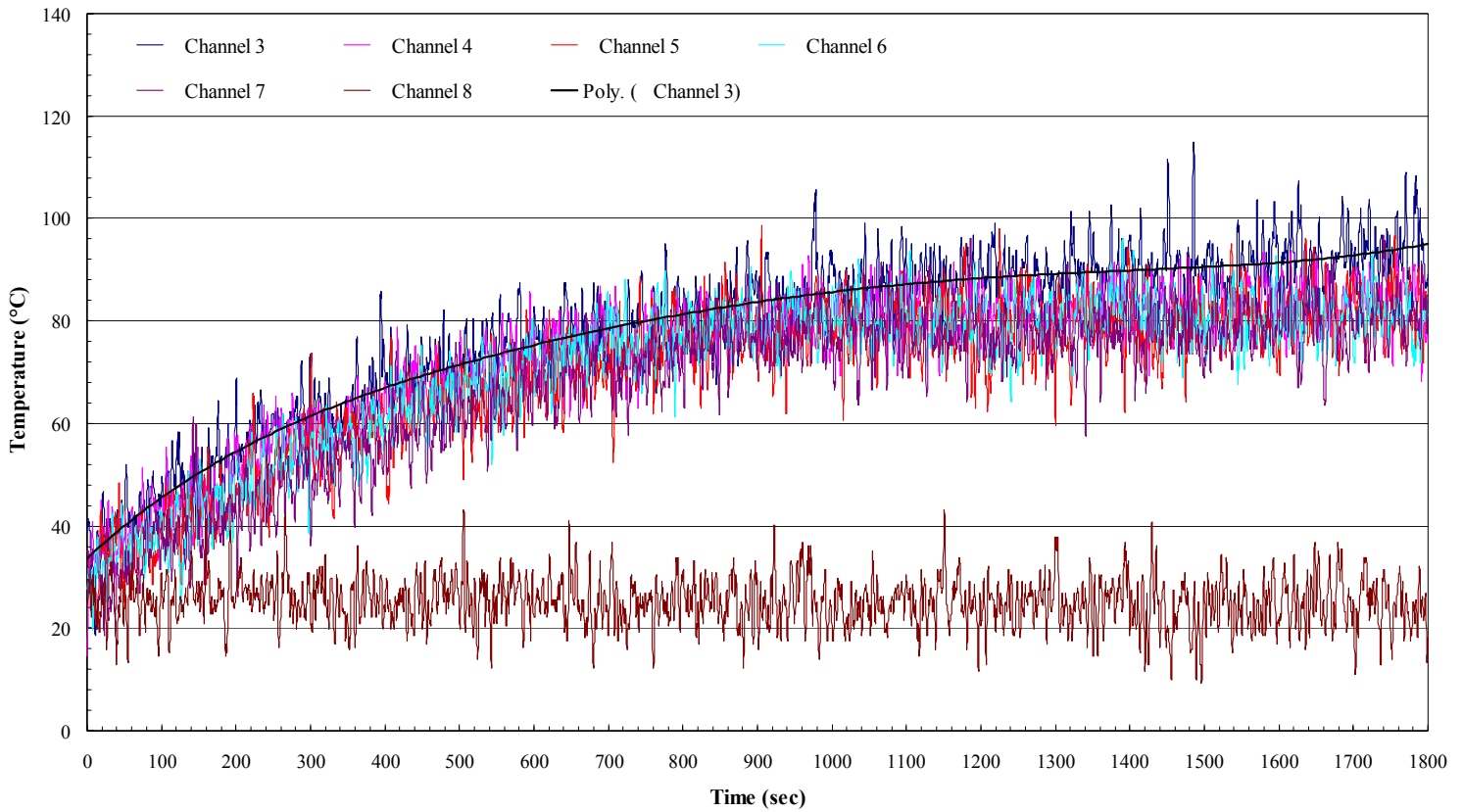
Aluminium plate painted with PEN
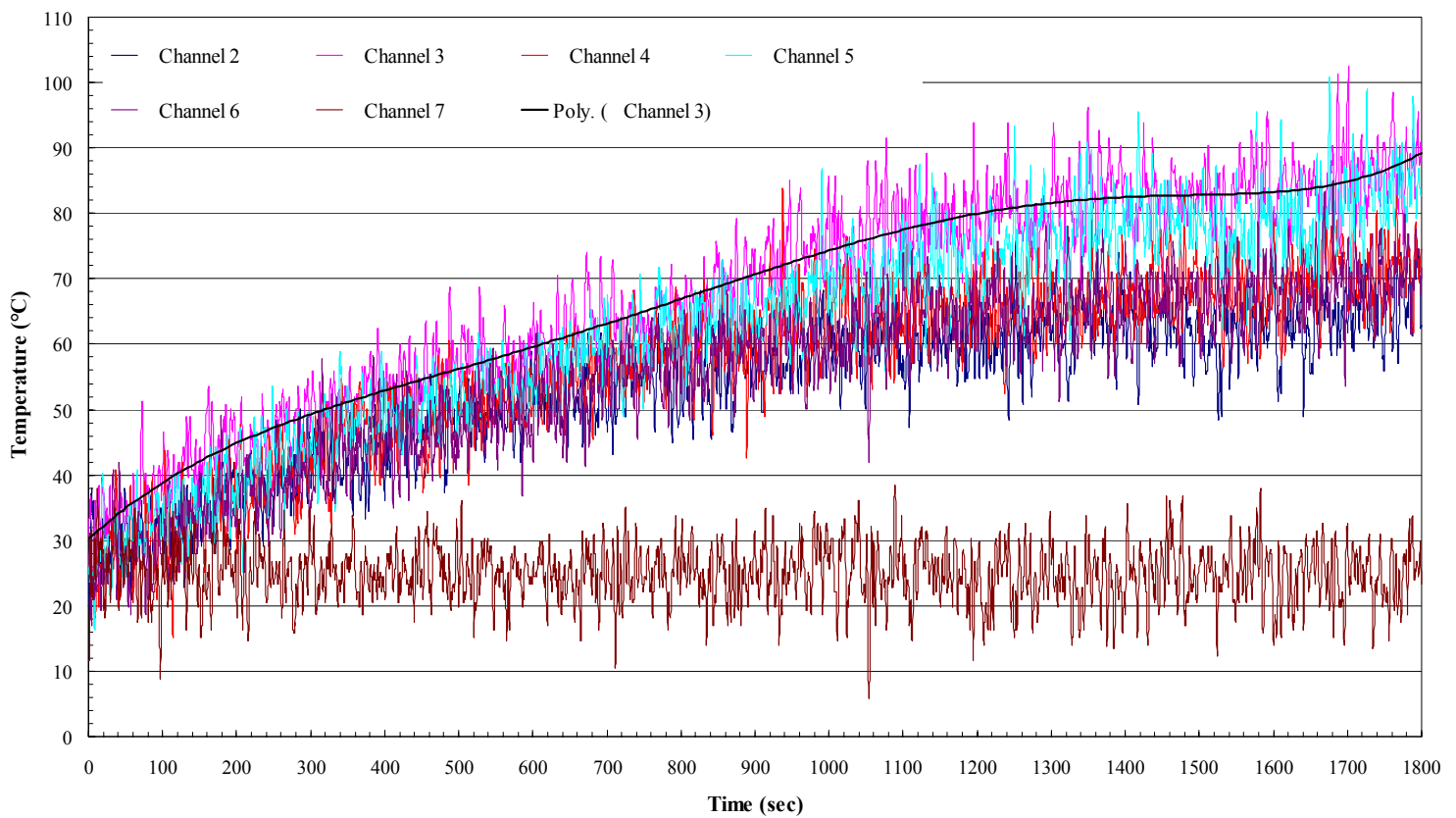
Aluminium plate painted with Calcium gluconate, Leached SiO2 and Expandable Graphite

7.19.4. Burn through tests for the painted aluminium plates – Pictures

AP750 coating: Left – 420 sec, Right – 1800 sec
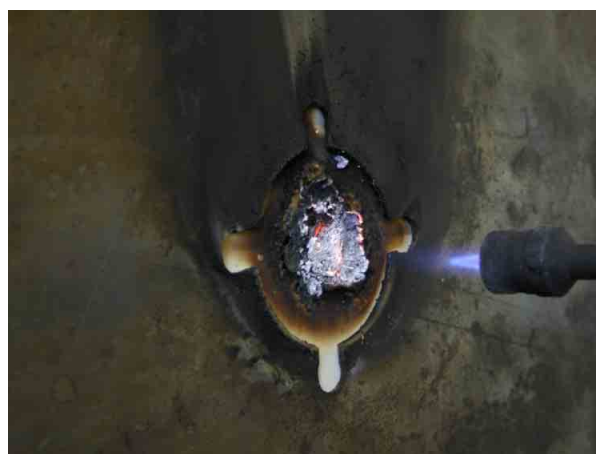
PEN coating: Left – 600 sec, Right – 1800 sec

Gluconate/graphite/silica coating: Left – 600 sec, Right – 1800 sec

7.19.5. Burn through tests for the painted cardboard sheets – Graphs
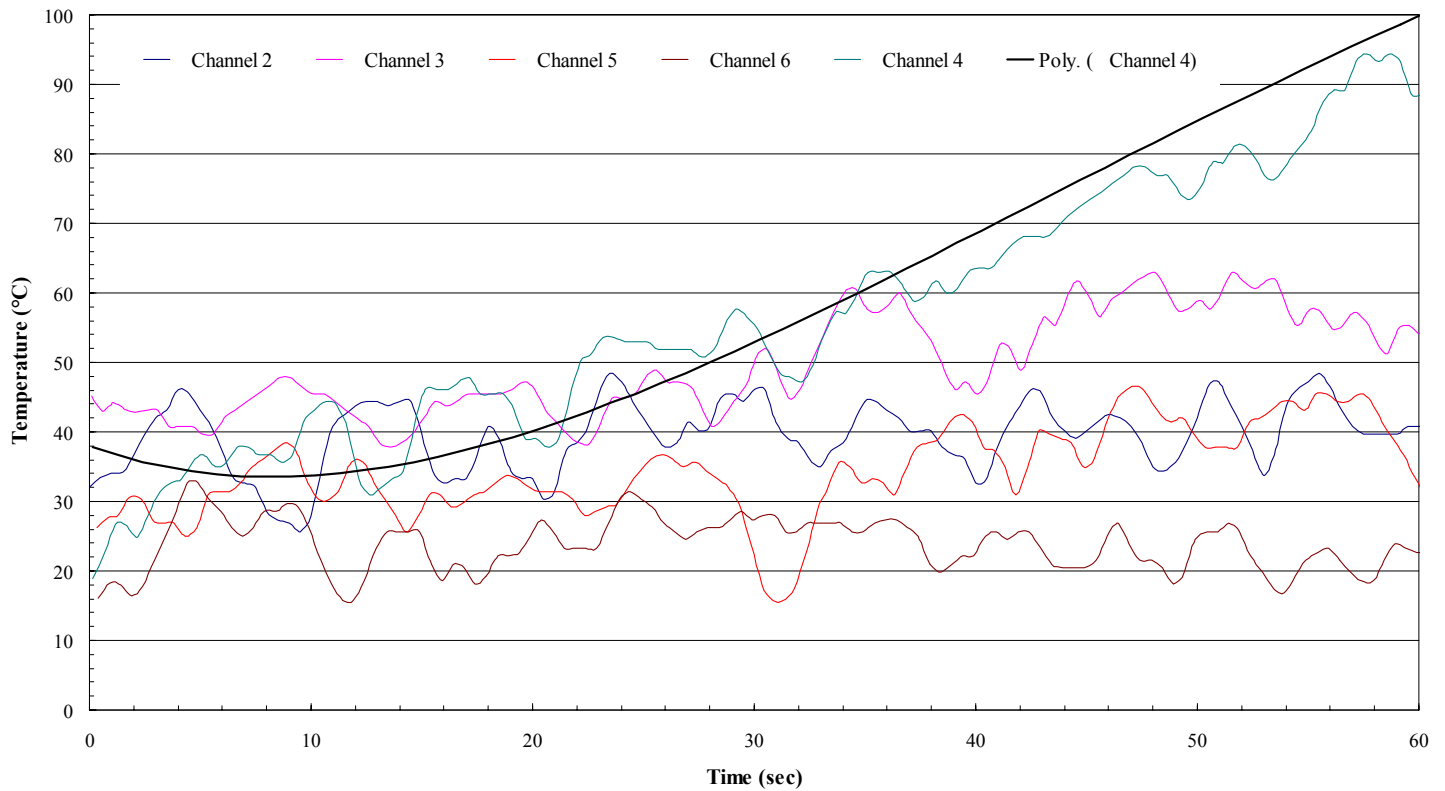
Cardboard sheet not painted (control)
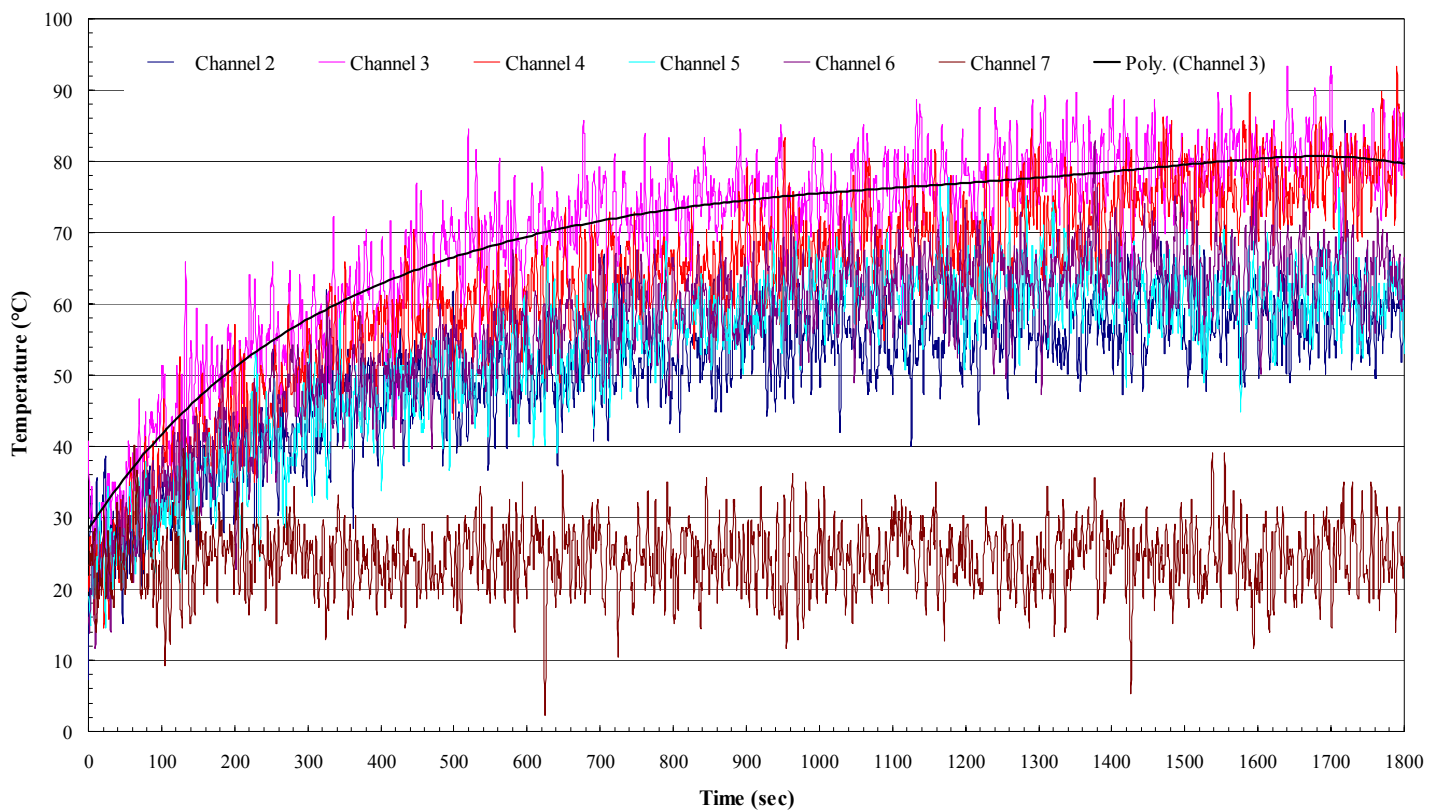
Cardboard sheet painted with AP750
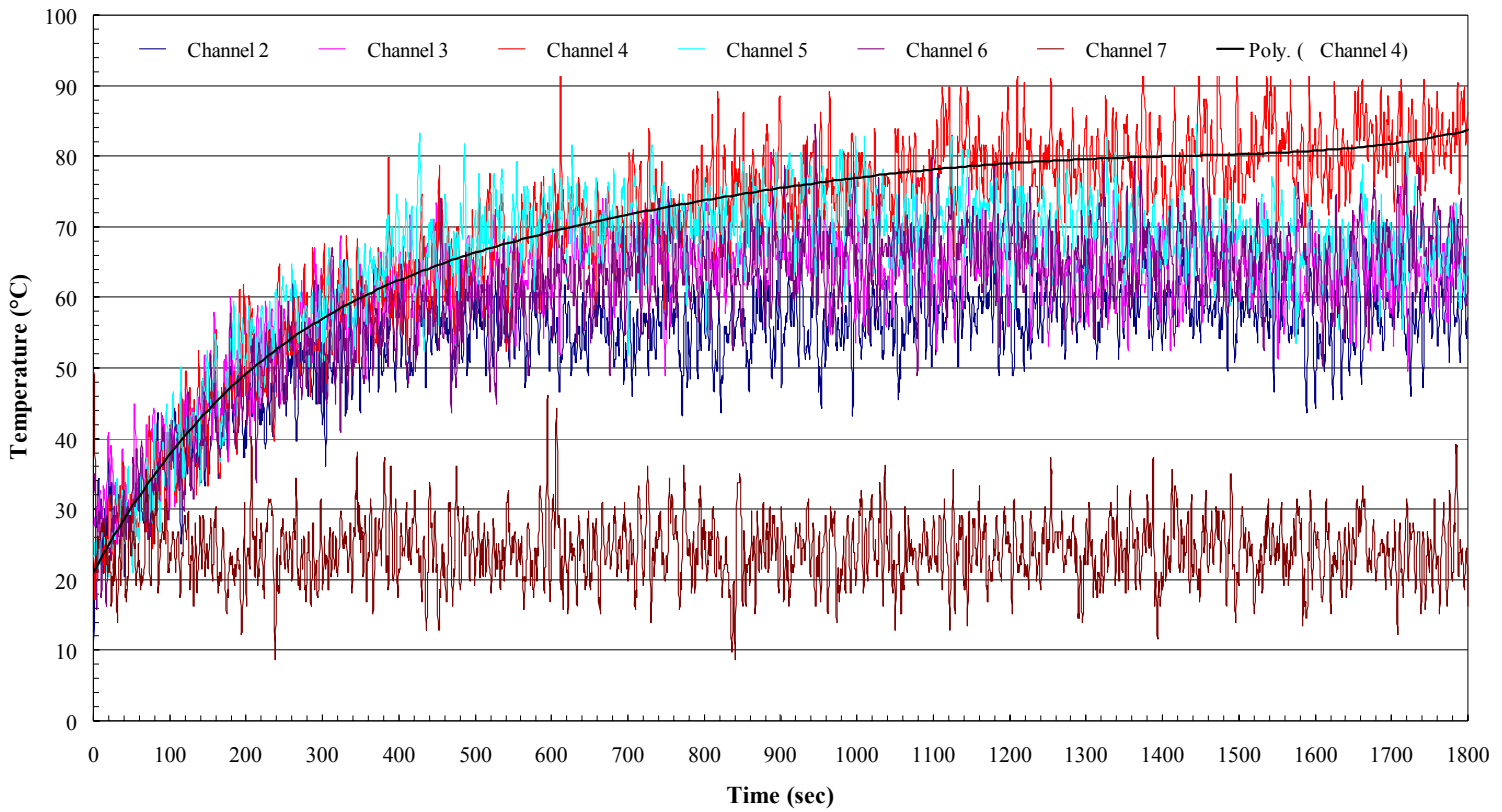
Card board sheet painted with PEN
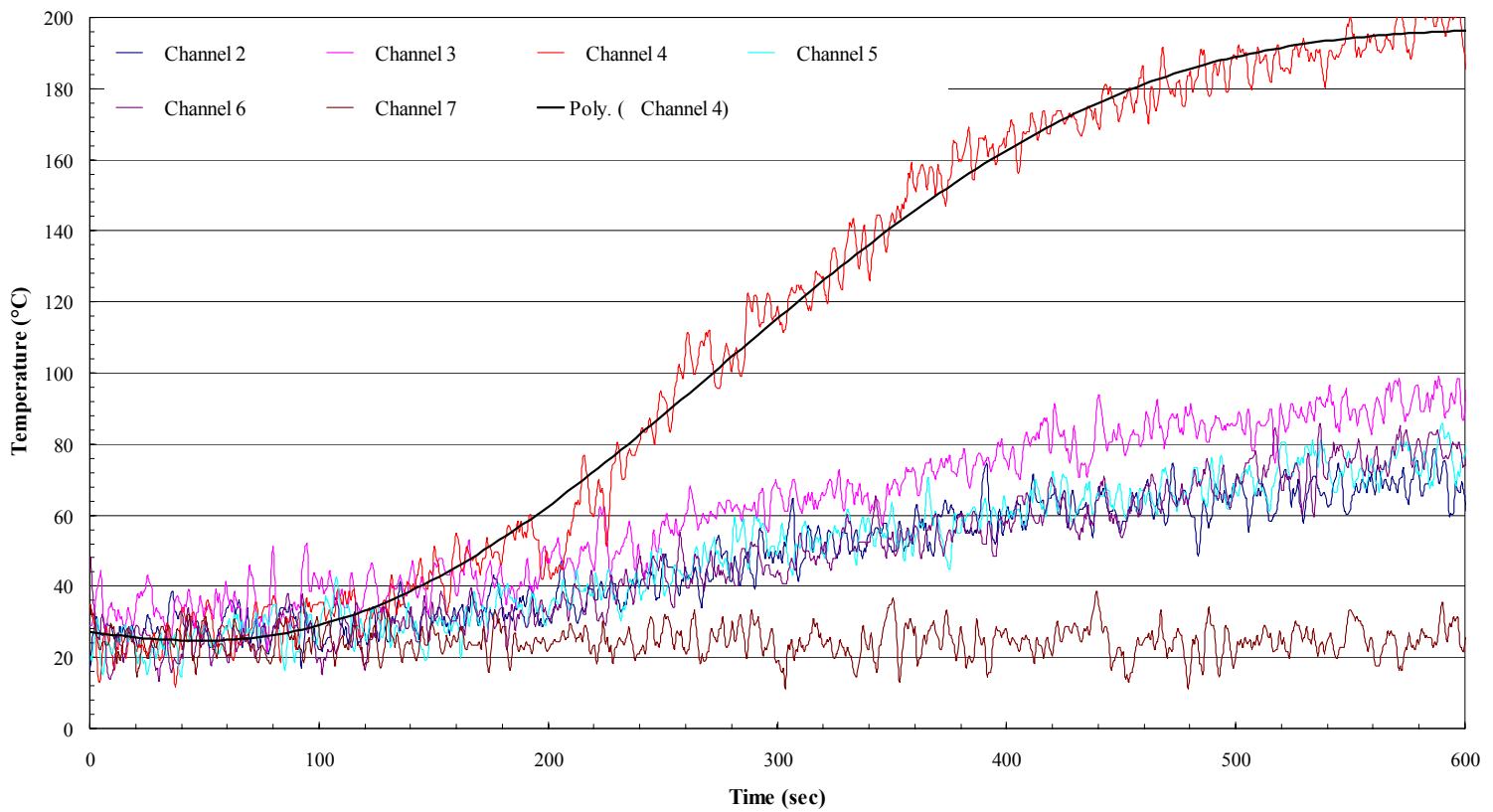
Cardboard sheet painted with Calcium gluconate, Leached SiO$_2$ and Expandable graphite

7.20. Appendix T

7.20.1. Light microscope and SEM images of calcium gluconate monohydrate crystals (powder)
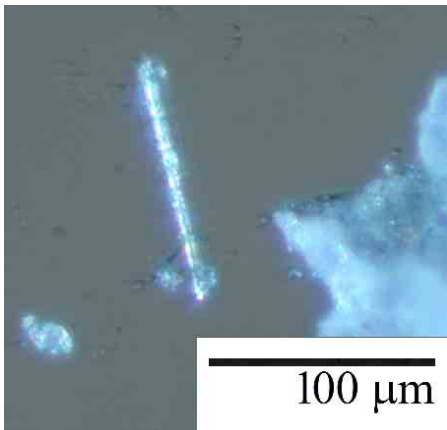
Light microscope images of calcium gluconate monohydrate crystals (powder)
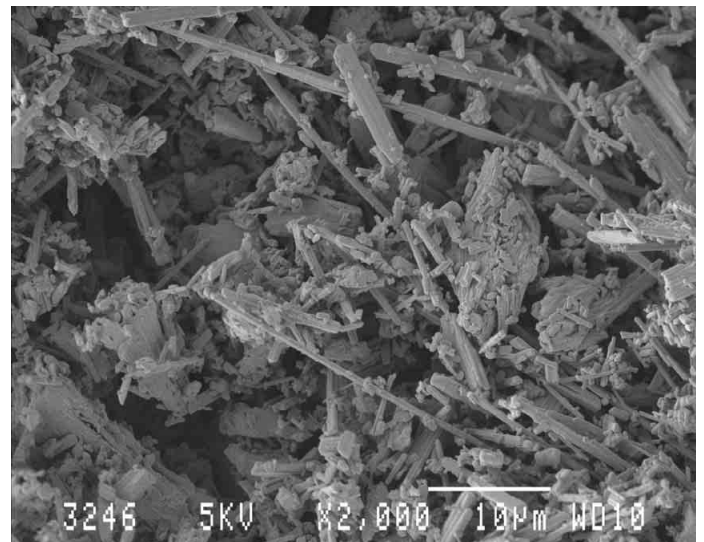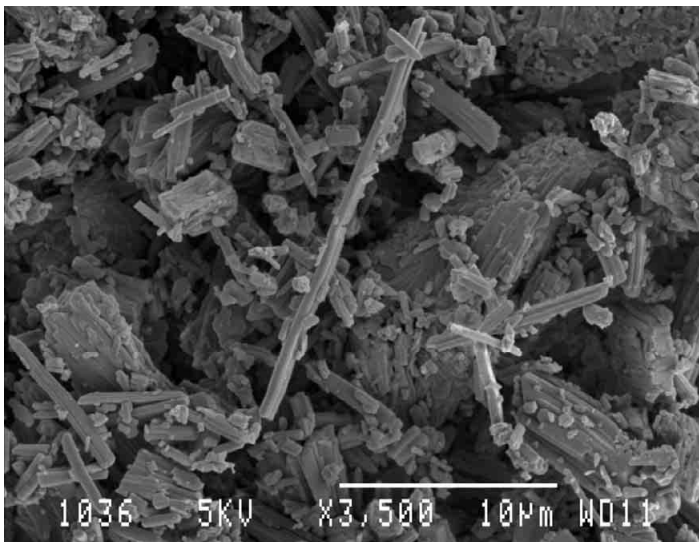
SEM images of calcium gluconate monohydrate crystals (powder)

7.20.2. Light microscope and SEM images of calcium gluconate monohydrate crystals recrystallised through diffusion technique
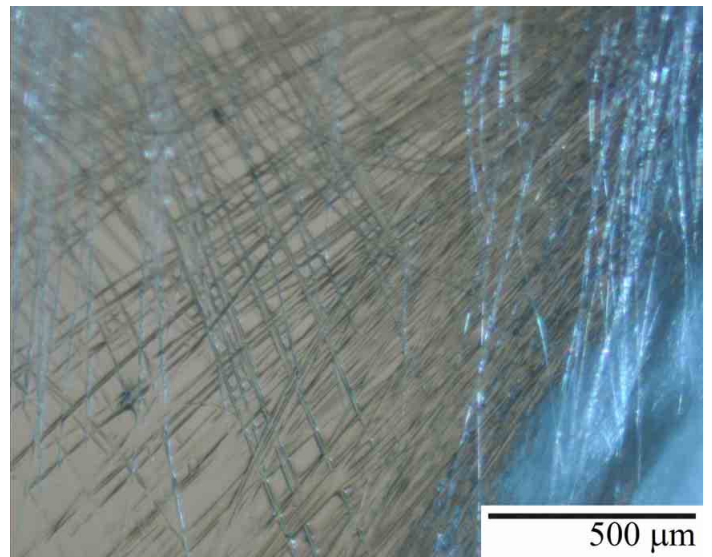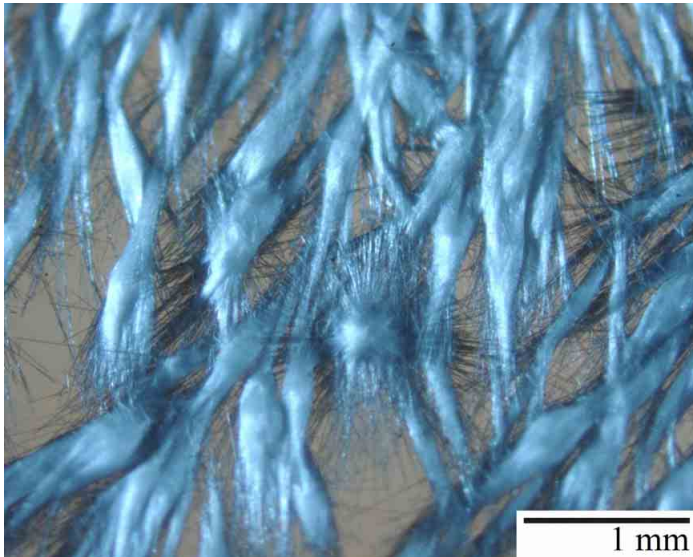
Light microscope images of calcium gluconate monohydrate recrystallised from water through diffusion with ethanol
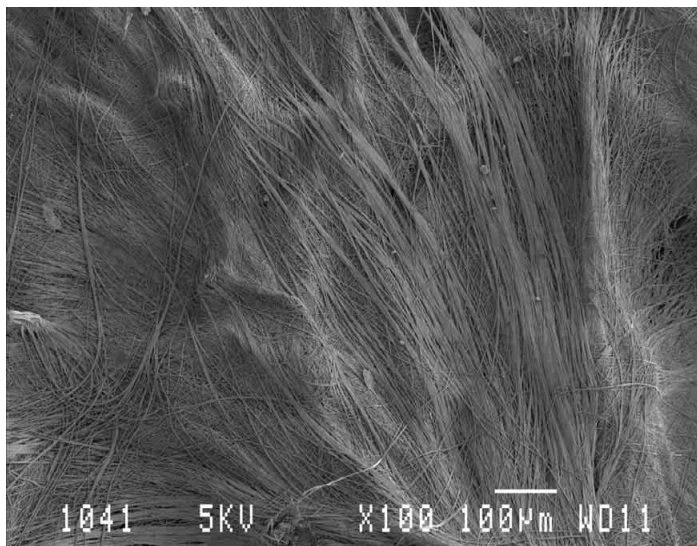
SEM images of calcium gluconate monohydrate recrystallised from water through diffusion with ethanol
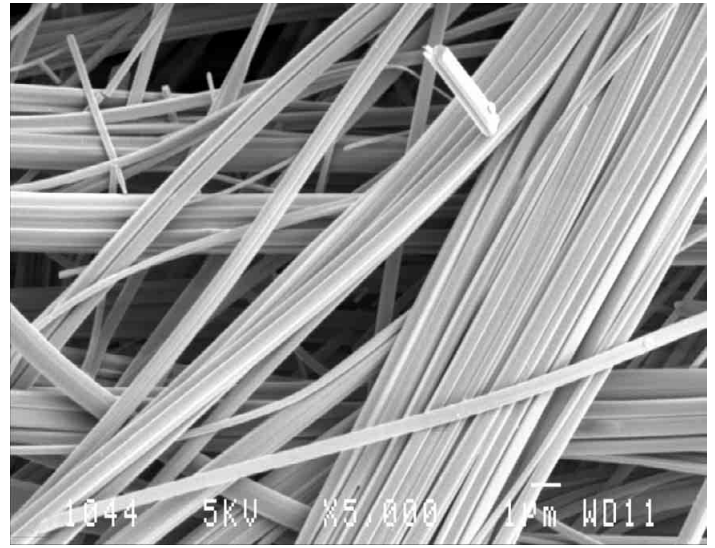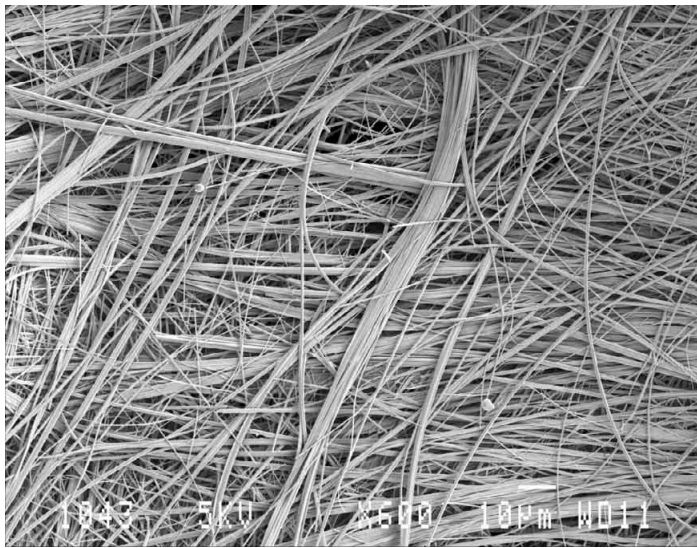
SEM images of calcium gluconate monohydrate recrystallised from water through diffusion with ethanol

7.21. Appendix U

7.21.1. Metal oxides and carbonates prepared from the metal dextrose solutions and calcium gluconate monohydrate
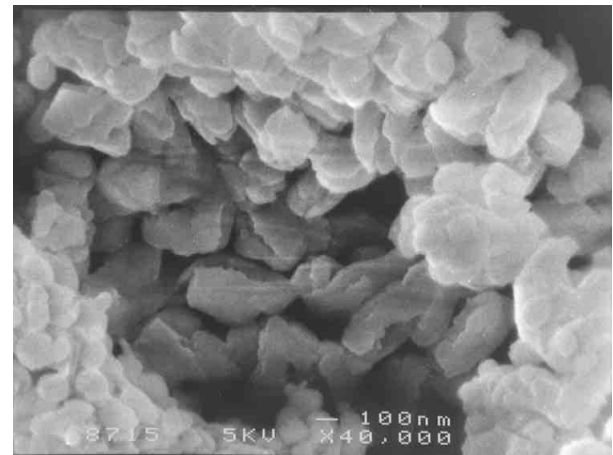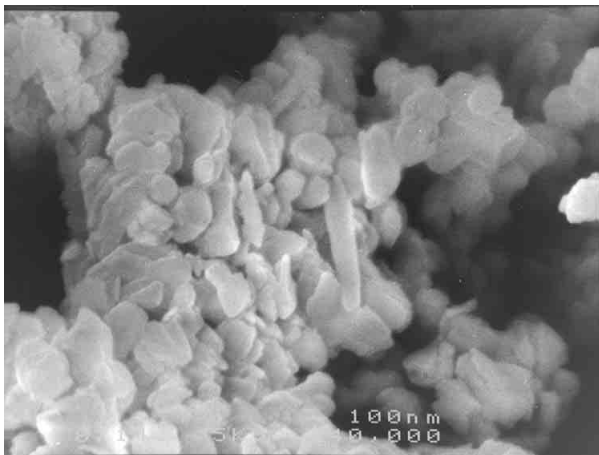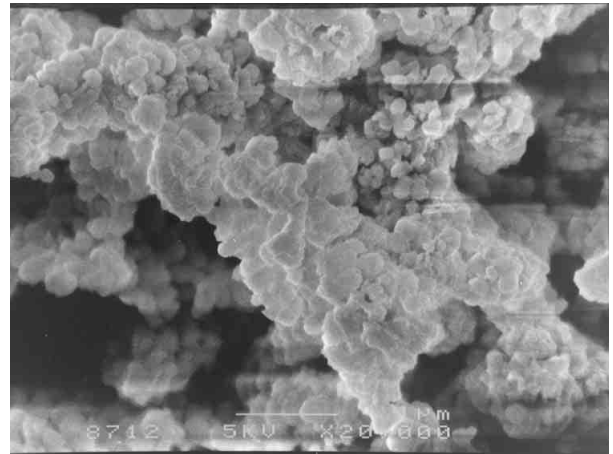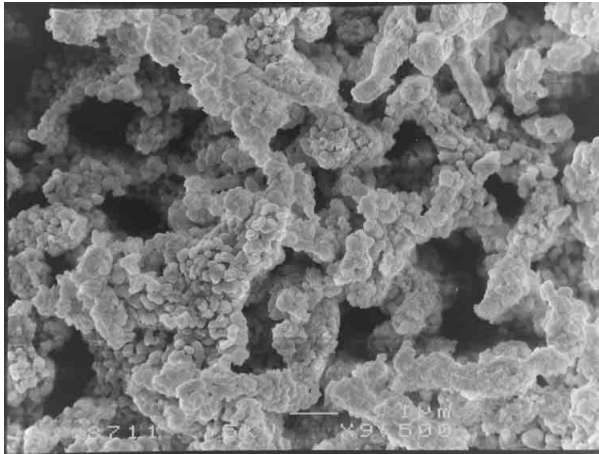
Calcium carbonate prepared from calcium gluconate monohydrate
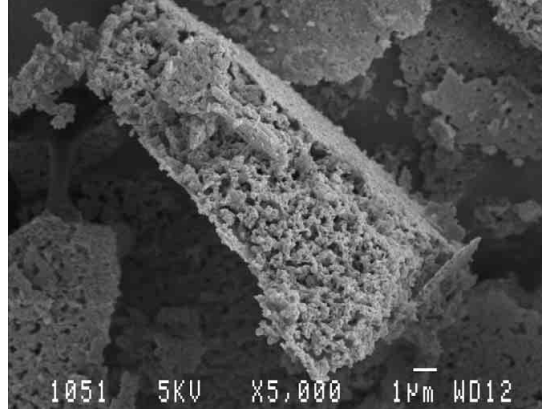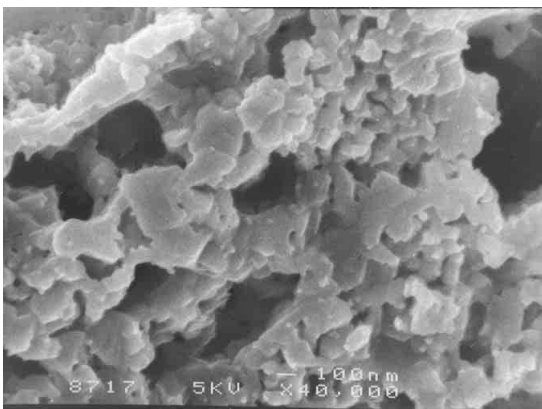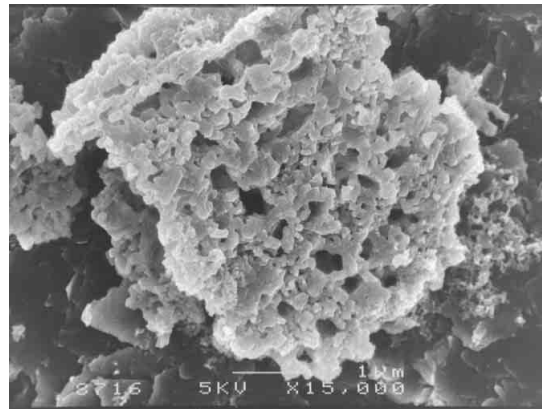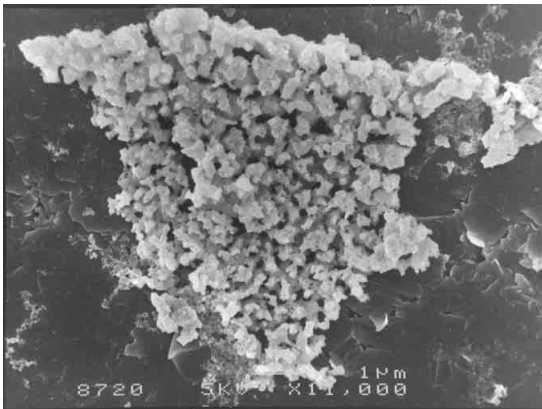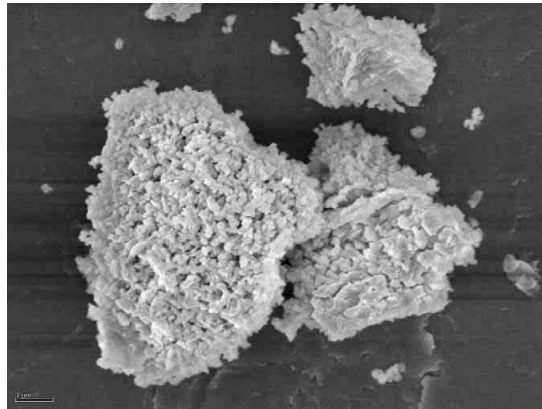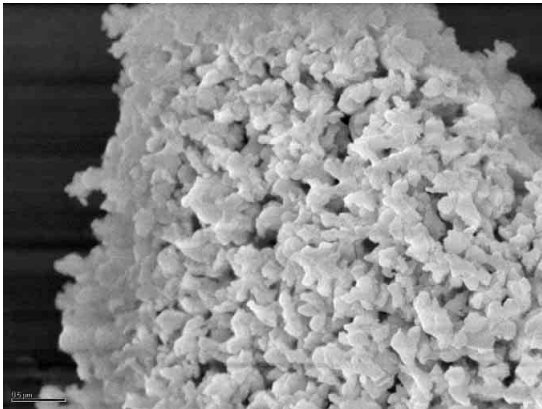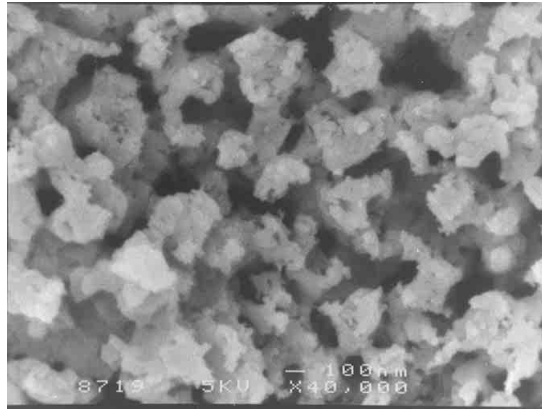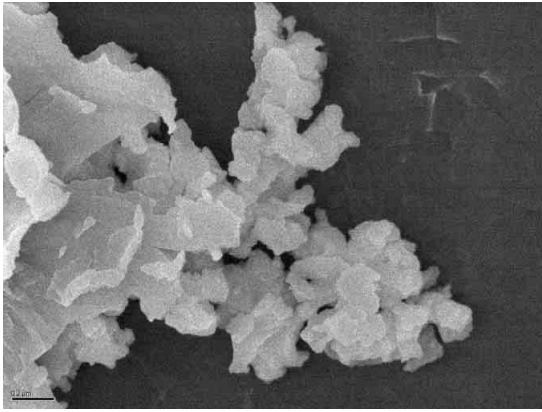
Calcium carbonate prepared from calcium dextrose solution
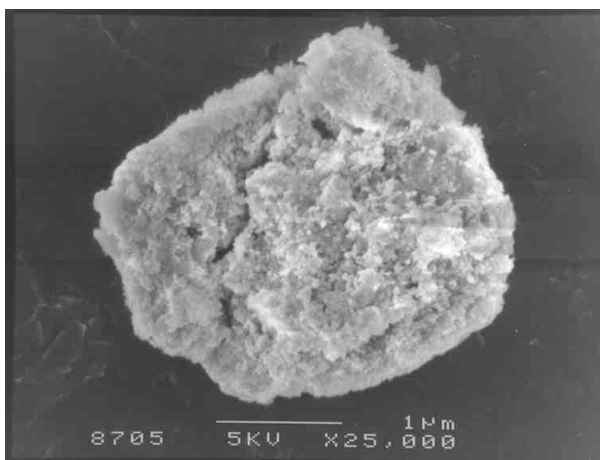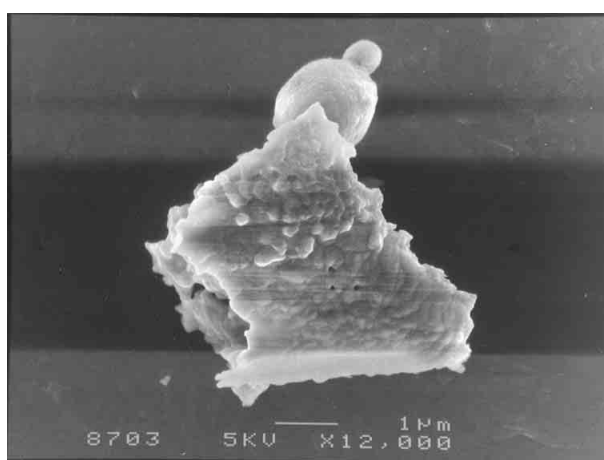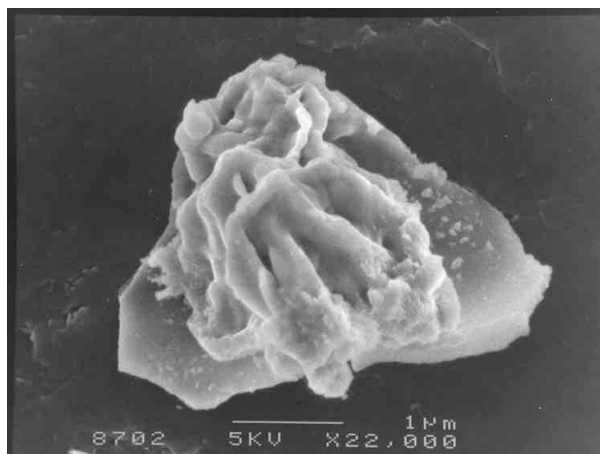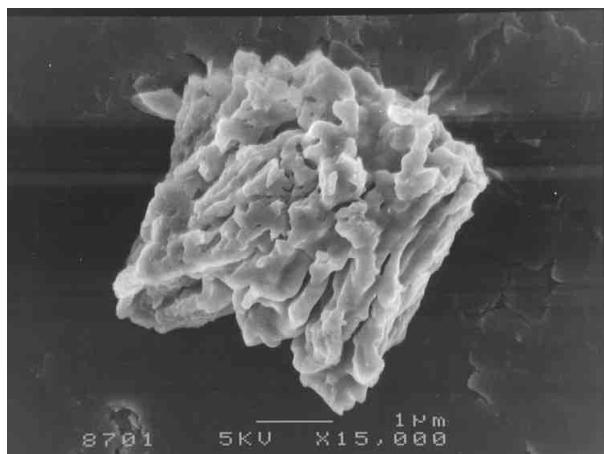
Aluminium oxide prepared from aluminium ammonium dextrose solution
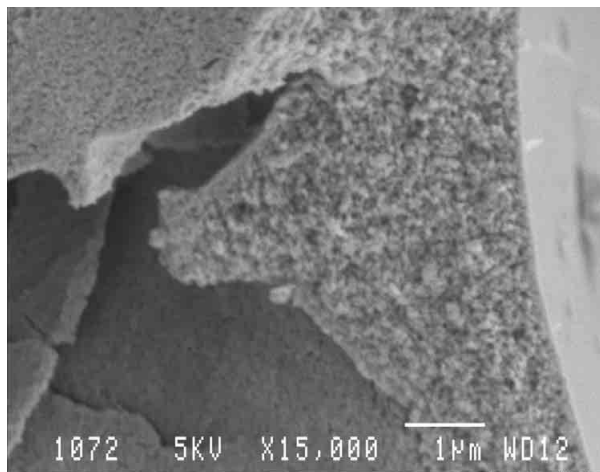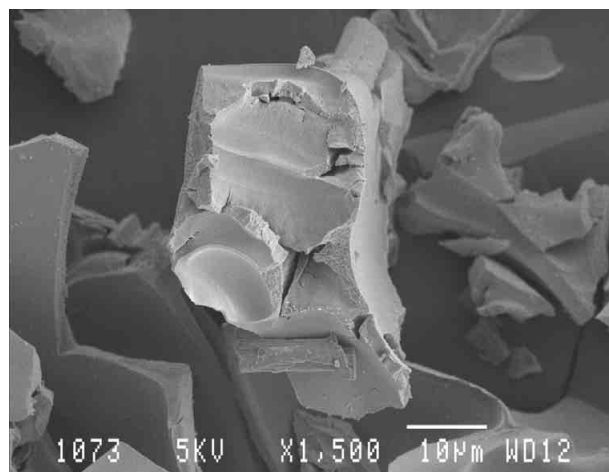
Zinc oxide prepared from zinc dextrose solution
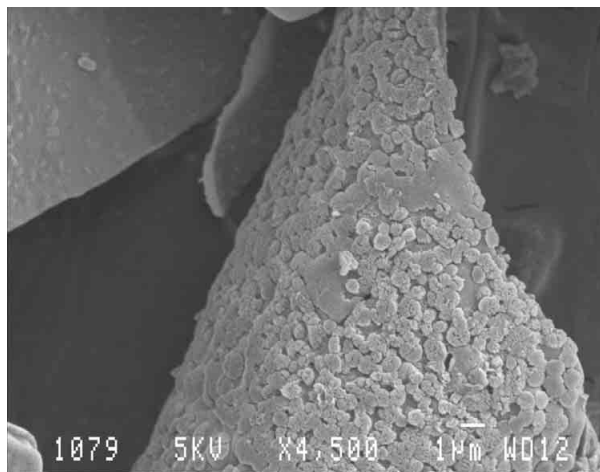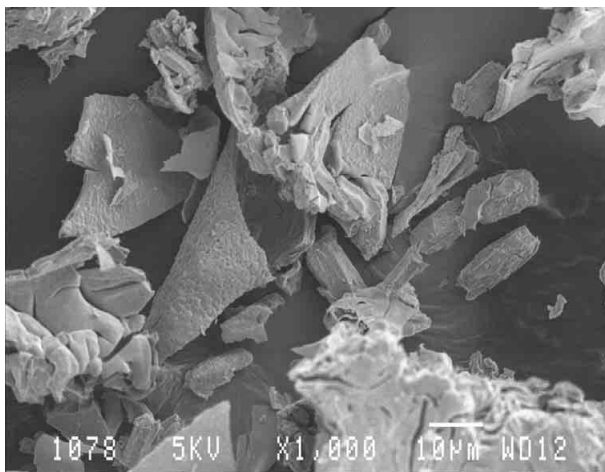
Iron oxide prepared from iron ammonium dextrose solution
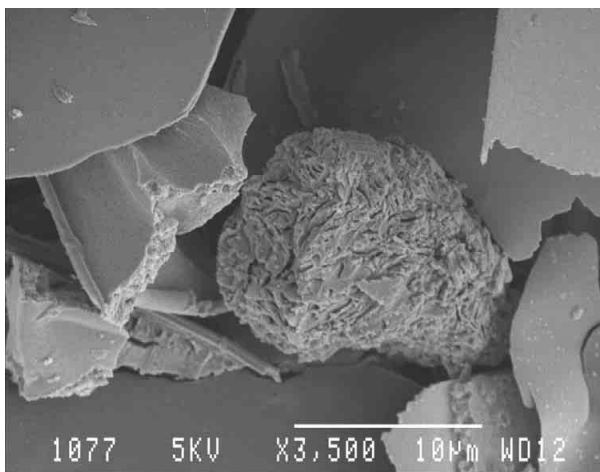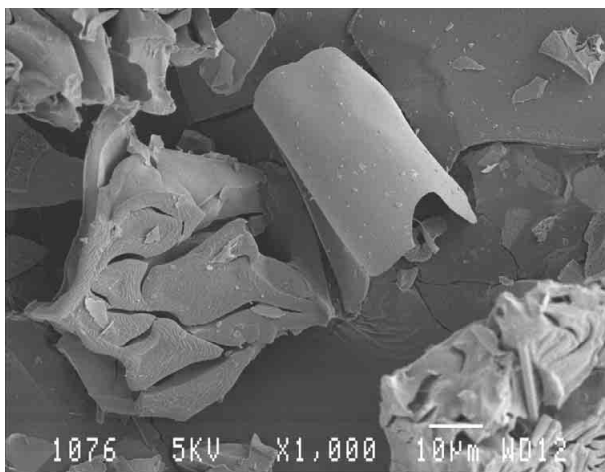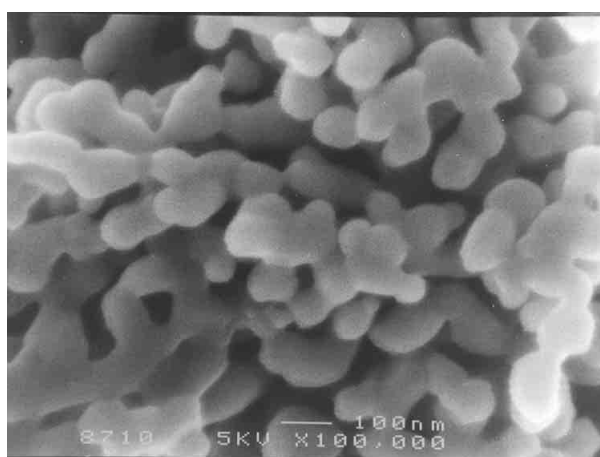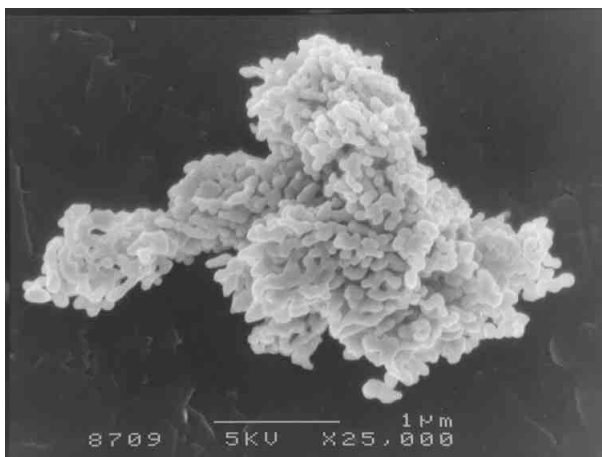
Iron oxide prepared from iron dextrose solution
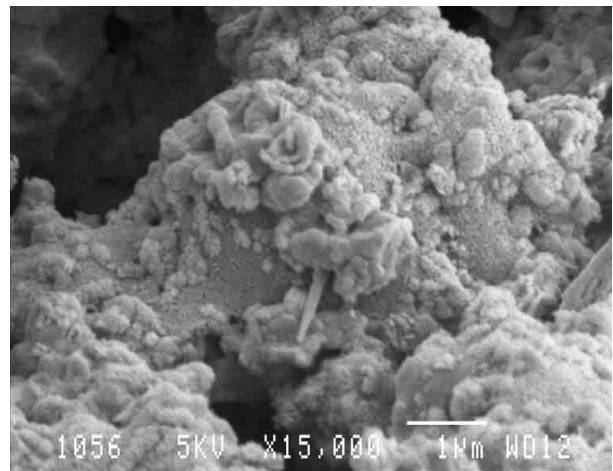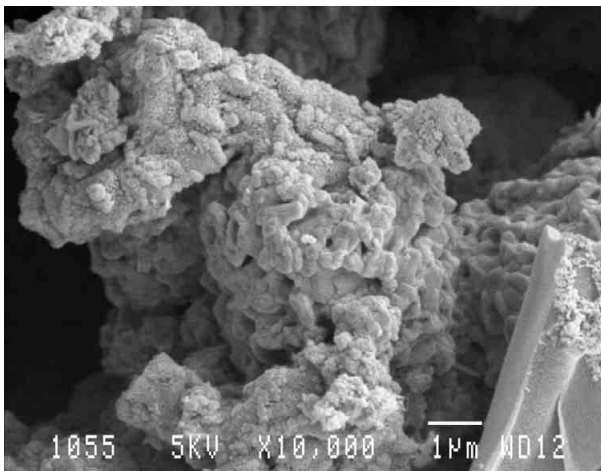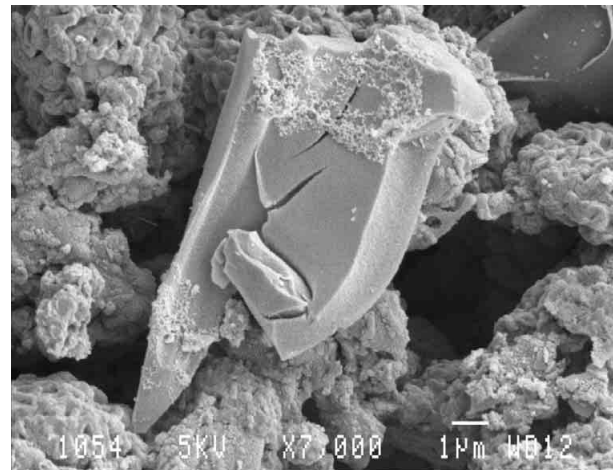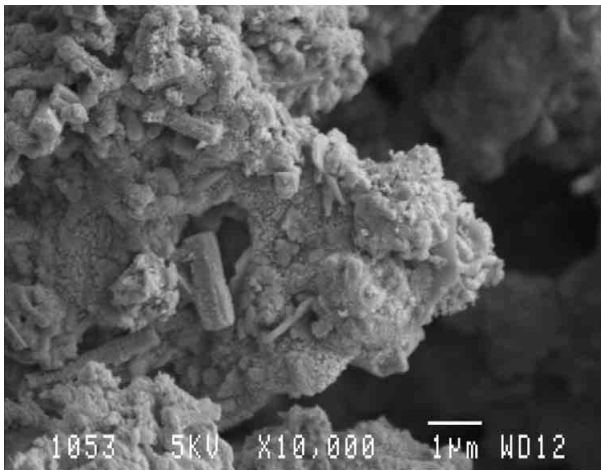
Copper oxide prepared from copper dextrose solution
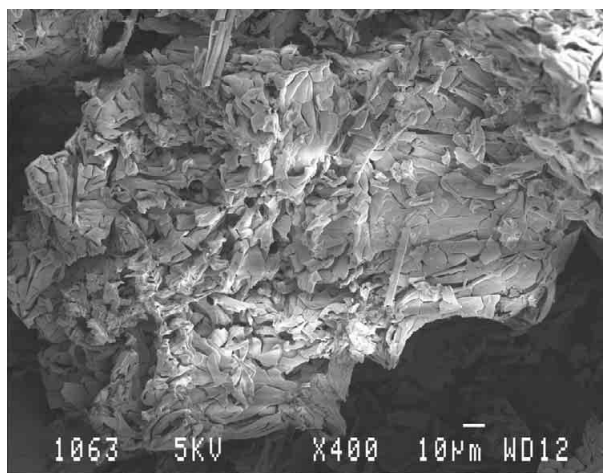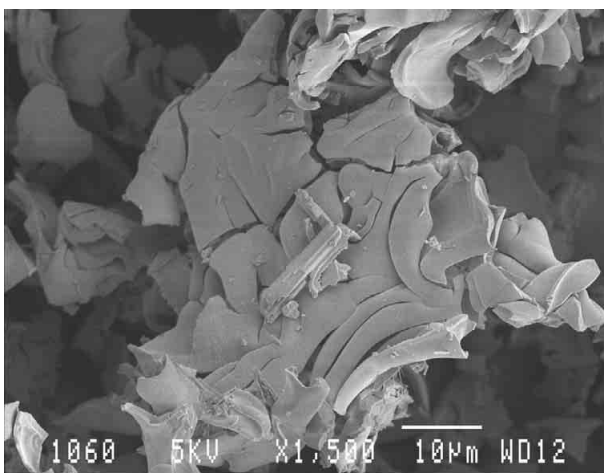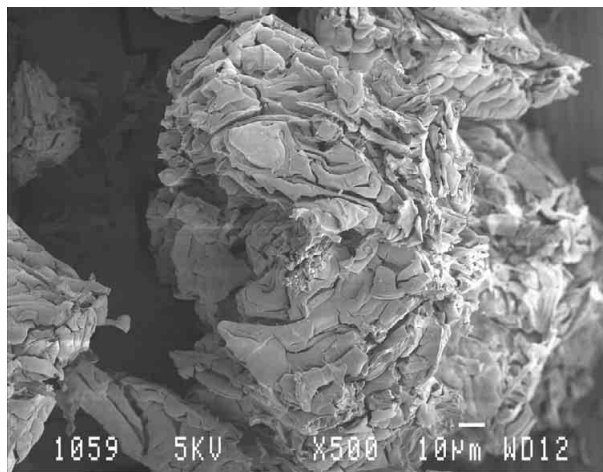
Zirconium oxide prepared from zirconium dextrose solution

7.22. Appendix V

7.22.1. Thermal analysis of selected calcium salts
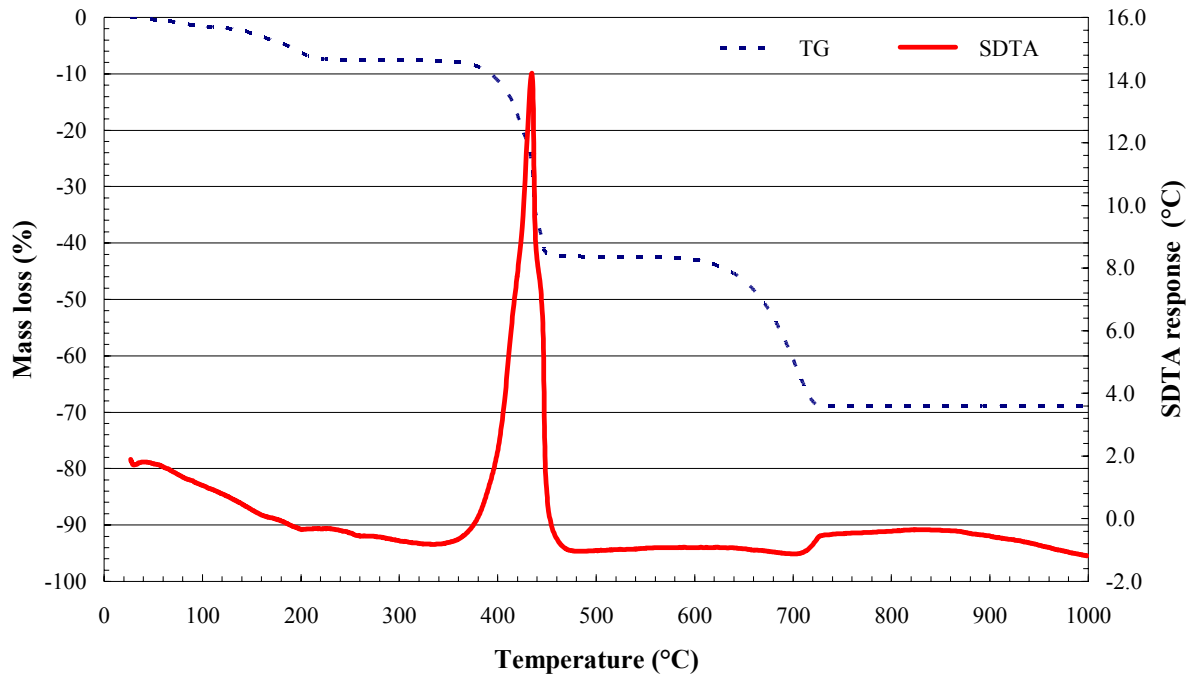
**Thermal analysis of acetic acid calcium salt hydrate in air at 10°C/min**
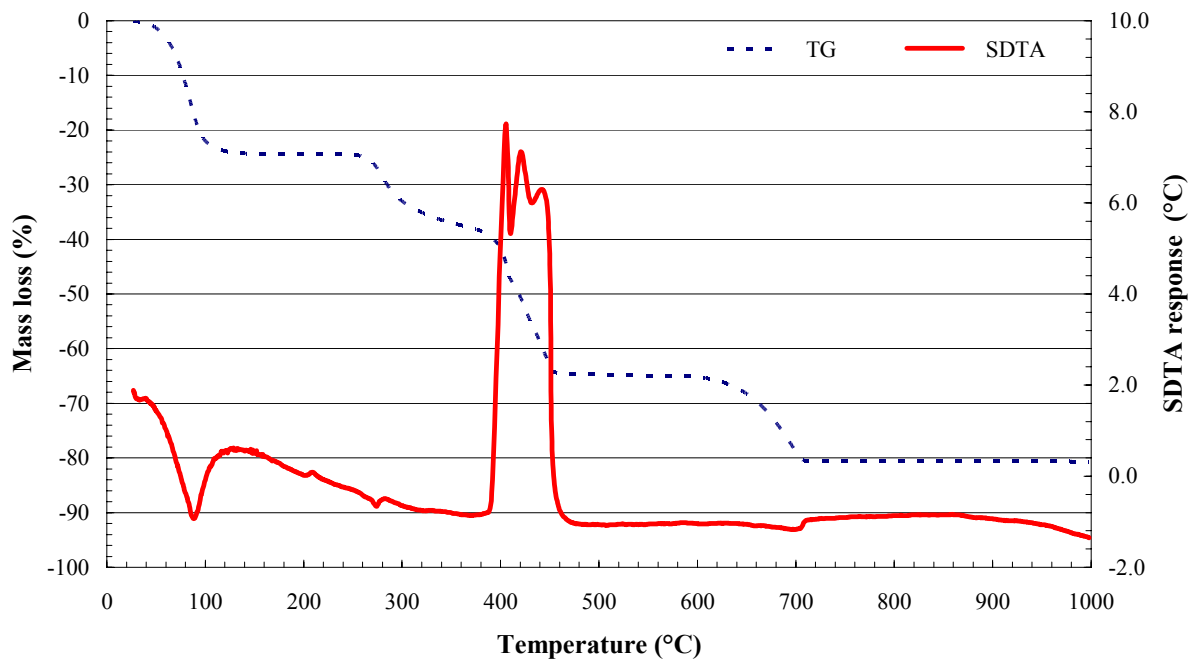
Thermal analysis of lactic acid calcium salt pentahydrate in air at 10°C/min
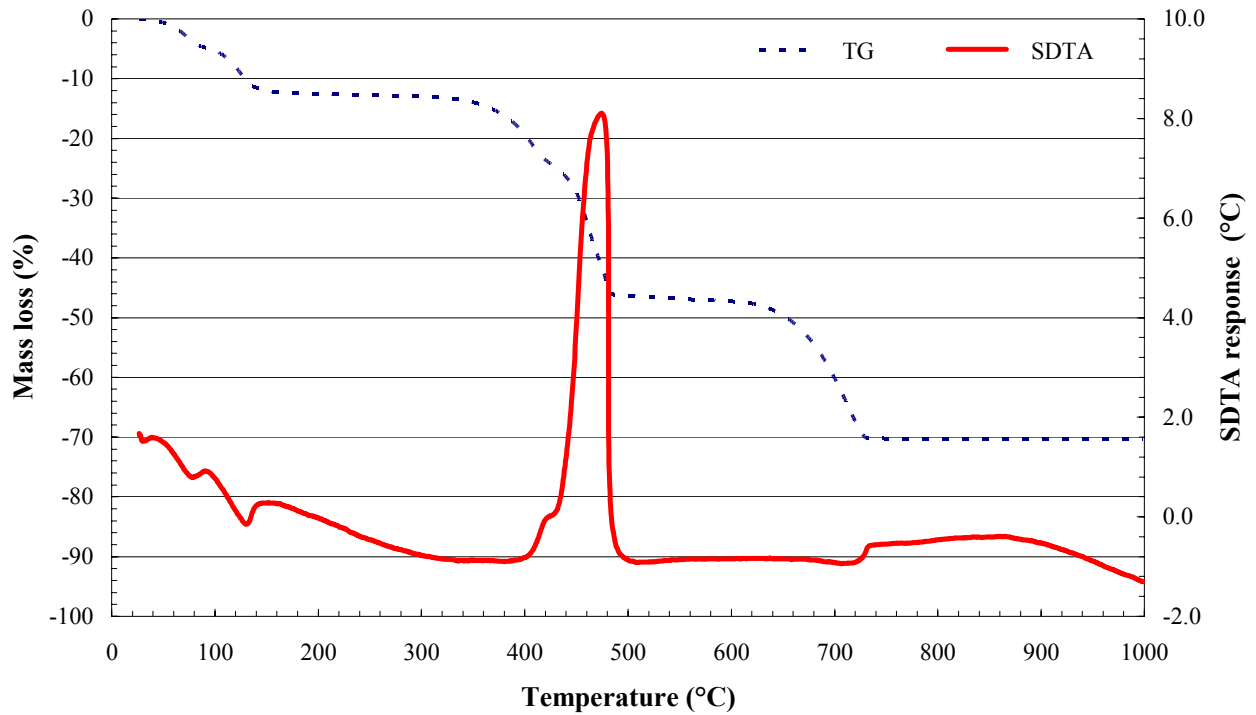
Thermal analysis of citric acid calcium salt tetrahydrate in air at 10°C/min
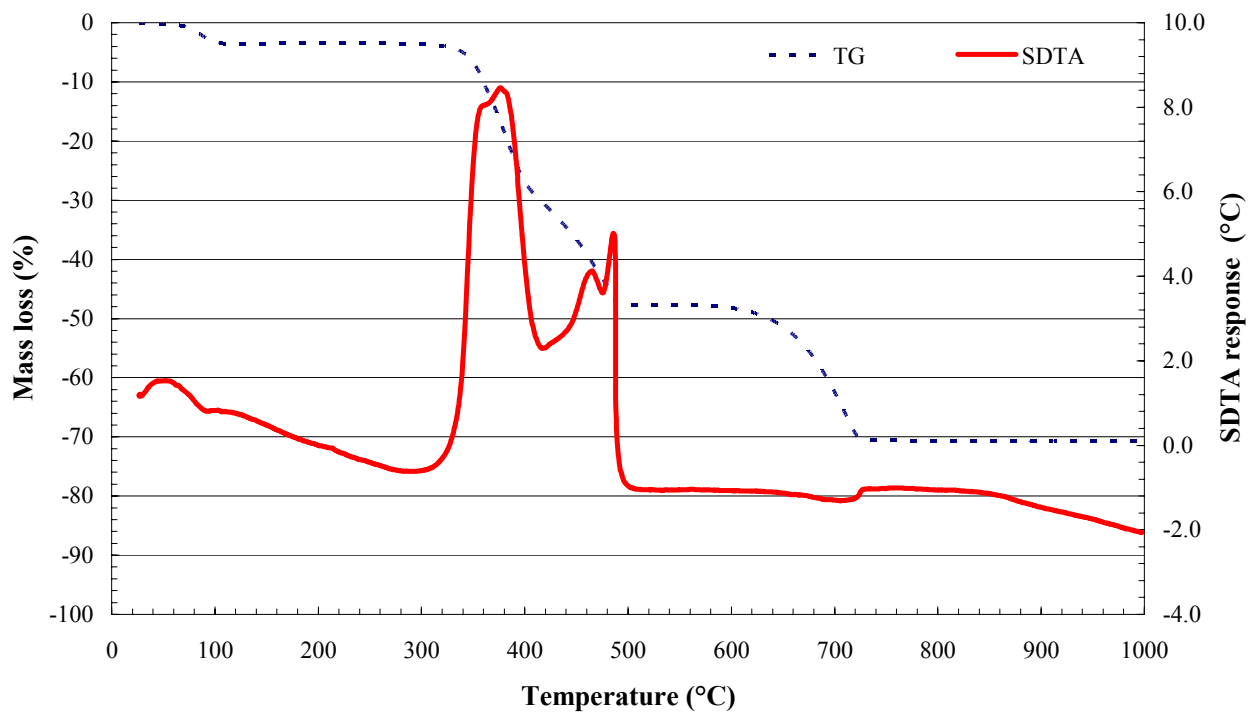
Thermal analysis of propionic acid calcium salt in air at 10°C/min
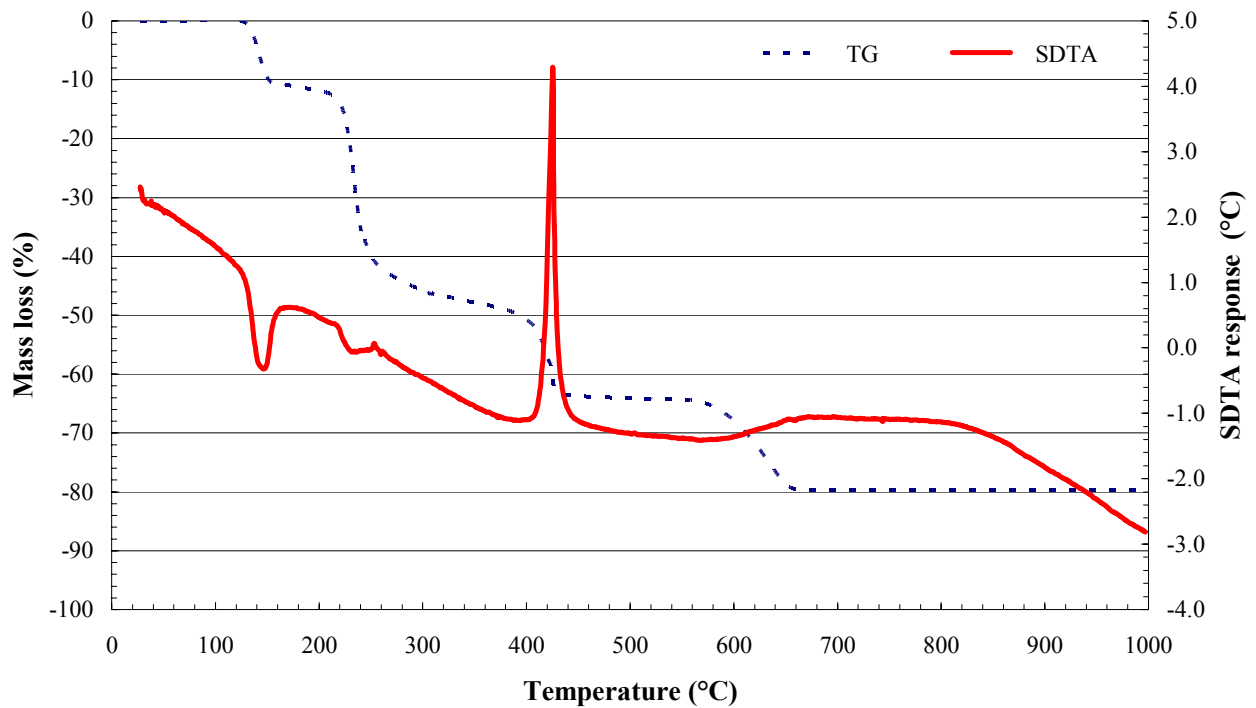
Thermal analysis of glyceric acid hemicalcium salt monohydrate in air at 10°C/min
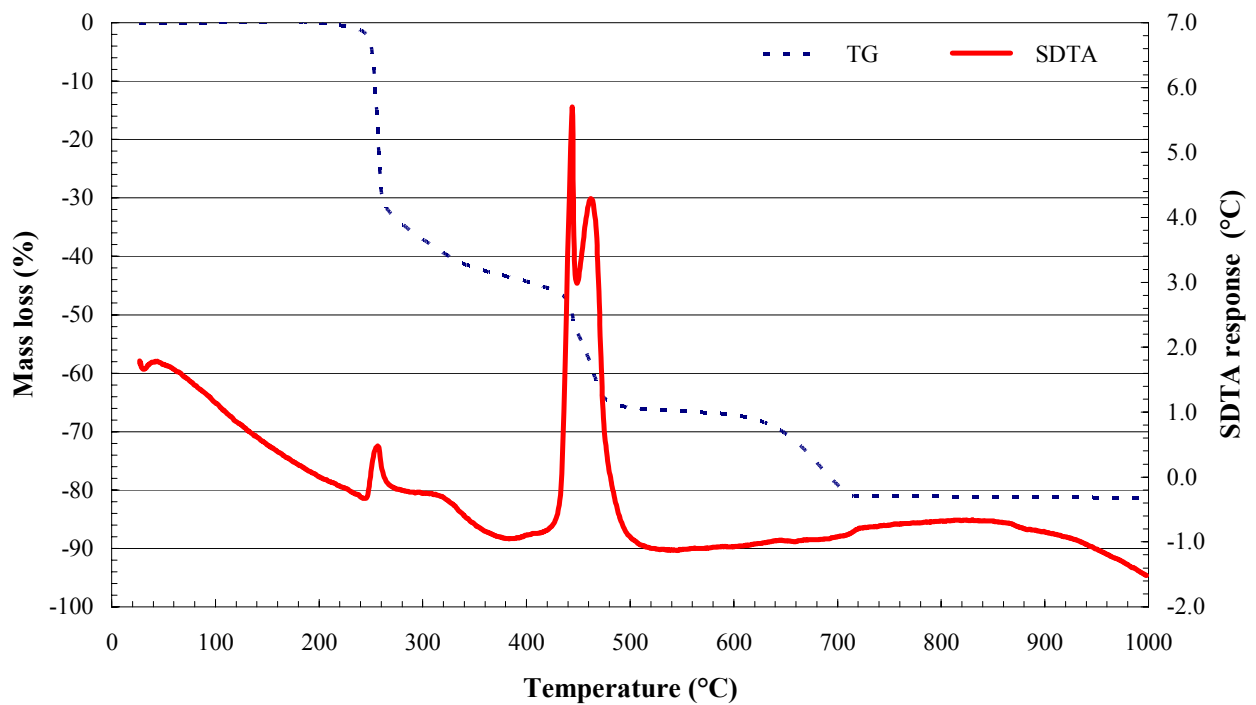
Thermal analysis of threonic acid hemicalcium salt in air at 10°C/min
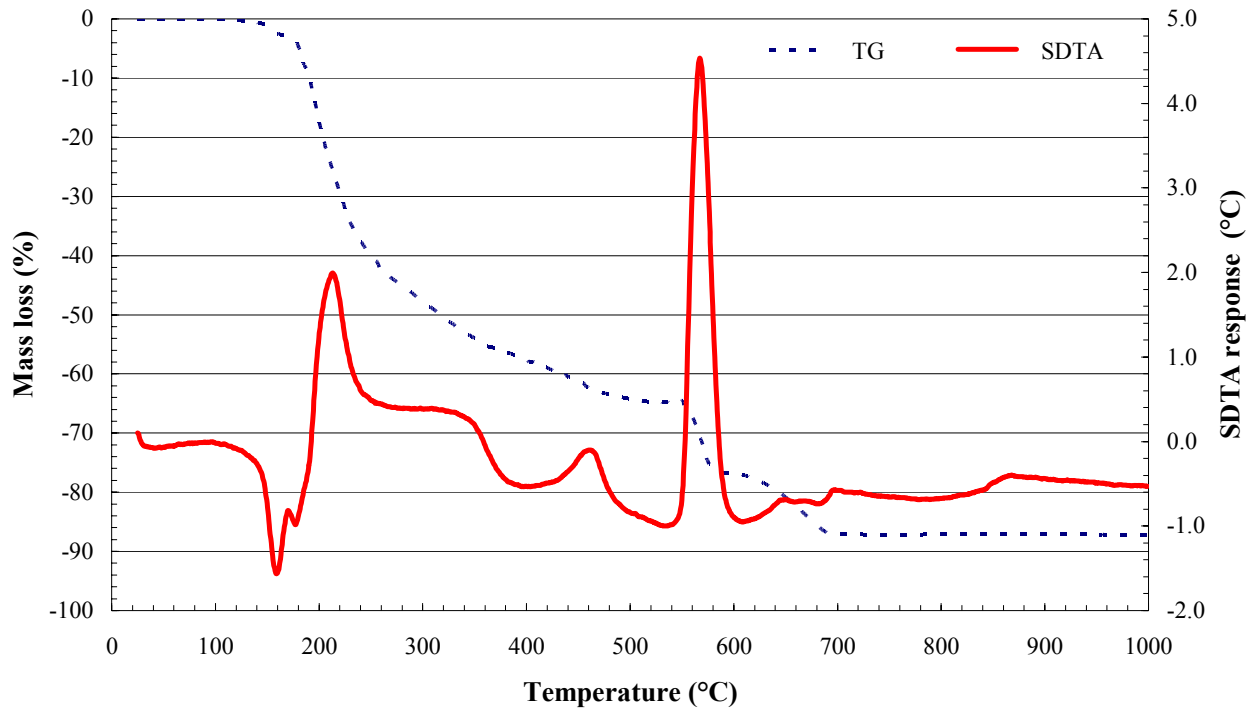
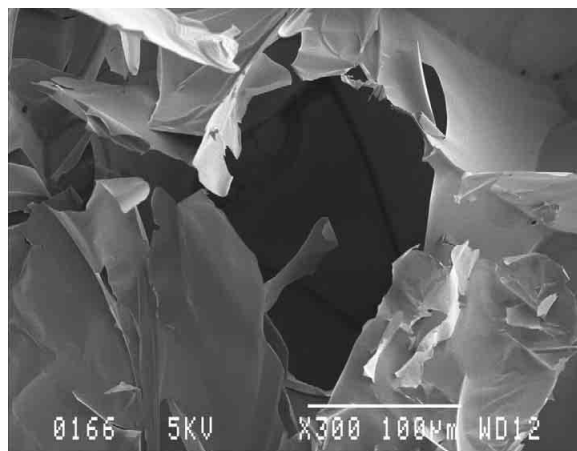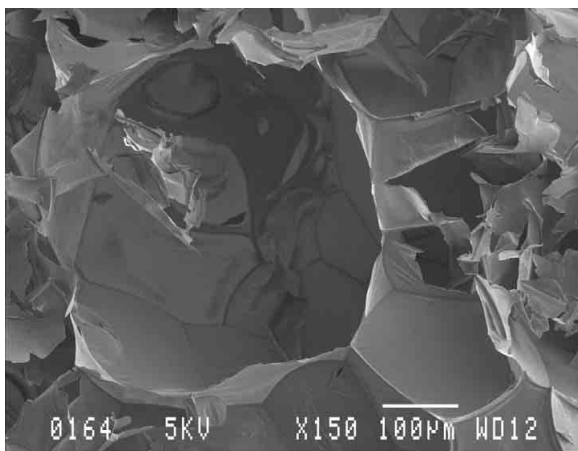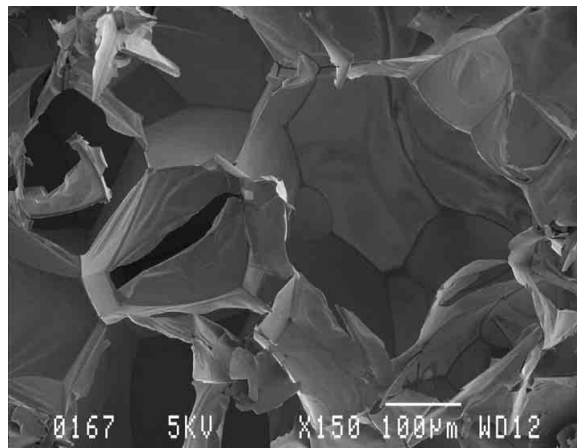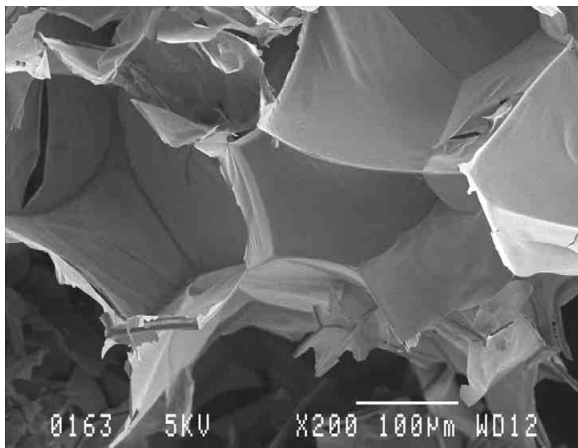**Thermal analysis of gluconic acid calcium salt monohydrate in air at 10°C/min**
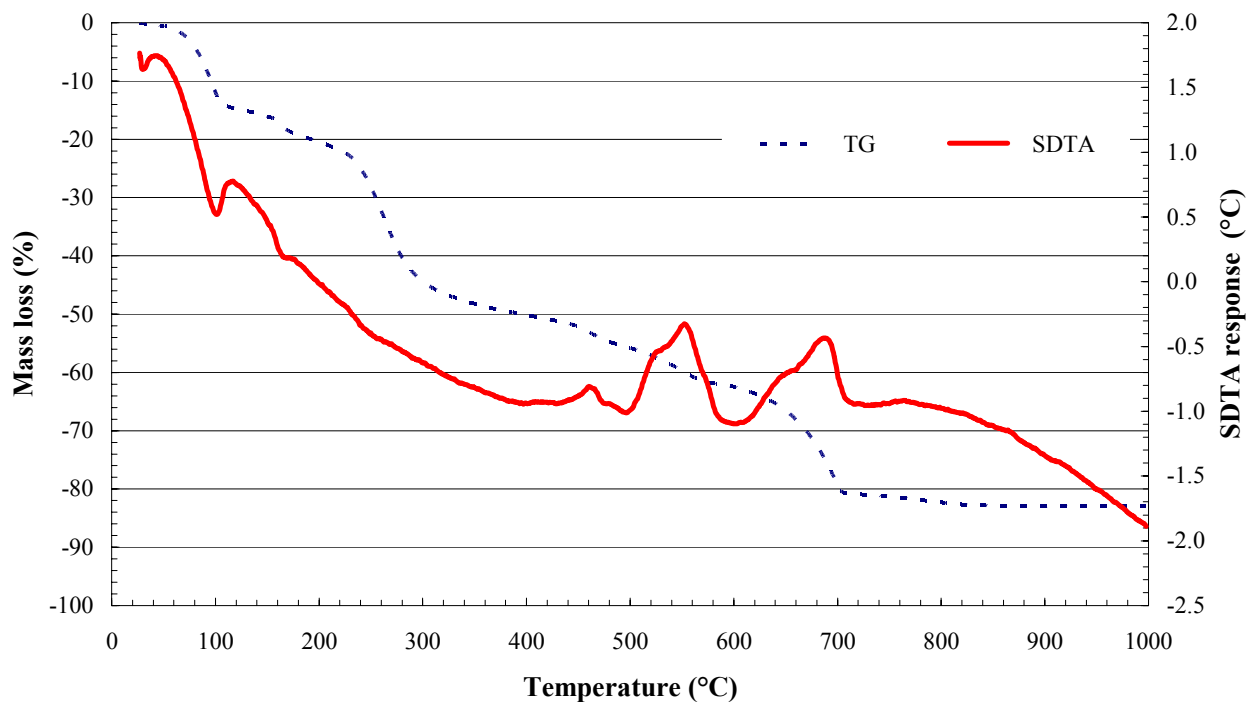
Thermal analysis of saccarinic acid calcium salt tetrahydrate in air at 10°C/min

7.22.2. SEM images of glyceric acid hemicalcium salt monohydrate at selected temperatures in air

Glyceric acid hemicalcium salt monohydrate pyrolysed at 200°C in air
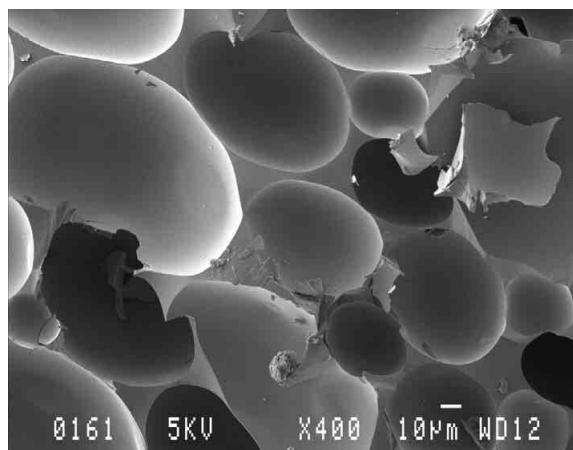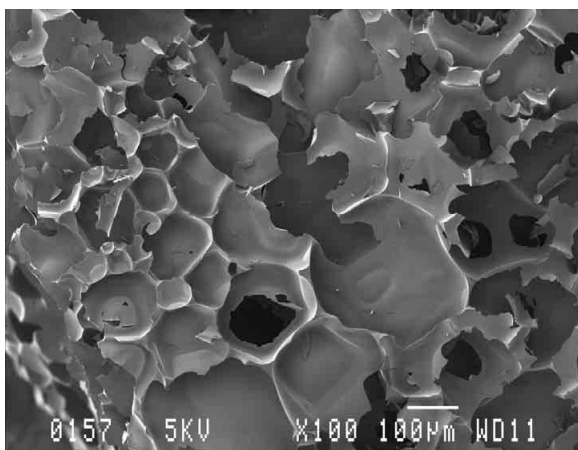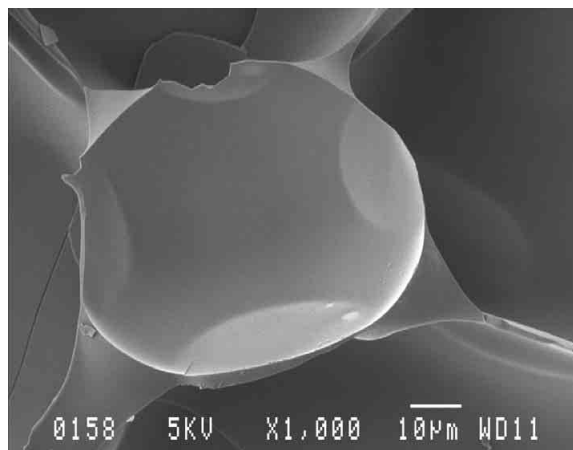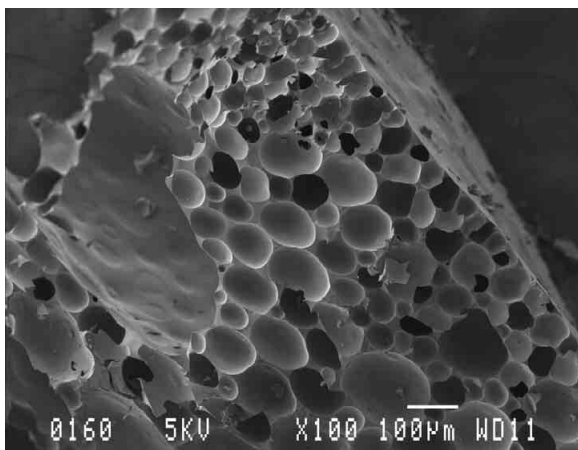
Glyceric acid hemicalcium salt monohydrate pyrolysed at 300°C in air

Glyceric acid hemicalcium salt monohydrate pyrolysed at 400°C in air